

The Development of the Relationships Governing
the Flow of Two-Phase Mixtures and their
Particular Application to
CIRCULATION IN WATER-TUBE BOILERS.

By

D. Chisholm, B.Sc., A.R.T.C.

A Thesis

Presented for the Ph.D., Degree
of The University of Glasgow.

May, 1953.

ProQuest Number: 13838743

All rights reserved

INFORMATION TO ALL USERS

The quality of this reproduction is dependent upon the quality of the copy submitted.

In the unlikely event that the author did not send a complete manuscript and there are missing pages, these will be noted. Also, if material had to be removed, a note will indicate the deletion.



ProQuest 13838743

Published by ProQuest LLC (2019). Copyright of the Dissertation is held by the Author.

All rights reserved.

This work is protected against unauthorized copying under Title 17, United States Code
Microform Edition © ProQuest LLC.

ProQuest LLC.
789 East Eisenhower Parkway
P.O. Box 1346
Ann Arbor, MI 48106 – 1346

ACKNOWLEDGEMENTS.

The research work presented in this thesis forms part of a major investigation on the problem of natural circulation in water-tube boilers being carried out at the Royal Technical College, Glasgow, on behalf of the British Shipbuilding Research Association. The Association have given permission for the use of results already submitted to them in the form of Progress Reports, and for this privilege the author records his grateful thanks.

The research work has been directed successively by Professor W. Kerr, C.B.E., Ph.D., and Professor A.S.T. Thomson, D.Sc., Ph.D., A.R.T.C.

Professor A.W. Scott, B.Sc., Ph.D., A.R.T.C., and Mr. A.M. Laird, B.Sc., A.R.T.C., gave helpful advice and criticism at all stages of the work.

Mr. D. Rooney and Mr. J. Holmes collaborated with the author in carrying out the tests on the experimental boiler.

Mr. D. Rooney carried out the greater part of the analysis of the experimental data using the standard theory which assumes homogeneous flow.

To all the above, and also to those who assisted indirectly the author gives his grateful thanks.

ABSTRACT.

The normal theory for the prediction of circulation in water-tube boilers assumes that the steam-water mixtures in the heated tubes behave as a homogeneous fluid. A theory is here developed which allows for the different vapour and liquid velocities; there is ample evidence to indicate that during two-phase flow even with horizontal tubes the gas, or vapour, flows faster than the liquid.

The flow pattern is assumed to consist of an annulus of liquid in contact with the tube wall, and a core of gas, or vapour, with entrained liquid. While this flow pattern may not occur at all flow rates the application of the theory gives good agreement over a wide range of experimental data. The "Prandtl mixing lengths" throughout the two phases are assumed to have the same values as during homogeneous flow. From these assumptions the application of Prandtl's Equation relating density, shearing stress, mixing length, and velocity profile gradient enables the velocity profile to be obtained for a particular shear distribution, and the respective phase velocities determined. This led to an expression for the ratio of the gas, or vapour, velocity to the liquid velocity.

The application of the expression is complicated by the presence of an unknown quantity of entrained liquid in the gas, or vapour. Where conditions are such that the liquid content of the gas may be assumed negligible, the equations may be directly applied. Good agreement was obtained with experimental/

experimental data for the downward flow of air-water mixtures under such conditions.

On the other hand where liquid is contained in the core, the quantity of liquid must be known before a solution is possible. So far no direct information is available regarding the probable liquid content of the core. The nearest possible approach to this information is to be obtained from Armand's work on air-water mixtures.

Examination of the problem led to the conclusion that the terms involving the water concentration in the core could be taken as common to both air-water and steam-water flow. This enabled the equations to be applied to steam-water flow.

Confirmation of the theory is obtained from the data of previous investigators both for air-water flow and steam-water flow. Test results which are obtained from a full-scale two-tube boiler operating up to a pressure of 1500 lb/in² and heat transfer rates up to 120,000 B.Th.U./hr. ft² of heated riser surface are also analysed. The proposed theory enabled the prediction of pressure changes during steam-water flow within 22%, in contrast to the homogeneous theory which gave errors as large as 60%.

The appendices include, in addition to detailed calculations and developments of a number of the theoretical equations, the details of test equipment designed to permit the study of steam-water mixtures flowing adiabatically at pressures/

pressures close to atmospheric. Also included is the development of the theoretical equations to permit their application to rough tubes.

CONTENTS.Page

ACKNOWLEDGEMENTS	ii.
ABSTRACT	iii.
INTRODUCTION	xi.
NOMENCLATURE	xiii.

PART I REVIEW OF PREVIOUS WORK.

1. Experimental work on water-tube boilers ..	2.
2. Hydrodynamic theories assuming homogeneous flow	11.
3. Determination and effect of the steam velocity relative to the water... ..	19.
4. Hydrodynamic theories introducing relative velocity	29.
5. Thermodynamic theories of natural circulation	34.
6. Two-phase flow in horizontal tubes.. ..	35.
7. General discussion of review.. ..	48.

PART II. THE PROPOSED THEORY FOR DETERMINATION OF PHASE VELOCITIES DURING TWO-PHASE FLOW.

8. Mode of flow	51.
9. Ratio of the gas to liquid velocity. ..	55.
10. Approximate form of the gas to liquid velocity ratio	59.
11. Shearing stress ratio τ_2/τ_1	63.
12. Distortion of the annulus profile... ..	67.
13. Effect of heat transfer on flow conditions	72.
14. Flow in downcomers	74.

PART III. THE PROPOSED THEORY FOR PRESSURE CHANGE DURING TWO-PHASE FLOW.

15. Pressure change due to friction	78.
16. Pressure change due to mixture weight ..	81.
17. Pressure change due to momentum forces ..	82.
18. Combined equations and method of solution	84.

PART IV. APPLICATION OF THE PROPOSED THEORY TO THE ANALYSIS OF THE EXPERIMENTAL DATA OF PREVIOUS INVESTIGATORS.

Page

19.	Liquid concentration in core (Armand's experiments)	87.
20.	Friction during air-water flow (Martinelli's experiments)	91.
21.	Pressure change during the flow of steam-water mixtures in vertical tubes (Schwab's experiments)	94.
22.	Pressure change during the downward flow of air-water mixtures in vertical tubes (Bergelin's experiments)	98.
23.	"Stagnation" point during flow in downcomers (Lowenstein's experiments)	103.

PART V. TWO-TUBE BOILER: TEST EQUIPMENT, PROCEDURE AND RESULTS.

24.	British Shipbuilding Research Association experimental boiler	108.
25.	Instrumentation	114.
26.	Calibration tests	117.
27.	Test programme, procedure and readings	122.
28.	Conversion and interpretation of test readings..	125.
29.	Test results	131.

PART VI. APPLICATION OF PROPOSED THEORY TO ANALYSIS OF TWO-TUBE BOILER TEST RESULTS.

30.	Pressure change with adiabatic flow in riser tube	144.
31.	Friction loss with adiabatic flow in riser tube.	151.
32.	Pressure change with heat transfer in riser tube	156.
33.	Steam-water velocity ratio in riser tube.. ...	167.
34.	Pressure change in downcomer tube and at riser entry	179.

PART VII. PREDICTION OF NATURAL CIRCULATION IN TWO-TUBE BOILER.

35.	Pressure changes over riser and downcomer tubes..	188.
36.	Circulation velocity	195.

TABLE INDEX.

<u>Table.</u>		<u>Page.</u>
1-2.	Steam-water flow pressure changes (Schwab)...	95-96.
3.	Specimen readings - two-tube boiler...	124.
4.	Overall heat balance - " " " " ...	130.
5-9.	Dryness fractions - " " " " ...	138-142.
10-11.	Pressure changes - steam drum-water drum ...	181-182.
12-13.	" " - riser bottom-water drum...	183-184.

FIGURE INDEX.

<u>Figure.</u>		<u>Page.</u>
1.	Thornycroft overall gauge. ...	3.
2.	Overall gauge data curve.. ...	5.
3.	Circulation velocity - Schmidt.. ...	8.
4.	U-tube circuit ...	12.
5.	Prediction of circulation in tube banks ...	16.
6.	Steam bubble velocity in a stationary column of water ...	20.
7.	Effect of "slip" on available pressure difference in U-tube circuit ...	22.
8.	X_c/X to a base of U_c/U_0 at 150 lb/in ²	24.
9.	X_c/X " " " " " " 32 atmos....	26.
10.	Correction for pressure... ...	27.
11.	Slug flow pattern... ...	30.
12.	X_c/X to a base of the ratio of air to total flow volume ...	40.
13.	Prandtl mixing length distribution ...	53.
14.	Two-phase velocity profile ...	56.
15.	Z to a base of X_c/X ...	61.
16.	Equilibrium of core element ...	64.
17.	Annulus equilibrium ...	68.
18.	Distortion of annulus profile... ...	71.
19.	Velocity profile - downcomer ...	75.
20.	Water concentration in core ...	89.
21.	Friction during air-water experiments (Martinelli)...	92.
22.	Pressure change - air-water flow in vertical tubes (Bergelin).. ...	100.
23.	Velocity ratio - " " " " ...	101.
24.	Mass flow producing "stagnation" ...	105.
25-27.	Two-tube boiler ...	110-112.
28.	Differential pressure recording system ...	115.
29.	Furnace heat loss ...	119.
30.	Boiler heat loss ...	120.

FIGURE INDEX.

<u>Figure.</u>		<u>Page.</u>
31-35.	Circulation velocities (experimental)..	...132-136.
36-40.	Pressure change - steam drum-riser top.	...145-149.
41.	Friction - steam-water flow 153.
42.	G to a base of boiler pressure... 154.
43-47.	Pressure change - riser top to riser bottom..	161-165.
48.	Velocity ratio K to a base of pressure.	... 168.
49.	The term z " " " " " 169.
50.	The ratio R_2/R_1 " " " " " 170.
51.	The ratio T_2/T_1 " " " " " 171.
52.	Pressure change - velocity ratio	... 173.
53.	" " " " " 174.
54.	Influence of heat transfer on K..	... 176.
55.	Variation of K along heated length	... 178.
56-60.	Pressure change - steam drum-water drum	...189-193.
61-64.	Circulation velocities - comparison of theoretical and experimental values196-199.
65-66.	Circulation velocity - sketch of graphical procedure	...203-204.
67.	Single phase velocity profile	231.
68.	U_3/U_1 to a base of X_c/X	233.
69.	Friction factor	235.
70.	K to a base of M/X (prediction of stagnation)	241.
71.	Determination of K and pressure gradient	... 249.
72.	Pressure gradients over heated length..	... 252.
73.	Determination of circulation velocity..	... 254.
74-75.	Equipment - steam-water tests 257.
76.	Single-phase velocity profile (rough tubes)..	261.
77.	$(U)_c/U_*$ to a base of X_2/X 263.
78.	C " " " " friction factor 264.

§

§

§

INTRODUCTION.

The present research was initiated to study the fundamental mechanism of circulation in water-tube boilers. To this end, a boiler was constructed consisting essentially of two drums interconnected by two tubes, one of which was heated by an electric furnace. The tube dimensions were of the same order as met with in practice, and the maximum operating pressure was 1500 lb/in², with heat transfer rates to the heated tube up to 120,000 B.Th.U/hr.ft.². The experimental data consisted of the circulation velocity, and the pressure changes over various tube lengths.

The circulation in water-tube boilers is governed by two relationships or laws. Firstly, in a tube bank all tubes are subject to a common pressure difference. Secondly, the net flow into a particular drum, or header, is zero.

These two statements are generally accepted as the basis of all circulation theories. What is not common to all theories is the method of calculating the pressure difference over tubes through which steam-water, or as they are more generally called, two-phase mixtures flow. The problem, therefore, reduces primarily to the study and analysis of the flow of the steam-water mixtures in the heated tube.

Until recently it has been commonly assumed that two-phase mixtures can be satisfactorily treated as homogeneous fluids. During the last decade considerable experimental and theoretical work has however indicated that such assumptions are untenable.

This/

This has also been confirmed by the data from the two-tube boiler.

This thesis contains an original development of the theoretical equations enabling the prediction of pressure changes during two-phase flow. Unlike previous investigators these equations are developed from the internal equilibrium conditions of the respective phases. The flow form assumed is symmetrical around the pipe axis, the liquid forming an annular ring at the wall, and the gas or vapour with entrained liquid occupying the core. It may appear that such a flow form is unlikely, particularly during horizontal flow, but experimental evidence indicates that, even during horizontal flow, with turbulence the liquid tends to form a ring round the wall.

The starting point of the theoretical development is the fact that during two-phase, and during homogeneous flow, the internal shearing stresses must be transferred by viscous or momentum shear. While this concept is inherent in the theories of certain previous investigators it has never been completely utilized.

- Fr. - Froude's Number $U^2/g.d.$
- K - Gas-liquid or vapour-liquid velocity ratio $U_g/U_L.$
- K_2 - Core-annulus velocity ratio $U_2/U_1.$
- M - Mass flow lb/sec.
- Re. - Reynolds Number $\rho.d.U/\mu$
- T - Shearing stress lb/ft².
- U - Velocity ft/sec.
- X - Cross-sectional area of tube ft².
- X_c - " " occupied by gas or vapour ft².
- X_L - " " " " liquid ft².
- X_A - " " " " annulus ft².
- X_2 - " " " " core ft².
- Z -
$$\frac{U_3}{U_1} \frac{1-q-w+w/K_2}{1-q} \sqrt{\frac{q}{q+w}}$$
- d - Tube diameter ft.
- g - Gravitational acceleration ft/sec².
- l - Axial length of tube ft.
- l_1 - Prandtl mixing length during single-phase flow ft.
- l_2 - " " " " two-phase flow ft.
- p - Pressure lb/ft².
- $\left(\frac{dp}{dl}\right)$ - total pressure gradient.
- $\left(\frac{dp}{dl}\right)_f$ - pressure gradient due to friction.
- $\left(\frac{dp}{dl}\right)_p$ - " " " " fluid weight.
- $\left(\frac{dp}{dl}\right)_m$ - " " " " momentum forces.
- q - Dryness fraction, or ratio by weight of gas to total flow rate. lb/lb.
- r - Radius ft.
- r_0 - tube radius ft.

- ω - Water content of core per lb. mixture lb/lb.
 γ - Distance from tube wall $r_0 - r$ ft.
 β - Ratio by volume of air to total flow rate ft³/ft³.
 λ + Friction factor.
 ρ - Density lb/ft³.
 θ - Inclination of tube to horizontal degrees.
 μ - Viscosity lb/ft. sec.

SUFFIXES.

- 1 - Applying to single-phase flow, or to the annular ring.
 2 - " " two-phase " " " " core.
 G - " " gas or vapour.
 L - " " liquid.
 b - " " boundary between phases.

PART I.REVIEW OF PREVIOUS WORK.

	<u>Page.</u>
1. Experimental work on water-tube boilers ...	2.
2. Hydrodynamic theories assuming homogeneous flow	11.
3. Determination and effect of the steam velocity relative to the water	19.
4. Hydrodynamic theories introducing relative velocity	29.
5. Thermodynamic theories of natural circulation	34.
6. Two-phase flow in horizontal tubes	35.
7. General discussion of review	48.

REVIEW OF PREVIOUS WORK.

1. EXPERIMENTAL WORK ON WATER-TUBE BOILERS.

Much of the early work was carried out on models having glass tubes and observation windows in the drums. The method proved valuable in confirming speculation based on operating experience and in guiding the formulation of theory.

Considerable full scale work was done by Thornycroft, Yarrow and others. Thornycroft introduced the use of an "overall" gauge between the steam and water drums, (see Fig.1) a device used by later experimenters.

The greater part of this work was carried out during the last ten years of the last century, and established the following important points:

- (a) Circulation due to density difference between riser and downcomer tubes.
- (b) Importance of circuit hydraulic losses.
- (c) Effect of steam-water mixtures entering downcomer tubes.
- (d) Possibility of alternating flow and reversal of flow.

The circuit hydraulic losses were known to be governed by the following factors:

- (a) The ratio of the tube length to diameter.
- (b) The tube form.
- (c) The discharge being above or below water level.

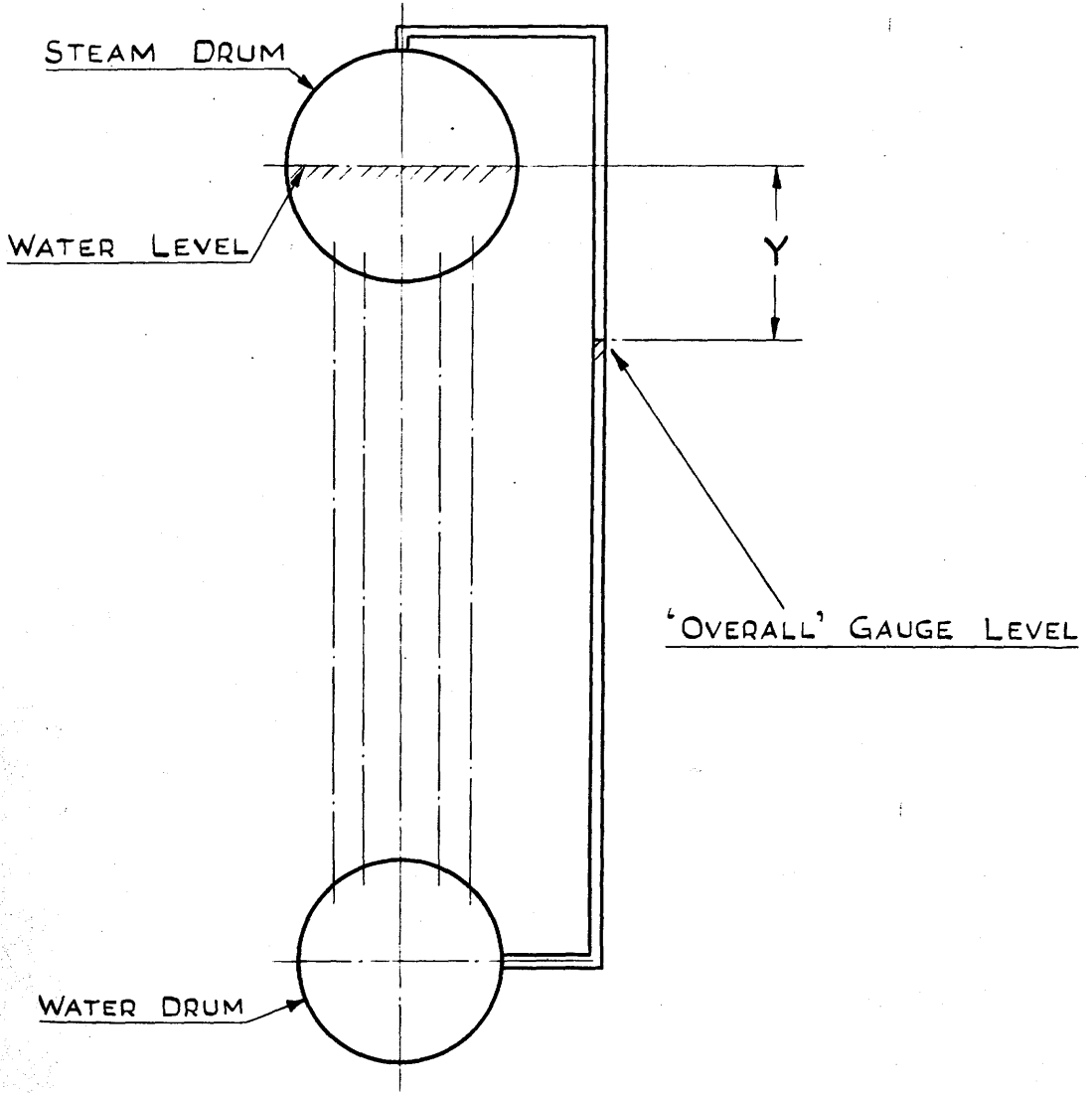


FIG. 1. THORNYCROFT OVERALL GAUGE

ROBINSON (1933) published results of tests on four full scale marine boilers. These tests covered:

- (a) Incidence of steam pockets in water drums.
- (b) Overall gauge readings.
- (c) Direction of flow in various tubes throughout the tube banks.

The velocities were measured by Pitot tubes.

A typical curve of the difference between the level in the steam drum and the overall gauge level (y -Figure 1) is shown in Figure 2 to a base of boiler evaporation. The drums were approximately a hundred inches apart.

The conclusions drawn from the tests were:

- (a) The difference between the steam drum level gauge and the overall gauge (y) is a measure of the difference in pressure between the steam and water drums.
- (b) The level in the overall gauge will change with evaporation rate and pressure.
- (c) Increase in evaporation decreases level in overall gauge till the point is reached where the level will tend to rise. This indicates a condition liable to cause overheating of riser tubes, and is associated with steam pockets collecting in the water drum.
- (d) y decreases with increase in gauge pressure.

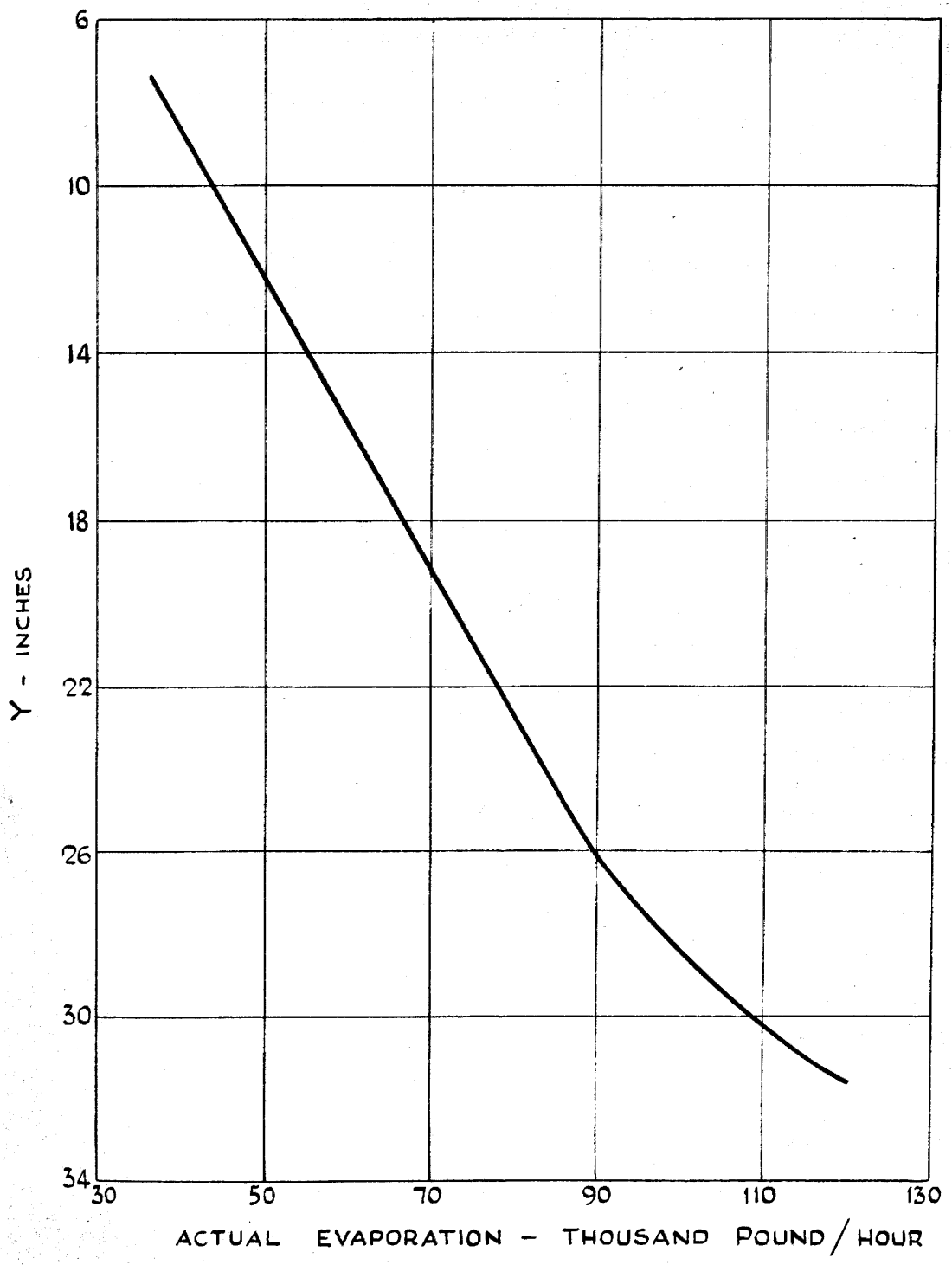


Fig. 2. Overall gauge data curve.

- (e) Increase in number of heated rows of generating tubes or the addition of unheated downcomers will cause an increase in the water level in the overall gauge for a given evaporation.
- (f) The majority of tubes act as risers even at low heat inputs, and no radical change occurs when the intensity of heating is increased, although reversal of flow may take place in some tubes. Alternating flow may take place in the intermediate zone up to high working rates.

In this zone downcomers were found among risers.

Dight (1933 and 1936) published results on Shop Trials of Naval Water-Tube Boilers of Yarrow type. The influence of firing rate on circulation was investigated using Pitot tubes.

The main observations may be summarised as follows:

- (a) Velocity in fire-row tubes upwards and increasing to a maximum of 4 feet/sec. for 0.2 lb/ft²/hr. fuel and then falling to 2.5ft/sec. at 1.2 lb/ft²/hr.
- (b) Velocity in outside row is downwards and has practically constant value of 0.6ft/sec.
- (c) Feed changes effect circulation : sudden change at high rating gave reduced flow in front row tubes, and in some cases complete reversal to about 2.5ft./sec. downwards.
- (d) Reverse flow once established persisted until firing rate reduced to low value.
- (e) No method discovered for producing reversal of flow at will.

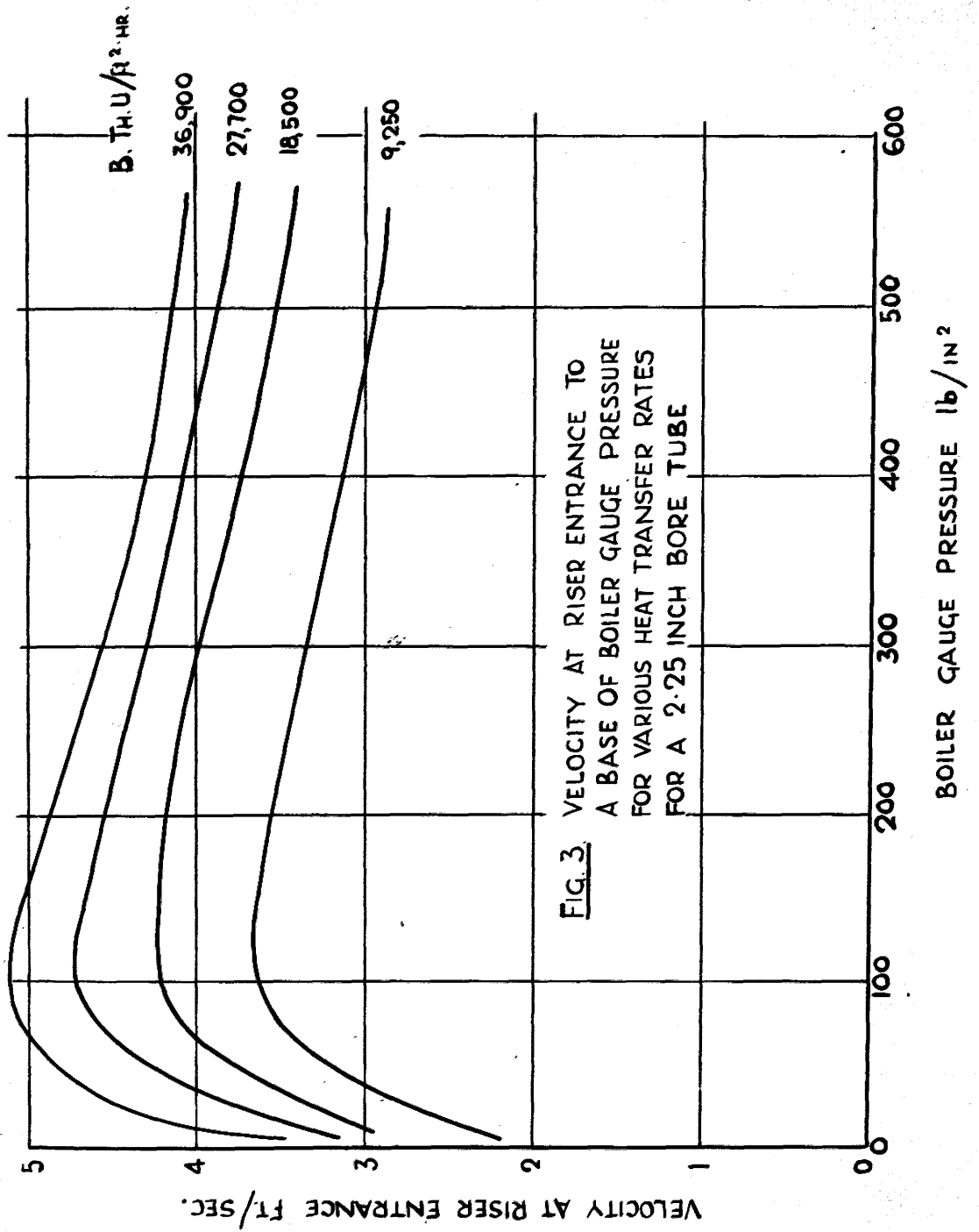
In later work, Dight stated the belief that fire-row tubes were the critical factor in forcing, and introduced the circulation augmentor, increased the diameter of fire-row tubes, added water walls, and fitted external downcomers to improve condition in front-row tubes.

Schmidt, Schurig, and Behringer (1933) carried out tests on an experimental two-tube boiler. The plant consisted of a steam and water drum connected by two vertical tubes of dimensions approximating to those obtained in normal boiler plant. One tube (the riser) was heated by conduction from metallic heating elements lying along the outer tube wall. The steam generated was condensed in a condenser operating at boiler pressure immediately above the steam drum, and from the condenser heat balance the steam generated was estimated. The circulation in the boiler was determined using a calibrated orifice at the foot of the downcomer.

Figure 3 which shows the circulation velocity to a base of boiler pressure for various heating rates, is representative of the data obtained. Sufficient data is not supplied, however, to enable the formulation of theory.

Further tests were carried out to investigate tube wall friction forces, and the effect of "relative velocity". These are dealt with later.

Lowenstein (1946) carried out tests on a gas fired two-tube boiler with an inclined riser tube and a vertical downcomer. The maximum pressure and heating rates were 1,100 lb/in². and 91,500 B.Th.U/hr. ft.².



A limited number of tests were carried out to determine the variation of circulation velocity with pressure and heat input.

Considerable testing was carried out to determine conditions producing tube rupture.

Schwab 1947 and Petersen and Baldina 1949. Both these papers use test results obtained at the Central Boiler and Turbine Research Institute in Russia. No details of the experimental layout are given. The experimental values given are mass flow, quality, and pressure drop over lengths of vertical tubes where steam water mixtures flow adiabatically. Some of the test results are given later.

Discussion.

The previous experimental work divides itself into three main categories, namely experimental work on model boilers, full-scale multi-tube boilers and full-scale two-tube boilers.

So far it has been found impracticable to obtain complete similarity between model and full-scale boilers. Results obtained from a model boiler are, therefore, useful only in so far as they may show general trends.

The disadvantage of experimental work on multi-tube boilers is the difficulty in determining the precise conditions under which individual tubes operate. In view of this, the full-scale two-tube boiler, when the tubes' length and diameters are of the same order as met with in multi-tube/

multi-tube boilers, offers the most satisfactory method of studying the mechanics of flow.

Both Schmidt's and Lowenstein's plant conform to the above requirements. Unfortunately Schmidt's and Lowenstein's published results are neither given nor analysed in sufficient detail to permit the formulation of an adequate circulation theory. On the other hand, the results quoted by Schwab and Petersen are given in sufficient detail. A number of these results are analysed later.

2. HYDRODYNAMIC THEORIES ASSUMING HOMOGENEOUS FLOW.

As already mentioned, early experimental work established many important factors influencing circulation. Nevertheless it was many years later that the first detailed paper on the determination of circulation velocity was published.

Lewis and Robertson (1940) presented the detailed solution of the circulation velocity where the mixture of steam and water in a heated tube is assumed homogeneous.

A U-tube circuit is examined (Figure 4) and the equations developed for the particular case of uniform heat distribution over the heated length.

The first step is to determine the point at which evaporation occurs, this point being referred to hereafter as the "point of evaporation". Evaporation does not necessarily commence where heating begins, as the temperature at this point may be below saturation temperature. The introduction of cold feed produces such an effect.

The average density over the heated section is shown to be

$$\frac{1}{q \left(\frac{1}{\rho_g} - \frac{1}{\rho_L} \right)} \text{Log}_e \left(1 + q \frac{\rho_L - \rho_g}{\rho_g} \right)$$

where q is the dryness fraction at the top of the heated length.

The "driving head" producing circulation is due to the difference in density between the heated and unheated tubes/

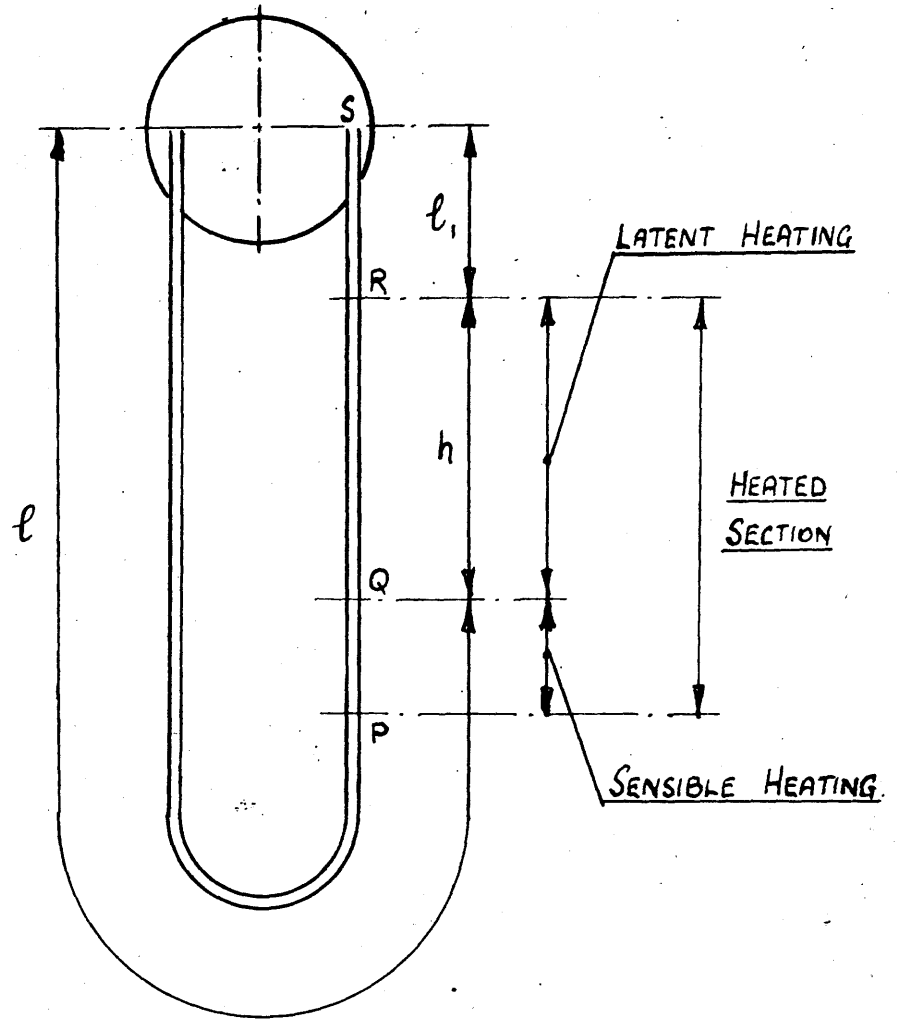


FIG. 4. U-TUBE CIRCUIT.

tubes, and is evaluated in feet of water

This is

$$(h + \ell_1) - \frac{h}{q \left(\frac{\rho_L - \rho_G}{\rho_G} \right)} \text{Log}_e \left(1 + q \frac{\rho_L - \rho_G}{\rho_G} \right) - \frac{\ell_1}{1 + q \frac{\rho_L - \rho_G}{\rho_G}}$$

for the circuit shown in Figure 4. No "driving head" is obtained from the liquid below the level of point Q, as the density is the same in both columns.

The driving head produces motion round the circuit, the theoretical circulation velocity being that velocity of flow at which the driving head balances the circuit losses.

Those losses will be

- (a) Entry losses to the downcomer.
- (b) Friction losses.
- (c) Losses due to the acceleration of
the expanding mixture in the heated length.

Evaporation with pressure decrease along the riser length is neglected.

The entry loss is assumed $\frac{1}{2} \cdot \frac{U^2}{2g}$ where U is the velocity at entry to the downcomer.

The friction loss from the top of the downcomer to the point of evaporation is

$$\frac{\lambda \cdot \ell \cdot U^2}{2 \cdot q \cdot d}$$

The friction loss over the heated length is shown to be

$$\frac{\lambda \cdot h \cdot U^2}{2 \cdot q \cdot d} \left(1 + \frac{q}{2} \cdot \frac{\rho_L - \rho_G}{\rho_G} \right)$$

Changes in steam and water densities are neglected.

The friction loss over the length RS is

$$\frac{\lambda \cdot \ell_1 \cdot U^2}{2 \cdot g \cdot d} \left(1 + q \frac{\rho_L - \rho_G}{\rho_G} \right)$$

The friction factor λ is assumed throughout the heated and unheated lengths to be 0.02.

The momentum, or acceleration, loss is

$$\frac{U^2}{\rho_G \cdot g} (\rho_L - \rho_G) q$$

The water is given its kinetic energy $\frac{U^2}{2g}$ at entry to the tube. This kinetic energy is treated as a loss as it is assumed to be dissipated as heat at exit from the tube.

As the driving head balances the circuit losses

$$\begin{aligned} (h + \ell_1) - \frac{h}{q \left(\frac{\rho_L - \rho_G}{\rho_G} \right)} \log_e \left(1 + q \frac{\rho_L - \rho_G}{\rho_G} \right) - \frac{\ell_1}{1 + q \frac{\rho_L - \rho_G}{\rho_G}} \\ = U^2 \left[\frac{3}{4g} + \frac{\lambda}{2g \cdot d} \left\{ \ell + h \left(1 + \frac{q}{2} \cdot \frac{\rho_L - \rho_G}{\rho_G} \right) + \ell_1 \left(1 + q \frac{\rho_L - \rho_G}{\rho_G} \right) \right\} \right. \\ \left. + \frac{q}{g} \cdot \frac{\rho_L - \rho_G}{\rho_G} \right] \end{aligned}$$

The circulation velocity U may be determined from this expression although a trial and error procedure is necessary as q is dependent on U .

Van Brunt (1941) The theory detailed by Lewis and Robertson, and developed for the simple case of a U-tube boiler is applied to the analysis of flow in a multi-tube high pressure boiler.

In addition, the effect of various heat transfer distributions on the available driving head is considered.

He/

He considers five different cases

- (a) Mean density based on heat absorption proportional to the square root of the length.
- (b) Mean density with 60% of heat absorbed in bottom half.
- (c) Mean density with 50% of heat absorbed in bottom half.
- (d) Mean density for uniform absorption.
- (e) Arithmetic mean density.

The variation in the driving head for the five methods is considerable.

Markson, Ravese and Humphreys (1942), Midtlyng (1942) and Ledinegg (1944) develop theories similar to Lewis and Robertson. The essential difference is in the method of solution.

Baker (1950) applied theoretical equations similar to those of Lewis and Robertson to the analysis of flow in an Admiralty 3-drum boiler.

As the equations are now applied to a multi-tube bank the form of the equation used by Lewis and Robertson cannot be applied directly.

The pressure change over each tube in the bank is determined for a number of assumed flows and graphed as shown in Figure 5. The pressure change is determined in feet of water, and is referred to as the depression head. This head is, in effect, the head obtained experimentally on an overall gauge, but duly corrected for density.

The/

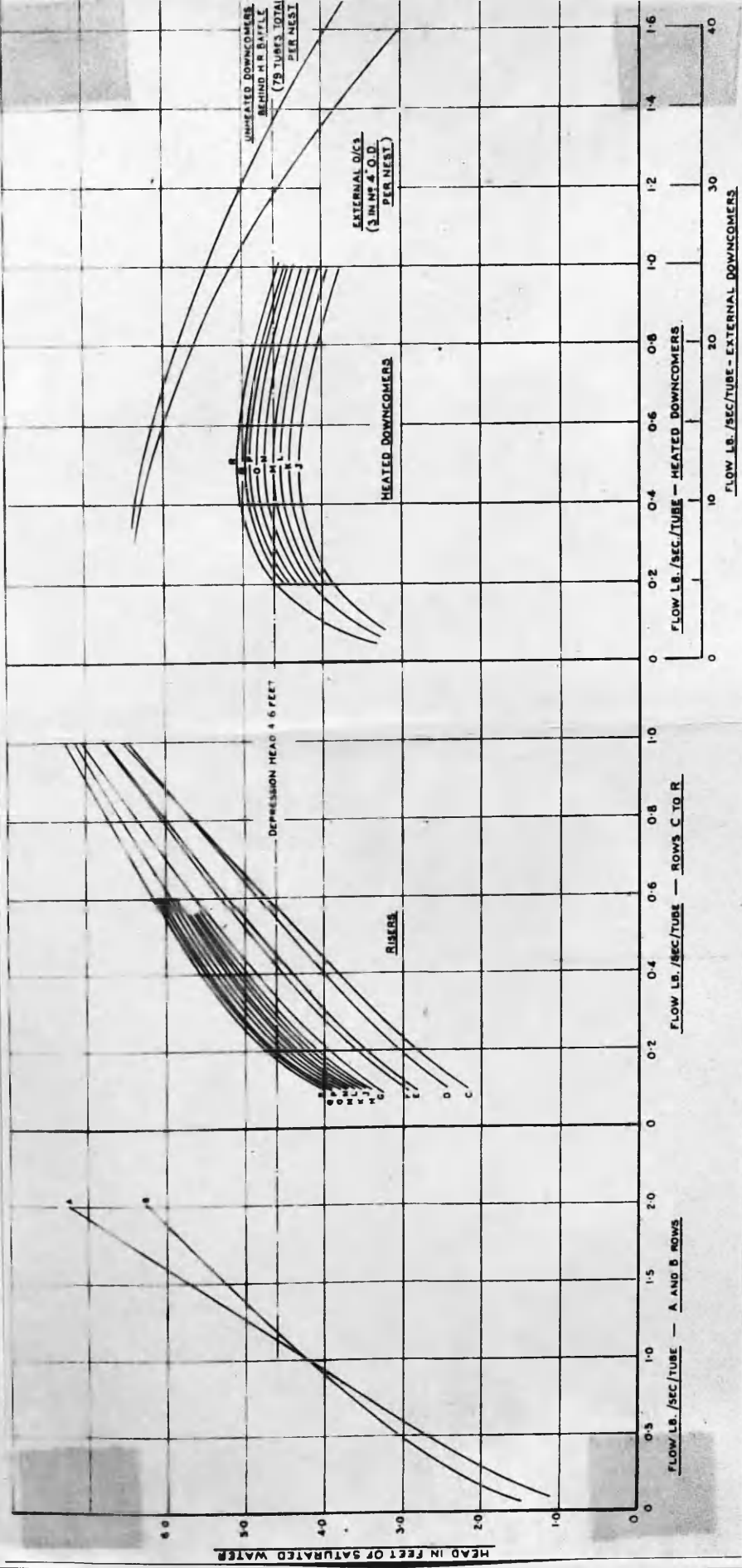


Fig. 5. Determination of flow in multi-tube banks (Baker).

The conditions to be satisfied by the circulation are that the downward flow must equal the upward, and that the pressure change over each tube in the bank must be the same, namely the pressure difference between the drums. By trial and error, the pressure change at which the downward flow balances the upward is obtained. The mass flow in each tube is then known.

Davis and Timmins (1933) dealt with the problem of flow in multi-tube banks in a similar manner.

Discussion.

It must be remembered that while this particular section of the review deals with homogeneous theories of circulation, the greater part of the theoretical approach is of a general nature. The assumption of homogeneous flow affects only the following:

- (a) The density determination during steam-water mixture flow.
- (b) The determination of friction during steam-water flow.
- (c) The determination of acceleration forces.

The point open to criticism in the majority of the papers referred to, in addition to the assumption of homogeneous flow, is that resistances and driving heads are evaluated in feet of water. During flow of an incompressible fluid there may be much to gain by such a procedure. There is little to gain where the fluid is compressible. It may, in fact, lead to misunderstanding.

For/

For example, there are instances where the energy per pound of mixture flow (i.e. ft. lb./lb.) has been treated as feet of water.

3. DETERMINATION AND EFFECT OF THE STEAM
VELOCITY RELATIVE TO THE WATER.

Where a steam-water mixture flows in a tube the apparent or effective density of the mixture is considerably increased if the steam moves relative to, and faster than, the water. It follows that in inclined boiler tubes the available driving head will be reduced by any relative movement with reduction in the boiler circulation.

Schmidt, Schurig and Behringer (1933) carried out tests to find the steam velocity in a stationary column of water in a vertical tube.

The steam bubbles were generated at an electric heating element at the foot of the tube, and the quantity of steam flowing estimated from the electrical heat input.

The pressure gradient in the tube was measured, and on the assumption that the pressure gradient was due only to the weight of the steam and water, the velocity of the steam bubbles was calculated. The results are shown in Figure 6.

Tests were then carried out on the two-tube boiler previously described. A liner was fitted inside the riser tube, and weighed to determine the friction drag on the wall of the tube. The results were not satisfactorily analysed, although it is of interest to note that with a "stationary" column of water, an upward flow of steam bubbles, and low steam contents, there was a noticeable downward drag on the tube.

Tests/

Behringer's Experimental Results.

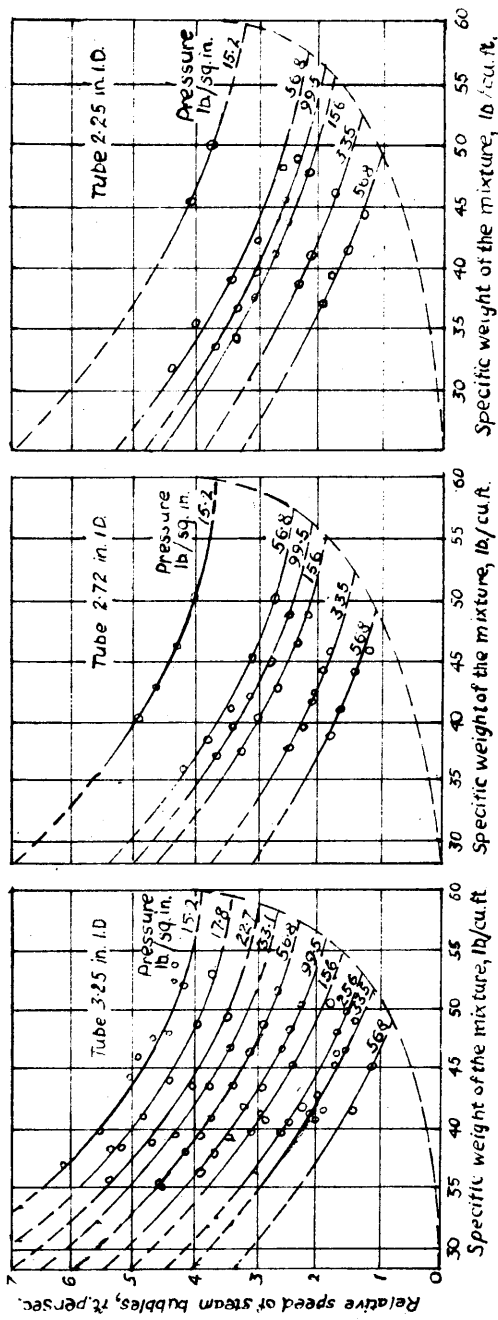


Fig. 6 — Relative velocity of steam in tubes of 3.25 in., 2.72 in. and 2.25 in. i. d. for various pressures in relation to the specific weight of the mixture.

Tests using steam and water had eventually to be abandoned due to serious fluctuations, and extensive tests were then carried out with air and water.

The final conclusion was that the relative velocity during flow of the water column is considerably greater than with a stationary column.

Nothman and Binder (1943) studied the effect of the relative velocity (slip) by determining the effective density for assumed relative velocities over a range of pressure.

Figure 7 shows the effect of the relative velocity on the available pressure difference, or driving head, based on the assumption that the mixture circulates in a U-tube circuit in which the downcomer contains water only, while the riser contains a mixture, the quality of which varies uniformly from 0 at the bottom to q at the top.

The quality q at any point is related to the effective density ρ in the expression

$$q = \frac{1 + K' \cdot \frac{\rho - \rho_g}{\rho_L - \rho_g}}{1 + \frac{\rho_L}{\rho_g} \cdot \frac{\rho - \rho_g}{\rho - \rho_L}}$$

where K' is the ratio of the steam relative velocity to the velocity in the downcomer.

The general conclusion was that the relative velocity can have an important effect on the effective density, but that to date it was not possible to predict the actual magnitude of the relative velocity or the effective density.

Petersen and Baldina (1949) analysed test results for the/

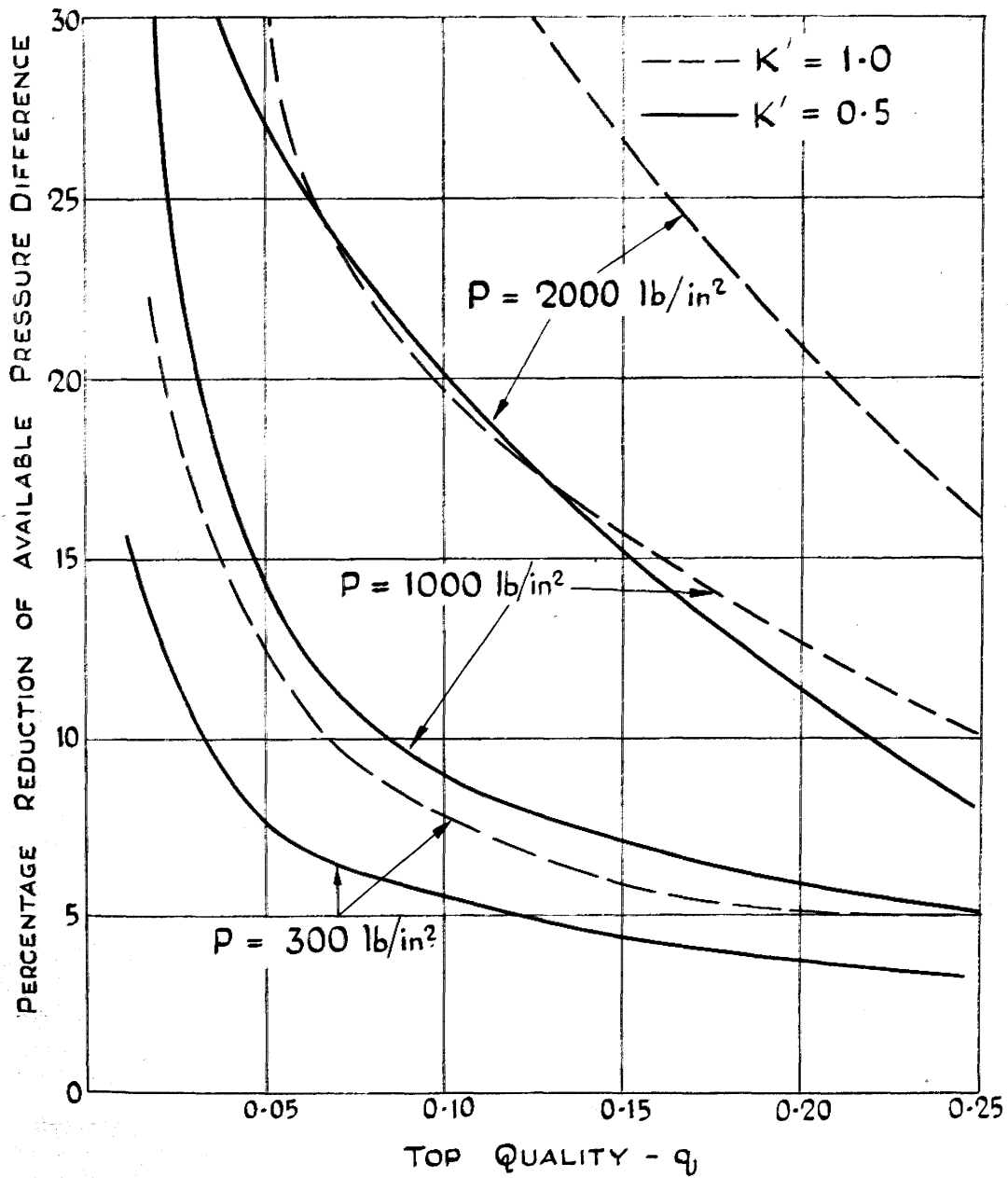


FIG. 7. EFFECT OF SLIP ON AVAILABLE PRESSURE DIFFERENCE

the vertical flow of steam-water mixtures by dimensional analysis.

The most important dimensionless quantities influencing flow are

$$(1) \frac{U_o''}{U_o'} \quad (2) \frac{\rho_g}{\rho_L} \quad (3) Fr \quad (4) \frac{e}{r}$$

where U_o'' and U_o' are the steam and water velocities when each occupies the total tube cross-section.

ρ_g and ρ_L are the steam and water densities respectively, Fr is Froude's Number based on the water velocity U_o' (i.e. $\frac{U_o'^2}{g \cdot d}$) and $\frac{e}{r}$ is the relative roughness coefficient of the tube.

Tests with horizontal tubes indicate that the normal friction equation assuming homogeneous flow holds within 20%. This formula is assumed to hold for vertical tubes.

The pressure change due to the mixture weight over a vertical tube length was obtained by subtracting the friction pressure change calculated assuming homogeneous flow from the experimental pressure change. From the mixture weight pressure change the ratio of the steam to tube cross-sections was determined. The ratios calculated are shown in Figure 8 to a base of U_o''/U_o' for various Froude's Numbers and for a boiler pressure of 150 lb/in² gauge. It should be noticed that the denominator of the base ratio is U_o' , the velocity of the water before evaporation commenced. This is a matter of convenience U_o' and U_o having similar magnitudes. As the tests were carried out at constant pressure and tube roughness, ρ_g/ρ_L and e/r do not influence/

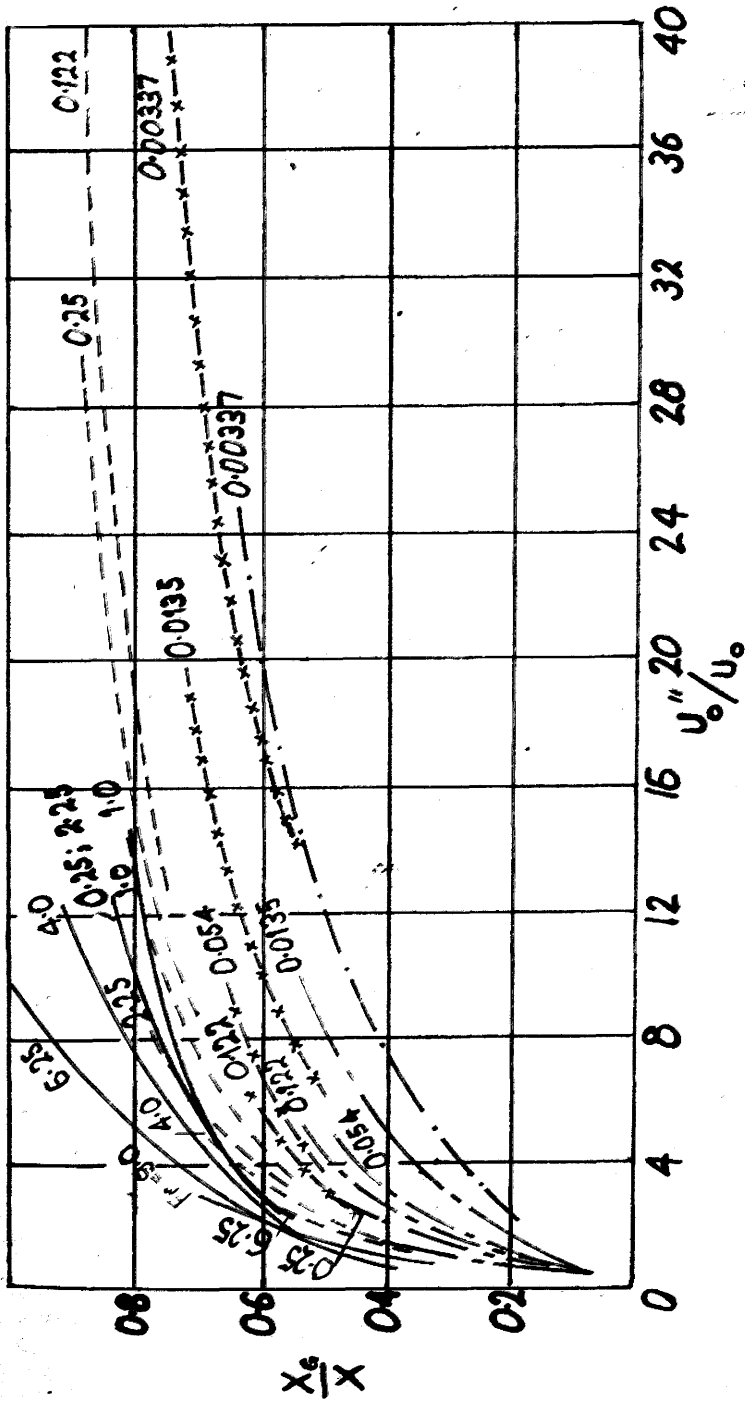


Fig. 8. Steam to tube cross-sectional ratio (X_s/X) to a base of U''/U_o for various Froude Numbers and tube diameters at a pressure of 150 lb/in².

— 25.5 m.m. diameter. - - - 32.0 m.m. diameter.
 - - - 56.0 m.m. diameter. - x - x - 76.0 m.m. diameter.

influence the graph form.

It was considered that the curves obtained confirmed the choice of dimensionless parameters despite the slight variation with tube diameter, i.e. at any particular pressure,

$$\frac{X_G}{X} = \phi \left(Fr \cdot \frac{U_o''}{U_o} \right)$$

However, for a general solution, the density dimensionless ratio must be included, i.e.

$$\frac{X_G}{X} = \phi \left(Fr \cdot \frac{U_o''}{U_o} \cdot \frac{\rho_G}{\rho_L} \right)$$

"The most suitable method for practical purposes was the representation of this function as a correction coefficient for the tube bore occupied by steam at a basic pressure

$$\frac{X_G}{X} = \left(\frac{X_G}{X} \right)_o \cdot \Delta_p$$

where Δ_p is also a function $\frac{U_o''}{U_o}$ and Fr ".

The basic pressure was chosen as 32 atmospheres, and the variation of $\frac{X_G}{X}$ with respect to Fr and $\frac{U_o''}{U_o}$ is as shown in Figure 9.

The magnitudes of Δ_p are as obtained from Figure 10.

The effect of tube inclination is also allowed for in a similar manner as the correction for pressure, although the limited number of results used in obtaining the necessary curves limits their value.

Discussion.

Schmidt, in calculating the relative velocity for the tests/

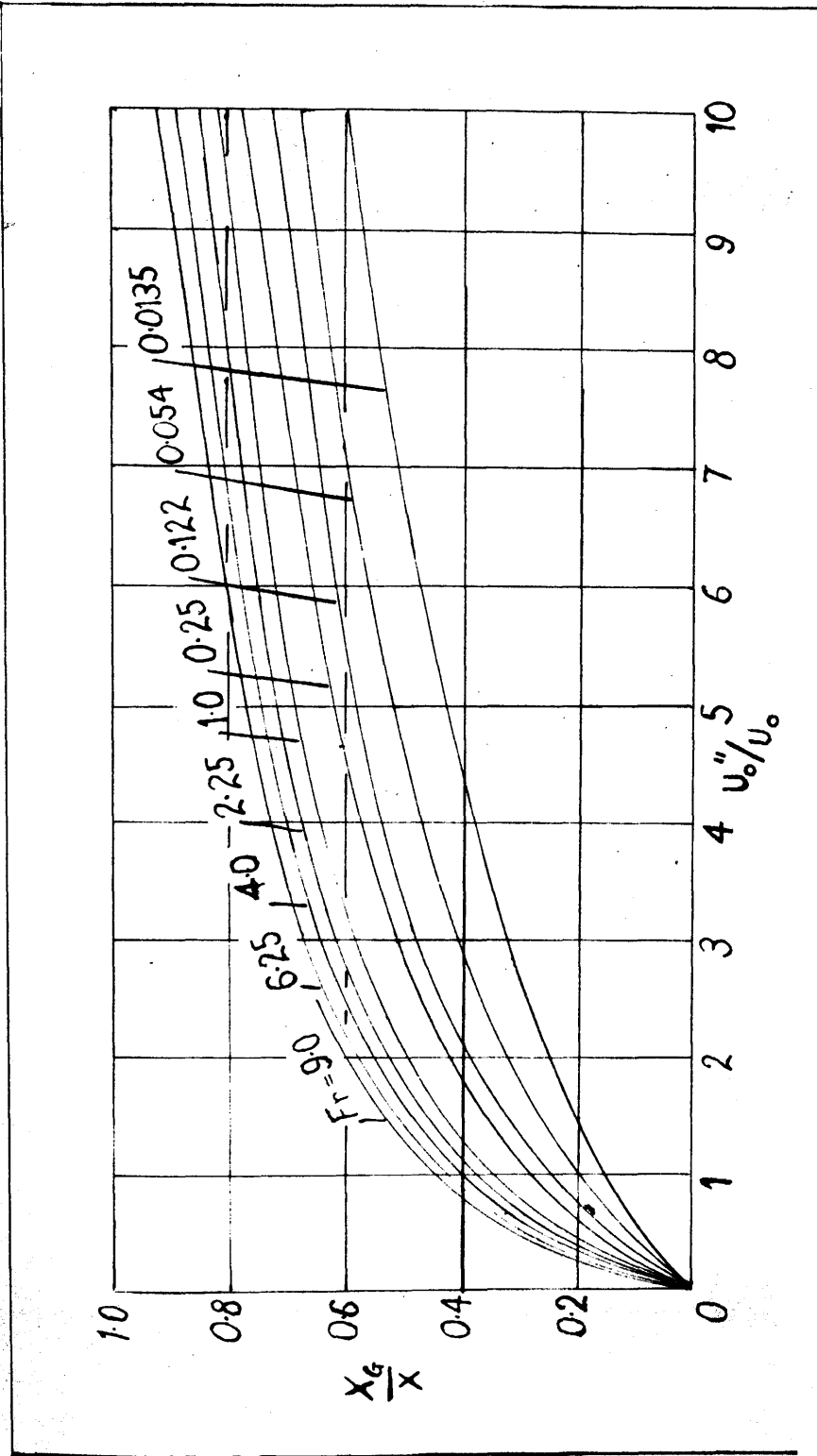


Fig. 9. Steam to tube cross-sectional ratio (X_g/X) to a base of U''/U_o for various Froude Numbers at a pressure of 32 atmospheres (influence of tube diameter neglected).

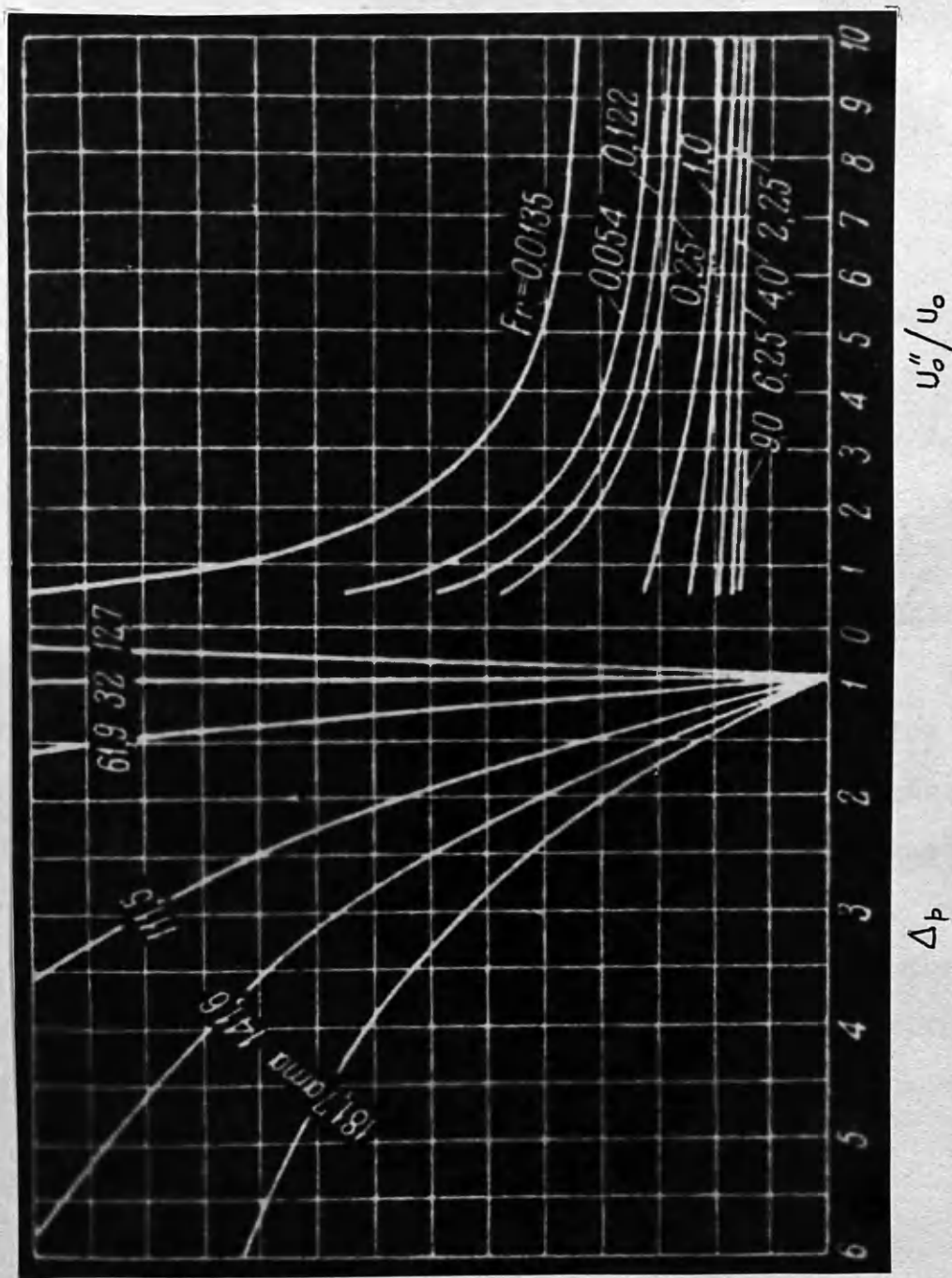


Fig. 10. The correction coefficient Δp as a function of U''/U_0 and Froude's Number for a series of pressures.

tests with a stationary water column, assumes the measured pressure gradient in the tube is due to the mixture weight only. But tests carried out by Schmidt with a liner tube, indicate that even where the water is stationary there is appreciable drag on the tube, hence it would appear that the pressure gradient is due to the combined effect of density and wall friction. This suggests that the relative velocities shown in Figure 6 are inaccurate.

Petersen and Baldina have made the most successful attempt to date in correlating results for the flow of steam-water mixtures. One disadvantage, however, is that the curves obtained are directly applicable only to cases where there are no momentum forces.

The friction equation used also detracts from the final curves obtained from the experimental data. It is assumed that the friction equation obtained for flow in horizontal tubes will be applicable to vertical tubes, an assumption which is hardly tenable when the increased relative velocities which will occur with vertical flow are considered.

These experiments also indicate conclusively that the assumption of a homogeneous mixture will give density values considerably different from the actual experimental values.

4. HYDRODYNAMIC THEORIES INTRODUCING
"RELATIVE VELOCITY".

Schwab (1947) in considering the flow of steam-water mixtures in vertical tubes, assumed the flow pattern to be that of a core of large steam bubbles with separating layers of water, and an annular ring of water as shown in Figure 11.

The friction pressure drop due to the flow of such a mixture was obtained by the following reasoning.

"The flow of water in the annular ring space is given by U , and hence it is possible to calculate with the aid of standard hydraulic formula the resistance to flow in all sections occupied by the steam bubbles,

$$\sum \delta p = \lambda \sum \frac{l'}{D} \cdot \frac{U^2}{2g} \cdot \rho$$

where λ is the coefficient of friction and D is the hydraulic diameter of the annular flow area.

Assuming that frictional resistance takes place only at the solid surface and neglecting friction resulting between the water annulus and the steam, the hydraulic diameter may be expressed as 4 times the annular area divided by the wetted perimeter of the tube

$$D = \frac{4(d^2 - d_n^2)\pi/4}{\pi d} = d \left(1 - \frac{d_n^2}{d^2}\right) \quad "$$

The normal friction equation for homogeneous flow is used over the lengths where the core is occupied by water.

From these assumptions the pressure drop over a given length can be readily expressed symbolically. A solution, however, requires knowledge of the values of l'_1 , l'_2 and d_n . These values can be determined if the ratio of the water in the/

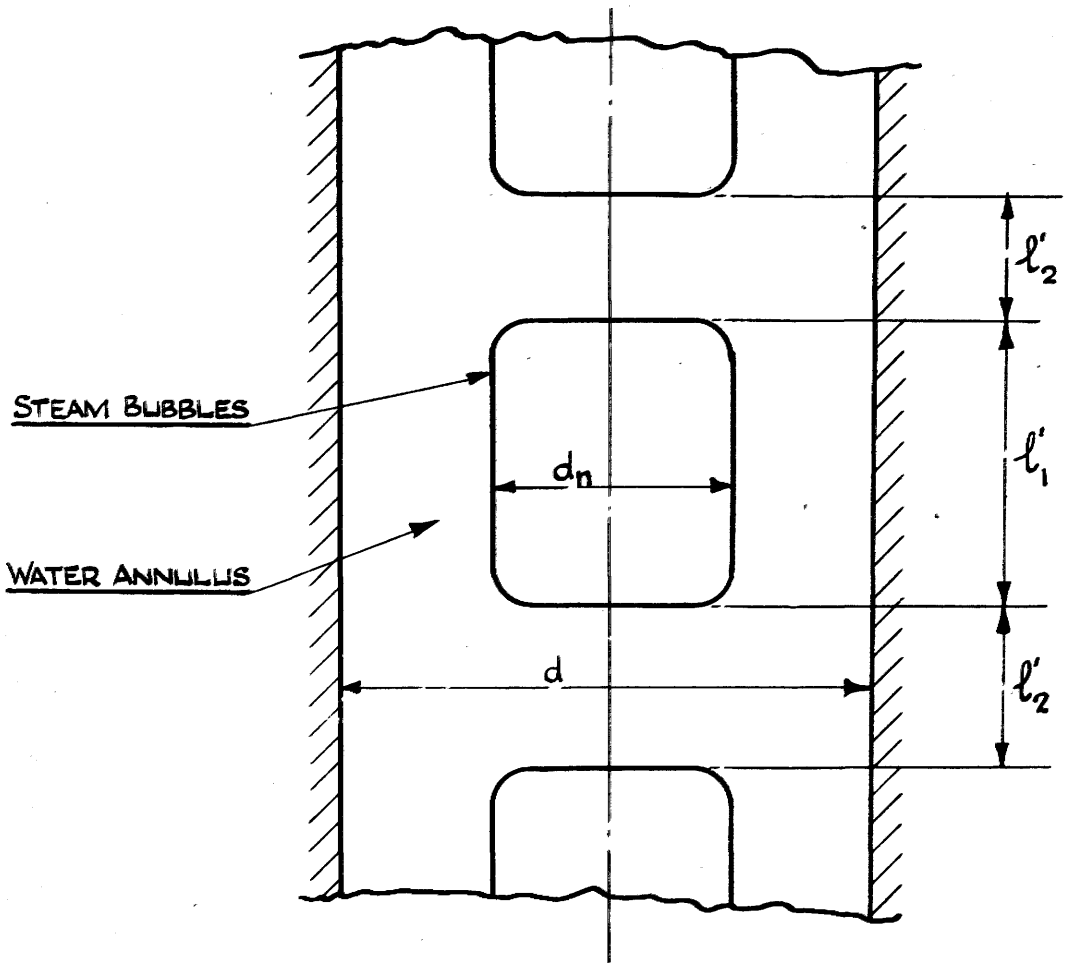


FIG. 11. FLOW FORM (SCHWAB).

the core to the total water flow, and the ratio of the core to annulus cross-sectional areas, are known.

The ratio of the water in the core to the total water flow is determined from the experimental results. The ratio of the core to annulus area is assumed to be that which will give the minimum pressure drop.

Very close agreement with the experimental results was obtained.

Waeselynck (1948) applied the experimental results obtained by Schmidt, Schurig, and Behringer for the flow of steam bubbles in stationary water columns. The theory is developed for the particular flow pattern where the central core is occupied by an emulsion consisting of water and steam bubbles with an annular ring of water.

Considering the equilibrium of a single bubble, the conventional equilibrium equation for a bubble under the force of gravity is

$$\bar{\pi} \cdot R^2 \cdot \frac{C'}{2g} \cdot \rho_2 \cdot (U_R)_i^2 = \frac{4}{3} \cdot \bar{\pi} \cdot R^3 (\rho_2 - \rho_g)$$

where R is the bubble radius,
 $(U_R)_i$ is the bubble velocity relative to the mean mixture velocity;

ρ_2 is the emulsion density,

ρ_g is the steam density,

and C' is a constant.

An interesting point is raised in that the relative velocity $(U_R)_i$ is not the value obtained by Schmidt, as Schmidt's/

Schmidt's value is the velocity of the bubble relative to the mean absolute velocity of the water. $(U_r)_1$ is the bubble velocity relative to the mean velocity of the mixture, where the mean velocity is defined as

$$U_m = \frac{X_L}{X} \cdot U_L + \frac{X_G}{X} \cdot U_G$$

X_L and X_G are the areas occupied by the liquid and steam, U_L is the mean liquid velocity, and U_G the steam velocity.

From this starting point it can be shown that

$$\frac{\rho_2}{\rho_L} \cdot U_r = U_0$$

where ρ_L is the liquid density,

U_r is the relative velocity obtained by Schmidt, and U_0 is a constant depending only on the pressure.

U_0 is the value of U_r obtained by extrapolating to the condition $\rho_2 = \rho_L$.

Graphs of the ratio of the core area to the tube area to a base of the ratio of the steam area to the tube area indicate that the theory is inapplicable at high steam contents. For example, at 100 lb/in² gauge a value of the ratio of steam to tube area of 0.7 gives a value of the ratio of core to tube area greater than unity, which is impossible.

By a series of graphs obtained by extrapolating Schmidt's results, the effective density of a steam water column can be determined .

The pressure drop during the flow of such a mixture due to friction is estimated in the following manner:

The/

The loss of head in an emulsion containing a large proportion of steam, can be calculated in the same manner as for a homogeneous fluid of the kinematic viscosity of water at saturation temperature, having the same mass flow as the emulsion, and a mean velocity U_m as defined above.

In the case of emulsions with relatively low steam contents, the equation approaches that of a homogeneous fluid with the kinematic viscosity of water at saturation temperature, and the emulsion density.

No indication of the accuracy of these friction equations or the range in which they are applicable is given.

Discussion.

The annulus hydraulic diameter used by Schwab in calculating the friction pressure change during two-phase flow is that which exists when there is no shearing force at the inter-face between the core and the annulus. The ratio of the core to annulus cross-sectional areas is assumed to be that which gives the minimum pressure drop. These assumptions are presumably the explanation of the large discrepancies found by Petersen on applying Schwab's theory to larger diameters (2 inches) than those tested by Schwab (1"inch). The error amounted to as much as 200% with a 2 inch diameter tube.

The theory developed by Waeselynck has the disadvantage that its theoretical basis is correct only for low steam contents and it may prove of considerable service under such conditions.

5. "THERMODYNAMIC" THEORIES OF
NATURAL CIRCULATION.

Silver (1946) considered the motive power of circulation to be due to the work done by the steam in expanding during formation. The expanding mixture was likened to that of a cylinder piston. No account was taken of any possible relative motion between the steam and water.

Davis (1948) expanded the above theory introducing the effect of relative velocity which was assumed to be that obtained by Schmidt with a stationary water column.

Heywood (1951) indicated that the thermodynamic equations give identical solutions to those obtained by the hydrodynamic equations.

Discussion.

The theories by Silver and Davis, while they may contribute to a clearer understanding of the driving force causing circulation, have been clearly shown by Heywood to be more laborious in application.

Heywood indicates the underlying unity of both theories, and it therefore, follows that due to its relative simplicity the hydromechanic theory is that to be recommended for use.

6. TWO-PHASE FLOW IN HORIZONTAL TUBES.

The first detailed paper on the flow of evaporating water through tubes was given by Bottomley (1936).

Throughout the theoretical development the steam and water mixtures were treated as a homogeneous fluid with the viscosity of the water content.

Benjamin and Miller (1942) and Allen (1951) used equations similar to those developed by Bottomley in indicating the method of designing piping to carry a "flashing" mixture of water and steam, as did Davidson and others (1943) in considering the flow of boiling water through heated coils at pressures in the region of from 500 to 3,300 lb/in.² and McAdams, Wood and Herman (1942) in analysing the flow of benzene-oil mixtures in tubes.

Both Davidson and McAdams evaluated the apparent friction factors during flow, and assumed that the discrepancies in the friction factors from the values expected were due to the velocity of the steam relative to the water.

Martinelli and others (1944) carried out an extensive experimental and theoretical investigation into the isothermal flow of two-phase mixtures through horizontal tubes.

Experimental readings consisted of the phase mass flows and pressure drops plus visual and photographic observations.

Tests were carried out with air and the following liquids, water, kerosene, diesel fuel, benzene, water plus nekal, and

water plus kemenol. The addition of nekal and kemenol enabled the effect of liquid surface tension to be investigated.

It/

It was observed that if increasing quantities of air are introduced to a tube flowing full of water, the following types of flow successively occur:

- (a) Bubbling flow in which the air flows along the top of the tube in the form of bubbles.
- (b) Stratified flow in which the liquid flows along the bottom of the tube with a smooth surface, and the air above.
- (c) Wave flow, which is similar to stratified flow, except that the interface is disturbed by waves.
- (d) Slugging flow in which occasional frothy slugs pass rapidly along the tube.
- (e) Annular flow in which the liquid flows along the pipe wall while the gas fills the central core.

The liquid surface was covered with capillary waves.

At very low liquid flow rates, the type of flow changes directly from wave to annular, with no intermediate region of slug form.

The reduction of the water surface tension by adding nekal produces considerable foaming, flow pattern (a) being predominant. It is also of interest to note that this change did not alter the pressure drop recorded.

The analysis commences by assuming that the pressure drop will be the same in both phases, and that the pressure drop in each phase can be represented by the normal friction formula;

$$-\frac{dp}{dl} = \frac{\lambda_L \cdot U_L^2 \cdot \rho_L}{2 \cdot g \cdot D_L} \dots \dots \dots R1.$$

for the liquid phase, and

$$-\frac{dp}{dl} = \frac{\lambda_L \cdot U_L^2 \cdot \rho_L}{2 \cdot g \cdot D_L} \dots \dots \dots R2.$$

for the gas phase.

The symbols D_L and D_G represent the hydraulic diameters of the respective phases.

For a cylindrical flow pattern $\frac{\bar{\Pi}}{4} D^2 = X$ relates the hydraulic diameter to the cross-sectional area.

For a more complex cross-sectional area the following relationships may be written:

$$X_L = \alpha \left(\frac{\bar{\Pi}}{4} D_L^2 \right) \dots \dots \dots R3$$

$$X_G = \beta' \left(\frac{\bar{\Pi}}{4} D_G^2 \right) \dots \dots \dots R4$$

where α and β' are, in effect, the ratios of the actual cross-sectional areas of flow to the area of circles of diameters D_L and D_G respectively. Consideration of the gas flow indicates that the gas flow area is approximately circular at all times, so that β' may be considered unity.

The friction factors λ_L and λ_G may be expressed in the general Blasius form

$$\lambda_L = \frac{\left(\frac{\bar{\Pi}}{4} \right)^n \cdot C_L}{\left(\frac{M_L}{\alpha \cdot D_L \cdot \mu_L \cdot g} \right)^n} \dots \dots \dots R5$$

and

$$\lambda_G = \frac{\left(\frac{\bar{\Pi}}{4} \right)^m \cdot C_G}{\left(\frac{M_G}{D_G \cdot \mu_G \cdot g} \right)^m} \dots \dots \dots R6.$$

The various diameters are related

$$\alpha \cdot \frac{\bar{\Pi}}{4} D_L^2 + \frac{\bar{\Pi}}{4} D_G^2 = \frac{\bar{\Pi}}{4} d^2$$

$$\therefore \alpha D_L^2 + D_G^2 = d^2 \dots \dots \dots R7$$

where d is the pipe diameter.

Combining Equations R1, R2, R5, R6 and R7 gives

$$\left(\frac{dp}{dl}\right) = \left(\frac{dp}{dl}\right)_g \left[1 + \alpha^{0.25} \left(\frac{\mu_L}{\mu_g}\right)^{0.83} \left(\frac{\rho_L}{\rho_g}\right)^{0.416} \left(\frac{M_L}{M_g}\right)^{0.75} \right]^{2.5} \quad R8$$

where $\left(\frac{dp}{dl}\right)_g$ is the pressure gradient when the gas flows alone through the pipe. This is the form for the particular case of both phases flowing turbulently, where $C_L = C_G = 0.184$ and $n = m = 0.2$. Using this equation to analyse the experimental results a plot of $\alpha^{0.25}$ to a base of its multiplier in Equation R8 gave results lying with a scatter of $\pm 30\%$ about a mean line. By means of this mean curve it would then be possible to predict pressure drops during two-phase flow.

Armand (1946) carried out tests with air-water mixtures similar to those carried out by Martinelli. In addition the tube was weighed during the mixture flow, so making it possible to estimate the respective cross-sectional areas occupied by the phases. The pipe length, weighed, was joined by flexible piping to the remainder of the plant. If L represents the effective length, and if W_0 represents the weight when filled with liquid, and W the weight when the mixture flows, then

$$W_0 = X \cdot L \cdot \rho_L$$

and

$$W = X_g \cdot L \cdot \rho_g + X_L \cdot L \cdot \rho_L$$

Therefore

$$\begin{aligned} \frac{W_0 - W}{W_0} &= \frac{X \cdot L \cdot \rho_L - X_g \cdot L \cdot \rho_g - X_L \cdot L \cdot \rho_L}{X \cdot L \cdot \rho_L} \\ &= \frac{X_g}{X} \cdot \frac{\rho_L - \rho_g}{\rho_L} \\ &= \frac{X_g}{X} \end{aligned}$$

as ρ_G is small compared with ρ_L .

The results are shown in Figure 12. The vertical axis represents $\frac{W_0 - W}{W_0}$ and the horizontal axis the ratio (β) of the steam flow volume to the total volume.

In addition, tests were carried out to determine the distribution of the mixture throughout the cross-section. This was done by traversing the tube with a small sampling tube, and, at exit, by cutting up the stream by knives and measuring the content in various cross-sections. From this work the following four fundamental flow patterns were defined:

- (a) The water wets fully the tube walls. The central portion of the water carries in it air bubbles non-uniformly distributed over the cross-section.
- (b) The water flows in the lower, and the air in the upper part of the tube.
- (c) The water forms a film on the wall, the air flowing in the central portion of the cross-section.
- (d) The same type of flow as (c) but the air entrains with it small water droplets. The water is distributed uniformly throughout the air.

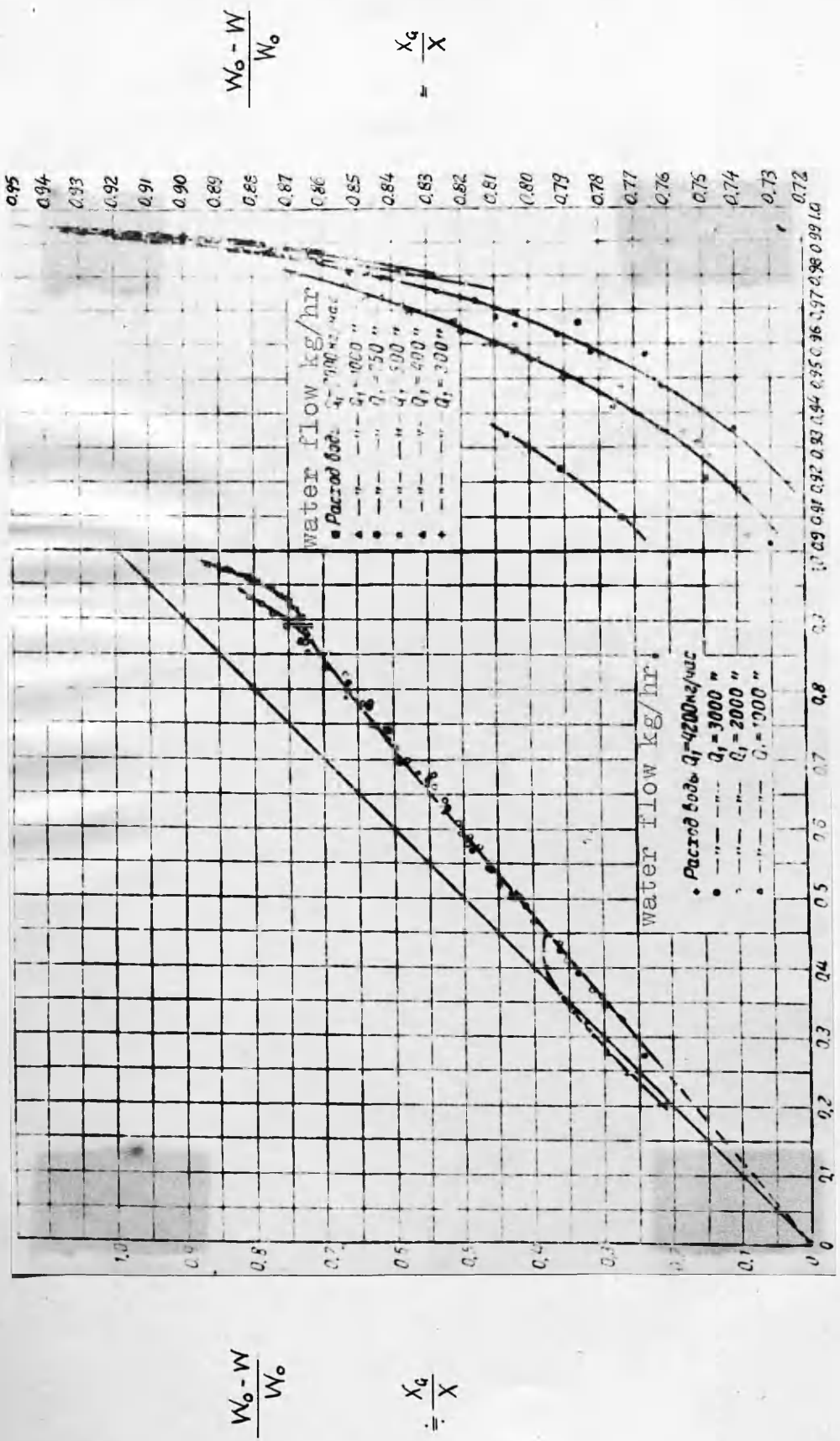
The analysis was developed along the following lines. The particular case of annular flow was considered.

The equations utilised are

$$M_L = 2\pi \cdot \rho_L \cdot \int_0^\delta U_i (r-y) dy$$

where δ equals the thickness of the water film on the wall and where

$$U_i = A \left(\frac{T_0 \cdot g}{\rho_L} \right)^{4/7} \cdot \left(\frac{g \cdot y}{\mu} \right)^{1/7}$$



β

Fig. 12. Ratio of the air to tube cross-sectional area to a base of air to total flow volume. Schwab. Tube 26 m.m. diameter.

$$\frac{W_0 - W}{W_0}$$

$$= \frac{X_g}{X}$$

$$\frac{W_0 - W}{W_0}$$

$$= \frac{X_g}{X}$$

A is a numerical constant.

Equilibrium of an element of length of the mixture gives

$$2\hat{u} \cdot r \cdot T_0 \cdot \delta l = \hat{u} \cdot r \cdot \delta p$$

and the geometry of the flow pattern gives

$$s = r \left(1 - \sqrt{\frac{X_G}{X}}\right)$$

Combining the above equations gives

$$\frac{dp}{dl} = \left(\frac{dp}{dl}\right)_0 \frac{A'}{\left(1 - \sqrt{\frac{X_G}{X}}\right) \left(1 + \frac{8}{7} \sqrt{\frac{X_G}{X}}\right)^{1/4}}$$

where $\left(\frac{dp}{dl}\right)_0$ is the pressure gradient if the liquid occupied the tube cross-section alone, and A' is a numerical constant.

This equation, which was developed for the particular case of annular flow, was further simplified to the form

$$\frac{dp}{dl} = \left(\frac{dp}{dl}\right)_0 \frac{A'}{\left(1 - \frac{X_G}{X}\right)^n} \quad R9$$

The value of A' and n were found to vary with the ratio $\frac{X_G}{X}$, the experimental pressure drop results giving the following:

$$\frac{X_G}{X} = 0 \text{ to } 0.65 \quad \frac{dp}{dl} = \left(\frac{dp}{dl}\right)_0 \frac{1}{\left(1 - \frac{X_G}{X}\right)^{1.42}}$$

$$\frac{X_G}{X} = 0.65 \text{ to } 0.9 \quad \frac{dp}{dl} = \left(\frac{dp}{dl}\right)_0 \frac{0.478}{\left(1 - \frac{X_G}{X}\right)^{2.2}}$$

$$\frac{X_G}{X} = 0.9 \text{ to } 0.99 \quad \frac{dp}{dl} = \left(\frac{dp}{dl}\right)_0 \frac{1.73}{\left(1 - \frac{X_G}{X}\right)^{1.64}}$$

To enable the prediction of $\frac{X_G}{X}$ an expression was developed as follows:

The air flowing in the core is assumed to obey the same friction law as in the case of flow inside a tube, i.e.

$$-\frac{dp}{dl} = \frac{\lambda (U_G - U_b)^2 \cdot \rho_G}{2 g \cdot d \sqrt{\frac{X_G}{X}}}$$

and it is finally shown that where $\frac{X_G}{X} > 0.72$ (or $\beta > 0.9$)

$$1 - \frac{X_G}{X} = \frac{4 + \frac{7}{8} m}{5 + m \left(\frac{\beta}{1-\beta} + \frac{8}{7} \right)}$$

where β is the ratio of the air volume content to the total volume of flow and where

$$m = 4 a \cdot Re^{\frac{1}{8}} \sqrt{\frac{\rho_G}{\rho_L}}$$

and where from the experimental results

$$a = 0.69 + (1-\beta)(4 + 21.9\sqrt{Fr}) \dots \dots \dots R10$$

The equations give satisfactory agreement with the extensive experimental data obtained.

Armand (1947) in the following year applied his theory, used in the air-water experiments, to the analysis of steam-water flow in horizontal rough tubes. The friction factor λ was 0.026. The term $1 - \frac{X_G}{X}$ was evaluated where $\beta > 0.9$ using Equation R10 and where $\beta < 0.9$ by the expression

$$\frac{X_G}{X} = c \cdot \beta$$

where $c = 0.833 + 0.05 \log_e p$ and where p is the pressure in Kg/m^2 .

The results on analysis gave the following forms of Equation R9.

$$-\frac{X_G}{X} = 0 \text{ to } 0.55 \qquad \frac{dp}{dl} = \left(\frac{dp}{dl} \right)_0 \frac{1}{\left(1 - \frac{X_G}{X} \right)^{0.5}} \dots \dots \dots R11$$

$$\frac{X_G}{X} > 0.55$$

$$\beta < 0.9$$

$$\frac{dp}{dl} = \left(\frac{dp}{dl}\right)_0 \frac{0.48}{\left(1 - \frac{X_G}{X}\right)^n} \dots \dots \dots R12$$

where $n = 1.9 + 1.48 \times 10^{-3} p$.

A variation in pressure from 10 to 180 atmospheres varies n from 1.9 to 2.17.

For β greater than 0.9 the most satisfactory correlation was obtained with the formula

$$\frac{dp}{dl} = \left(\frac{dp}{dl}\right)_0 \frac{0.025 \beta + 0.005}{(1 - \beta)^{1.75}} \dots \dots \dots R13$$

Equations R.11 to R.13 enable the prediction of the pressure gradient due to friction during the horizontal flow of steam-water mixtures with considerable accuracy. The majority of the results are within $\pm 20\%$.

Burnell (1947) dealt with steam-water mixtures flowing adiabatically through pipes where the pressure at exit was normally the critical pressure. Analysing the test results by the method detailed by Bottomley, considerable discrepancy was obtained between the theoretical and experimental critical pressure, and the theoretical and experimental mass flows. The theoretical mass flows were lower, and the pressures higher than those measured.

Burnell showed that this discrepancy could only be due to the wrong assumption that the steam and water moved with the same velocity. He showed that for certain tests the steam velocity must be approximately twice that of the water.

Bergelin/

Bergelin and Gazley (1949) continued the work of Martinelli. The paper is primarily devoted to stratified flow, where the liquid occupies the lower and the gas the upper part of the tube.

During experiments on stratified flow "the interfacial position was measured by connecting a calibrated height gauge across opposed pressure taps located on the top and bottom of the section."

The interfacial measurement indicated that in particular circumstances there was a change in the respective cross-sectional areas occupied by the phases along the length of the tube. It follows that there will be an exchange of kinetic energy between the phases, a condition not allowed for in Martinelli's theoretical development nor in other theoretical developments to date.

Analysis showed considerable discrepancy between theoretical (Martinelli) and experimental results, the error being as great as 100%.

Bergelin, Kegel, Carpenter and Gazley (1949) carried out tests with air-water mixtures flowing vertically downwards. The conditions at entry to the pipe were such that the liquid flowed along the wall. The data, compared with values based on Martinelli's Theory, showed a scatter of 30%. The trend of the experimental results, however, was counter to that expected from the theoretical development, suggesting that all relevant factors had not been considered.

Application/

Application of the theory to vertical tube condensers with a wide range of condensing vapour gave a maximum error of 142%.

Linning (1952) carried out tests similar to those carried out by Burnell, but with considerably smaller tube diameters. Burnell's tests were carried out with tubes from $\frac{1}{2}$ to $1\frac{1}{2}$ inches diameter. Linning tested with tubes of 0.128 inches bore and 0.06 inches bore.

A theory is developed for the cases of annular and stratified flow, and introduces the effect of variation in velocity between the steam and water.

The method of obtaining the ratio of the steam and water velocities is by equating the following equations:

- (a) Steam phase continuity.
 - (b) Water phase continuity.
 - (c) Overall momentum.
 - (d) Liquid momentum.
 - (e) Overall energy.
 - (f) Steam phase energy.
- and (g) Relation of water velocity to interface velocity.

The friction pressure drop is assumed calculable by the normal equation, where the velocity used is that of water, and where the friction factor is that corresponding to a Reynolds Number based on the water velocity, density, and viscosity, and on the tube diameter. Satisfactory agreement between theoretical and experimental results is obtained over/

over the limited pressure range investigated by the author.

Discussion.

The experimental results and analysis of Armand, Burnell and Linning indicate conclusively that considerable error is involved in the assumption of homogeneous flow. The steam velocity is considerably greater than the water velocity.

The theories developed to date to include the effect of this relative velocity are either applicable to a restricted set of conditions, or are based on untenable assumptions.

Martinelli's, theory falls within the first category. Martinelli, in effect, relates the liquid hydraulic diameter to the respective phase mass flows, densities and viscosities, the relationship being obtained from results with horizontal tubes. This relationship, will however only hold under the above conditions. For example, inclining the tube will increase the velocity of the gas relative to the liquid with a consequent change in the liquid hydraulic diameter. This is a possible explanation of the large divergence obtained by Bergelin on comparing experimental results for vertical tubes with theoretical results based on Martinelli's theory.

The experimental work and analysis of Armand is exemplary, although the formula proposed for the determination of the ratio of the steam to tube cross-sectional area is not in a form applicable to inclined tubes or to flow where inertia forces occur.

The/

The theory developed by Linning has already been criticised in a contribution to his published paper.

7. GENERAL DISCUSSION.

During the flow of steam-water mixtures through horizontal or inclined tubes the work of many experimenters indicates that the steam moves relative to the water. Petersen and Baldina show that this relative velocity is of such a magnitude that the effective density of the steam-water mixture is appreciably influenced.

Therefore, theories of circulation, such as that of Lewis and Robertson, based on the assumption of no relative movement, will give inaccurate results. A satisfactory theory of circulation will require consideration of the effect of relative velocity. This will affect the density, the momentum forces, and tube friction.

The problem is primarily the theoretical determination of the relative velocity. The theoretical development should be made on a basis which allows for the influence on the relative velocity of the following important considerations:

- (a) The effect of momentum forces.
- (b) The effect of tube inclination.
- (c) The effect of tube roughness.

Of the papers published to date, those by Schwab and Linning are the only theories which would appear to satisfy the above important considerations. Schwab assumed that in the flow of steam-water mixtures through vertical tubes, the flow velocities were such as to give the minimum pressure drop over the tube. This assumption has no theoretical foundation.

Linning/

Linning in developing his theory, introduces an error into his steam phase energy equation. Developed correctly it will no longer be independent of the equations used in determining the velocity ratio.

It may be said in conclusion that as yet no theory has been developed on a sufficiently broad basis to enable its application to the various conditions of flow met with in boiler practice.

In the theory developed in the following sections an attempt has been made to fill this gap.

PART II.THE PROPOSED THEORY FOR THE DETERMINATION
OF PHASE VELOCITIES DURING TWO-PHASE FLOW.

	<u>Page</u>
8. Mode of flow	51.
9. Ratio of the gas to liquid velocity	55.
10. Approximate form of the gas to liquid velocity ratio	59.
11. Shearing stress ratio τ_2/τ_1	63.
12. Distortion of the annulus profile	67.
13. Effect of heat transfer on flow conditions	72.
14. Flow in downcomers	74.

INTRODUCTION.

One of the main difficulties in developing satisfactory relationships enabling the prediction of pressure changes during two-phase flow is the present lack of knowledge regarding the respective phase velocities. The following sections contain the development of the fundamental relationships governing these velocities.

8. MODE OF FLOW.

The experimental work of Armand indicates that during the flow of a liquid and a gas, or a liquid and a vapour, through a horizontal tube there are four possible flow patterns.

- (a) The liquid flows in the lower, and the gas in the upper part of the tube. The liquid wets only part of the tube wall. This form is referred to hereafter as stratified flow.
- (b) The liquid wets fully the tube walls. The central portion of the liquid carries in it gas bubbles non-uniformly distributed over the cross-section.
- (c) The liquid forms a film on the wall fully wetting the surface. Gas flows in the central portion of the tube.
- (d) The flow pattern is similar to (c), but the gas now entrains with it small liquid droplets, which are uniformly distributed throughout the gas.

Forms (b), (c) and (d) may be described by the general term "annular flow" in so far as there is an annulus of liquid surrounding a core of lighter density. Flow pattern (d), where the core consists of gas entraining with it small liquid droplets uniformly dispersed, may be regarded as the more general case, and it is for this form that the following theory/

theory has been developed. Separated flow occurs only with small gas contents.

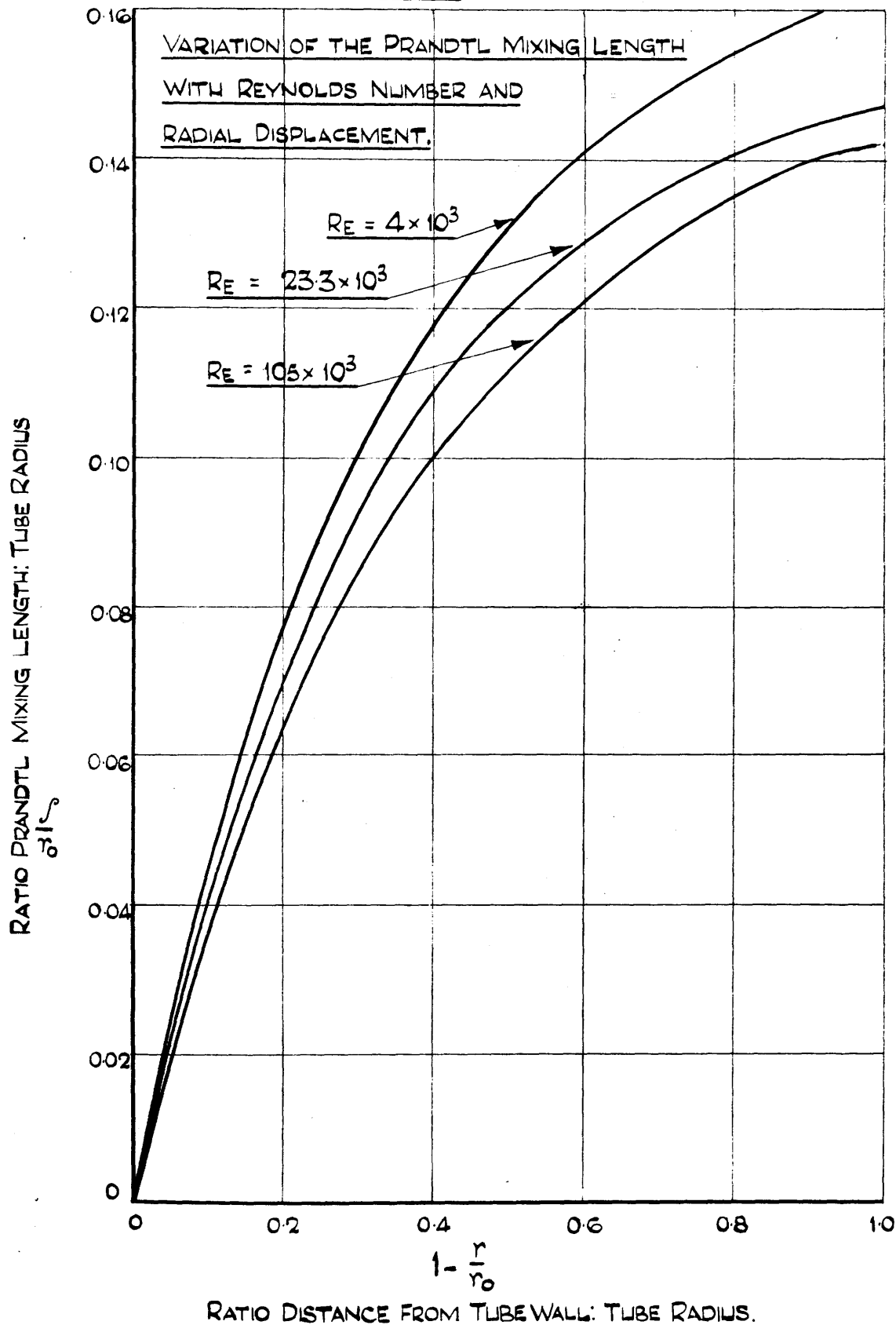
In addition the following assumptions are made:

- (a) Both phases flow turbulently.
- (b) The central core is uniformly dispersed around the tube axis.
- (c) The gas and entrained liquid forming the core behave as a homogeneous fluid, the liquid having the same velocity as the gas.
- (d) The Prandtl mixing length distribution is the same during single and two-phase flow. The distribution calculated by Nikuradse for single-phase flow is shown in Figure 13.

This above assumption would appear contrary to the observation that diffusion does not occur throughout the two-phase mixture. If the above assumed independence of the mixing length on the respective phase densities is true, it might be expected that the liquid would disperse throughout the gas, the equilibrium condition during horizontal flow being when diffusion upwards in the vertical plane balances the "free" downward velocity of the liquid relative to the gas.* That this does not occur must be attributed to the effects of surface tension, as Martinelli has shown that decreasing the surface tension tends to produce foaming or diffusion.

Martinelli also observed that at the interface the liquid surface was covered with capillary waves. While

FIG. 13.



the surface tension tends to prevent diffusion at the boundary, the wave amplitude is analogous in its effect to that of the prandtl mixing length. The action of the gas on the liquid wave produces forces similar to those occurring due to momentum transfer within the phases. It may therefore be approximately the case that within the phases the mixing length is not affected by the surface tension at the phase boundary.

Having assumed the above mode of flow, the ratio of the gas to liquid velocities follows as shown in the following.

* "Turbulent Transfer Mechanism and Suspended Sediment in Closed Channels" - Ismail.
Am. Soc. Civ. Engrs. Vol.77, Feb. 1951.

9. RATIO OF THE GAS TO LIQUID VELOCITY.

Prandtl has shown that, during the turbulent flow of a homogeneous fluid in a pipe, the shearing stress T_1 at a radial distance y from the wall can be expressed in the form

$$T_1 = \rho_1 \cdot \ell_1^2 \cdot \left(\frac{du}{dy}\right)_1^2 / g \dots \dots \dots 1$$

where ρ_1 , ℓ_1 , and $\left(\frac{du}{dy}\right)_1$ are respectively the density, Prandtl mixing length, and the gradient of the velocity profile.

For liquid flow under such conditions the velocity profile is represented by curve oco' in Figure 14.

During two-phase flow with the same liquid mass flow in the annulus as for the single-phase case, and with a central core of gas, or vapour, and entrained liquid the velocity profile is shown by curve $oabfdeo'$.

The velocity profile in the annulus is assumed at present to be the same for both the single and two-phase cases. This latter point is dealt with in further detail in Section 12.

At a point a distance y from the wall, within the core, Prandtl's Equation will be

$$T_2 = \rho_2 \cdot \ell_2^2 \cdot \left(\frac{du}{dy}\right)_2^2 / g \dots \dots \dots 2$$

The suffix 2 denotes properties of the core.

Combining Equations 1 and 2 gives

$$\left(\frac{du}{dy}\right)_2 = \frac{\ell_1}{\ell_2} \cdot \left(\frac{du}{dy}\right)_1 \sqrt{\frac{\rho_1}{\rho_2} \cdot \frac{T_2}{T_1}} \dots \dots \dots 3$$

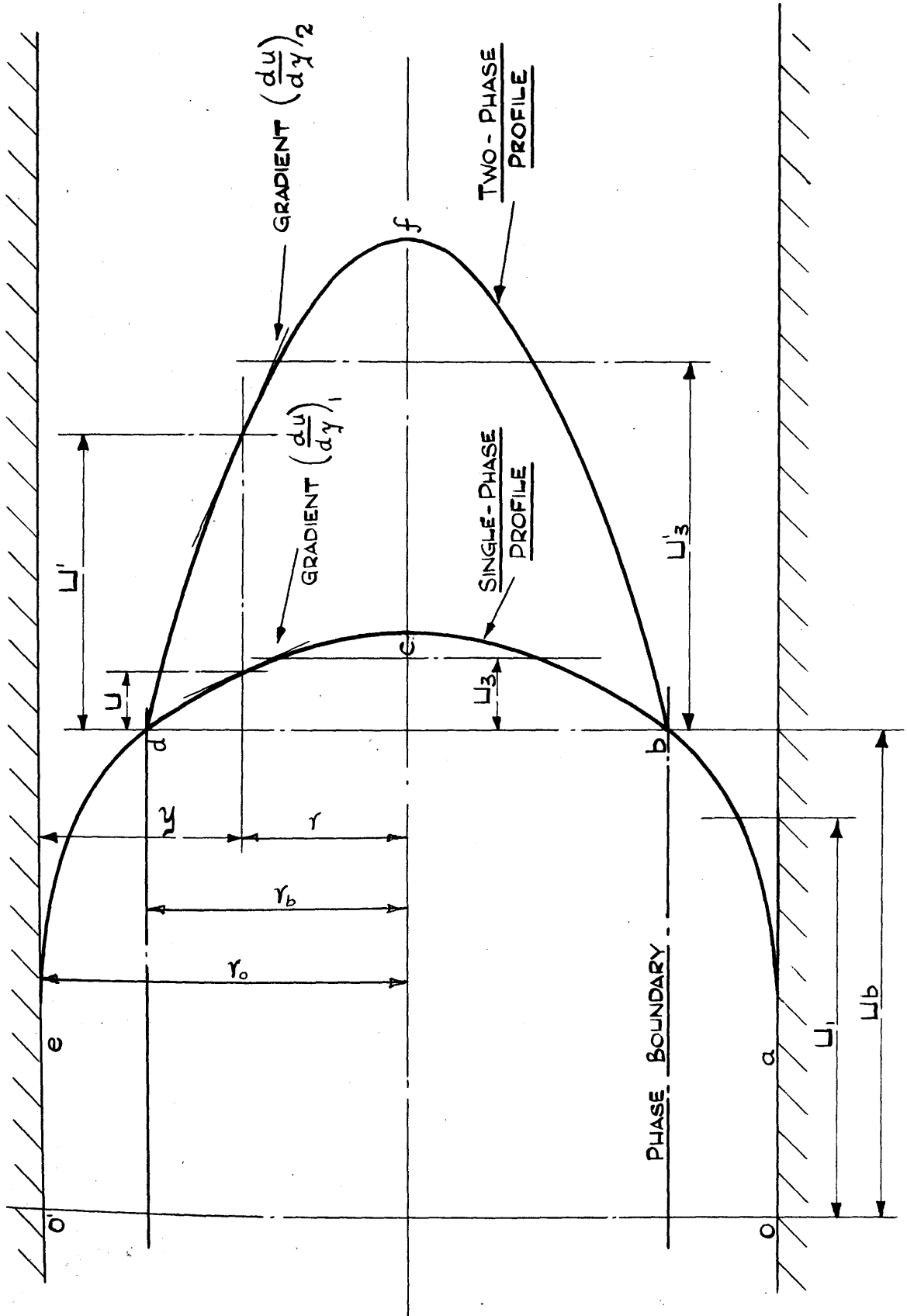


FIG. 14. VELOCITY PROFILE DURING SINGLE AND TWO PHASE FLOW.

As discussed in the previous section the mixing length ratio l_1/l_2 is assumed unity, giving

$$\left(\frac{du}{dy}\right)_2 = \left(\frac{du}{dy}\right)_1 \sqrt{\frac{\rho_1}{\rho_2} \cdot \frac{T_2}{T_1}} \dots \dots \dots 4$$

It will be shown that T_2/T_1 is constant throughout the core, hence U_3 and U_3' the mean velocities in the core during single and two-phase flow relative to the velocity at the phase boundary are related thus (See Appendix C).

$$U_3' = U_3 \sqrt{\frac{\rho_1}{\rho_2} \cdot \frac{T_2}{T_1}} \dots \dots \dots 5$$

If U_b is the phase boundary velocity, the absolute velocity of the core mixture U_2 is

$$U_2 = U_b + U_3' = U_b + U_3 \sqrt{\frac{\rho_1}{\rho_2} \cdot \frac{T_2}{T_1}} \dots \dots \dots 6$$

Now the core contains a mixture of gas and entrained liquid. Let q and w represent the respective proportions of gas and liquid in the core by weight per pound of flow.

Then

$$\rho_2 = \frac{q + w}{q/\rho_g + w/\rho_L} \dots \dots \dots 7$$

As w/ρ_L is presumably small relative to q/ρ_g this expression may be reduced to

$$\rho_2 = \frac{q + w}{q} \cdot \rho_g \dots \dots \dots 8$$

Also as the annular ring contains liquid only

$$\rho_1 = \rho_L \dots \dots \dots 9$$

It/

It can be shown from the continuity equations that the mean liquid velocity U_L is related to the mean annulus velocity U_1 in the expression (Equation A.11, Appendix A).

$$U_L = U_1 \frac{1-q}{1-q-\omega+\omega/k_2} \dots \dots \dots \text{A11}$$

where K_2 is the ratio of the core to annulus velocity, and is obtained by dividing Equation 6 by the annulus velocity, i.e.

$$K_2 = \frac{U_b}{U_1} + \frac{U_3}{U_1} \sqrt{\frac{\rho_1}{\rho_2} \frac{T_2}{T_1}} \dots \dots \dots \text{10}$$

This ratio is greater than the gas to liquid velocity ratio, as the mean liquid velocity is greater than the mean annulus velocity, due to part of the liquid possessing the core velocity. On the other hand, the core velocity is also the gas velocity.

The gas to liquid velocity ratio is obtained by substituting Equations 8 and 9 for ρ_2 and ρ_1 respectively in Equation 6, then dividing by Equation A.11, i.e.

$$K = \frac{U_G}{U_L} = \frac{U_2}{U_L} = \frac{U_b}{U_1} \frac{1-q-\omega+\omega/k_2}{1-q} + \frac{U_3}{U_1} \frac{1-q-\omega+\omega/k_2}{1-q} \sqrt{\frac{q}{q+\omega} \frac{\rho_L}{\rho_G} \frac{T_2}{T_1}} \dots \dots \dots \text{11}$$

It should be noted that $\frac{U_b}{U_1}$ and $\frac{U_3}{U_1}$ are velocity ratios associated with a single-phase velocity profile.

10. APPROXIMATE FORM OF THE
GAS TO LIQUID VELOCITY RATIO.

Present knowledge does not extend to the evaluation of the liquid content of the core, hence it is not possible to apply Equation 11 in its present form.

From inspection of a single-phase velocity profile it is evident that the ratio U_b/U_1 is slightly greater than unity. As its multiplier in Equation 11 will be slightly less than unity for small values of ω and/or for values of near unity, it is reasonable to assume the product unity.

Equation 11 therefore becomes

$$K = 1 + \frac{U_3}{U_1} \cdot \frac{1-q-\omega+\omega/K_2}{1-q} \sqrt{\frac{q}{q+\omega} \cdot \frac{\rho_L}{\rho_G} \cdot \frac{T_2}{T_1}} \dots \dots \dots 12$$

If the symbol Z is used to denote the expression

$$\frac{U_3}{U_1} \cdot \frac{1-q-\omega+\omega/K_2}{1-q} \sqrt{\frac{q}{q+\omega}}$$

Equation 12 reduces to

$$K = 1 + Z \sqrt{\frac{\rho_L}{\rho_G} \cdot \frac{T_2}{T_1}} \dots \dots \dots 13$$

At a particular pressure during steam-water flow the term Z will be dependent on the core to tube cross-sectional ratio, and on the annulus mass flow. The variation in turbulence with annulus mass flow rate will be an important factor governing the mixing between the phases.

Consider now the possible variation of Z with pressure.
For/

For a particular core to tube cross-sectional ratio, U_3/U_1 , will vary only slightly with Reynolds' Number. The change in dryness fraction with increasing pressure may be predicted from Equation A12, i.e.

$$\frac{X_g}{X} = \frac{q/\rho_g}{q/\rho_g + K(1-q)/\rho} \dots \dots \dots A12$$

The velocity ratio equation indicates that K does not vary as rapidly as ρ_g hence for a particular X_g/X ratio the dryness fraction will increase with increasing density. Both the viscosity and surface tension of water decrease with increasing pressure suggesting that the mixing will increase with increasing pressure. Hence both q and w will increase with increasing pressure, with the result that Z will tend to remain constant with pressure variation. This also suggests that Z may have approximately the same value during both steam-water and air-water flow.

As K may be determined from Armand's experiments with air-water flow, Z may be calculated from Equation 13. The procedure is detailed in Appendix D, and the values obtained graphed in Figure 15. They are plotted to a base of gas to tube cross-sectional ratio for various liquid flow rates. It was not possible to relate Z to the more correct reference axis of core to tube cross-sectional ratio for various annulus flow rates, as the water content w was unknown.

No direct measurements of the velocity ratio K for steam-water mixtures are available, hence the values of obtained/

THE TERM Z - RATIO OF $\frac{\text{GAS CROSS-SECTIONAL AREA}}{\text{TUBE CROSS-SECTIONAL AREA}}$
 FOR VARIOUS VALUES OF $(1-q) \frac{M}{X}$ LBS/SEC. FT.².

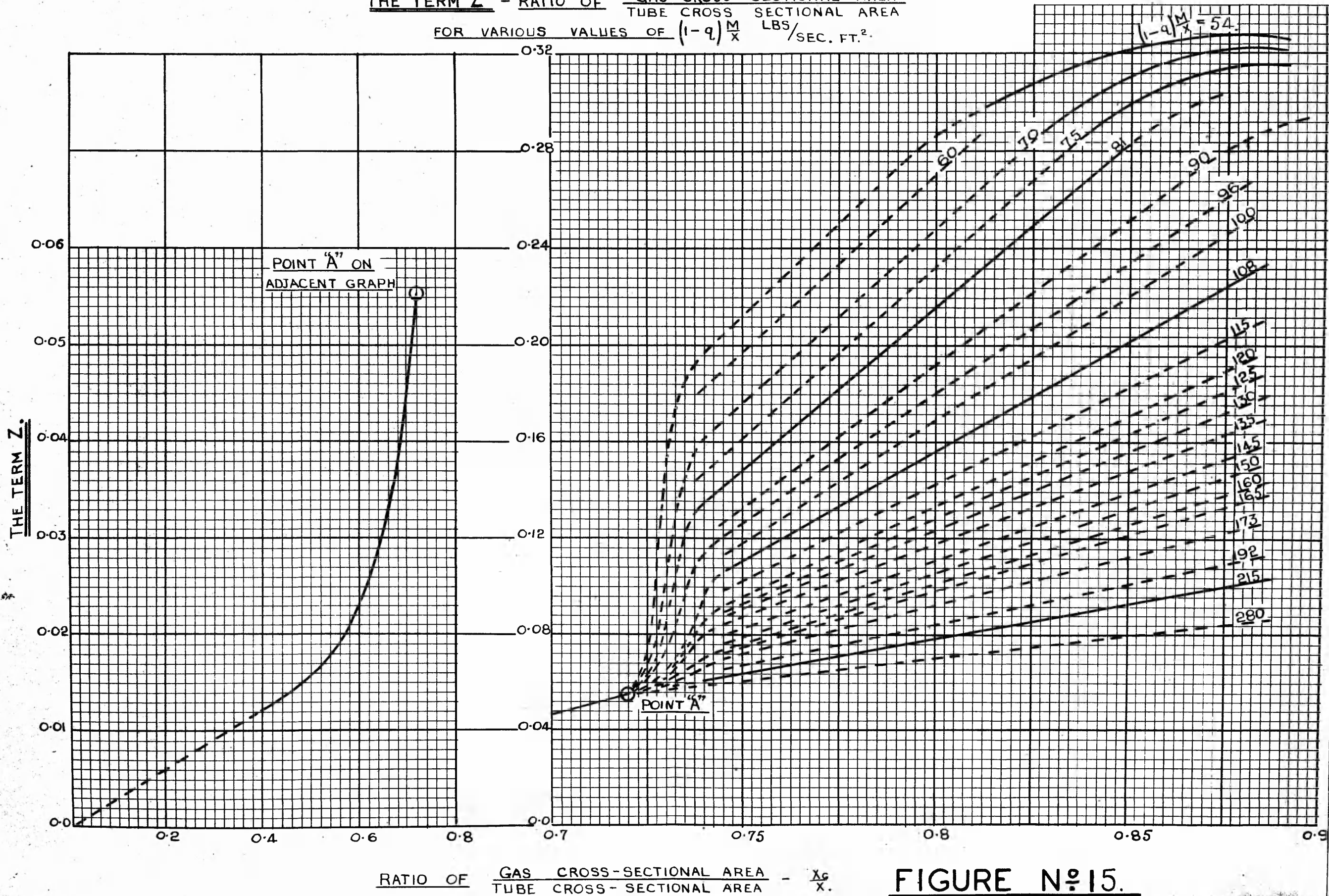


FIGURE N°15.

obtained with air-water mixtures are assumed to hold for the flow of steam-water mixtures. The values of Z will however, be applicable only to smooth tubes, as the air-water tests were carried out for this condition. The equations are developed to include the effect of tube roughness in Appendix K.

11. SHEARING STRESS RATIO T_2/T_1 .

Equation 13 for the ratio of the gas to liquid velocities contains the shearing stress ratio T_2/T_1 . This ratio is now determined by considering the equilibrium of an elementary cylinder in the core as shown in Figure 16. The tube is inclined at an angle θ to the horizontal, and the flow is upwards. Increments in the direction of motion are taken as positive.

The following are the forces acting on the cylinder in the direction of motion. (Second order differentials are neglected),

- (a) due to pressure change

$$- \left(\frac{dp}{dl} \right)_2 \cdot \delta l \cdot \pi \cdot r^2$$

- (b) due to shearing stresses on the cylinder walls.

$$- T_2 \cdot 2\pi \cdot r \cdot \delta l$$

- (c) due to the weight of the cylinder.

$$- \rho_2 \cdot \pi r^2 \cdot \delta l \cdot \sin \theta$$

- (d) due to the core mixture momentum force

$$- \rho_2 \cdot \pi r^2 \cdot \frac{U_2 \delta U_2}{g}$$

In developing this expression, and all similar expressions, the velocity and velocity changes are treated as the mean phase velocity and velocity changes respectively. This involves the substitution of mean velocity for root mean/

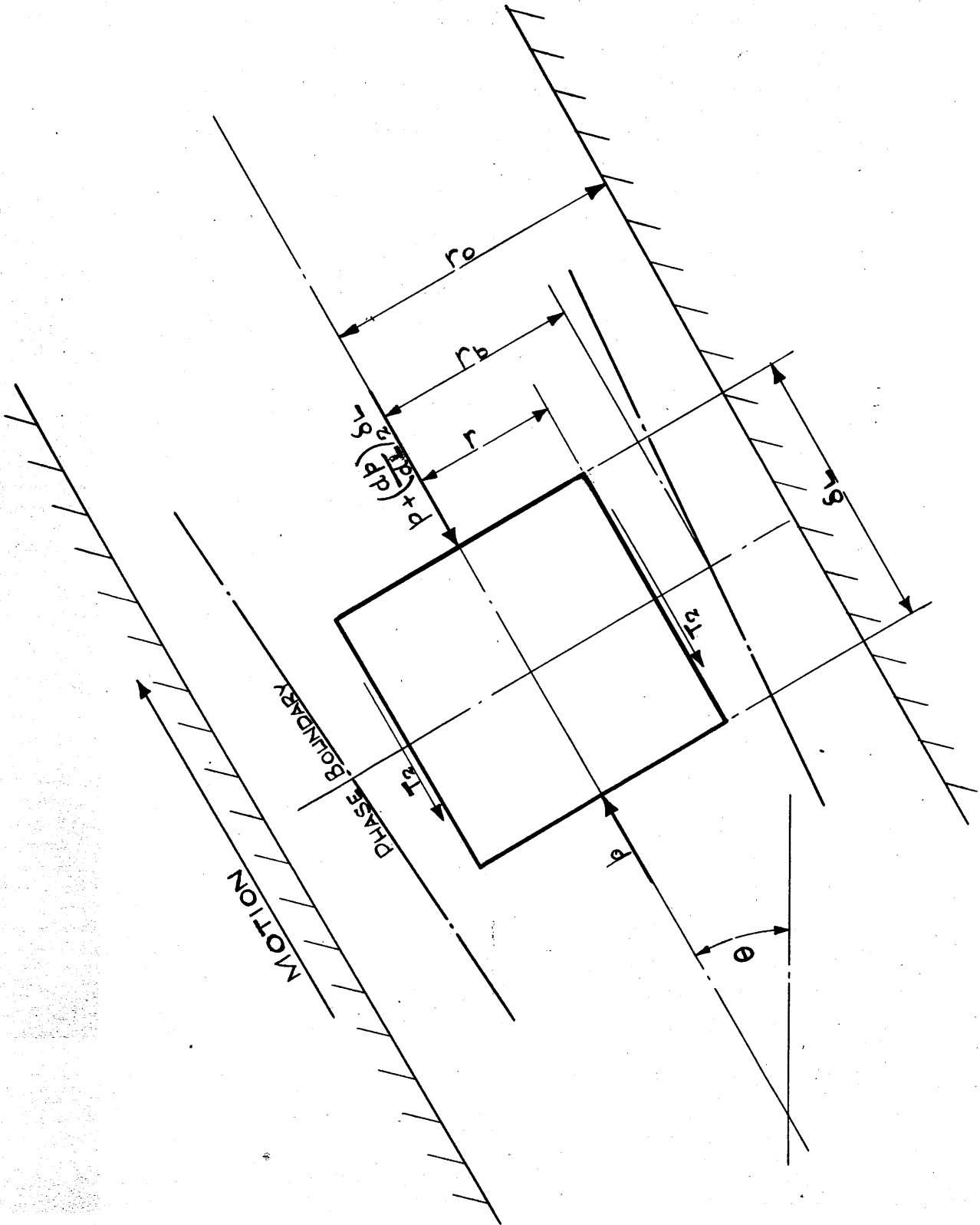


FIG. 16. EQUILIBRIUM OF CORE ELEMENT.

mean square velocity, together with a simplification of the same order in which the variation of mean velocity with cylinder radius is ignored.

As the above forces are in equilibrium,

$$\begin{aligned}
-\left(\frac{db}{dl}\right)_2 \cdot \delta l \cdot \bar{n} r^2 - T_2 \cdot 2\bar{n} \cdot r \cdot \delta l - \rho_2 \cdot \bar{n} r^2 \cdot \delta l \sin \theta \\
- \rho_2 \cdot \bar{n} r^2 \cdot \frac{U_2 \cdot \delta U_2}{g} = 0
\end{aligned}$$

or

$$T_2 = -\frac{r}{2} \left[\left(\frac{db}{dl}\right)_2 + \rho_2 \sin \theta + \frac{\rho_2 \cdot U_2 \cdot \delta U_2}{\delta l \cdot g} \right] \dots \dots \dots 14$$

For the case of single-phase flow this reduces to

$$T_1 = -\frac{r}{2} \left(\frac{db}{dl}\right)_{F1} \dots \dots \dots 15$$

where T_1 and $(db/dl)_{F1}$ are the shearing stress and friction on pressure gradient respectively during single-phase flow.

Hence by dividing Equation 14 by 15

$$\frac{T_2}{T_1} = \frac{\left(\frac{db}{dl}\right)_2 + \rho_2 \sin \theta + \frac{\rho_2 \cdot U_2 \cdot \delta U_2}{\delta l \cdot g}}{\left(\frac{db}{dl}\right)_{F1}} \dots \dots \dots 16$$

It will be seen that, as assumed in the development, the ratio is constant over the core.

In applying this equation ρ_G is substituted for ρ_2 as w is unknown. Since the gradients due to the core weight and momentum force are small relative to the total pressure gradient, little error is normally involved in this assumption.

Also, as will be discussed in detail in the following section, the pressure gradient during single-phase flow is assumed the same as that obtained during two-phase flow for a/

a particular annulus flow rate.

This reduces Equation 16 to

$$\frac{T_2}{T_1} = \frac{\left(\frac{db}{dl}\right)_2 + \rho_G \sin \theta + \frac{\rho_G \cdot U_2 \cdot \delta U_2}{\delta l \cdot g}}{\left(\frac{db}{dl}\right)_{F2}} \dots \dots \dots 17$$

If there are no momentum forces this becomes

$$\frac{T_2}{T_1} = \frac{\left(\frac{db}{dl}\right)_2 + \rho_G \cdot \sin \theta}{\left(\frac{db}{dl}\right)_{F2}} \dots \dots \dots 18$$

and further if the tube is in the horizontal plane

$$\frac{T_2}{T_1} = \frac{\left(\frac{db}{dl}\right)_2}{\left(\frac{db}{dl}\right)_{F2}} = \frac{\left(\frac{db}{dl}\right)_{F2}}{\left(\frac{db}{dl}\right)_{F2}} = 1 \dots \dots \dots 19$$

Final Equations. The velocity ratio equations are therefore applied in the following forms:

(a) Horizontal Tube No momentum force.

$$K = 1 + Z \sqrt{\frac{\rho_L}{\rho_G}} \dots \dots \dots 20$$

(b) Inclined Tube. No momentum force.

$$K = 1 + Z \sqrt{\frac{\rho_L \left(\frac{db}{dl}\right)_2 + \rho_G \sin \theta}{\rho_G \left(\frac{db}{dl}\right)_{F2}}} \dots \dots \dots 21$$

(c) Vertical Tube ($\sin \theta = 1$) No momentum force.

$$K = 1 + Z \sqrt{\frac{\rho_L \cdot \left(\frac{db}{dl}\right)_2 + \rho_G}{\rho_G \left(\frac{db}{dl}\right)_{F2}}} \dots \dots \dots 22$$

(d) Vertical Tube Momentum forces.

$$K = 1 + Z \sqrt{\frac{\rho_L \cdot \left(\frac{db}{dl}\right)_2 + \rho_G + \frac{\rho_G \cdot U_2 \cdot \delta U_2}{\delta l \cdot g}}{\rho_G \left(\frac{db}{dl}\right)_{F2}}} \dots \dots \dots 23$$

12. DISTORTION OF THE ANNULUS PROFILE.

In developing the theory it has been assumed that the velocity profile in the annulus is the same for both the single and two-phase profiles considered. The actual profile will be determined by the shearing stress distribution in the annulus. This distribution is now determined by considering an elementary cylinder with a radius r , greater than the core radius r_b as shown in Figure 17.

The following forces act on the elemental cylinder in the direction of motion (Second order differentials are neglected)

- (a) due to the pressure change

$$- \left(\frac{dp}{dl} \right)_2 \cdot \pi r^2 \cdot \delta l$$

- (b) due to shearing stresses on the cylinder walls

$$- \tau_1' \cdot 2\pi r \cdot \delta l$$

- (c) due to the weight of cylinder

$$- \left\{ \rho_2 \cdot \pi r_b^2 \cdot \delta l + \rho_1 \cdot \pi (r^2 - r_b^2) \delta l \right\} \sin \theta$$

- (d) due to the core mixture momentum force

$$- \rho_2 \cdot \pi r_b^2 \cdot \frac{u_2 \cdot \delta u_2}{g}$$

- (e) due to the momentum force of the annular ring of liquid

$$- \rho_1 \pi (r^2 - r_b^2) \frac{u_1 \cdot \delta u_1}{g}$$

As/

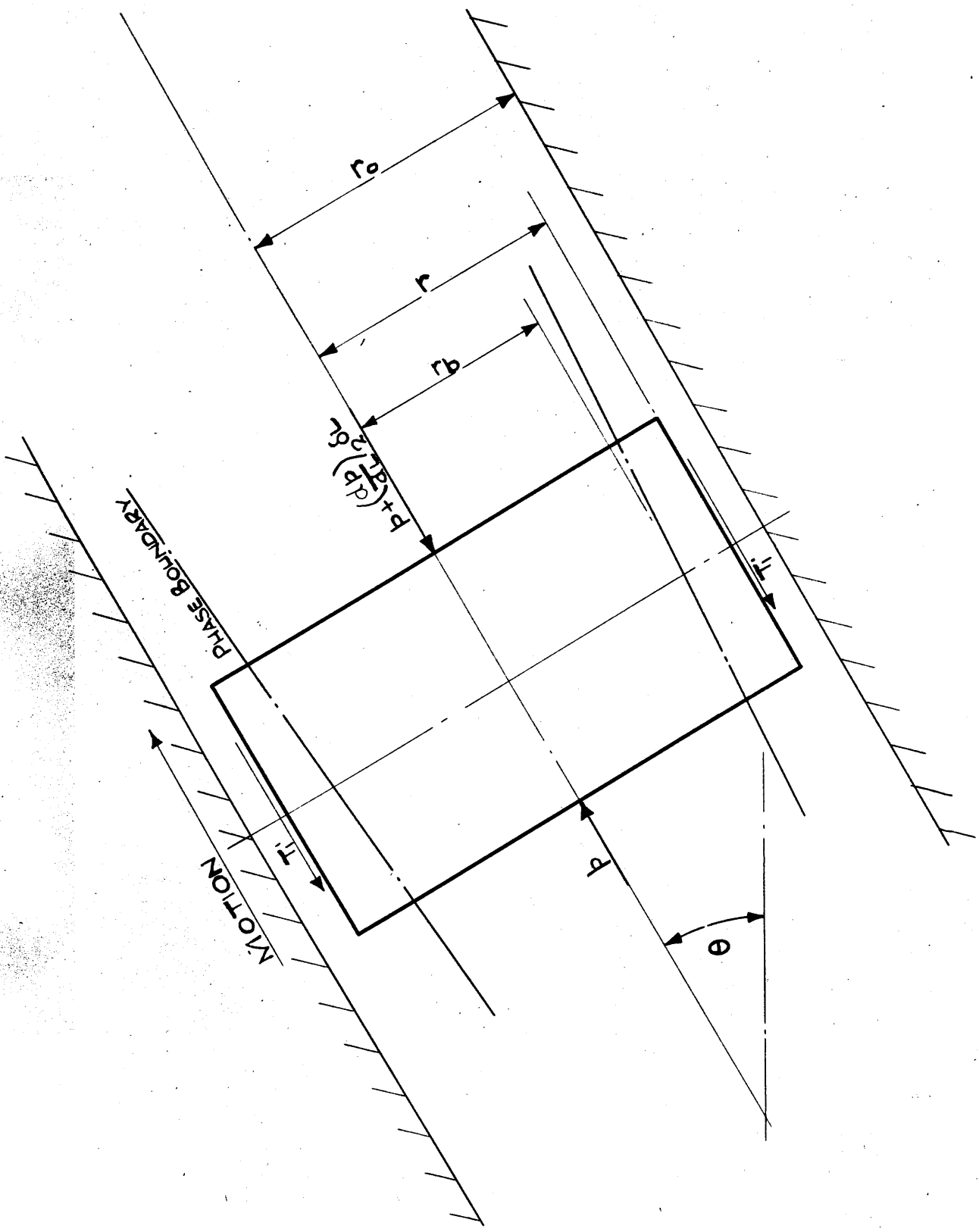


FIG. 17. ANNULUS EQUILIBRIUM.

As the above forces are in equilibrium

$$T_1' = -\frac{r}{2} \left[\left(\frac{dp}{dl} \right)_2 + \rho_1 \sin \theta - (\rho_1 - \rho_2) \frac{r_b^2}{r^2} \sin \theta + \frac{\rho_2}{\delta l} \cdot \frac{r_b^2}{r^2} \frac{u_2 \delta u_2}{g} + \frac{\rho_1}{\delta l} \left(1 - \frac{r_b^2}{r^2} \right) \frac{u_1 \delta u_1}{g} \right] \dots 24$$

Now the pressure gradient $\left(\frac{dp}{dl} \right)_2$ is equal to the sum of the pressure gradients due to friction $\left(\frac{dp}{dl} \right)_{F2}$ mixture weight $\left(\frac{dp}{dl} \right)_{\rho_2}$, and momentum force $\left(\frac{dp}{dl} \right)_{M2}$

It can be readily shown that

$$\left(\frac{dp}{dl} \right)_{\rho_2} = -\rho_1 \sin \theta + (\rho_1 - \rho_2) \frac{r_b^2}{r_o^2} \sin \theta \dots 25$$

and

$$\left(\frac{dp}{dl} \right)_{M2} = -\frac{\rho_2}{\delta l} \cdot \frac{r_b^2}{r_o^2} \cdot \frac{u_2 \delta u_2}{g} - \frac{\rho_1}{\delta l} \left(1 - \frac{r_b^2}{r_o^2} \right) \frac{u_1 \delta u_1}{g} \dots 26$$

Substituting Equations 25 and 26 in 24 gives

$$T_1' = -\frac{r}{2} \left[\left(\frac{dp}{dl} \right)_{F2} - (\rho_1 - \rho_2) r_b^2 \left(\frac{1}{r^2} - \frac{1}{r_o^2} \right) \sin \theta - \frac{r_b^2}{\delta l} \left(\frac{1}{r^2} - \frac{1}{r_o^2} \right) \left(\frac{\rho_1 u_1 \delta u_1}{g} - \frac{\rho_2 u_2 \delta u_2}{g} \right) \right] \dots 27$$

This equation indicates more clearly than Equation 24 the variation of the shearing stress within the annulus. For a single-phase fluid the shearing stress distribution bears a linear relationship with the radius. Equation 27 indicates that with two-phase flow the shearing stresses vary non-linearly, except for the case of horizontal flow, with no momentum forces, when Equation 27 reduces to

$$T_1' = -\frac{r}{2} \left(\frac{dp}{dl} \right)_{F2} \dots 28$$

For the case of upward flow (i.e. $\sin \theta$ positive) the shearing stresses vary less rapidly with decreasing radius, than/

than for the case of single-phase flow, as will also the velocity profile gradient. With reference to Figure 18, if $o'ed$ represents the annulus profile with linear shear distribution, then $o'e'd'$ represents the profile with the non-linear stress variation obtained during upward flow in inclined tubes. The mean velocity is the same for both curves as the mass flow in the annulus is the same for both the single and two-phase cases considered.

The actual profile during two-phase flow is, therefore, represented by $o'e'd'f'$ rather than $o'edf$ as assumed in the development. As T_2/T_1 is constant throughout the core there is no distortion within the core. The only outcome, therefore, of this effect is its influence on the magnitude of U_b/U_1 . The form of the theoretical equation for the gas-liquid velocity ratio (Equation 11) is unchanged. The approximations made regarding the term containing U_b/U_1 will still be approximately true. No allowance for this effect is made in applying the equations.

A further influence of distortion is the change of the shearing stresses at the wall for a particular annulus mass flow. For the same velocity profile in the annulus during single and two-phase flow, the wall shearing stress, and consequently the friction pressure change, must be the same during both flow conditions. If, however, the two-phase profile is distorted then the velocity gradient in the laminar wall layer must change (for the same thickness of laminar layer), altering the shearing stresses at the wall and the friction pressure change. However, in developing the friction equation (Section 15) this distortion effect is neglected.

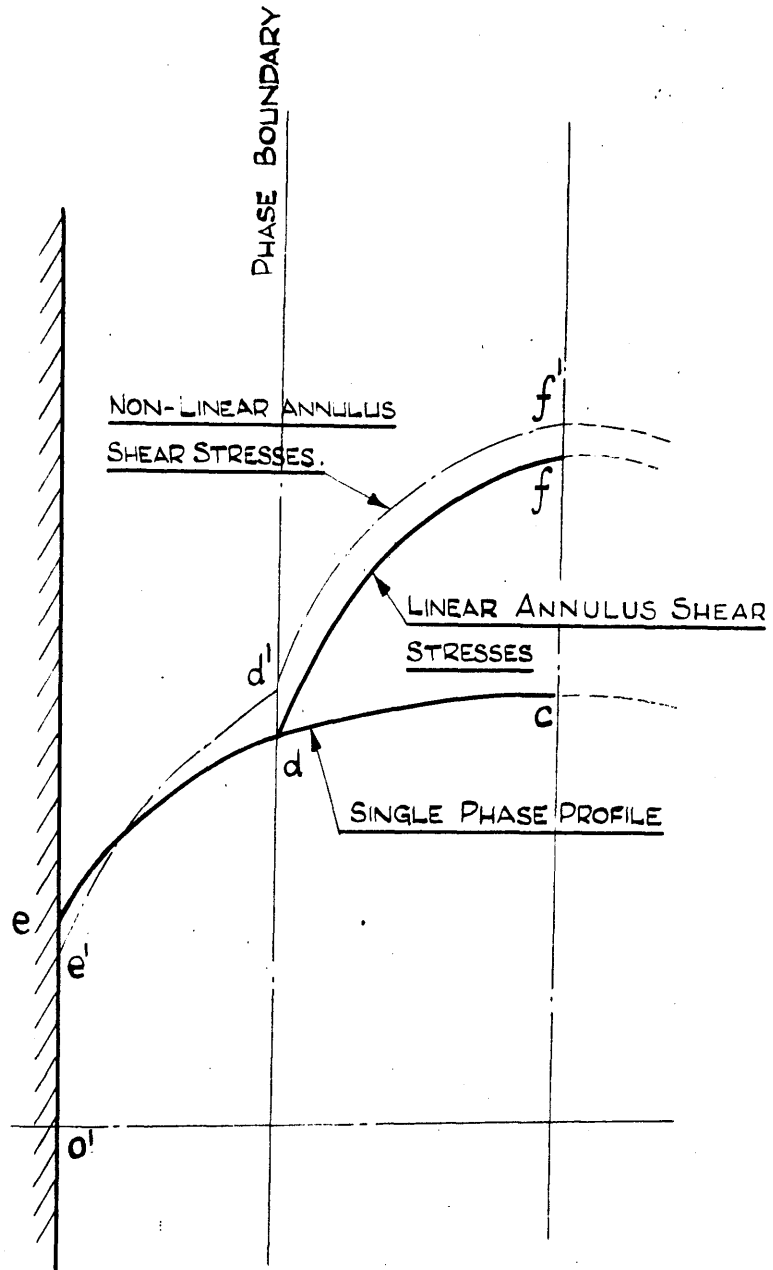


FIG. 18. DISTORTION OF ANNULUS PROFILE.

13. EFFECT OF HEAT TRANSFER ON FLOW CONDITIONS.

The mechanism of heat transfer will have a considerable effect on the flow of an evaporating liquid. Where the heat is transferred through the tube walls evaporation will occur close to the wall. Presumably bubbles of vapour form close to the wall and move axially relative to the liquid, and also radially inwards to coalesce with the core of the liquid and vapour flowing in the centre of the tube.

Annulus Density. In the development contained in Section 9, the flow in the annulus has been assumed that of a homogeneous liquid. It will be appreciated however, that in the case of heat transfer there is a mixture of liquid and vapour in the annulus.

Present knowledge of the axial and radial movements of vapour bubbles in an annulus of liquid is insufficient to predict the annulus equivalent density, hence it is suggested that the theoretical equation be applied assuming the density in the annulus is that of the liquid. The velocity ratio values thus obtained will be greater than those obtained using the actual annulus density, as inspection of Equation 11 indicates that K increases with the annulus density.

Laminar Boundary Layer. The formation of steam bubbles in the region of the wall will presumably produce disturbances at the wall similar to those produced by rough tubes. Hence the velocity change over the laminar layer will be reduced/

reduced, which will have the effect of increasing the ratios U_b/U_1 and U_3/U_1 in Equation 11. The effect is neglected. This approximation will tend to counterbalance the assumption made above in neglecting the change in density of the annulus liquid.

14. FLOW IN DOWNCOMER TUBES.

The theory has been developed for the case where the shearing stress ratio T_2/T_1 is positive. During the downward flow in inclined tubes this ratio may be negative. The manner of applying the equation under these circumstances requires care.

Let T_2' denote negative values of T_2 . The fundamental relationship between the velocity gradients and the shearing stresses can be written

$$\left(\frac{du}{dy}\right)_2^2 = \left(\frac{du}{dy}\right)_1 \frac{\rho_1}{\rho_2} \cdot \frac{T_2'}{T} \dots \dots \dots 29$$

However, on this occasion, as the shearing stress ratio has changed sign, so also must the gradient. Hence the velocity profile will be as shown in Figure 19. The remainder of the theoretical development is unaffected.

The final form of the Velocity Ratio Equation is, therefore,

$$K = 1 - Z \sqrt{\frac{\rho_L}{\rho_G} \cdot \frac{T_2'}{T}} \dots \dots \dots 30$$

The general form may, therefore, be expressed

$$K = 1 \pm Z \sqrt{\frac{\rho_L}{\rho_G} \cdot \frac{\pm T_2}{T}} \dots \dots \dots 31$$

If the positive sign of T_2 is chosen, then the positive sign must be used before the square root term. Similarly with the negative sign. The appropriate sign is that which will give a real value to the square root term.

Where/

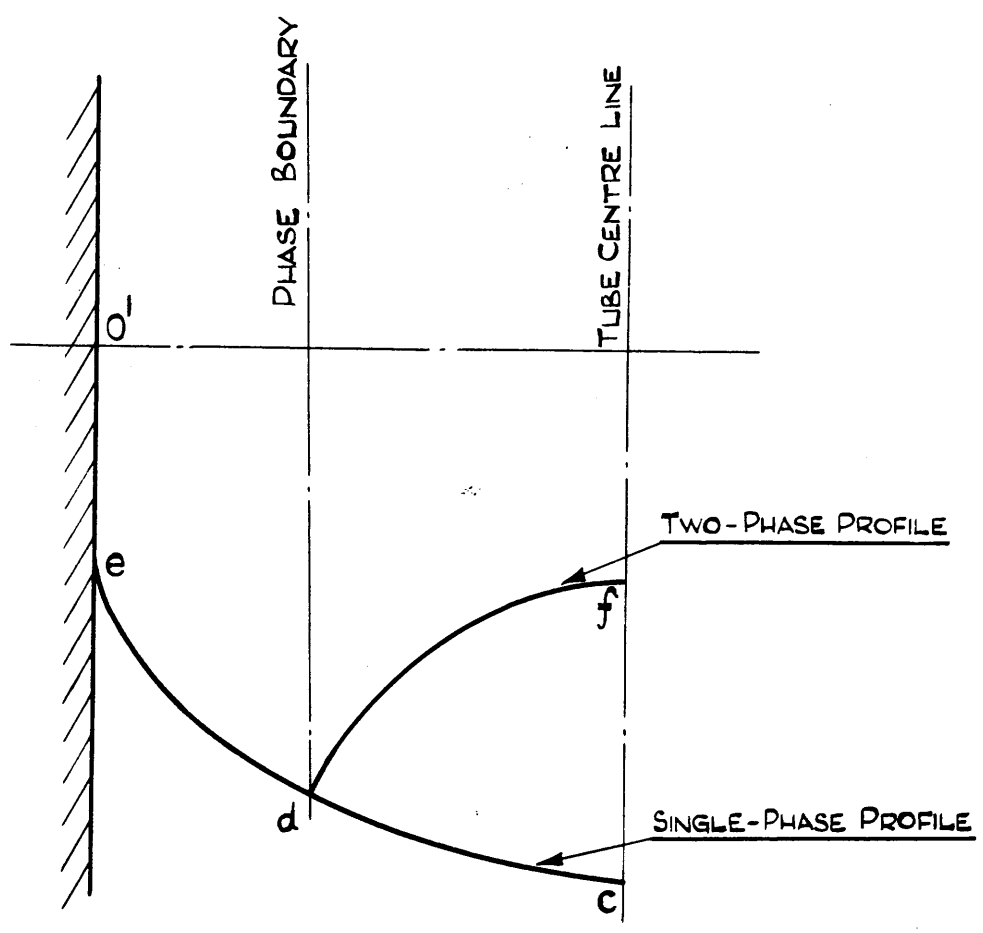


FIG. 19. VELOCITY PROFILE DOWNCOMER

Where flow occurs in a vertical downcomer tube, and inertia forces are negligible, Equation 31 is obtained in the form

$$K = 1 \pm Z \sqrt{\frac{\rho_L \pm \left[\left(\frac{dp}{dl} \right)_2 - \rho_G \right]}{\rho_G \left(\frac{dp}{dl} \right)_{F2}}} \dots \dots \dots 32$$

PART III.THE PROPOSED THEORY FOR
PRESSURE CHANGE DURING TWO PHASE-FLOW.

	<u>Page.</u>
15. Pressure change due to friction	78.
16. Pressure change due to mixture weight ...	81.
17. Pressure change due to momentum forces...	82.
18. Combined equations and solution	84.

INTRODUCTION.

During the flow of a homogeneous fluid, or a two-phase mixture the pressure change along the pipe may be due to the three distinct actions: firstly, to the friction at the tube walls; secondly, to the effect of the mixture weight; thirdly to forces required to accelerate the fluid. These effects are dealt with in turn in the following sections.

15. PRESSURE CHANGE DUE TO FRICTION.

During the flow of a single-phase liquid the friction pressure change is obtained from the equation

$$-\left(\frac{dp}{dl}\right)_{F1} \cdot \delta l = \frac{\lambda \cdot \delta l \cdot U^2 \cdot \rho_1}{2g \cdot d} \dots \dots \dots 33$$

where U is the mean velocity. Let U_1 represent the velocity in an annular ring during such flow conditions where $U_1 = \frac{U}{\alpha}$.

The friction equation may now be written

$$-\left(\frac{dp}{dl}\right)_{F1} \cdot \delta l = \frac{\lambda \cdot \delta l \cdot (\bar{\alpha} U_1)^2 \rho_1}{2g \cdot d} \dots \dots \dots 34$$

If during two-phase flow the velocity in the annulus is U_1 , and the annulus profile is the same as for the single-phase case, then the friction pressure change is also

$$-\left(\frac{dp}{dl}\right)_{F2} \cdot \delta l = \frac{\lambda \cdot \delta l \cdot (\bar{\alpha} U_1)^2 \rho_1}{2g \cdot d} \dots \dots \dots 35$$

As already discussed in Section 12, distortion of the annulus profile will influence the friction pressure gradient. This effect is, however, neglected and the above equation is assumed to hold where the annulus profile is distorted.

Now from Equation All(Appendix A), the mean velocity of the total water flow is related to the annulus velocity in the expression

$$U_L = U_1 \frac{1-q}{1-q-\omega + \omega/k_2} \dots \dots \dots All$$

and

$$\rho_1 = \rho_L \dots \dots \dots 9$$

Substituting Equation A11 and 9 in 35 gives

$$-\left(\frac{dp}{d\ell}\right)_{F2} \cdot \delta\ell = \left\{ \bar{a} \cdot \frac{1-q-\omega+\omega/k_2}{1-q} \right\}^2 \frac{\lambda \cdot \delta\ell \cdot U_L^2 \cdot \rho_L}{2q \cdot d}$$

$$= G \cdot \frac{\lambda \cdot \delta\ell \cdot U_L^2 \cdot \rho_L}{2q \cdot d} \dots \dots \dots 36$$

where

$$G = \left\{ \bar{a} \cdot \frac{1-q-\omega+\omega/k_2}{1-q} \right\}^2 \dots \dots \dots 37$$

The term \bar{a} from inspection of a single-phase velocity profile is slightly greater than unity. The second term, as discussed in Section 10 will be slightly less. Consequently G was assumed unity giving

$$-\left(\frac{dp}{d\ell}\right)_{F2} \cdot \delta\ell = \frac{\lambda \cdot \delta\ell \cdot U_L^2 \cdot \rho_L}{2q \cdot d} \dots \dots \dots 38$$

It is evident that where evaporation occurs at the wall the additional turbulence will tend to disrupt the laminar layer causing an increase in the friction pressure change. Inspection of the experimental data suggests a correction factor of 1.25 to allow for evaporation with heat transfer giving for this condition

$$-\left(\frac{dp}{d\ell}\right)_{F2} \cdot \delta\ell = 1.25 \cdot \frac{\lambda \cdot \delta\ell \cdot U_L^2 \cdot \rho_L}{2q \cdot d} \dots \dots \dots 39$$

For certain purposes the friction equations are more conveniently expressed in terms of mass flow rates.

From the liquid continuity equation (Equation A5)

$$(1-q) \frac{M}{X_L} = U_L \cdot \rho_L \dots \dots \dots A5$$

Substituting this in Equation 36 gives on rearranging

$$-\left(\frac{dp}{d\ell}\right)_{F2} \cdot \delta\ell = G \cdot \frac{\lambda \cdot \delta\ell}{2q \cdot d} \left\{ (1-q) \frac{M}{X} \right\}^2 \frac{1}{\rho_L} \left\{ \frac{X}{X_L} \right\}^2 \dots \dots \dots 40$$

The friction factor λ will be that corresponding to the Reynold's Number associated with the annulus mass flow. This is arrived at in a similar manner to the development of the friction equation.

During flow of a single-phase fluid, Reynold's Number is defined as

$$Re_1 = \frac{\rho_1 \cdot d \cdot U}{\mu_1} \dots \dots \dots 41$$

If U_1 is the flow in an annular cross-sectional area of the tube where $U_1 = \frac{U}{\bar{a}}$ then

$$Re_1 = \frac{\rho_1 \cdot d \cdot \bar{a} \cdot U_1}{\mu_1} \dots \dots \dots 42$$

During two-phase flow it may therefore be assumed that for a velocity U_1 in the annular ring

$$Re_2 = \frac{\rho_1 \cdot d \cdot \bar{a} \cdot U_1}{\mu_1} \dots \dots \dots 43$$

Now

$$U_L = U_1 \cdot \frac{1-q}{1-q-\omega+\omega/k_2} \dots \dots \dots A11$$

$$\rho_1 = \rho_L \dots \dots \dots 9$$

and

$$\mu_1 = \mu_L \dots \dots \dots 44$$

Substituting the above equations gives

$$Re_2 = \left\{ \bar{a} \frac{1-q-\omega+\omega/k_2}{1-q} \right\} \cdot \frac{\rho_L \cdot d \cdot U_L}{\mu_L} \dots \dots \dots 45$$

Here again the bracketed term may be assumed unity giving

$$Re_2 = \frac{\rho_L \cdot d \cdot U_L}{\mu_L} \dots \dots \dots 46$$

This is the Reynold's Number used in evaluating the friction factor λ .

16. PRESSURE CHANGE DUE TO MIXTURE WEIGHT.

The weight of mixture over a length δl is balanced by the pressure change along the tube, i.e.

$$-\left(\frac{dp}{dl}\right)_{\rho_2} \cdot \delta l \cdot X = \left\{ X_1 \cdot \delta l \cdot \rho_1 + X_2 \cdot \delta l \cdot \rho_2 \right\} \sin \theta \dots 47$$

where the equation is developed from consideration of the annulus and core weight, during upward flow.

This may also be written

$$-\left(\frac{dp}{dl}\right)_{\rho_2} \cdot \delta l \cdot X = \left\{ X_L \cdot \delta l \cdot \rho_L + X_G \cdot \delta l \cdot \rho_G \right\} \sin \theta \dots 48$$

where the equation is developed from consideration of the gas and liquid weight.

The final form is the same from either starting point.

Equation 48 reduces to

$$-\left(\frac{dp}{dl}\right)_{\rho_2} = \left\{ \frac{X_L}{X} \cdot \rho_L + \frac{X_G}{X} \cdot \rho_G \right\} \sin \theta \dots 49$$

Substituting Equation A12, and A13, from Appendix A for $\frac{X_G}{X}$ and $\frac{X_L}{X}$ respectively gives finally

$$-\left(\frac{dp}{dl}\right)_{\rho_2} = \left\{ \frac{q + K(1-q)}{q/\rho_G + K(1-q)/\rho_L} \right\} \sin \theta \dots 50$$

17. PRESSURE CHANGES DUE TO MOMENTUM FORCES.

The equations may be developed using either the core and annulus velocities or the gas and liquid velocities. The equations will differ from either starting point due to the use of mean velocities, rather than the root of the mean square velocities. The equation developed using the core annulus velocities would presumably more closely approach the actual values as it allows more completely for the variation in liquid velocity. However, as the application of these equations would necessitate a knowledge of the water concentration w , the more approximate equations developed from the gas and liquid velocities are used.

These equations are now developed considering the momentum change over an element of length δl . Second order differentials are neglected.

The liquid momentum rate at the beginning of the element is

$$\frac{(1-q)}{q} \cdot M \cdot U_L$$

The gas momentum rate at the beginning of the element is

$$\frac{q}{q} \cdot M \cdot U_G$$

The liquid momentum rate at the end of the element is

$$\frac{(1-q-\delta q)}{q} \cdot M \cdot (U_L + \delta U_L) = \frac{(1-q)}{q} \cdot M \cdot U_L + \frac{(1-q)}{q} \cdot M \cdot \delta U_L + \frac{\delta q}{q} \cdot M \cdot U_L$$

The gas momentum rate at the end of the element is

$$\frac{(q+\delta q)}{q} \cdot M \cdot (U_G + \delta U_G) = \frac{q}{q} \cdot M \cdot U_G + \frac{q}{q} \cdot M \cdot \delta U_G + \frac{\delta q}{q} \cdot M \cdot U_G$$

The rate of change of momentum is therefore

$$\frac{q}{g} \cdot M \cdot \delta U_a + \frac{q}{g} \cdot M \cdot \delta U_L + \frac{\delta q}{g} \cdot M (U_a - U_L)$$

Hence if $\left(\frac{db}{dl}\right)_{M_2}$ is the pressure gradient due to momentum forces

$$-\left(\frac{db}{dl}\right)_{M_2} \cdot X \cdot \delta l = \frac{q}{g} \cdot M \cdot \delta U_a + \frac{1-q}{g} \cdot M \cdot \delta U_L + \frac{\delta q}{g} \cdot M (U_a - U_L) \dots 51$$

which gives

$$-\left(\frac{db}{dl}\right)_{M_2} = \frac{1}{\delta l} \left[\frac{q}{g} \cdot \frac{M}{X} \cdot \delta U_a + \frac{1-q}{g} \cdot \frac{M}{X} \cdot \delta U_L + \frac{\delta q}{g} \cdot \frac{M}{X} (U_a - U_L) \right] \dots 52$$

18. COMBINED EQUATIONS AND SOLUTION.

During two-phase flow the total pressure change during the upward flow of the mixture is determined by combining Equations 38, 50 and 52

$$\begin{aligned}
 -\left(\frac{dp}{dl}\right)_2 \cdot \delta l &= -\left(\frac{dp}{dl}\right)_{F2} \cdot \delta l - \left(\frac{dp}{dl}\right)_{P2} \cdot \delta l - \left(\frac{dp}{dl}\right)_{M2} \cdot \delta l \\
 &= \frac{\lambda \cdot \delta l \cdot U_L^2 \cdot \rho_L}{2g \cdot d} + \left\{ \frac{q + K(1-q)}{q/\rho_G + K(1-q)/\rho_L} \right\} \delta l \cdot \sin \theta \\
 &+ \left\{ \frac{q}{g} \cdot \frac{M}{X} \delta U_G + \frac{1-q}{g} \cdot \frac{M}{X} \delta U_L + \frac{\delta q}{g} \cdot \frac{M}{X} (U_G - U_L) \right\} \dots \dots \dots 53
 \end{aligned}$$

The velocity ratio K is obtained from Equations 23 and 38 in the form

$$K = 1 + Z \sqrt{\frac{\rho_L \left(\frac{dp}{dl} \right)_2 + \rho_G \sin \theta + \rho_G \frac{U_2 \delta U_2}{\delta l \cdot g}}{\rho_G - \frac{\lambda \cdot U_L^2 \cdot \rho_L}{2g \cdot d}}} \dots \dots \dots 54$$

The method of solution is a trial and error process whereby for various assumed values of K the pressure change is first calculated, and then a theoretical value calculated for K from Equation 54. The correct solution is found when the assumed and calculated values of agree.

Where upward flow in vertical tubes occurs and there are no momentum forces, Equation 53 reduces to

$$-\left(\frac{dp}{dl}\right)_2 \cdot \delta l = \frac{\lambda \cdot \delta l \cdot U_L^2 \cdot \rho_L}{2g \cdot d} + \left\{ \frac{q + K(1-q)}{q/\rho_G + K(1-q)/\rho_L} \right\} \delta l \dots \dots 55$$

and Equation 54 to

$$K = 1 + Z \sqrt{\frac{\rho_L \left(\frac{dp}{dl} \right)_2 + \rho_G}{\rho_G - \frac{\lambda \cdot U_L^2 \cdot \rho_L}{2g \cdot d}}} \dots \dots \dots 56$$

Where/

Where the flow is vertically downwards and there are no momentum forces the equations are slightly changed as $\sin \theta$ is now -1 in contrast to the positive value of unity when the flow is up a vertical tube.

Equation 53 becomes

$$-\left(\frac{dp}{dl}\right)_2 \cdot sl = \frac{\lambda \cdot sl \cdot u_L^2 \cdot \rho_L}{2g \cdot d} - \left\{ \frac{q + K(1-q)}{q/\rho_a + K(1-q)/\rho_L} \right\} sl \dots \dots \dots 57$$

and Equation 54 (See Section 14)

$$K = 1 \pm Z \sqrt{\frac{\rho_L + \left[\left(\frac{dp}{dl}\right)_2 - \rho_a \right]}{\rho_a - \frac{\lambda \cdot u_L^2 \cdot \rho_L}{2g \cdot d}}} \dots \dots \dots 58$$

PART IV.APPLICATION OF THE PROPOSED THEORY TO
THE ANALYSIS OF THE EXPERIMENTAL DATA OF
PREVIOUS INVESTIGATORS.

	<u>Page.</u>
19. Liquid concentration in core (Armand's experiments)	87.
20. Friction during air-water flow (Martinelli's experiments) 	91.
21. Pressure change during the flow of steam-water mixtures in vertical tubes (Schwab's experiments)	94.
22. Pressure changes during the downward flow of air-water mixtures in vertical tubes (Bergelin's experiments) 	98.
23. "Stagnation" point during flow in downcomers (Lowenstein's experiments) 	103.

INTRODUCTION.

The theoretical equations just developed are applied in this section to the analysis of results from previous investigators.

19. LIQUID CONCENTRATION IN CORE
(ARMAND'S EXPERIMENTS)

An approximate check on the validity of Equation 12, viz:

$$K = 1 + \frac{U_3}{U_1} \cdot \frac{1-q-\omega+\omega/k_2}{1-q} \sqrt{\frac{q}{q+\omega} \cdot \frac{\rho_L}{\rho_G} \cdot \frac{T_2}{T_1}}$$

is obtained by using it to analyse the results obtained by Armand for air-water mixtures flowing through smooth horizontal tubes. (Figure 12)

As the tests were carried out in the horizontal plane $\frac{T_2}{T_1} = 1$ (Equation 19). Also as ω is small $(1-q-\omega+\omega/k_2)/(1-q)$ may be assumed unity. This reduces Equation 12 to

$$K = 1 + \frac{U_3}{U_1} \sqrt{\frac{q}{q+\omega} \cdot \frac{\rho_L}{\rho_G}} \dots \dots \dots 59$$

Armand weighed the tube while the two-phase mixture flowed, from which it was possible to determine the cross-sectional areas occupied by the respective phases. From this data the author determined the velocity ratio K as shown in Appendix D.

The ratio U_3/U_1 can be calculated from a single-phase velocity profile, and it will be that corresponding to the Reynold's Number in the annulus. As the variation of U_3/U_1 with Reynold's Number is slight, all values used correspond to a Reynold's Number of 105,000. This is an approximate mean value of Reynold's Number during the/

the tests.

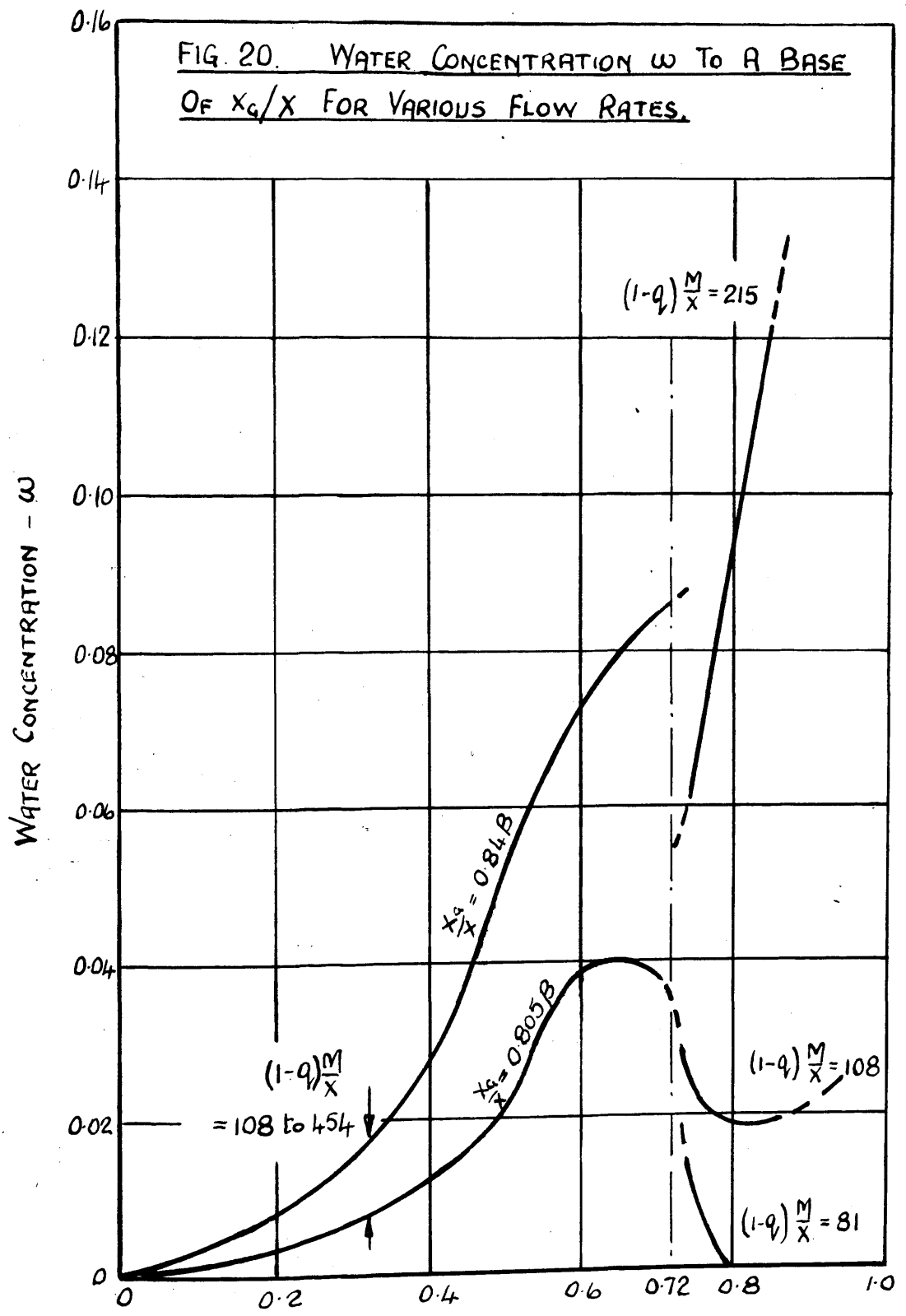
Armand measured the respective flow rates of air and water, hence q is known, and consequently the only unknown in Equation 59 is the water content ω of the core. This was evaluated and plotted to a base of the ratio of gas to tube cross-sectional areas in Figure 20. A specimen calculation is given in Appendix D.

Discussion.

The small magnitude of the water concentration throughout is consistent with the assumptions made in developing the theory.

Above $\frac{X_g}{X} = 0.72$ there is a marked variation of the water content with the water flow rate. The increasing water concentration in this region with increasing mass flow is due to the greater turbulence with larger flows. The increased turbulence will increase the mixing between the phases. The concentration ω in the core decreases to zero with decreasing water flow rates, and, in fact, slightly negative water concentrations are obtained with the smallest experimental mass flow. This is, no doubt, due to the approximate nature of the equations, and the most likely explanation lies in the ratio of the Prandtl mixing lengths l_1/l_2 being assumed unity.

Below $\frac{X_g}{X} = 0.72$ it was not possible to discern a variation of the experimental data with mass flow rate. It is probable that a variation with flow rate exists in this region also, but that the experimental technique lacked



$\frac{X_G}{X}$ - RATIO OF THE GAS TO TUBE CROSS-SECTIONAL AREA.

the necessary sensitivity. The majority of the experimental results on Figure 12 lie between lines represented by the equations $\frac{X_c}{X} = 0.84\beta$ and $\frac{X_g}{X} = 0.805\beta$ and the water concentration has been determined for these two cases. The magnitude of the water concentration throughout indicates the equations are approximately true.

The results analysed in this section are those obtained by Martinelli for the flow of air-water mixtures through horizontal tubes.

In Section 15 the pressure drop due to friction has been obtained in the form (Equation 40)

$$-\left(\frac{dp}{dl}\right)_{F2} \cdot \delta l = G \cdot \frac{\lambda \cdot \delta l}{2g \cdot d} \left(\frac{1-q}{1} \frac{M}{X}\right)^2 \frac{1}{\rho_L} \left(\frac{X}{X_L}\right)^2$$

Regrouping and substituting n for the power of $\frac{X}{X_L}$

$$-\left(\frac{dp}{dl}\right)_{F2} / \frac{\lambda}{2g \cdot d} \left(\frac{1-q}{1} \frac{M}{X}\right)^2 \frac{1}{\rho_L} = G \left(\frac{X}{X_L}\right)^n \dots \dots \dots 60$$

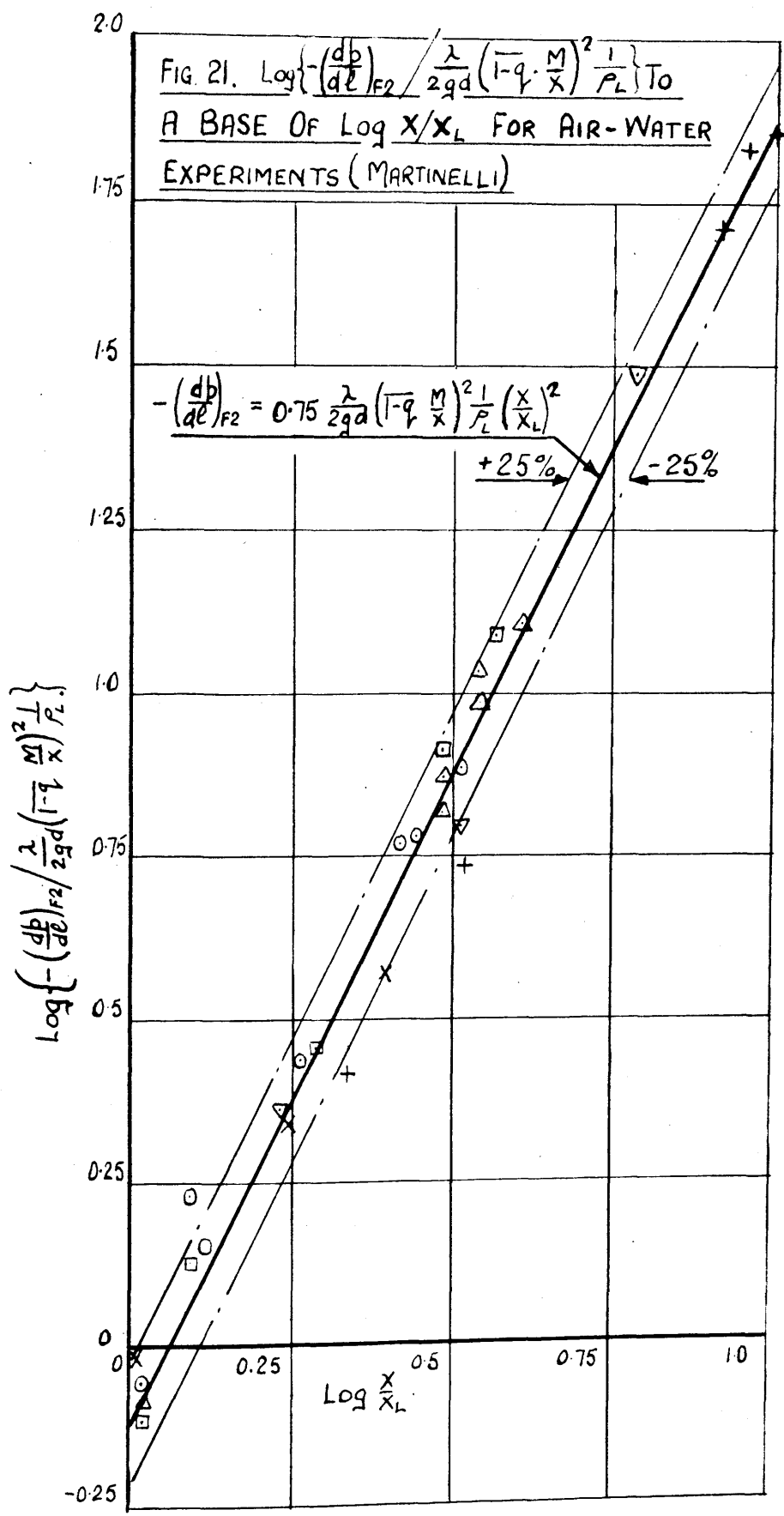
In logarithmic form this is

$$\text{Log} \left\{ -\left(\frac{dp}{dl}\right)_{F2} / \frac{\lambda}{2g \cdot d} \left(\frac{1-q}{1} \frac{M}{X}\right)^2 \frac{1}{\rho_L} \right\} = \text{Log } G + n \text{Log} \left(\frac{X}{X_L}\right) \dots \dots \dots 61$$

In view of this relationship Martinelli's results were graphed using $\log \left\{ \left(\frac{dp}{dl}\right)_{F2} / \frac{\lambda}{2g \cdot d} \left(\frac{1-q}{1} \frac{M}{X}\right)^2 \frac{1}{\rho_L} \right\}$ as the vertical axis, and $\log X/X_L$ as the base. In this manner if the results lie on a single line, the slope of the line represents n and the value of G will be the value of $-\left(\frac{dp}{dl}\right)_{F2} / \frac{\lambda}{2g \cdot d} \left(\frac{1-q}{1} \frac{M}{X}\right)^2 \frac{1}{\rho_L}$ when X/X_L is zero.

In evaluating X/X_L the velocity ratio K is assumed that obtained from Armand's experiments for air-water mixtures flowing under similar conditions.

The results are shown in Figure 21. The slope of the line through the experimental results is 2 and G is 0.75, i.e. a mean line through the experimental points represents/



- x 4.5 lb/sec.
- o 3 lb/sec.
- 2 lb/sec.
- △ 1.5 lb/sec.
- ▽ 1 lb/sec.
- + 0.7 lb/sec.

represents the equation

$$-\left(\frac{db}{dl}\right)_{F_2} \cdot \delta l = 0.75 \frac{\lambda \cdot \delta l}{2g \cdot d} \left(\frac{1-q}{x}\right)^2 \frac{1}{\rho_L} \left(\frac{x}{x_L}\right)^2$$

All but three of the test results lie within 25% of the mean line.

The value of G is rather further from unity than expected though it is sufficiently close to confirm on a broad basis the reasoning leading to Equation 40, as does also the slope of the mean line through the experimental points.

21. PRESSURE CHANGE DURING THE FLOW OF
STEAM-WATER MIXTURES IN VERTICAL TUBES.
(SCHWAB'S EXPERIMENTS)

The theory developed in Parts II and III of this report is applied to the analysis of results given by Schwab for the adiabatic flow of steam-water mixtures in vertical tubes.

The pressure gradients during the various flow conditions are small enough to allow the changes in steam density and in mixture quality to be neglected, with the result that the pressure change may be considered as due solely to the mixture weight and to friction, the momentum forces being neglected.

The pressure change is (Equation 55)

$$-\left(\frac{dp}{dl}\right)_2 \cdot sl = \frac{\lambda \cdot sl \cdot u_L^2 \cdot \rho_L}{2g \cdot d} + \left\{ \frac{q + K(1-q)}{q/\rho_g + K(1-q)/\rho_L} \right\} sl$$

The friction factor λ is that corresponding to a Reynold's Number $Re_2 = \frac{\rho_L \cdot d \cdot u_L}{\mu_L}$

The velocity ratio K is determined using Equation 56

$$K = 1 + Z \sqrt{\frac{\rho_L}{\rho_g} \cdot \frac{\left(\frac{dp}{dl}\right)_2 + \rho_g}{-\frac{\lambda \cdot u_L^2 \cdot \rho_L}{2g \cdot d}}}$$

where the Z term is that obtained from experiments with air-water mixtures as given in Figure 15.

The theoretical pressure change and velocity ratio are those which make Equations 55 and 56 compatible. The values obtained are given in Tables 1 and 2 where, to facilitate comparison, the pressure change actually measured/

TABLE I.PRESSURE 172 lb/ft² GAUGE.

TUBE 1" BORE.

TEST No.	M/x lb/sec.ft ²	DRYNESS FRACTION. q	STEAM- WATER VELOCITY RATIO K	PRESSURE CHANGE lb/ft ² .		
				MEASURED	CALCULATED - PROPOSED THEORY	CALCULATED - STANDARD THEORY.
1	35.5	0.0742	4.15	0.102	0.114	0.0415
2	62.9	0.105	5.7	0.114	0.119	0.042
3		0.0585	3.15	0.119	0.122	0.053
4		0.0212	2.08	0.154	0.169	0.106
5	107.5	0.148	4.5	0.184/0.201	0.162	0.08
6		0.0665	2.95	0.153	0.15	0.072
7		0.0248	1.8	0.163	0.166	0.102
8	143	0.11	3.1	0.241	0.248	0.114
9		0.041	2.1	0.184	0.185	0.096
10	177.5	0.0875	2.45	0.266/0.284	0.352	0.141
11		0.0382	2.0	0.21/0.219	0.222	0.116
12		0.0128	1.45	0.228	0.229	0.164
13	218	0.0312	1.75	0.251	0.27	0.142
14		0.0116	1.4	0.254	0.246	0.183
15	286.5	0.0158	1.4	0.306/0.297	0.302	0.193
16		0.007	1.3	0.306	0.297	0.24

TABLE II

PRESSURE 1615 lb/□" GAUGE

TUBE 1" BORE.

TEST No.	M/x lb/sec.ft ²	DRYNESS FRACTION q	STEAM-WATER VELOCITY RATIO K	PRESSURE CHANGE		1b/□" ft.
				MEASURED.	CALCULATED - PROPOSED THEORY.	
17	36.9	0.306	1.78	0.096	0.106	0.0785
18		0.1985	1.5	0.115	0.127	0.104
19	73.8	0.306	1.75	0.108/0.110	0.117	0.087
20		0.225	1.32	0.118	0.127	0.105
21		0.135	1.22	0.146	0.151	0.136
22		0.09	1.19	0.181	0.177	0.164
23		0.0719	1.18	0.19/0.192	0.191	0.179
24		104	0.224	1.28	0.133	0.138
25	0.141		1.18	0.157	0.156	0.141
26	0.051		1.14	0.206/0.211	0.213	0.206
27	134	0.173	1.18	0.152/0.156	0.165	0.14
28		0.109	1.13	0.177/0.179	0.179	0.166
29		0.040	1.10	0.229	0.232	0.228
30	164	0.142	1.14	0.172/0.176	0.183	0.164
31		0.101	1.10	0.195/0.199	0.193	0.181
32		0.037	1.08	0.238	0.24	0.238
33	206.5	0.116	1.10	0.21	0.219	0.196
34		0.0825	1.09	0.224	0.218	0.21
35	274	0.0876	1.08	0.257	0.254	0.244
36		0.0571	1.07	0.258	0.26	0.261

PRESSURE 1615 lb/□" GAUGE.

TUBE 2.2" BORE.

37	52	0.083	1.42	0.176	0.188	0.165
38		0.0563	1.40	0.20	0.211	0.192
39		0.0367	1.35	0.224	0.232	0.217
40	78	0.0605	1.27	0.20	0.213	0.199
41		0.0409	1.25	0.212/0.215	0.224	0.212
42		0.0256	1.20	0.236/0.238	0.244	0.236
43	96.8	0.0381	1.20	0.219/0.222	0.255	0.217
44		0.0305	1.19	0.228/0.232	0.237	0.23

measured is tabulated alongside the values calculated for both the proposed theory and the standard homogeneous flow theory.

The latter theory gives the equation for the pressure change in the form.

$$-\left(\frac{dp}{dl}\right)_2 \cdot \delta l = \frac{\lambda \cdot \delta l \cdot U^2}{2g \cdot d \left(\frac{q}{\rho_a} + \frac{(1-q)}{\rho_L} \right)} + \frac{\delta l}{\frac{q}{\rho_a} + \frac{(1-q)}{\rho_L}}$$

where the velocity U is obtained from the equation

$$U = \frac{M}{X} \left(\frac{q}{\rho_a} + \frac{1-q}{\rho_L} \right)$$

Lewis and Robertson suggested the value of λ be assumed 0.02, and this value has been used throughout where the homogeneous theory has been used.

The methods of calculation are shown in Appendix H.

Discussion.

The proposed theory gives good agreement with the experimental results, the maximum error, with the exception of Test No. 10, being of the order of 14%, whereas with the homogeneous theory the error is as much as 60%. As might be expected, where K approaches unity the error with either theory is small.

It will be observed that the maximum value of K is 5.7 with a minimum value close to 1. In general the velocity ratio decreases with increasing pressure, due to the increase in steam density.

22. PRESSURE CHANGE DURING THE DOWNWARD FLOW
OF AIR-WATER MIXTURES.
(BERGELIN'S EXPERIMENTS).

Where mixtures flow downward in smooth vertical tubes with no inertia forces, the pressure change is determined using Equation 57.

$$-\left(\frac{dp}{dl}\right)_2 \cdot \delta l = \frac{\lambda \cdot \delta l \cdot U_L^2 \cdot \rho_L}{2g \cdot d} - \left\{ \frac{q + K(1-q)}{q/\rho_G + K(1-q)/\rho_L} \right\} \delta l$$

The velocity ratio is obtained from Equation 58

$$K = 1 \pm Z \sqrt{\frac{\rho_L \pm \left[\left(\frac{dp}{dl}\right)_2 - \rho_G \right]}{\rho_G - \frac{\lambda \cdot U_L^2 \cdot \rho_L}{2g \cdot d}}}$$

where

$$Z = \frac{U_3}{U_1} \cdot \frac{1-q-\omega + \omega/K_2}{1-q} \sqrt{\frac{q}{q+\omega}} \dots \dots \dots 63$$

In the experiments of Bergelin, conditions at entry to the pipe tend to ensure that the liquid flowed down the tube wall. The liquid mass flow rates and the probable gas to tube cross-sectional ratios are of such an order that from the analysis contained in Section 19 it would appear likely that there would be little mixing between the phases. As the water concentration ω is therefore small it is possible to reduce Equation 63 to

$$Z = \frac{U_3}{U_1} \dots \dots \dots 64$$

Hence Equation 58 becomes

$$K = 1 \pm \frac{U_3}{U_1} \sqrt{\frac{\rho_L \pm \left[\left(\frac{dp}{dl}\right)_2 - \rho_G \right]}{\rho_G - \frac{\lambda \cdot U_L^2 \cdot \rho_L}{2g \cdot d}}} \dots \dots \dots 65$$

It is essential to reduce the equation to this form as the Z curve (Figure 15) does not cover the necessary range of liquid mass flows or gas to tube cross-sectional ratios. The values of U_3/U_1 are determined from the single-phase velocity profile during flow through smooth tubes.

The solution of the equations is similar to that used in the analysis of steam-water flow in the preceding section, the theoretical values of the pressure change and velocity ratio being those which make Equations 57 and 65 compatible. A detailed calculation is given in Appendix E.

The theoretical values of the pressure change are compared with the experimental values in Figure 22 where they are plotted to a base of air flow rate for various water flow rates.

The theoretical values of the velocity ratio K are plotted to similar axes in Figure 23, where they are compared with the velocity ratio values which, on substitution in Equation 57, would give the experimental pressure change. This latter velocity ratio is referred to hereafter as the experimental value of the velocity ratio.

In the region where the line through the experimental points is represented by a dotted line the pressure gradient varied along the pipe length. In this region the velocity ratio K is presumably changing along the tube length, with an interchange of kinetic energy between the phases. It is not possible to allow for this in the analysis.

Discussion /

FIG. 22. PRESSURE CHANGE DURING THE DOWNWARD FLOW OF AIR-WATER MIXTURES IN VERTICAL TUBES TO A BASE OF AIR FLOW FOR VARIOUS WATER FLOW RATES.

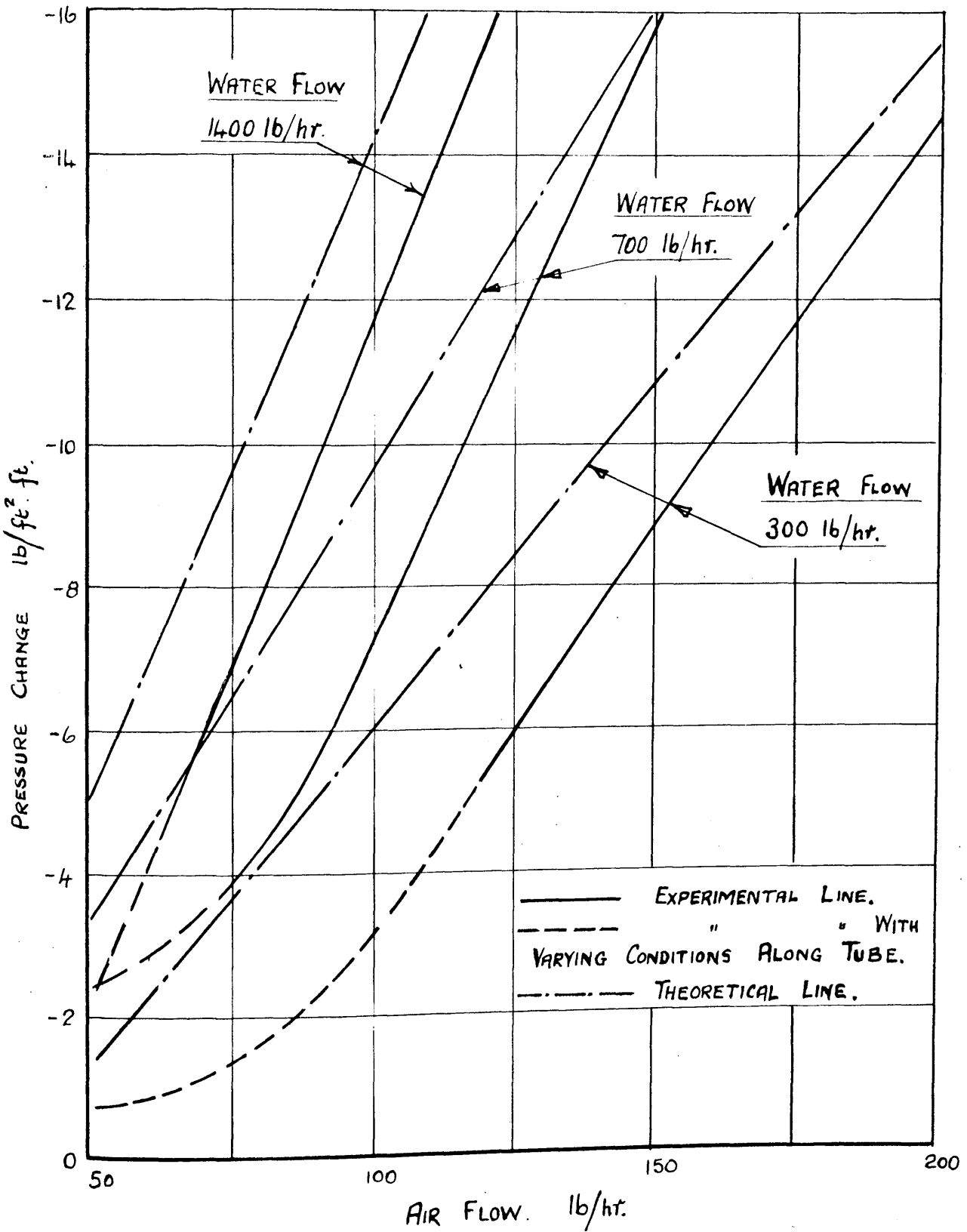
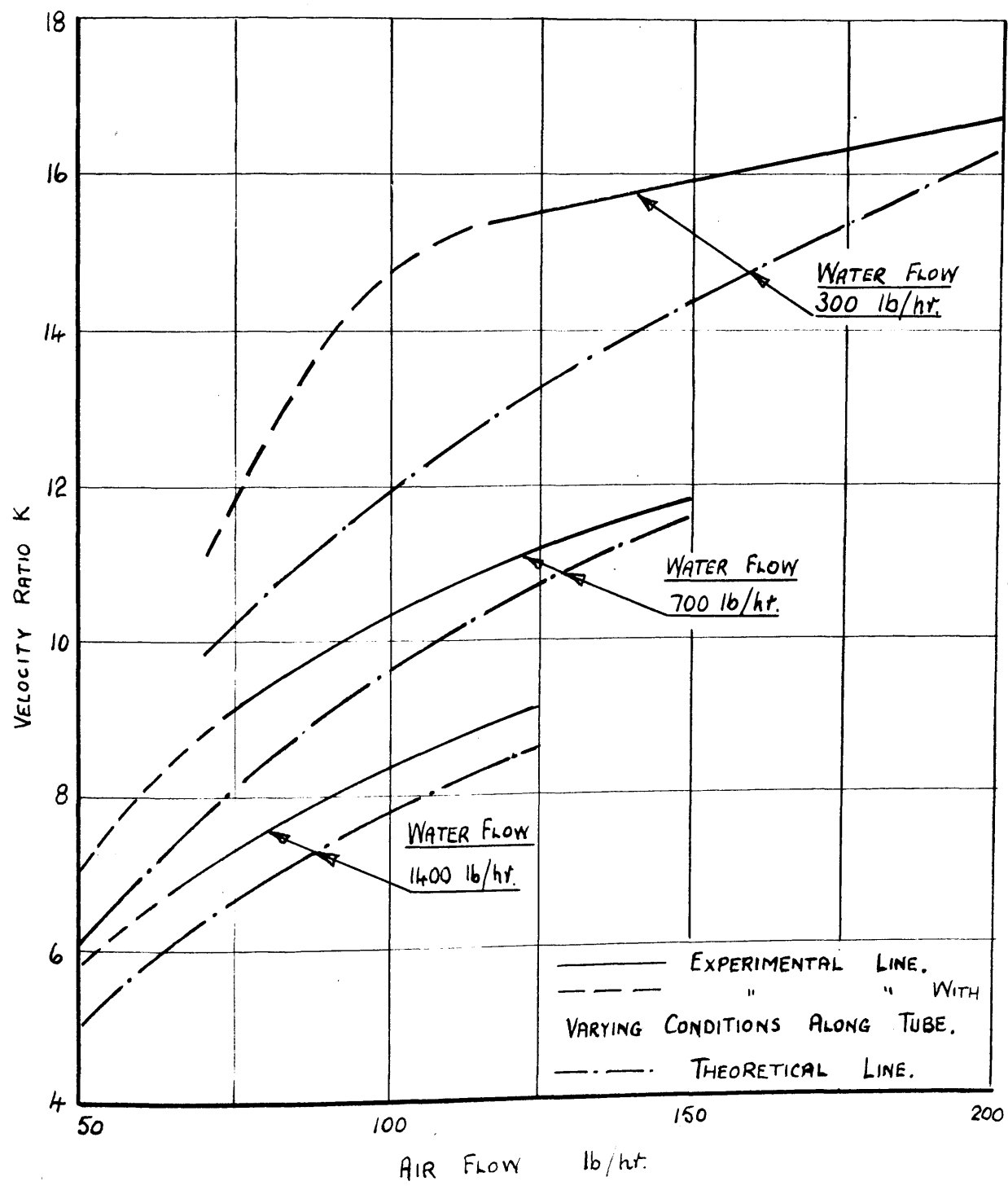


FIG. 23. THE AIR-WATER VELOCITY RATIO K TO A BASE OF AIR FLOW FOR VARIOUS WATER FLOW RATES



Outwith the region where the velocity ratio appears to vary along the tube length, the theoretical values of the pressure change agree with the experimental values within - 62%. This agreement is not as satisfactory as that obtained by Bergelin using Martinelli's Theory which gave agreement within $\pm 30\%$. It should be remembered, however, that Martinelli's approach is empirical.

The agreement obtained by the application of the Martinelli Theory to vertical tubes would appear fortuitous, as the pressure change due to the weight of the mixture has not been introduced. The reasoning behind this omission would appear to be that the equations give the friction pressure change in the air phase, and that, as the weight of the air is negligible, this will be the total pressure change. This approach would appear fundamentally unsound.

With the proposed theory the mixture weight has an appreciable influence. For example, where the water and air flow rates are 1400, and 80 lb/hr. respectively, the friction pressure change and the mixture weight pressure change are 18.6 and 8 lb/ft² ft. respectively, giving the resultant pressure change as 10.6 lb/ft² ft. as compared with the experimental value of 7.9 lb/ft² ft.

The values of the theoretical and experimental velocity ratios outwith the region where conditions vary along the tube, agree within 20%, which gives further confirmation of the equation enabling the determination of the velocity ratio.

Under certain conditions natural circulation in a water-tube boiler breaks down completely, the riser tube no longer receiving sufficient water from the downcomer tubes. This condition is referred to as stagnation, and Lowenstein, after an extensive experimental investigation with a two-tube boiler, concluded that this can be due to two causes. Firstly, due to an excessive evaporation rate in the downcomer, the steam forms a restriction such that insufficient water passes down the downcomer tube. Secondly, due to a considerably smaller evaporation rate, where the steam velocity is zero, the steam forms with continued evaporation, a restriction in the downcomer as in the first case. The steam velocity will be zero when the upward flow of the steam relative to the water equals the downward water velocity.

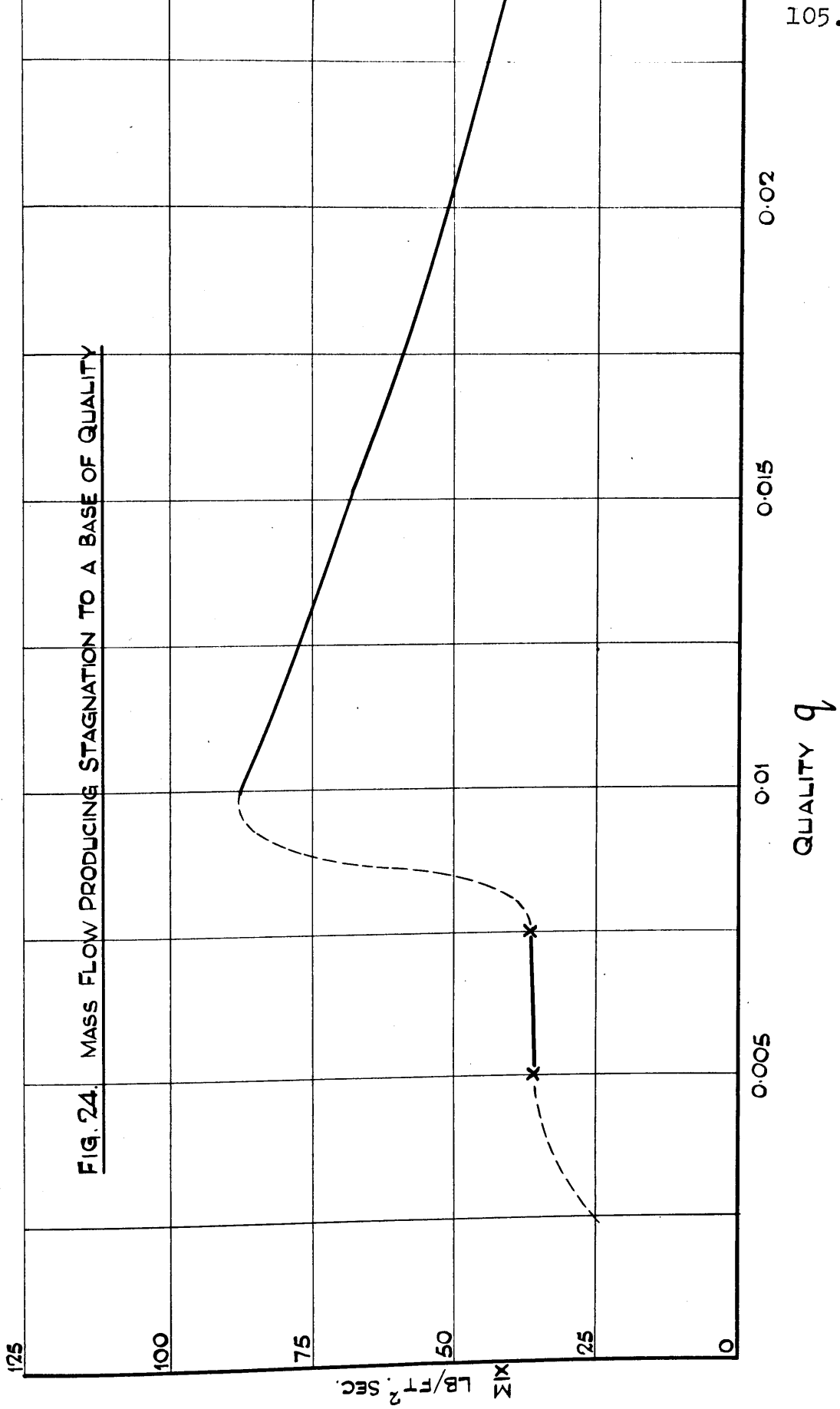
In attempting to obtain stagnation due to the latter cause, Lowenstein produced evaporation in the downcomer by subjecting the boiler to pressure drops from a pressure of 60 atmospheres to 40 atmospheres. Lowenstein found that where the mass flow in the downcomer before commencing the pressure drop was in the region of 95.8 to 103.5 lb/ft.² sec., circulation was maintained as the steam flowed downwards with the water. Where the mass flow was initially 50.6 to 60.5 lb/ft².sec., circulation continued as the steam flowed upwards to the steam drum. Where the mass flow was initially 80.3 to 87.9 lb/ft.² sec., the steam velocity was in/

in the vicinity of zero, with the result that the downcomer tube was blocked. The results do not indicate the precise mass flow at which the steam velocity is zero as the mass flows quoted are those present prior to the pressure drop. It is to be assumed that the evaporation produced would tend to reduce the mass flow in the downcomer. Therefore, it can only be said with certainty that the velocity of the steam in the downcomer will be zero for certain mass flow rates less than $87.9 \text{ lb/ft.}^2 \text{ sec.}$ This will naturally only apply with the tube diameter (1.18 in.) and pressure region investigated by Lowenstein.

It is of interest to investigate the theoretical stagnation point. In applying the theoretical equation it is not possible to apply the equation to the limiting condition where the steam velocity is zero, i.e. where the velocity ratio $K = 0$. The theoretical equations are applied to find the mass flow in the downcomer compatible with $K = 0.1$, this being an approximation to the condition when the steam velocity is zero. The procedure is detailed in Appendix F, the calculations assuming a pressure of 50 atmospheres.

The theoretical mass flows giving $K = 0.1$ are shown in Figure 24 to a base of mixture quality. The change in the mass flow curve at $q = 0.009$ is associated with the critical Z value at $\frac{X_g}{X} = 0.72$. The range of quality investigated is limited by the range of the $Z - \frac{X_g}{X}$ curve.

Figure 24 suggests that the critical condition occurs with/



with mass flows in the region from 36.6 to 88 lb/ft.² sec., which agrees with the observations of Lowenstein. It is not suggested that the proposed equations will give an accurate solution to the problem of stagnation. For one thing, the Prandtl mixing length distribution when K is near zero is a matter of some conjecture. However, the agreement obtained with experimental observation for this limiting condition gives valuable confirmation of the general form of the equations.

PART V.

TWO-TUBE BOILER:

TEST EQUIPMENT, PROCEDURE AND RESULTS.

	<u>Page</u>
24. B.S.R.A. experimental boiler	108.
25. Instrumentation	114.
26. Calibration tests	117.
27. Test programme, procedure and specimen readings	122.
28. Conversion and interpretation of test readings	125.
29. Test results	131.

24. BRITISH SHIPBUILDING RESEARCH ASSOCIATION
EXPERIMENTAL BOILER.

The plant was designed to enable the investigation of the fundamental laws governing natural circulation. It consists of a two-tube water-tube boiler designed for a maximum working pressure of 1500 lb/in.² and a maximum heat transfer rate of 120,000 B. Th.U/ft.² hr. over a heated length of 10'6" with a tube 2 $\frac{1}{4}$ " O.D.

The plant operates on a simple closed system, the steam generated being condensed in a condenser integral with the steam drum, the condensate refluxing into the steam drum. Boiler. The steam drum is 23" internal diameter and 5'9 $\frac{1}{2}$ " long, and the water drum is 10" internal diameter and 6'0" long.

The steam drum has, in addition to the usual manholes and mountings, a 4" bore stand pipe to take the integral condenser, which stands vertically above the drum. The stand pipes for the riser and downcomer tubes take internal sleeves so that the internal tube diameters may be uniform throughout. The internal sleeve for the downcomer tube stops 10" below mid-drum level, and for the riser 3" above mid-drum level. This ensures above water discharge from the tube.

The water drum is fitted with inspection doors, stand pipes for tubes, and blow down valve.

The downcomer and riser tubes each consist of a 13 foot length of tube, 2 $\frac{1}{4}$ " O.D. and 1.698" I.D. flanged at both/

both ends to 1'0" long distance pieces. The distance pieces are introduced to carry pressure tapping points, thermocouple pockets and Pitot tubes. The system is shown in Figures 25 and 26.

Integral Condenser. The condenser is fitted directly above the steam drum. It comprises a single tube $6\frac{1}{4}$ " O.D., $5\frac{1}{2}$ " I.D. and 5'6" long, surrounded by an annular cooling water jacket. The cooling water enters the bottom of the annulus discharges at any one of four exit pipes fitted at 12" intervals up the length of the condenser. Exit valves allow the effective cooling surface to be varied. The cooling water flow is controlled by a hand operated stop valve with a small bye-pass valve for fine adjustment. The system is indicated in Figure 27.

Furnace. The furnace space, 18" square and 10'6" long, is surrounded on all sides by a 9" thick insulating refractory lining backed by a steel shell. The heating elements are silica carbide "Globars" 1" diameter, 39" long, of which the mid 20" length is the effective heating portion. They are placed horizontally along each 18" side of the furnace space pitched vertically at 3" centres. Thus the "Globars" form a cage approximately 15" square by 10'6" high with the riser tube passing through the centre.

Six copper bus-bars are carried on insulators up each outside face of the furnace and flexible connections are taken from these to the "Globalar" ends to which they are secured by metal clips. The connections are so arranged that/

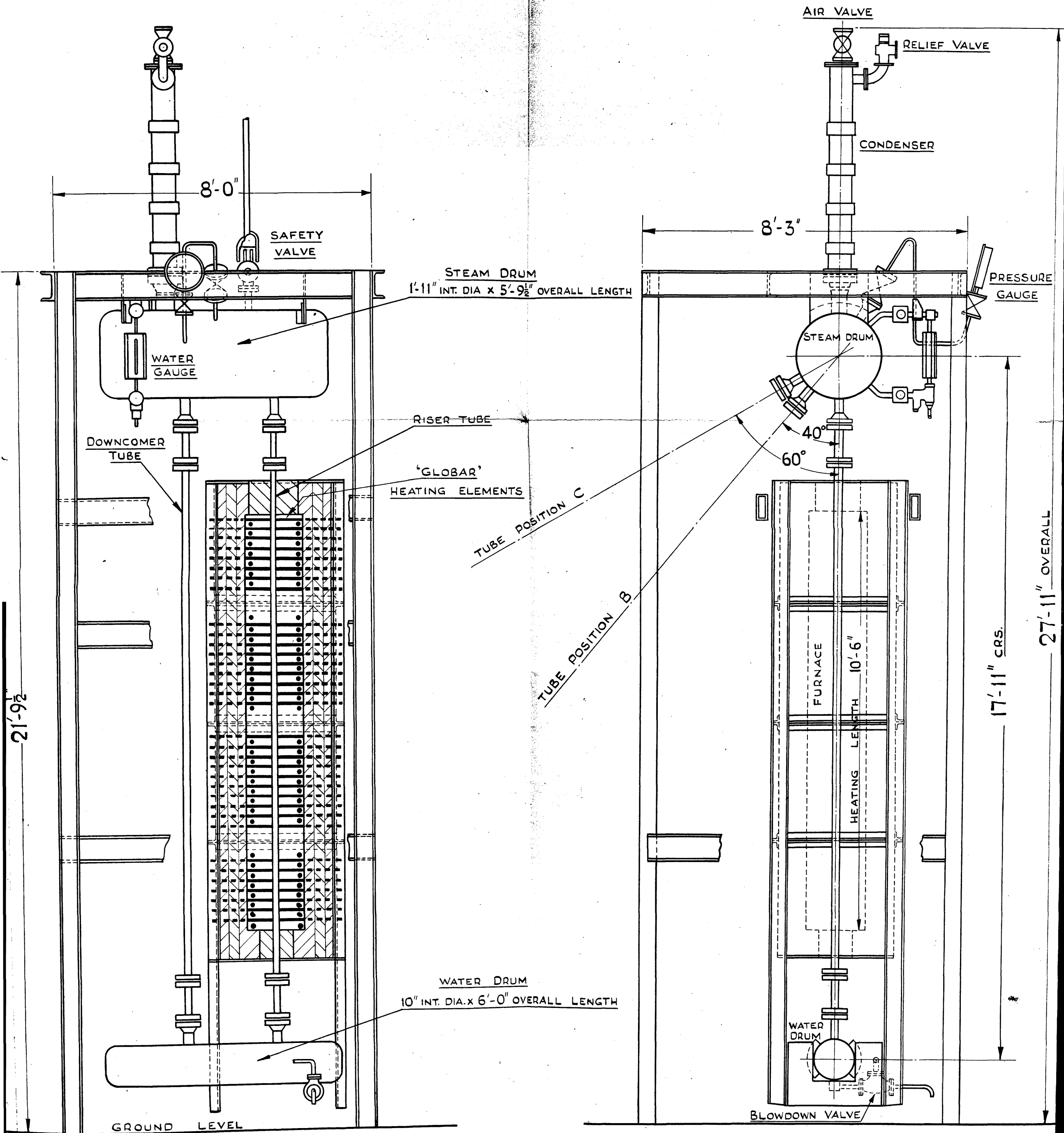


FIG. 25. SKETCH OF B.S.R.A. EXPERIMENTAL BOILER & FURNACE

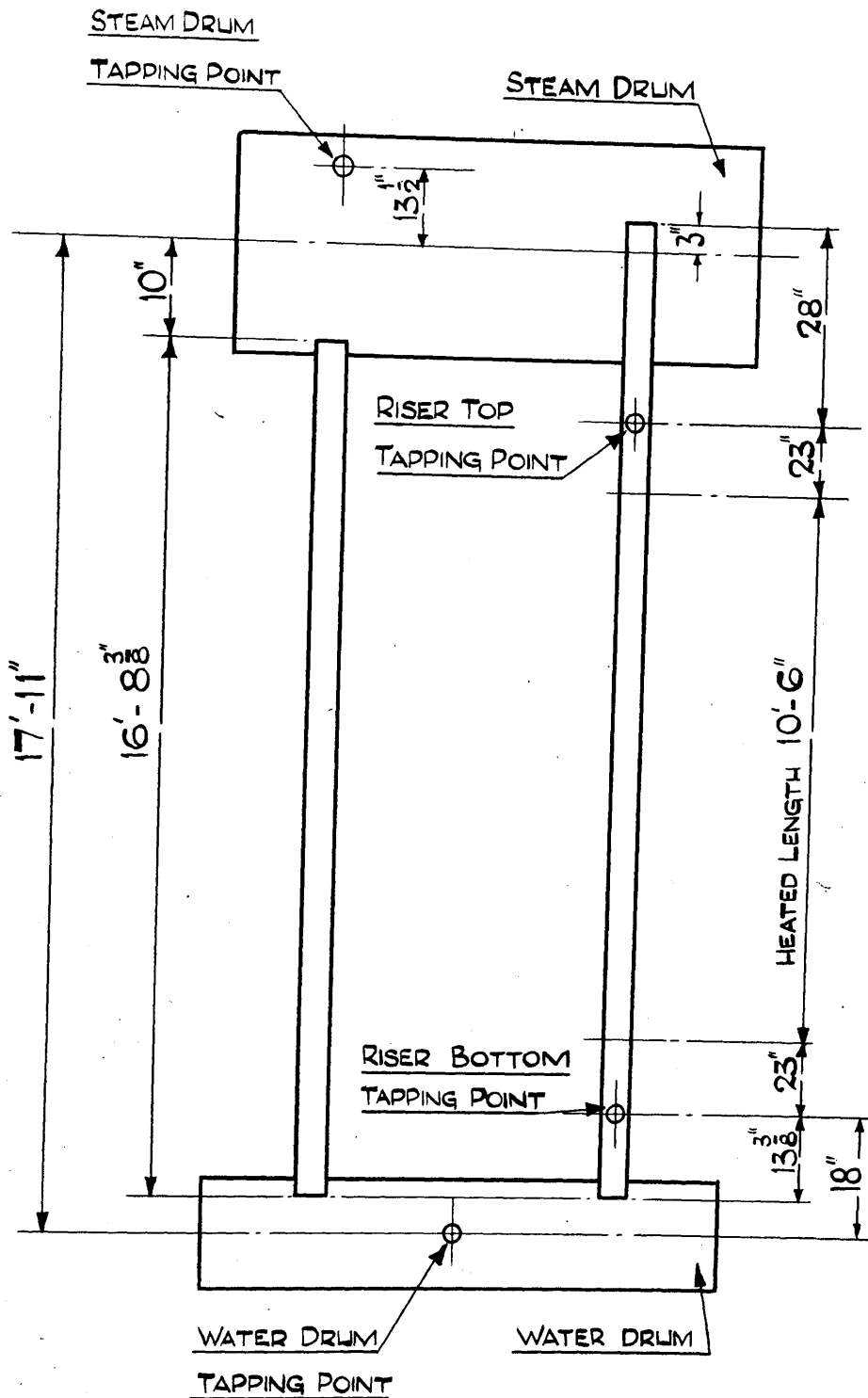
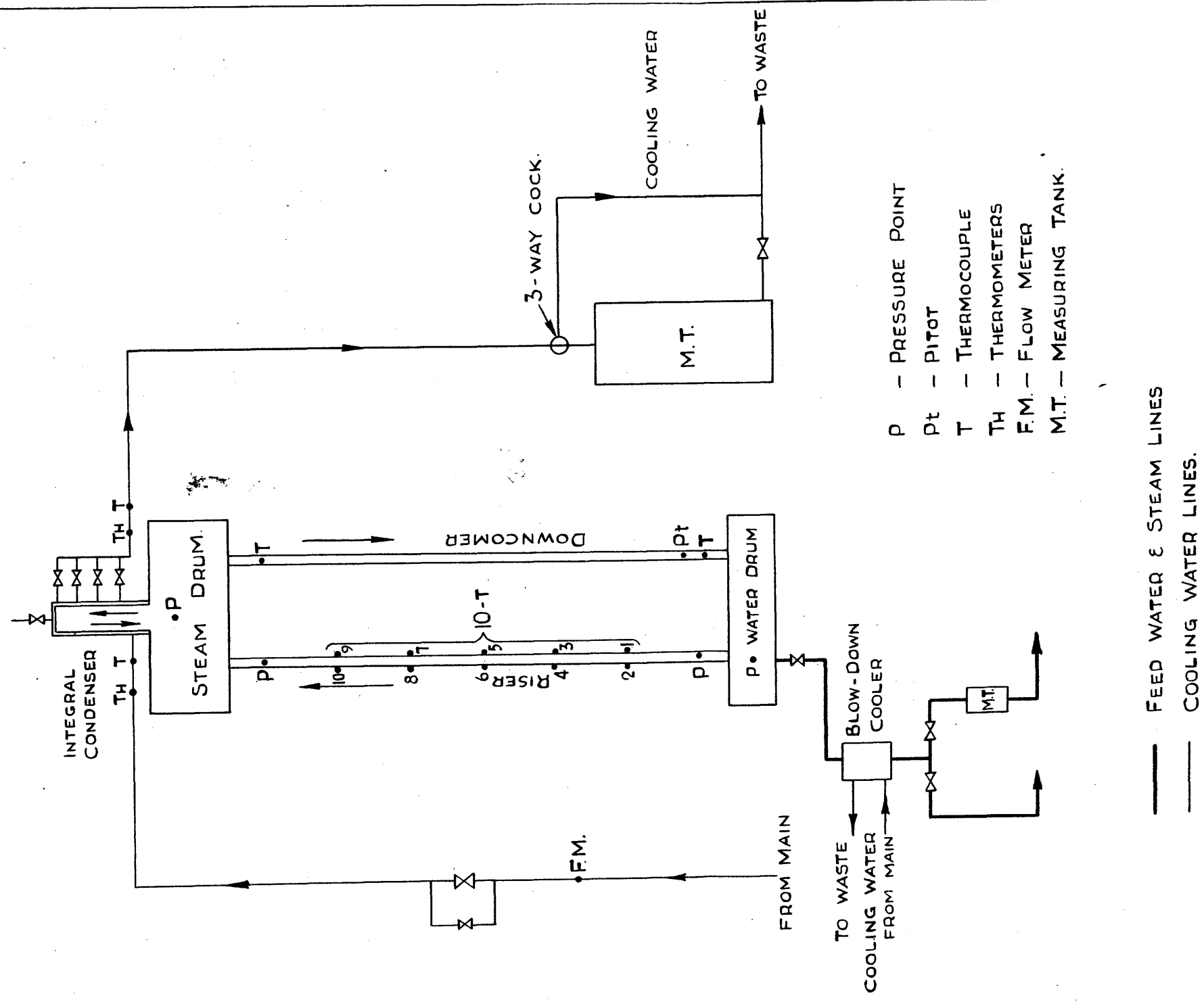


FIG. 26. DIAGRAM SHOWING DIMENSIONS OF TWO-TUBE BOILER CIRCUIT.



P - PRESSURE POINT
 Pt - PITOT
 T - THERMOCOUPLE
 Th - THERMOMETERS
 F.M. - FLOW METER
 M.T. - MEASURING TANK.

FIG. 27. FLOW DIAGRAM SHOWING INSTRUMENT POINTS CLOSED CIRCUIT

that the three phases are approximately balanced. The bus-bars are fed by flexible cables to the secondary terminals of a transformer.

Transformer. The transformer is of the oil-cooled type and has the following rating:- KVA 300, 3-phase, 50 cycles, Volts (No Load) 440/80.6/32.8, Amperes 394/1820.

By a system of tapings, the following secondary voltages are available: 80.6, 72.6, 66.5, 58.5, 46.5, 41.7, 38.4 and 33.8.

The transformer is fed from the 440 volt main through an air circuit breaker.

Miscellaneous. In addition, the boiler is equipped with an air valve, pressure gauge, safety valve, level gauge and an Igema "remote" level gauge.

Operational Procedure. The boiler is first filled with distilled water to mid-drum level, then the furnace switched on with the transformer at a suitable voltage tapping to give the approximate heat input required. The air valve is kept open during the preliminary heating, and is closed when all air has been expelled from the steam drum. The pressure then rises until the condenser is brought into operation. The boiler pressure is conveniently controlled by adjustment of the condenser cooling water valve.

25. INSTRUMENTATION.

As far as possible continuous records were taken of all important readings. Where greater accuracy was required these were supported, where necessary, by independent readings.

Pressures. A pressure recorder gives a continuous record of the boiler pressure. This was used for control purposes, the actual test readings being taken from the boiler pressure gauge.

A differential pressure recorder can be connected through manifolds and valves as indicated in Figure 28, to any of the following points:- steam drum, water drum, riser tube top, riser tube bottom. Thus the differential pressure between any two of these points can be obtained and checked by integration.

Flow Quantities. The cooling water flow rate is continuously recorded on a flow recorder. Again the recorder is used simply for purposes of control, and the actual test readings are taken by direct measurement in a 240 gallon calibrated tank.

The circulation is measured by a reverse type Pitot tube positioned at the bottom of the downcomer tube, the head readings being taken continuously on a flow recorder.

Temperatures. The instruments for temperature readings comprise thermocouples used in conjunction with a "6-point" Kent "Multelec" recorder, and a 24-point "Manual" indicator, an optical pyrometer, and mercury thermometers.

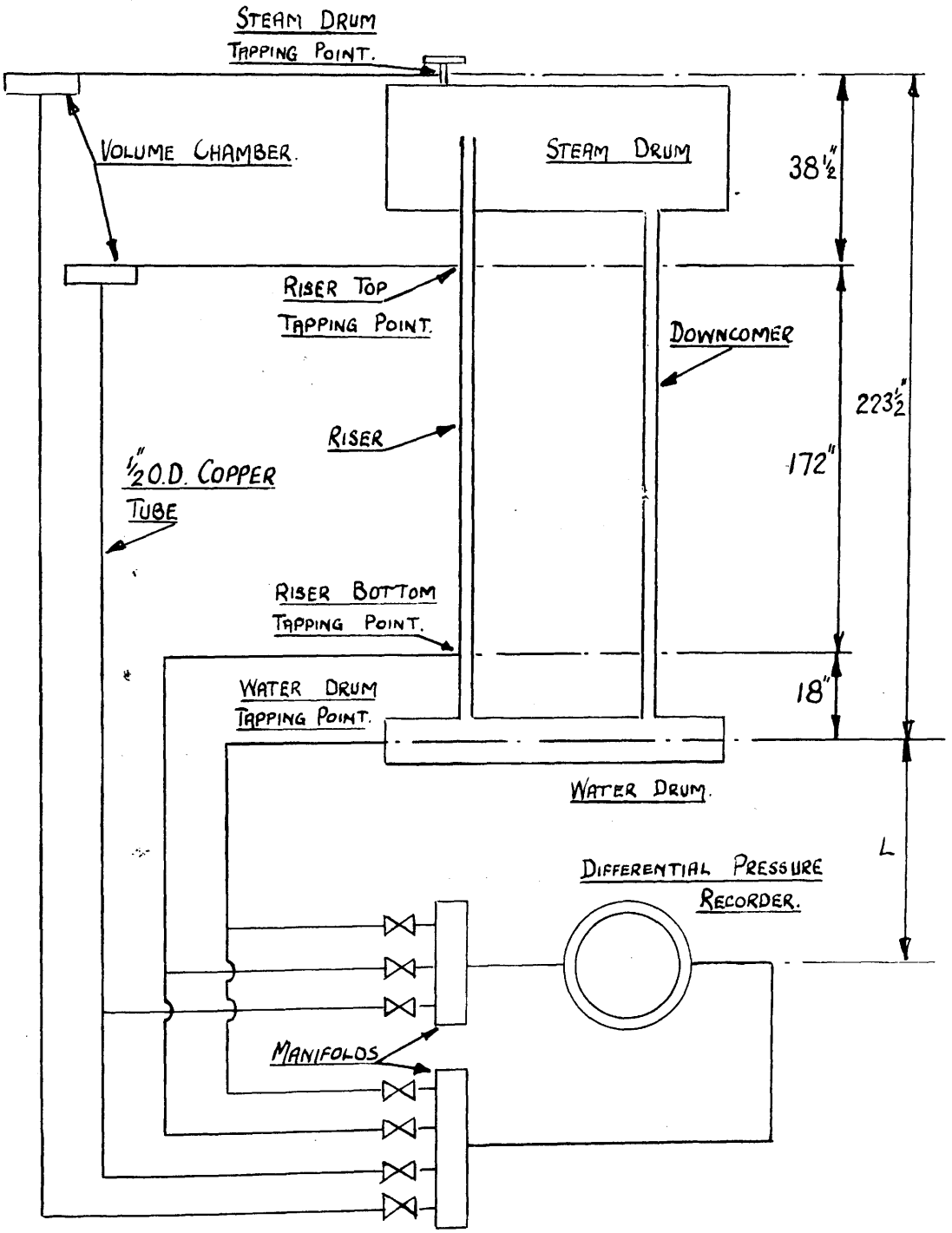


FIG. 28. LAYOUT OF DIFFERENTIAL PRESSURE
RECORDING SYSTEM.

The following temperatures are observed:-

Cooling water at condenser inlet and outlet by thermocouples and thermometers;

Boiler water at top and bottom of downcomer;

Furnace inner wall temperature, and "Globar" element temperature.

The thermocouples were of Chromel-Alumel. The furnace and "Globar" surfaces were taken by optical pyrometer through eye holes in the furnace wall, the holes being plugged when not in use.

26. CALIBRATION TESTS.

This section of the report does not concern itself with the routine checks required on the calibration of pressure gauges, differential recorders etc., but with those tests which were necessary for a full interpretation of experimental data obtained.

Pitot Tube. The Pitot tube was calibrated in situ by pumping water into the steam drum, blocking the riser tube, and taking the water away from the water drum. The water flow was measured in a calibrated tank. The head reading in feet was found to be related to the downcomer velocity in the expression.

$$h = 1.938 \cdot \frac{U^2}{2g} \dots \dots \dots .66$$

Tube Friction. The tubes used were tested in the horizontal for tube friction, the pressure drop over the tube being measured using water manometers for various water flow rates. All tubes, when new, were found to be smooth. During the period of the tests, the downcomer tube became rough due to corrosion, having eventually a friction factor $\lambda = 0.0288$. The riser tubes were frequently changed due to the tube distorting. During their period of use they remained smooth.

Furnace Heat Losses. A certain proportion of the electrical heat input to the furnace is lost through the furnace walls. The method of determining the heat loss was as follows. The riser tube was extracted from the furnace and the ends sealed. The furnace was then operated. Using an optical/

optical pyrometer, the furnace wall temperature was noted when it became constant. The furnace heat input was measured using wattmeters. When the temperature was constant the electrical input balanced the heat loss from the furnace. Figure 29 was obtained from a series of such experiments.

Boiler Heat Loss. The method of determining the heat loss from the boiler is now described. The boiler pressure was raised to approximately 1,000 lb/in.², then the furnace switched off. The pressure was maintained by reducing the cooling water flow to the condenser. When the cooling water was completely shut off the pressure began to fall and the pressure drop on a time base was obtained from the pressure recorder. Assuming that by this time no heat is being transferred from the furnace, the heat loss from the boiler may be estimated from the pressure time gradient. This calculation gave the curves of heat loss to saturation temperature shown in Figure 30. It will be seen that with decreasing saturation temperature the heat loss apparently rises and falls. The initial rise is presumably due to the heat still being transferred to the riser from the furnace. It will be seen that the curves tend to become linear, and on projecting give zero heat loss at approximately 150°F. This heat loss curve is for the case where the furnace is not in operation, consequently the temperature around the boiler will be considerably less than during actual operating conditions. When the furnace is in/

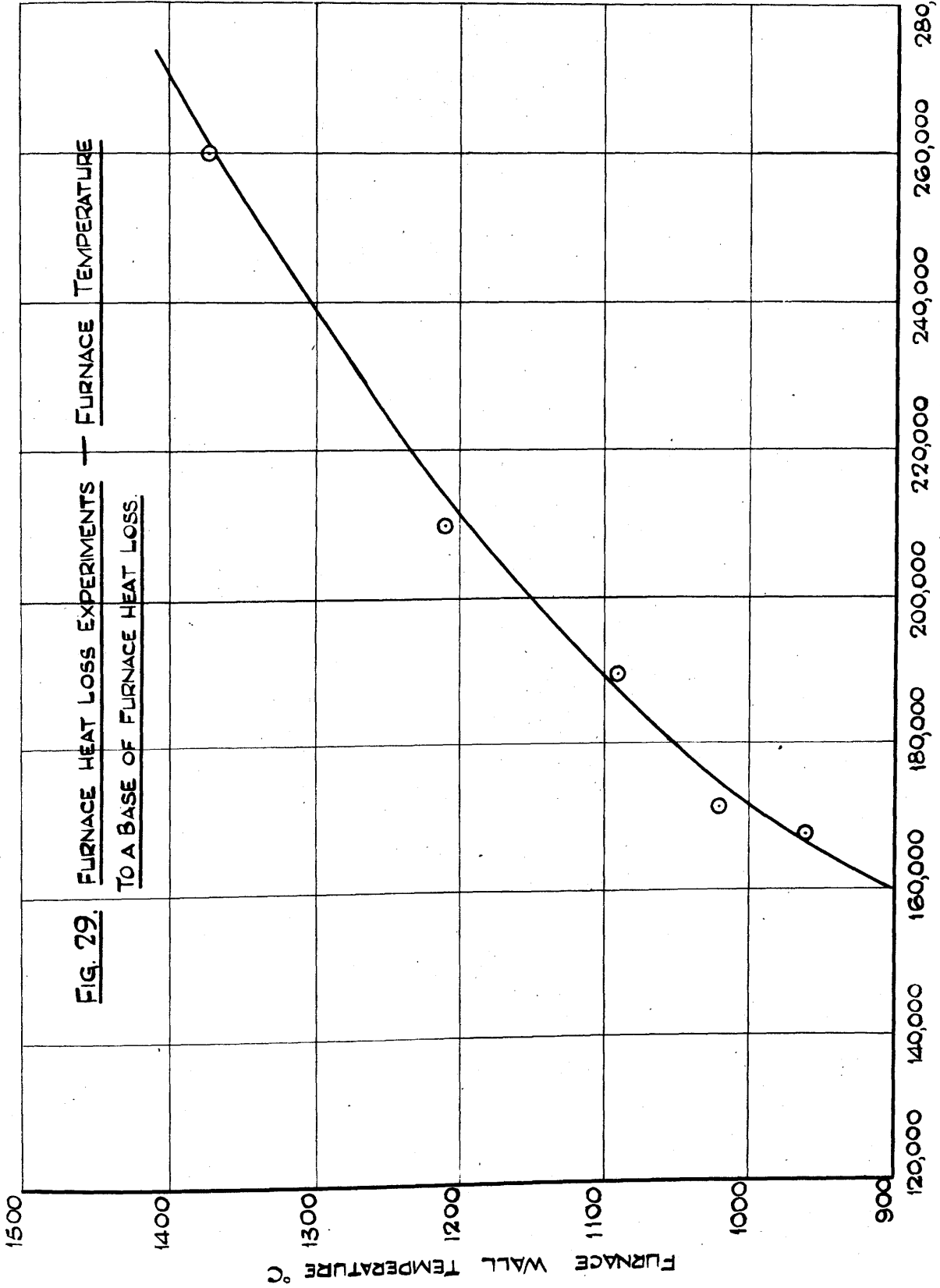
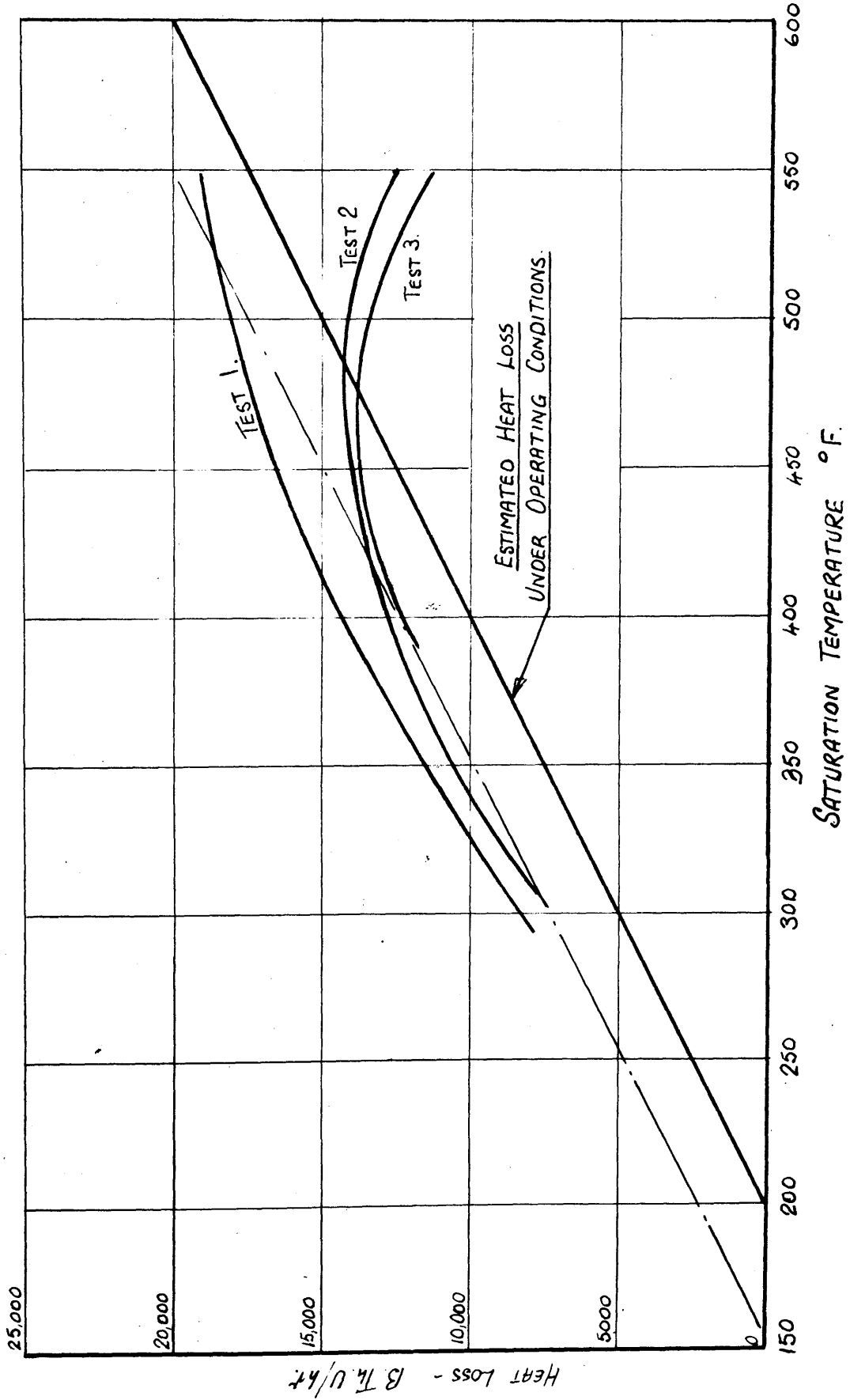


FIG. 29.
FURNACE HEAT LOSS EXPERIMENTS — FURNACE TEMPERATURE
TO A BASE OF FURNACE HEAT LOSS.

FURNACE HEAT LOSS B.T.U./HR.

FIG. 30. BOILER HEAT LOSS TO A BASE OF SATURATION TEMPERATURE.



HEAT LOSS - Btu/ft

in operation if the temperature of the surroundings be assumed 50° F. higher, and the slope of the experimental line still holds, then the estimated boiler heat loss might well be that shown by the proposed line in Figure 30.

$$Q_B = 50(t_s - 200) \dots \dots \dots 67$$

where Q_B is the boiler heat loss in B.Th.U./hr. and t_s is the saturation temperature.

All tests were carried out using a vertical tube 1.698 inch bore. The heat input was varied to give a range of heat transfer rates from 23,000 B.Th.U/hr.ft.² to 120,000 B.Th.U/hr.ft.² of outer tube surface.

Tests were carried out, first with no restriction, then with a series of restricting orifices at entry to the tube. Without the introduction of the orifice the circulation velocity at any particular pressure is solely dependent on the heat input. The introduction of the restricting orifice widens the scope of the analysis by introducing another variable. The orifice produces the same characteristics in the riser as would be obtained by the introduction of a downcomer of smaller diameter.

The orifices used were $\frac{7}{8}$ ", $\frac{3}{4}$ ", $\frac{5}{8}$ " and $\frac{1}{2}$ " diameter.

With the smaller restricting orifices the maximum heating was not used, due to the danger of overheating with reduced flow.

Test Procedure. The test procedure is as follows:-

First the transformer is adjusted to a suitable voltage tapping and the appropriate restricting orifice fitted at entry to riser.

The power is then switched on and the boiler pressure raised to approximately 50 lb/in.² gauge. Test readings are not taken until all readings have become steady. Normally the furnace brick temperature takes longest to attain a steady temperature. When steady conditions have been obtained the following readings are taken over a period of approximately 1 hour

- (a) The condenser heat balance is taken at the beginning/

beginning, middle and end of the test, i.e. cooling water mass flow and inlet and outlet temperatures measured.

- (b) Every possible combination of differential pressure using the four tapping points is recorded on the differential pressure recorder, i.e. six differential pressure readings are taken. Each differential pressure is recorded for a period of approximately 10 minutes to ensure a steady reading is obtained. The duration of each test is primarily determined by this procedure.
- (c) All temperature readings are taken twice during each test.
- (d) The Pitot reading, which remains constant is recorded.
- (e) The wattmeters giving the electric power to the furnace are read.

This procedure is repeated for a series of pressures over the operating range. More tests are carried out in the lower pressure region, as the physical variables change more rapidly with pressure in this region.

Test Results. A typical set of test readings are shown in Table 3.

TABLE 3. EXPERIMENTAL READINGS.

RESTRICTING ORIFICE: $\frac{3}{4}$ ". VOLTAGE TAPPING: 41.9. TEST SERIES No 11.

BOILER PRESSURE (GAUGE)		lb/□"	50	105	165	200
DOWNCOMER VELOCITY		INS	3.125	3.375	3.56	3.50
PRESSURE RECORDER	STEAM DRUM - WATER DRUM	INS	36	40.5	45.5	46.5
	STEAM DRUM - RISER BOTTOM	INS	78	85	87	86.5
	RISER TOP - RISER BOTTOM	INS	53	58	60.5	60.5
	RISER TOP - WATER DRUM	INS	11	14.5	19	20.5
	STEAM DRUM - RISER TOP	INS	25	27	27	26
	RISER BOTTOM - WATER DRUM	INS	-41.5	-44	-41.5	-39.5
COOLING WATER	MASS FLOW	GALLS/SEC.	0.12	0.054	0.166	0.089
			0.121	0.054	0.164	0.092
	INLET TEMPERATURE	°F	42	42	41	43
			42	42	41.5	43
OUTLET TEMPERATURE	°F	105	176	85	117	
		103	177	85	117	
ELECTRICAL INPUT TO FURNACE.		WATTS X 10 ⁻⁵	4.55	4.53	4.505	4.33
			4.33	4.51	4.605	4.30
					4.455	4.33
FURNACE WALL TEMP°		°C	1000	1045	1049	1038
TEMPERATURE - DOWNCOMER BOTTOM		°F	302	336	373	390
TEMPERATURE - DOWNCOMER TOP		°F	302	336	374	390.5

1. Pitot Velocity. The instrument was calibrated at atmospheric pressure using water at approximately 60°F., and calibration indicated that the head in feet was related to the downcomer velocity in the expression.

$$h = 1.938 \cdot \frac{U^2}{2g} \dots \dots \dots 68$$

It is assumed that the calibration constant will hold over the range of conditions met with in the tests.

It must be remembered in using Equation 68 that h is in feet of water at the conditions prevailing at the Pitot tube. The recorder on the other hand gives the Pitot head (h_R) in inches of water at atmospheric conditions, thus a density correction must be applied. If ρ_a and ρ_b are the densities at atmospheric and Pitot conditions respectively then,

$$\frac{h_R}{12} \cdot \frac{\rho_a}{\rho_b} = 1.938 \frac{U^2}{2g} \dots \dots \dots 69$$

from which

$$U = \sqrt{\frac{2g}{1.938} \cdot \frac{h_R}{12} \cdot \frac{\rho_a}{\rho_b}} \dots \dots \dots 70$$

2. Differential Pressures. The differential pressure recorder was calibrated with water at 60°F. and atmospheric pressure.

A recorder reading of h_R inches of water, therefore, represents a pressure difference of

$$\frac{h_R}{12} \cdot \rho_a$$

where ρ_a is the density of water at atmospheric pressure and a temperature of 60°F.

When the valves are arranged to give the pressure difference between the steam and water drum tapping points, the steam drum is exerting a pressure of

$$P_{SD} + \left(L + \frac{228.5}{12} \right) \rho_c$$

at the instrument, where P_{SD} is the pressure at the steam drum tapping point, ρ_c is the density of water in the pressure limbs connecting the tapping point with the instrument, and L is the height from the water drum to the pressure recorder. (See Figure 28).

Similarly, the water drum exerts a pressure of

$$P_{WD} + L \rho_c$$

at the instrument, where P_{WD} is the pressure at the water drum.

Consequently,

$$\frac{h_R}{12} \cdot \rho_a = P_{SD} + \left(L + \frac{228.5}{12} \right) \rho_c - P_{WD} - L \rho_c$$

Hence,

$$\begin{aligned} P_{WD} - P_{SD} &= \left(\frac{228.5}{12} \cdot \rho_c - \frac{h_R}{12} \cdot \rho_a \right) \\ &= \left(228.5 \frac{\rho_c}{\rho_a} - h_R \right) \frac{\rho_a}{12} \dots \dots \dots 71 \end{aligned}$$

where the units are pounds and feet.

similarly/

Similarly,

$$P_{WO} - P_{RB} = \left(18 \frac{\rho_c}{\rho_a} - h_R \right) \frac{\rho_a}{12} \dots \dots \dots 72$$

$$P_{WO} - P_{RT} = \left(190 \frac{\rho_c}{\rho_a} - h_R \right) \frac{\rho_a}{12} \dots \dots \dots 73$$

$$P_{RT} - P_{SD} = \left(38.5 \frac{\rho_c}{\rho_a} - h_R \right) \frac{\rho_a}{12} \dots \dots \dots 74$$

$$P_{RB} - P_{SD} = \left(210.5 \frac{\rho_c}{\rho_a} - h_R \right) \frac{\rho_a}{12} \dots \dots \dots 75$$

$$P_{RB} - P_{RT} = \left(172 \frac{\rho_c}{\rho_a} - h_R \right) \frac{\rho_a}{12} \dots \dots \dots 76$$

Where the suffixes RT and RB refer to the riser top and riser bottom tapping points.

The density of the water varies along the lengths of the copper pressure limbs due to temperature variations, consequently the ratio ρ_c/ρ_a varies over the lengths.

Tests with thermocouples on the pressure limbs indicated that the temperature in the limbs adjacent to the furnace had a temperature variation from 110 to 160°F. while in the region of the steam and water drums the limb temperatures were of the order of 100°F.

Having regard to the above temperature variations the following ratios of ρ_c/ρ_a were adopted:-

Water drum to riser bottom - $\rho_c/\rho_a = 0.99$

Riser bottom to riser top - $\rho_c/\rho_a = 0.98$.

Riser top to steam drum - $\rho_c/\rho_a = 0.99$.

The/

The allowances over the other lengths can be estimated from these assumptions.

3. Steam Evaporation. The steam is condensed by the condenser heat transfer and the heat loss through the top half of the steam drum. This total heat transfer divided by the latent heat gives the pound of steam evaporated. From knowledge of the mass flow the dryness fraction at the top of the riser tube may then be determined.

The method of obtaining the heat transfer through the upper half of the steam drum is as follows.

The areas of the outer insulation surfaces of the boiler are -

Steam drum	7276 square inches.
Water drum	3676 square inches.
Downcomer tube and riser distance pieces	2120 square inches.

The steam and water drum insulation thicknesses are $3\frac{1}{4}$ inches, and the downcomer $\frac{7}{8}$ inches thick.

The proportion of the boiler heat loss through the top half of the steam drum will be approximately

$$\frac{7276}{2(7276 + 3676 + 2120 \times \frac{3.25}{0.875})} = 0.193$$

$$\doteq 0.2$$

of the total heat loss. The total loss may be obtained from Figure 30. A detailed calculation of the dryness fraction at tube exit is given in Appendix H.

The heat transfer at the condenser is the product of the cooling water mass flow and the temperature rise. It is/

is evident that the condenser may cool the condensate below saturation temperature, or in other words, remove more than the latent heat. It is implicit in the method of calculation that this does not take place. To avoid this, a tray is placed below the condenser, in the steam space, to catch the condensate. The condensate flows along the four foot length of tray in contact with the steam, a condition which should ensure the condensate being at saturation temperature before leaving the tray. Thermocouples indicated that at the downcomer top the temperature corresponded to that in the steam space.

Converted Results. A detailed example of the conversions are given in Appendix G.

Accuracy. The differential pressure recorder can be read to the nearest half inch. Inspection of the results by summing the various readings against the overall readings suggests that the readings are obtained to the nearest inch of water.

The Pitot recorder can be read to the nearest $\frac{1}{8}$ inch.

An overall heat balance for the furnace and boiler such as shown in Table 4 gave agreement within 5% in all but a few tests.

TABLE 4. OVERALL HEAT BALANCE.

TEST SERIES No 11.

BOILER PRESSURE lb/p" (GAUGE).	SATURATION TEMPERATURE °F.	FURNACE WALL TEMPERATURE °F.	CONDENSER HEAT TRANSFER B. Th. U/HR.	BOILER HEAT LOSS B. Th. U/HR. (FROM FIGURE)		FURNACE HEAT LOSS. B. Th. U/HR. (FROM FIGURE)	ESTIMATED HEAT INPUT. B. Th. U/HR.	MEASURED HEAT INPUT B. Th. U/HR.
				A	B			
51	299	1000	269,250*	5,000	172,500	446,750	444,000.*	
103	340	1045	261,670	7,000	179,500	448,170	452,000.	
165	373	1049	260,170	8,600	180,000	448,770	453,600.	
200	388	1038	241,500	9,300	178,400	429,200	432,000.	

* AVERAGE VALUES.

3/12

29. TEST RESULTS.

It was originally hoped that a particular voltage tapping would imply a particular heat input to the tube over the whole range of test pressures. However, increasing furnace losses with increasing pressure and variations in the main's voltage make the heat input vary as much as 30% from the mean heat input for a particular voltage tapping.

In relating the test results the voltage tapping nevertheless has been taken as the common denominator of a particular test series. It should, therefore, be remembered that, where mean lines are drawn through test data plotted in this manner, the scatter of the points does not necessarily imply experimental error, but rather that there is a considerable fluctuation in main's voltage between various tests. The mean heat transfer figure quoted for a particular voltage tapping, is a "weighted" mean figure allowing for the fact that a greater proportion of the tests were carried out at low pressures.

Relating data at particular pressures was also considered, but due to the difficulty of testing at particular specified pressures this had to be abandoned.

Figures 31 to 35 show the circulation velocity, as measured at the downcomer Pitot tube, plotted to a base of boiler gauge pressure for particular voltage tappings. These are plotted for tests with and without restricting orifices.

The/

CIRCULATION VELOCITY - BOILER PRESSURE

TUBE :- 2 1/4 O.D. x 2 S.W.G. HEATING: UNIFORM RESTRICTION ORIFICE: NONE
TUBE POSITION: VERTICAL HEATED LENGTH: 10'-6"

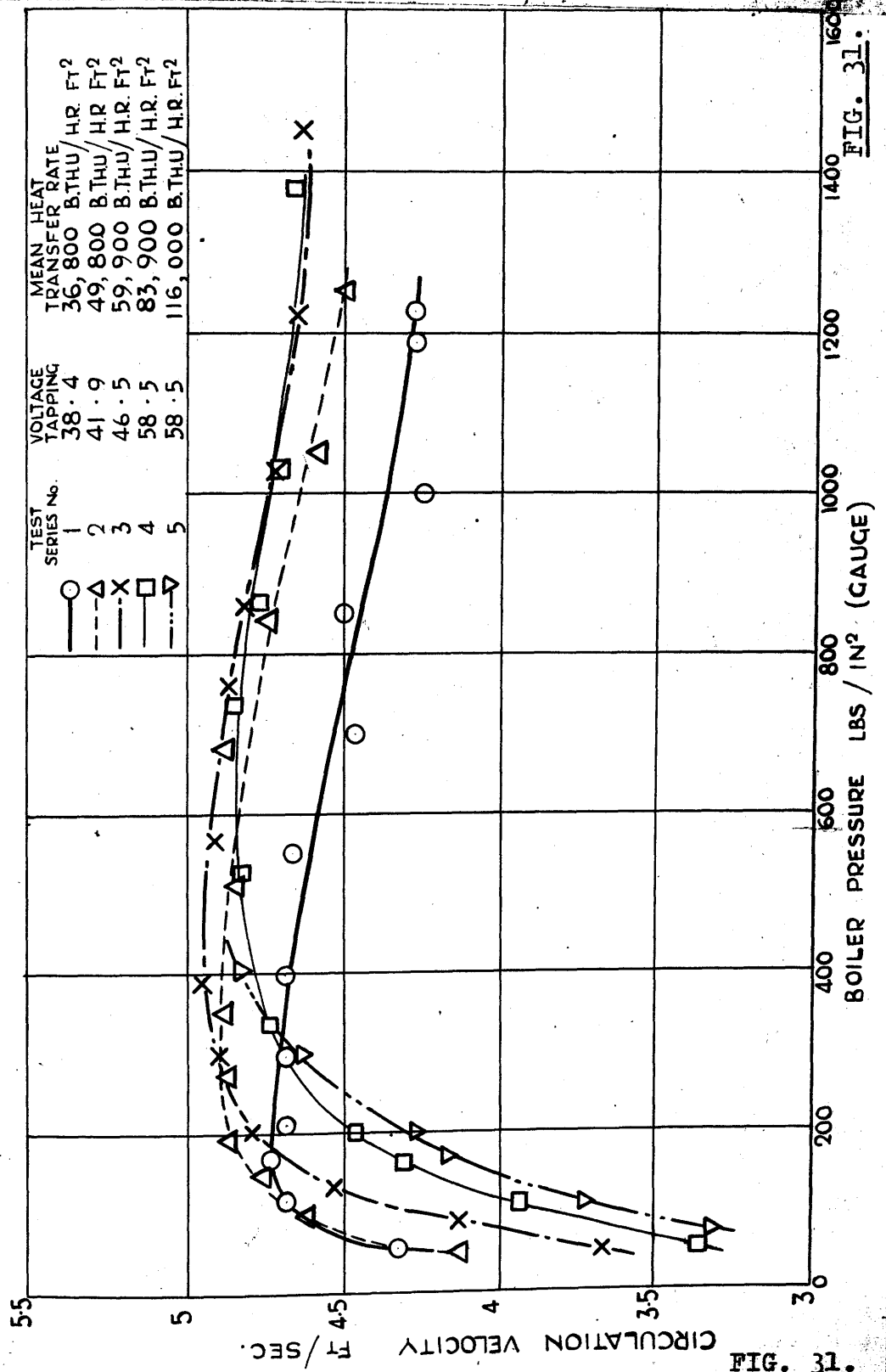


FIG. 31.

FIG. 31.

CIRCULATION VELOCITY - BOILER PRESSURE

TUBE: $2\frac{1}{4}$ O.D. x 2 SWG. HEATING: UNIFORM RESTRICTING ORIFICE $\frac{7}{8}$ DIA.

TUBE POSITION: VERTICAL HEATED LENGTH 10'-6"

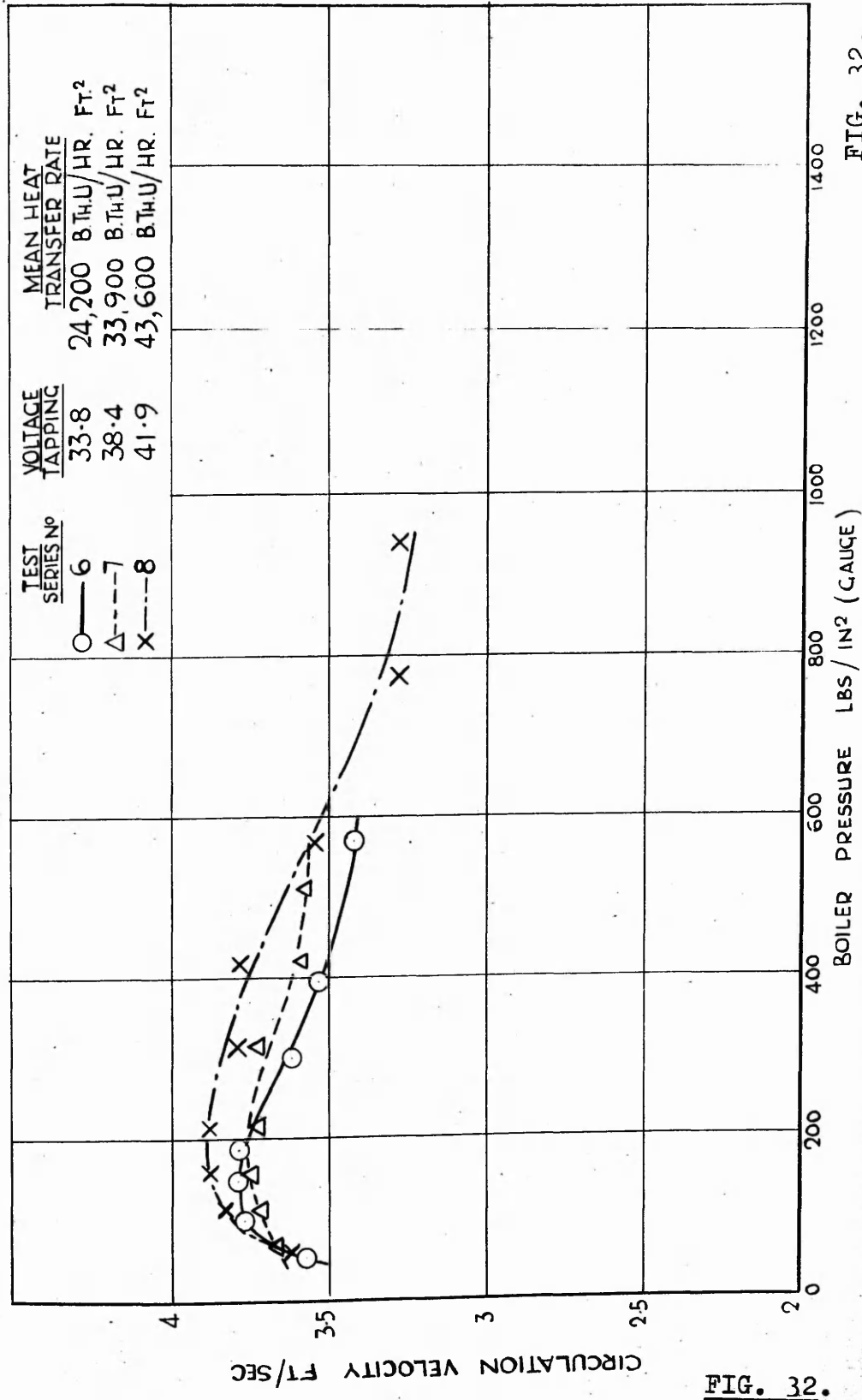


FIG. 32.

FIG. 32.

CIRCULATION VELOCITY - BOILER PRESSURE

TUBE: $2\frac{1}{4}$ O.D. x 2 SWG. HEATING: UNIFORM RESTRICTING ORIFICE $\frac{3}{4}$ DIA.

TUBE POSITION: VERTICAL HEATED LENGTH 10'-6"

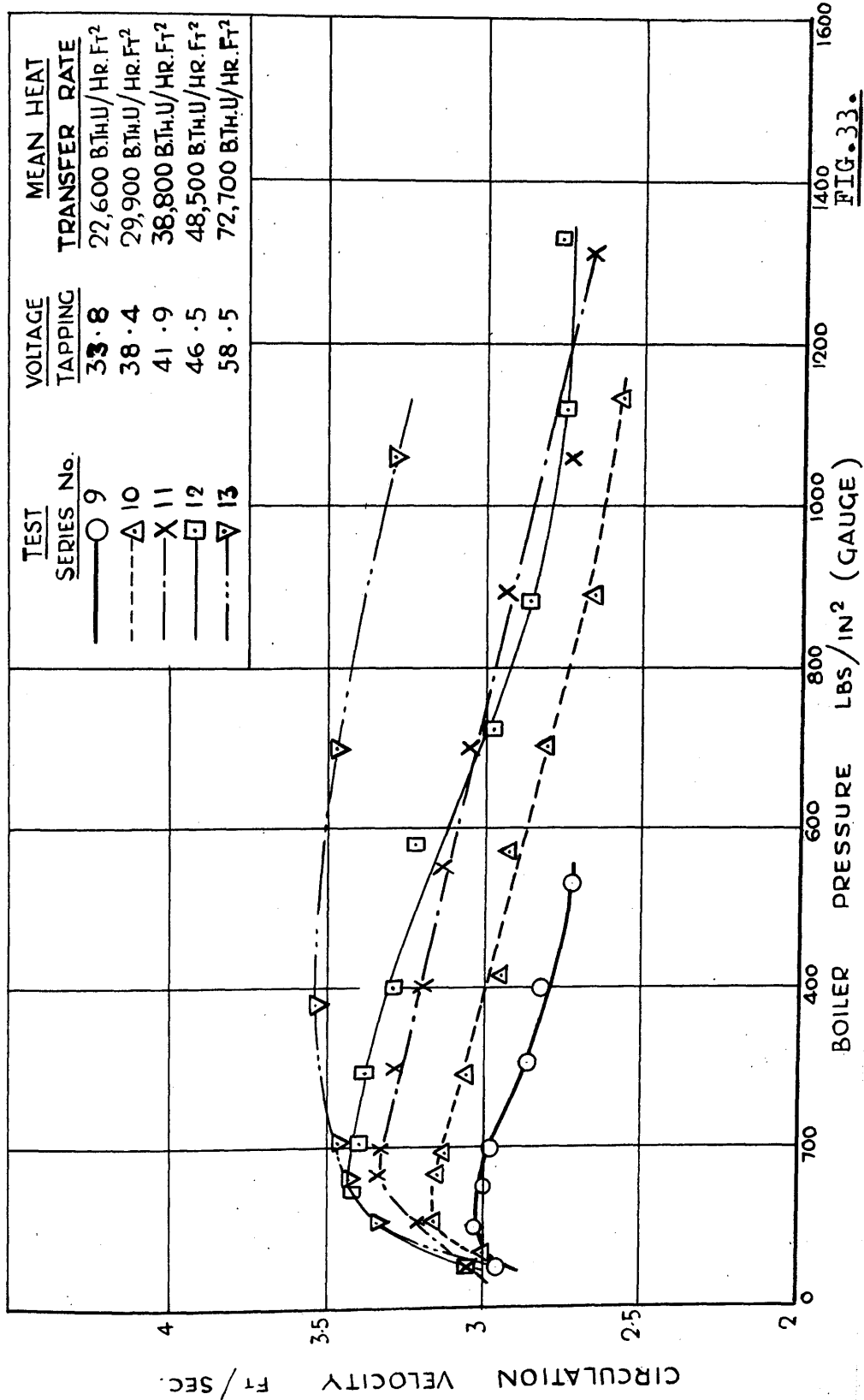


FIG. 33.

FIG. 33.

CIRCULATION VELOCITY — BOILER PRESSURE

TUBE: 2 1/4" O.D. x 2 SW.G. HEATING: UNIFORM RESTRICTING ORIFICE: 5/8" DIA.

TUBE POSITION: VERTICAL HEATED LENGTH: 10'-6"

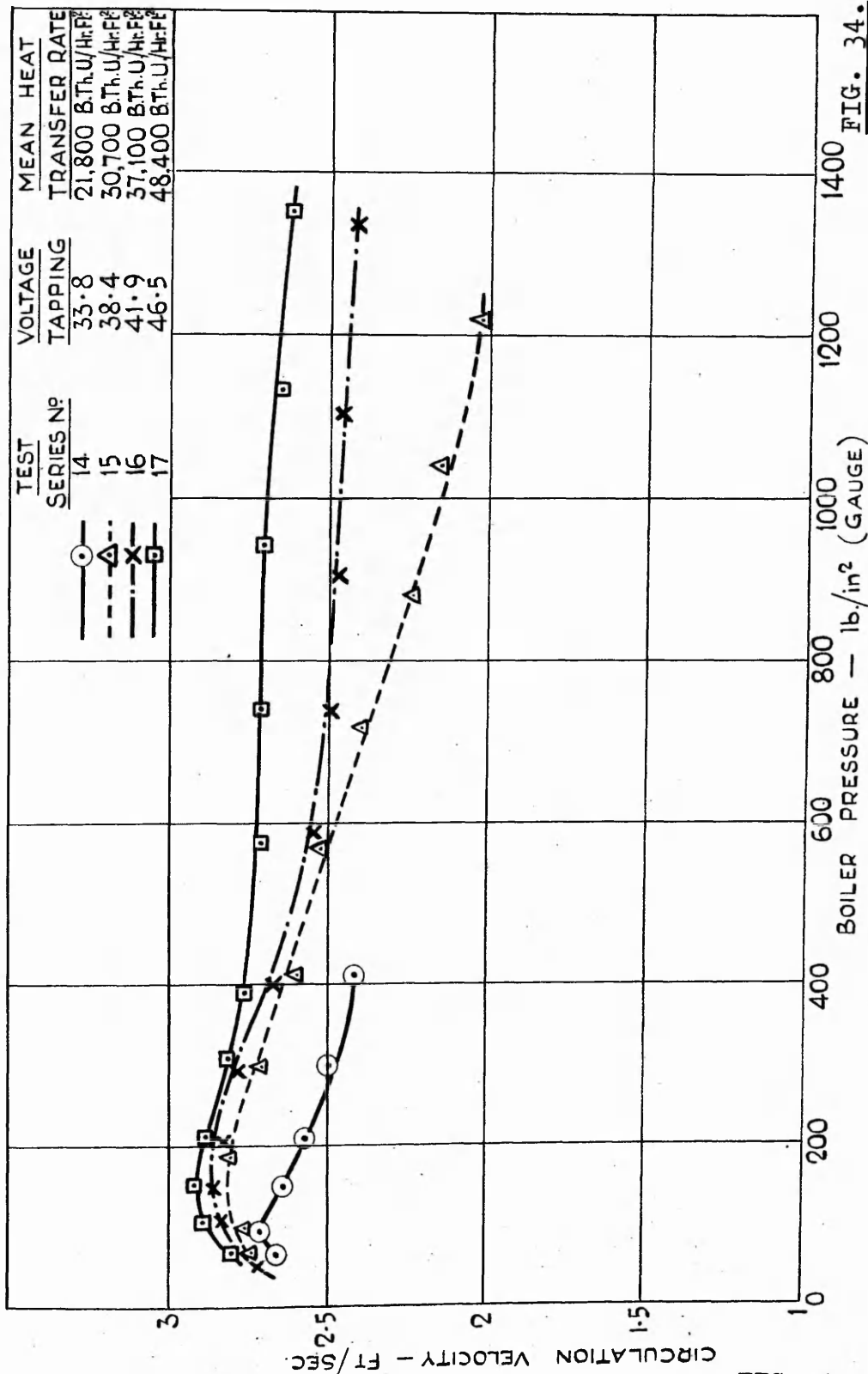


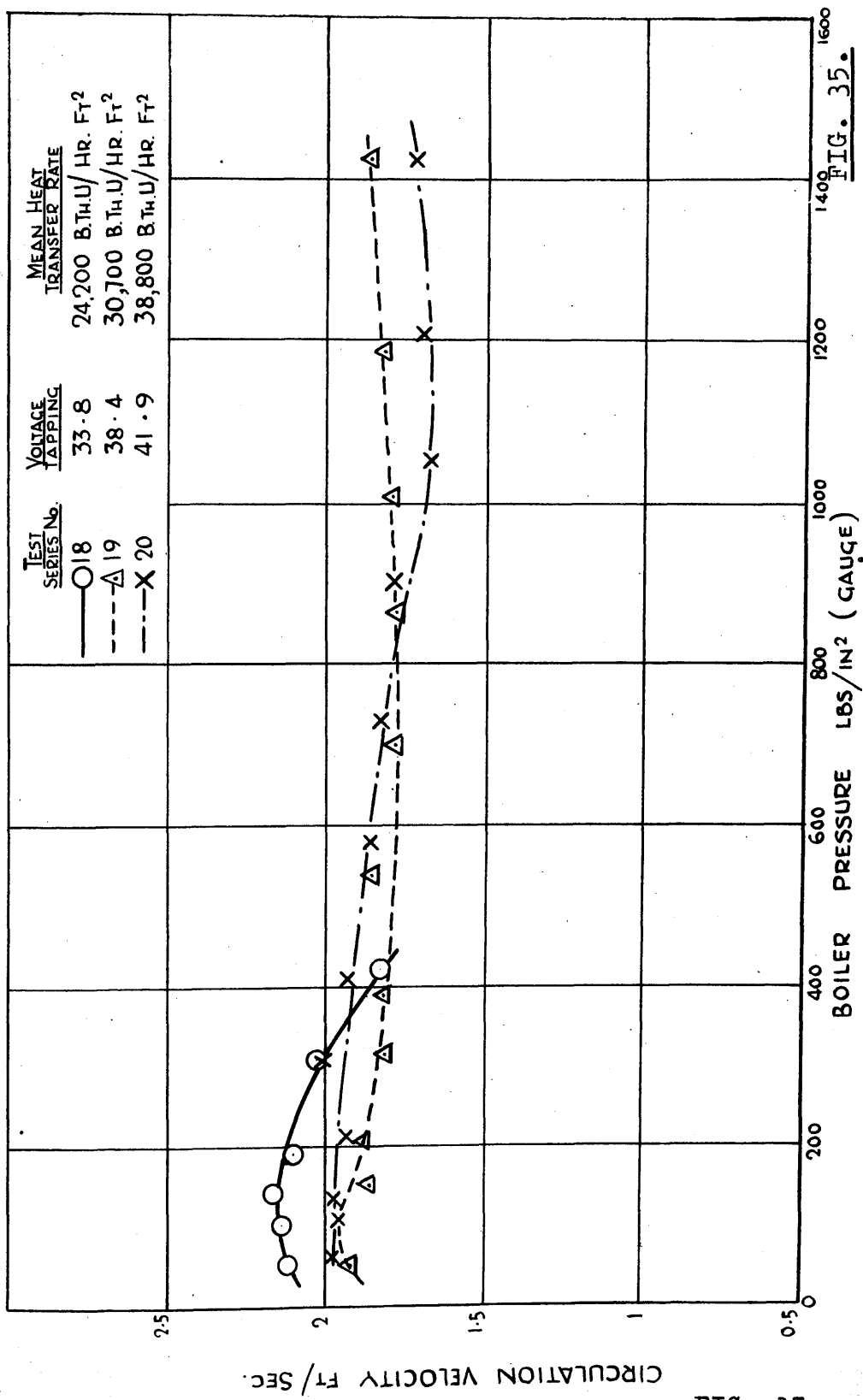
FIG. 34.

FIG. 34.

CIRCULATION VELOCITY - BOILER PRESSURE

TUBE: $2\frac{1}{4}$ O.D. x 2 SWG.
 HEATING: UNIFORM
 HEATED LENGTH: 10'-6"
 RESTRICTION ORIFICE $\frac{1}{2}$ DIA.

TUBE POSITION: VERTICAL



CIRCULATION VELOCITY FT/SEC.

FIG. 35.

FIG. 35.

The dryness fractions at the top of the riser tube are shown on Tables 5 to 9.

The curves of differential pressure are shown later when comparison is made between experimental and calculated values. The values are not given for the pressure differences to the steam drum tapping point for Tests Series Nos. 1 and 2, as these readings were unreliable. This was due to the volume chamber being placed above the tapping point with the result that the water tended to syphon from the chamber. In later tests the volume chamber was placed slightly below the tapping point.

DRYNESS FRACTIONS

TABLE 5.

TUBE : $2\frac{1}{4}$ O.D. x 2 S.W.G. HEATING : UNIFORM RESTRICTING ORIFICE NONE

TUBE POSITION : VERTICAL HEATED LENGTH : 10'-6"

TEST SERIES N° 1		VOLTAGE TAPPING		38.4		MEAN HEAT TRANSFER RATE		36,800		B.Th.U./HR.Ft ²	
PRESSURE	55	116	167	210	298	400	550	700	850	1,000	1,190
DRYNESS FRACTION	.0192	.0174	.0205	.0165	.0180	.0231	.0205	.0254	.0292	.0251	.0324

TEST SERIES N° 2		VOLTAGE TAPPING		41.9		MEAN HEAT TRANSFER RATE		49,800		B.Th.U./HR.Ft ²	
PRESSURE	49	99	146	192	270	350	510	680	840	1050	1250
DRYNESS FRACTION	.0249	.0235	.025	.0253	.0256	.0257	.0312	.0333	.0367	.0371	.0436

TEST SERIES N° 3		VOLTAGE TAPPING		46.5		MEAN HEAT TRANSFER RATE		59,900		B.Th.U./HR.Ft ²	
PRESSURE	49	87	133	202	300	390	570	760	860	1025	1220
DRYNESS FRACTION	.0357	.0342	.0350	.0336	.0316	.033	.0353	.0411	.0484	.0455	.0447

TEST SERIES N° 4		VOLTAGE TAPPING		58.5		MEAN HEAT TRANSFER RATE		83,900		B.Th.U./HR.Ft ²	
PRESSURE	54	105	160	200	339	525	735	860	1,030	1380	
DRYNESS FRACTION	.0497	.0465	.0464	.0471	.0506	.054	.0565	.0546	.0592	.0722	

TEST SERIES N° 5		VOLTAGE TAPPING		58.5		MEAN HEAT TRANSFER RATE		116,000		B.Th.U./HR.Ft ²	
PRESSURE	72	110	169	200	300	405					
DRYNESS FRACTION	.0739	.0703	.0666	.0671	.0650	.0671					

DRYNESS FRACTIONS

TABLE 6.

TUBE : $2\frac{1}{4}$ O.D. x 2 S.W.G.

HEATING : UNIFORM $7\frac{1}{8}$ "
RESTRICTING ORIFICE

TUBE POSITION : VERTICAL

HEATED LENGTH : 10'-6"

TEST SERIES N^o 6 VOLTAGE TAPPING 33.8 MEAN HEAT TRANSFER RATE 24,200 B.Th.U./HR.Ft²

PRESSURE	50	100	149	185	300	395	570		
DRYNESS FRACTION	.0127	.0157	.0157	.0168	.0164	.0193	.0215		

TEST SERIES N^o 7 VOLTAGE TAPPING 38.4 MEAN HEAT TRANSFER RATE 33,900 B.Th.U./HR.Ft²

PRESSURE	62	111	159	215	315	420	510		
DRYNESS FRACTION	.0181	.0205	.0194	.0214	.0285	.0308	.033		

TEST SERIES N^o 8 VOLTAGE TAPPING 41.9 MEAN HEAT TRANSFER RATE 43,600 B.Th.U./HR.Ft²

PRESSURE	58	115	166	215	315	415	565	770	940
DRYNESS FRACTION	.0258	.0265	.0266	.0268	.029	.029	.0362	.0354	.0392

TEST SERIES N^o VOLTAGE TAPPING MEAN HEAT TRANSFER RATE B.Th.U./HR.Ft²

PRESSURE									
DRYNESS FRACTION									

TEST SERIES N^o VOLTAGE TAPPING MEAN HEAT TRANSFER RATE B.Th.U./HR.Ft²

PRESSURE									
DRYNESS FRACTION									

DRYNESS FRACTIONS

TABLE 7.

TUBE : $2\frac{1}{4}$ O.D. x 2 S.W.G. HEATING : UNIFORM RESTRICTING ORIFICE $\frac{3}{4}$ DIA.

TUBE POSITION : VERTICAL HEATED LENGTH : 10'-6"

TEST SERIES N°	9	VOLTAGE TAPPING			33.8	MEAN HEAT TRANSFER RATE			22,600	B.Th.U./HR.Ft ²
PRESSURE	50	100	151	200	305	400	530			
DRYNESS FRACTION	.0159	.0167	.0175	.0194	.0205	.0213	.0245			

TEST SERIES N°	10	VOLTAGE TAPPING			38.4	MEAN HEAT TRANSFER RATE			29,900	B.Th.U./HR.Ft ²
PRESSURE	68	110	164	197	290	415	570	700	890	1130
DRYNESS FRACTION	.0204	.0214	.0218	.0238	.0258	.0276	.0305	.035	.0316	.0380

TEST SERIES N°	11	VOLTAGE TAPPING			41.9	MEAN HEAT TRANSFER RATE			38,800	B.Th.U./HR.Ft ²
PRESSURE	50	105	165	200	300	402	550	700	890	1060
DRYNESS FRACTION	.0297	.0292	.0296	.0284	.0286	.0278	.0382	.0392	.0442	.0455

TEST SERIES N°	12	VOLTAGE TAPPING			46.5	MEAN HEAT TRANSFER RATE			48,500	B.Th.U./HR.Ft ²
PRESSURE	51	100	145	207	295	400	580	720	880	1120
DRYNESS FRACTION	.0366	.036	.0362	.0376	.0402	.0421	.047	.0512	.0539	.0561

TEST SERIES N°	13	VOLTAGE TAPPING			58.5	MEAN HEAT TRANSFER RATE			72,700	B.Th.U./HR.Ft ²
PRESSURE	49	105	160	208	380	700	1,060			
DRYNESS FRACTION	.05	.0496	.0508	.0524	.0587	.0662	.0778			

TABLE 9.

DRYNESS FRACTIONS

TUBE : 1" O.D. x 2 S.W.G. HEATING : UNIFORM RESTRICTING ORIFICE 1/2 DIA

TUBE POSITION : VERTICAL HEATED LENGTH : 10'-6"

TEST SERIES N°	18	VOLTAGE TAPPING			33.8	MEAN HEAT TRANSFER RATE			24,200	B.Th.U./Hr.Ft ²
PRESSURE	56	104	145	191	308	420				
DRYNESS FRACTION	.0212	.0280	.0298	.0289	.0298	.0378				

TEST SERIES N°	19	VOLTAGE TAPPING			38.4	MEAN HEAT TRANSFER RATE			30,700	B.Th.U./Hr.Ft ²
PRESSURE	50	100	157	205	315	390	540	700	865	1,010
DRYNESS FRACTION	.0276	.0370	.0412	.0387	.0471	.0461	.0496	.0562	.055	.0621

TEST SERIES N°	20	VOLTAGE TAPPING			41.9	MEAN HEAT TRANSFER RATE			38,800	B.Th.U./Hr.Ft ²
PRESSURE	64	108	137	213	304	405	580	730	900	1050
DRYNESS FRACTION	.0441	.0483	.0512	.0525	.0524	.0585	.066	.0718	.0726	.0659

TEST SERIES N°	VOLTAGE TAPPING			MEAN HEAT TRANSFER RATE			B.Th.U./Hr.Ft ²
PRESSURE							
DRYNESS FRACTION							

TEST SERIES N°	VOLTAGE TAPPING			MEAN HEAT TRANSFER RATE			B.Th.U./Hr.Ft ²
PRESSURE							
DRYNESS FRACTION							

PART VI.APPLICATION OF PROPOSED THEORY TO
ANALYSIS OF TWO-TUBE BOILER TEST RESULTS.

	<u>Page.</u>
30. Pressure change during adiabatic flow in vertical tubes	144.
31. Friction during adiabatic flow in vertical tubes	151.
32. Pressure change during flow with heat transfer in vertical tubes	156.
33. The steam-water velocity ratio	167.
34. Pressure change during flow in the downcomer tube and at riser entry	179.

INTRODUCTION.

This section contains the analysis of the pressure changes measured over the various lengths of the two-tube boiler circuit described in the previous section.

30. PRESSURE CHANGE DURING ADIABATIC FLOW IN VERTICAL TUBES.

The method of predicting the theoretical pressure change has already been discussed in Section 21, in analysing the results of Schwab.

The theoretical equations are (Equation 56)

$$K = 1 + Z \sqrt{\frac{\rho_L}{\rho_G} \cdot \frac{\left(\frac{dp}{dl}\right)_2 + \rho_G}{\rho_G - \frac{\lambda \cdot u_L^2 \cdot \rho_L}{2g \cdot d}}}$$

where the momentum forces are neglected, and (Equation 55)

$$-\left(\frac{dp}{dl}\right)_2 \cdot sl = \frac{\lambda \cdot sl \cdot u_L^2 \cdot \rho_L}{2g \cdot d} + \left\{ \frac{q + K(1-q)}{q/\rho_G + K(1-q)/\rho_L} \right\} sl$$

The friction factor λ is that corresponding to a Reynold's Number of $\frac{u_L \cdot d \cdot \rho_L}{\mu_L}$.

These equations are applied to determine the pressure change over the 28" length of 1.7" bore vertical tube between the riser top tapping point and the steam drum. The slight change in densities of the phases due to pressure change up the short length of tube, and also the change in quality, are negligible.

The theoretical values of velocity ratio and pressure change are those which make Equations 55 and 56 compatible. The procedure is detailed in Appendix H.

The values obtained by calculation are plotted along with corresponding experimental results in Figures 36 to 40. For certain tests the theoretical pressure changes calculated on the assumption of homogeneous flow are also plotted.

PRESSURE DIFFERENCE, STEAM DRUM TO RISER TOP - BOILER PRESSURE

TUBE: 2 1/4" O.D. x 2 SW.G.

HEATING: UNIFORM

RESTRICTING ORIFICE: NONE

TUBE POSITION: VERTICAL

HEATED LENGTH: 10'-6"

HOMOGENEOUS FLOW THEORY

○— EXPERIMENTAL

— · — · — ANNULAR FLOW THEORY

----- HOMOGENEOUS FLOW THEORY

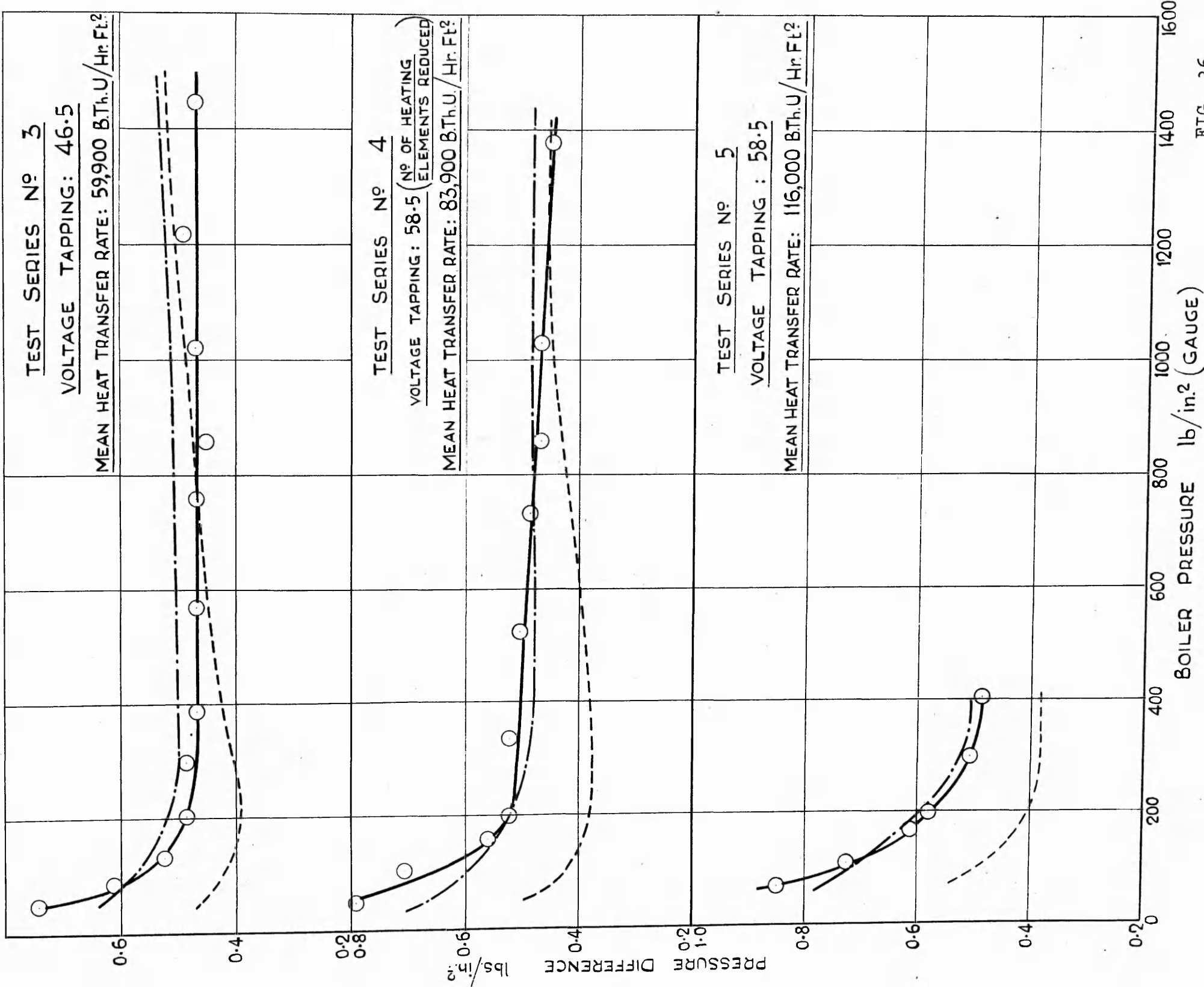


FIG. 36.

PRESSURE DIFFERENCE, STEAM DRUM TO RISERTOP - BOILER PRESSURE

TUBE: $2\frac{1}{4}$ " O.D. x 2 S.W.G.

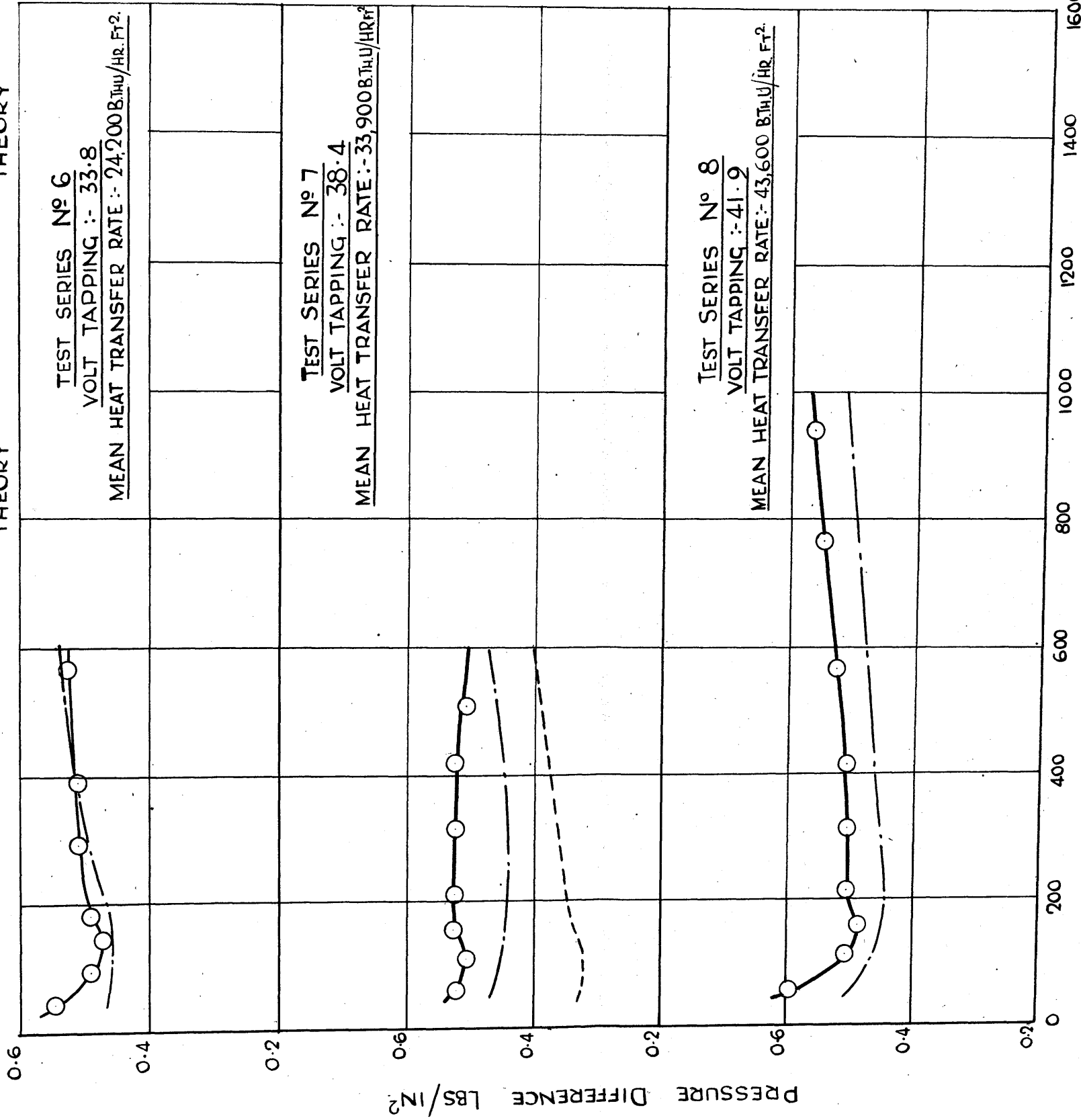
HEATING: UNIFORM

RESTRICTING ORIFICE: $8\frac{7}{8}$ " DIA.

TUBE POSITION: VERTICAL

HEATED LENGTH: 10'-6"

EXPERIMENTAL ANNULAR FLOW THEORY HOMOGENEOUS FLOW THEORY

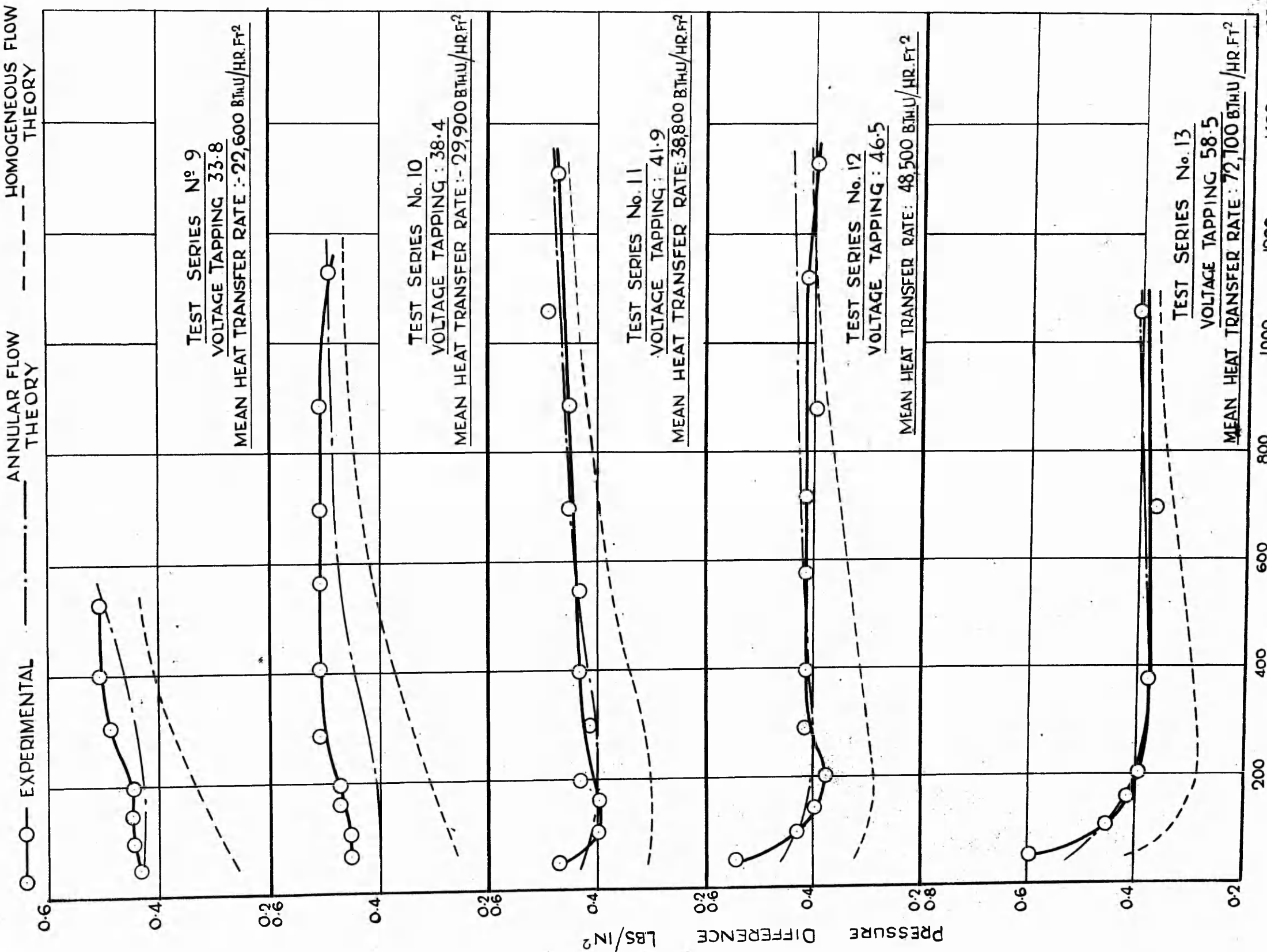


BOILER PRESSURE LBS/IN². (GAUGE)

FIG. 37

PRESSURE DIFFERENCE, STEAM DRUM TO RISER TOP - BOILER PRESSURE

TUBE: $2\frac{1}{4}$ O.D x 2 SWG. HEATING: UNIFORM RESTRICTING ORIFICE: $\frac{3}{4}$ DIA.
 TUBE POSITION: VERTICAL HEATED LENGTH: 10'6"

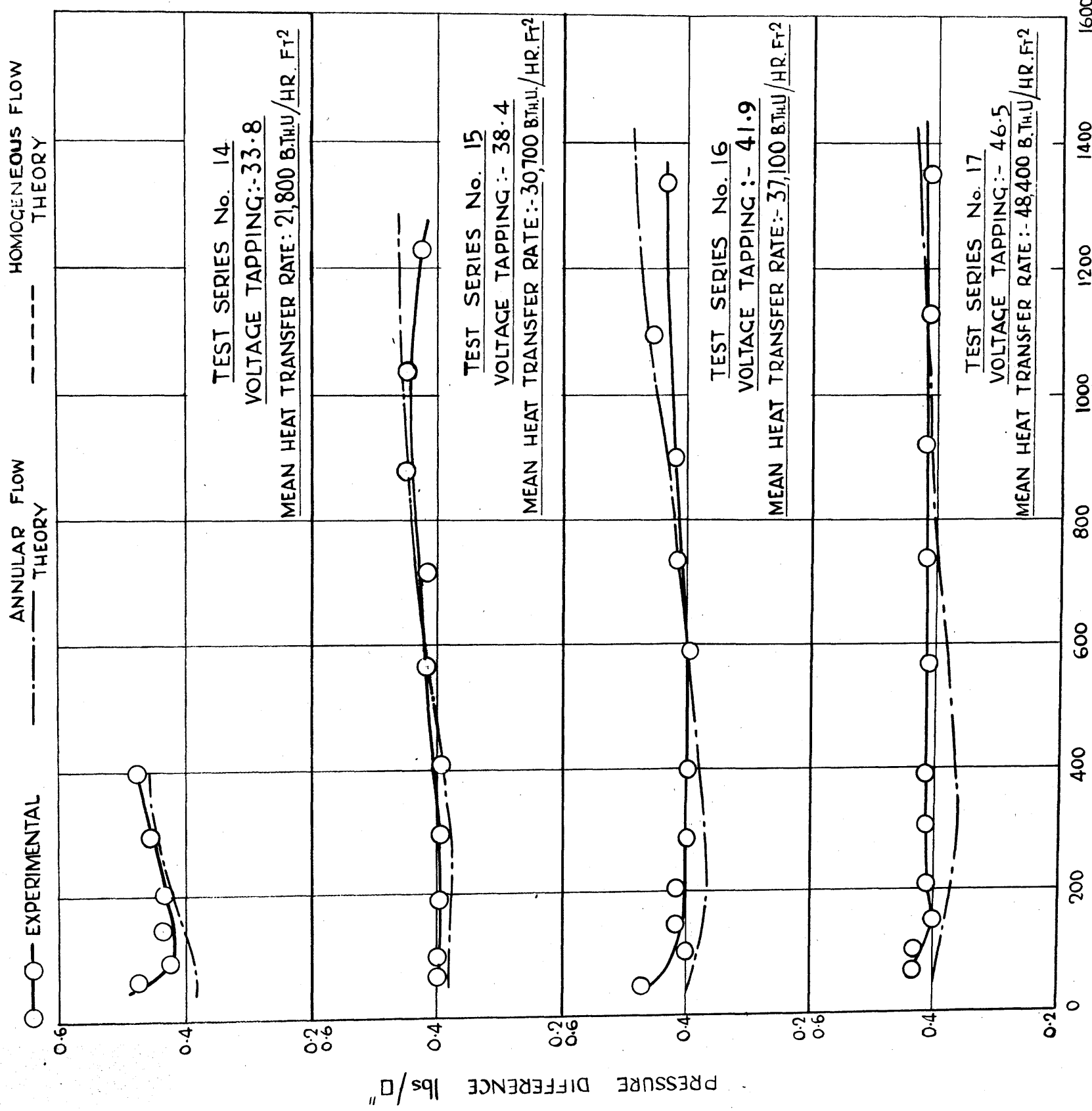


BOILER PRESSURE LBS./IN² (GAUGE)

PRESSURE DIFFERENCE, STEAM DRUM TO RISER TOP - BOILER PRESSURE

TUBE: $2\frac{1}{4}$ " O.D. x 2 SWG. HEATING: UNIFORM RESTRICTED ORIFICE: $\frac{5}{8}$ " DIA.

TUBE POSITION: VERTICAL HEATED LENGTH: 10' 6"



BOILER PRESSURE lbs/ft² (GAUGE)

PRESSURE DIFFERENCE, STEAM DRUM TO RISER TOP- BOILER PRESSURE

TUBE: 2 1/4" O.D. x 2 S.W.G. HEATING: UNIFORM RESTRICTING ORIFICE: 1/2" DIA.

TUBE POSITION: VERTICAL HEATED LENGTH: 10'-6"

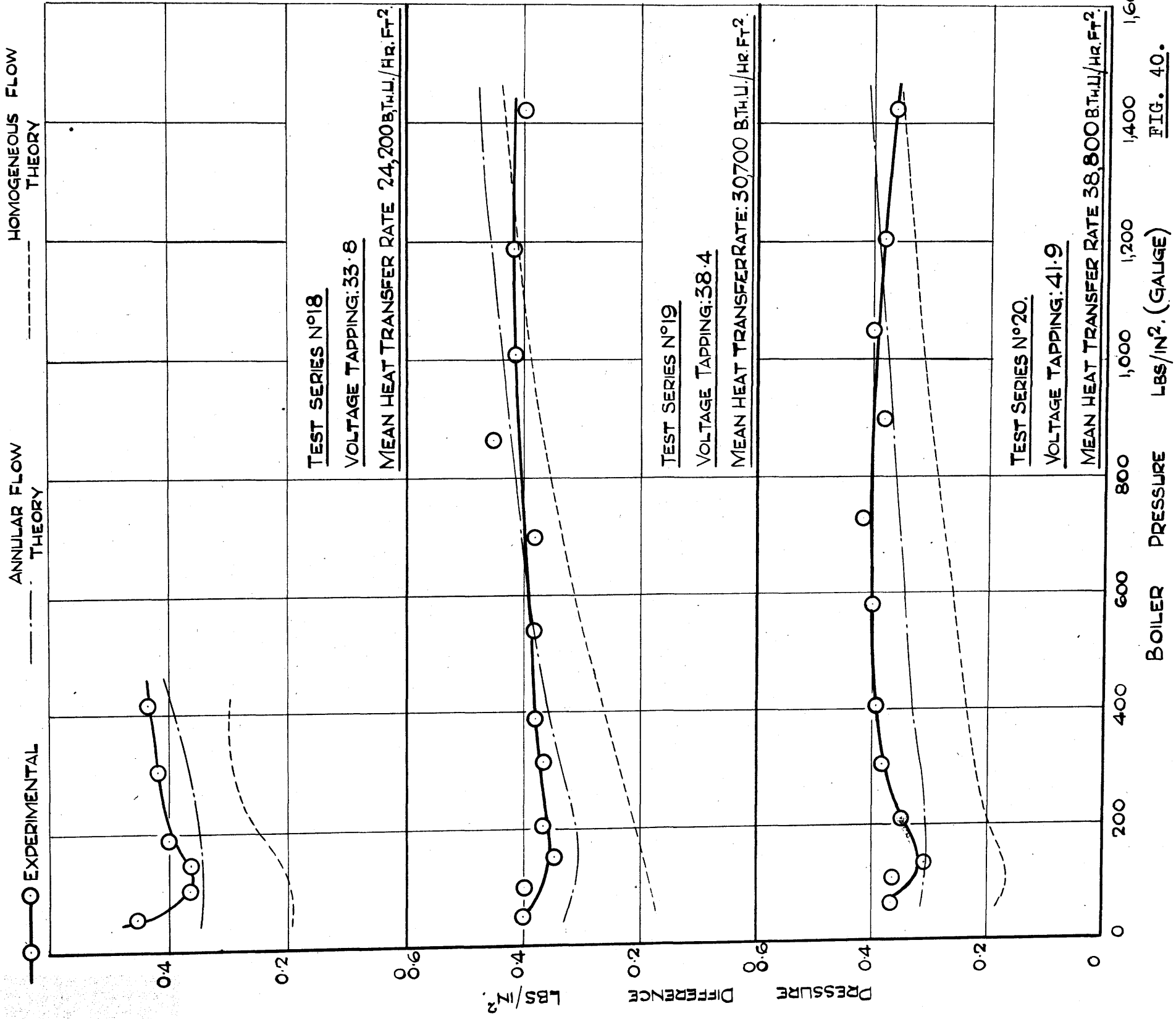


FIG. 40.

Discussion.

The proposed theory gives considerable improvement in the agreement between the calculated and experimental values, as compared with the homogeneous theory. The proposed theory gives 45% of the predicted pressure changes within 5% of the experimental value, 87% within 15% and all within 22%.

The homogeneous theory, on the other hand, gives only 40% of the predicted pressure changes within 22%. The maximum error is 55%.

It will be observed that at pressures above 1000 lb/in.² the proposed theory tends to give values slightly higher than the experimental values. This may be partly due to the effects of distortion. At high pressures, due to the relatively small steam volume content, the friction pressure change is normally small relative to the total pressure change. The shearing stress ratio T_2/T_1 is therefore large, a condition giving considerable annulus profile distortion. The proposed friction equation, therefore, will probably give an excessive estimate of the friction pressure change under such conditions.

31. FRICTION DURING ADIABATIC FLOW IN VERTICAL TUBES.

In Section 15 theoretical considerations led to the development of the formula for the friction pressure gradient during two-phase flow (Equation 40).

$$-\left(\frac{dp}{dl}\right)_{F2} \cdot sl = G \cdot \frac{\lambda \cdot sl}{2g \cdot d} \left(\frac{1-q}{x} \frac{M}{\rho_L}\right)^2 \left(\frac{x}{x_L}\right)^2$$

In Section 20 this was applied in the logarithmic form (Equation 61).

$$\text{Log} \left\{ -\left(\frac{dp}{dl}\right)_{F2} / \frac{\lambda}{2g \cdot d} \left(\frac{1-q}{x} \frac{M}{\rho_L}\right)^2 \right\} = \text{Log } G + n \text{Log} \left(\frac{x}{x_L}\right)$$

to the analysis of air-water experiments, where n is the power of $\frac{x}{x_L}$. G and n were found to be 0.75 and 2 respectively. G has been assumed unity in applying the theoretical equations.

In view of the uncertainty of the precise magnitude of G , Equation 61 is applied to the analysis of results obtained for the adiabatic flow between the riser top and steam drum tapping points.

During flow in vertical tubes the friction pressure change cannot be measured directly, as the mixture weight will be present in any overall pressure change measurement. The total pressure gradient is given by

$$-\left(\frac{dp}{dl}\right)_2 \cdot sl = -\left(\frac{dp}{dl}\right)_{F2} \cdot sl + \left\{ \frac{q + K(1-q)}{q/\rho_g + K(1-q)/\rho_L} \right\} sl$$

where/

where the inertia forces are neglected.

The value of $\left(\frac{db}{dl}\right)_{F_2}$ determined from this equation, using the measured total pressure change, is substituted in Equation 61, and a log plot made in Figure 41, which enables the evaluation of G and .

Only tests where the friction contributed a large proportion of the total pressure gradient were analysed, otherwise experimental errors in the overall change would produce considerably larger errors in the apparent friction change. The tests analysed were Test Series Nos. 3,4,5,12 and 13. For this reason also the results were plotted up to a maximum pressure of 225 lb/in² gauge. The friction decreases with increasing pressure due to the higher steam density, and the correspondingly lower value of the ratio

$$\frac{x}{x_L} \left(\text{i.e. } \frac{q/\rho_g + K(1-q)/\rho_L}{K(1-q)/\rho_L} \right) \text{ in Equation 61.}$$

First inspection of Figure 41 suggests a wide scatter of the experimental results, but closer inspection indicates that results in the same pressure region lie on straight lines having a slope with $\eta = 2$. This suggests that G varies with pressure. To illustrate this point, G is calculated for each test using Equation 42, and plotted to a base of pressure as shown in Figure 42.

The maximum scatter about a mean line is $\pm 7\%$, with the exception of a single test result.

G has already been shown to be a function of ω , the water content in the core. The variation with pressure, therefore, may well be due to the change in respective phase/

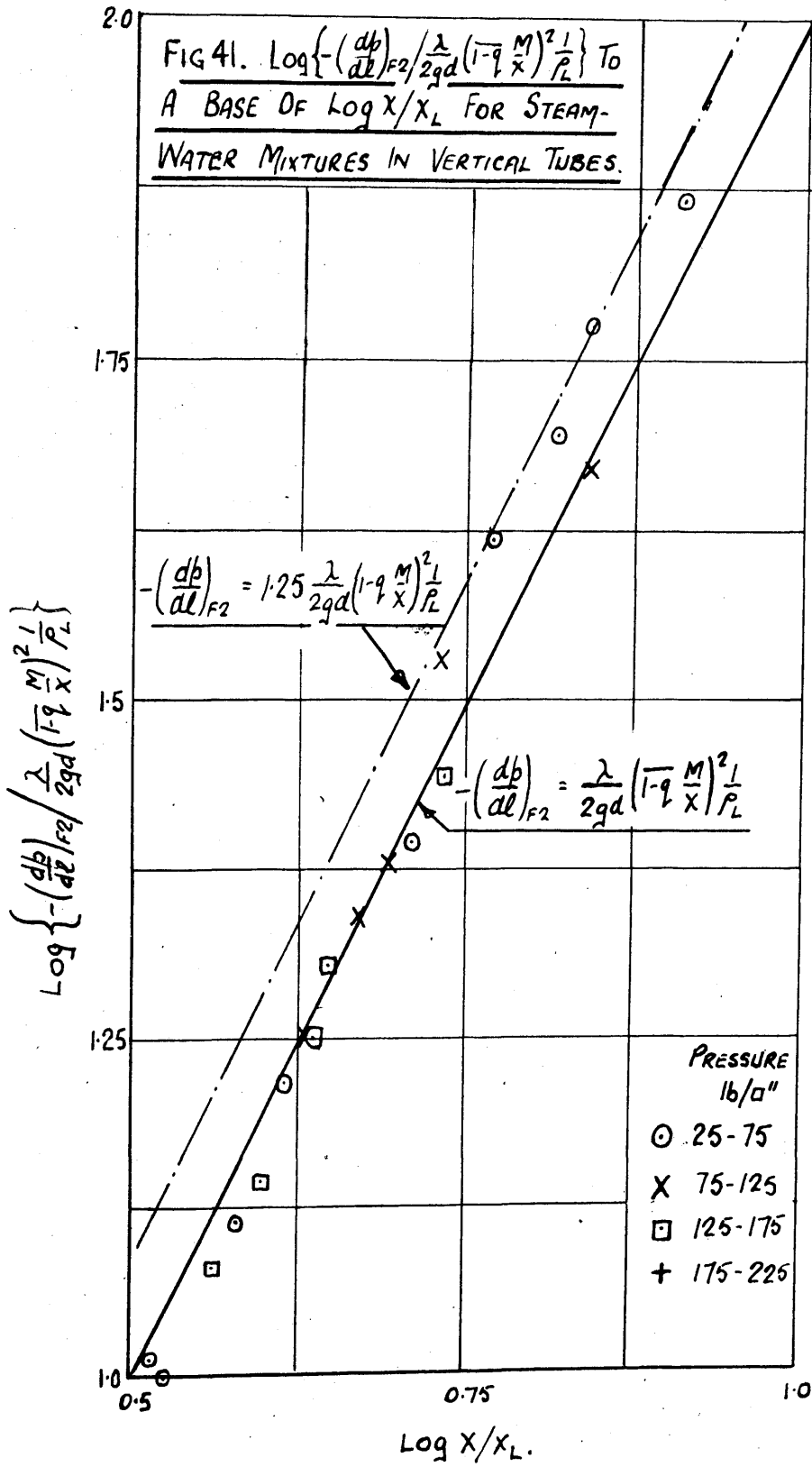
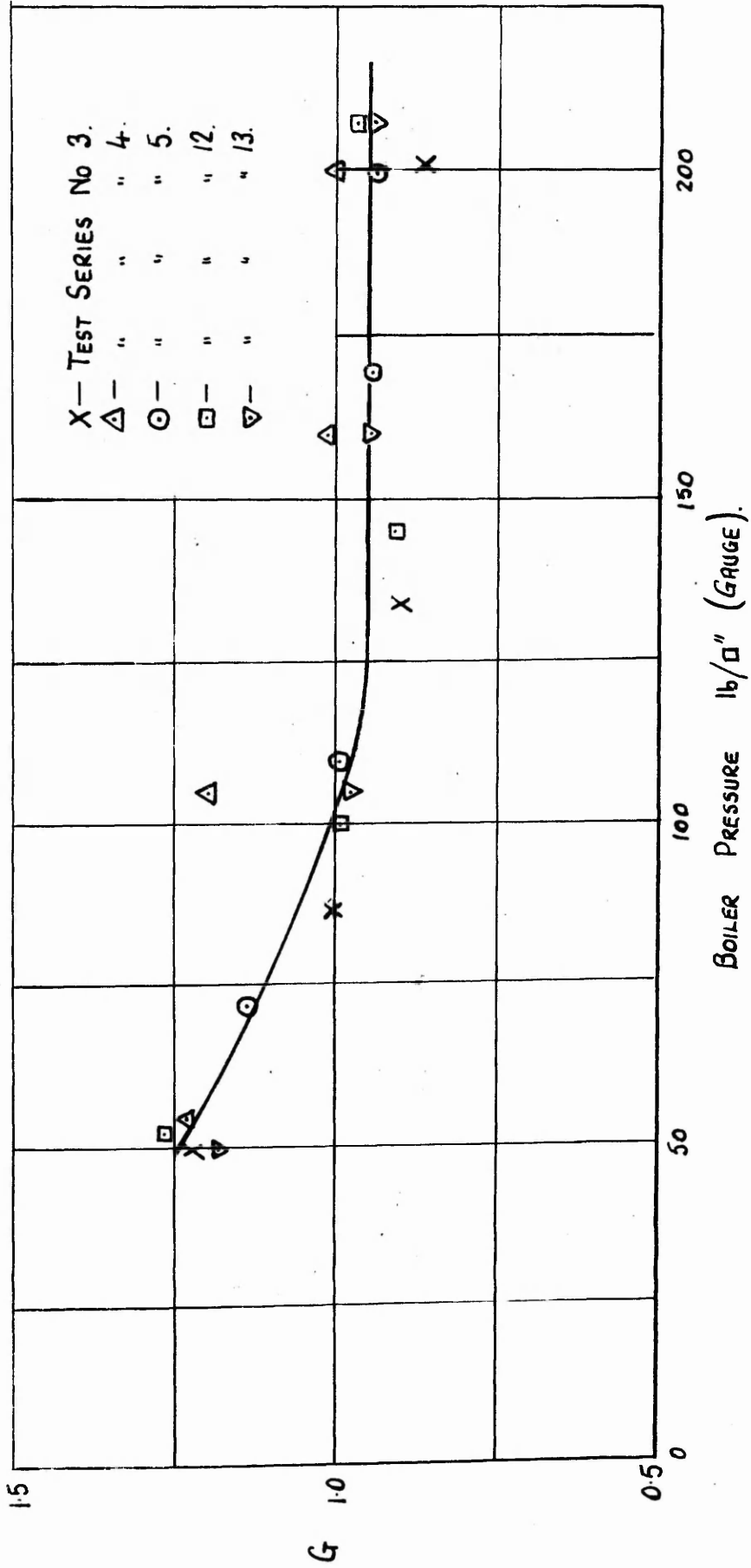


FIG. 42. GRAPH OF "G" TO A BASE OF BOILER PRESSURE.



phase densities and viscosities with pressure, altering the core water content.

Above 135 lb/in² gauge, G assumes a constant value of 0.95. This agrees well with the value of unity used throughout the theoretical analysis.

The use of values of G obtained from Figure 42 in the theoretical analysis would give considerable improvement at pressures below 100 lb/in² between the theoretical and experimental pressure changes.

The results analysed in this section of the report are the differential pressure readings between the riser top and the riser bottom tapping points. With reference to Figure 26 it is seen that the tapping points are 23" respectively from the beginning and end of the heated length. Hence the experimental pressure change over the length between the riser top and the riser bottom tapping points comprises the pressure change over the heated length, the pressure change over a length in which water flows, and the pressure change over a length in which the steam-water mixture flows adiabatically.

Points of Evaporation. The water does not commence to evaporate immediately heat is transferred to it, as at that point in the circuit the liquid temperature is below saturation temperature due to the following reasons:-

- (a) The pressure at all points in the tube is greater than the steam drum pressure, consequently, assuming that water only enters the downcomer, the temperature of the water must be equal to or less than the steam drum temperature, which in turn must be less than the saturation temperature at all points in the tube.
- (b) Heat is lost from the water flow in the tubes and in the water drum.

The method of calculating the point of evaporation is

as/

as follows:-

Let Q = heat transfer per lb. of flow to bring the water to saturation temperature.

$$\frac{dH}{dp} = \text{gradient of total heat of saturated water}$$

with respect to pressure.

δp = pressure difference between the point of evaporation and the steam drum.

$$\frac{Q_B}{M \cdot 3600} = \text{heat loss from boiler per lb. flow where } Q_B$$

is the heat loss from the boiler per hour and M is the mass flow per second.

Only a fraction of this total boiler heat loss is from the flowing water, as it is assumed in determining the mixture quality that heat transfer through the upper half of the steam drum contributes to the action of the condenser. The proportion of the heat loss utilised in this manner was estimated to be $\frac{1}{5} Q_B$, hence the heat loss from the water is $\frac{4}{5} Q_B$.

It can be shown that approximately

$$Q = \frac{dH}{dp} \cdot \delta p + \frac{4}{5} \cdot \frac{Q_B}{M \cdot 3600} \dots \dots \dots 77$$

The gradient $\frac{dH}{dp}$ may be calculated from the steam tables.

The point of evaporation is assumed a certain distance L from the furnace bottom. Using the experimental reading for the pressure difference between the steam drum/

drum and riser bottom tapping points, the pressure change to the point of evaporation is then estimated, and Q calculated from Equation 77. The heat transfer Q over the length L is then calculated by assuming a uniform heat transfer over the heated length. If L has been assumed correctly, Q calculated by both methods should be the same. By trial and error the correct length L is obtained.

End of Evaporation. Adiabatic conditions are assumed to start immediately following the top of the furnace. The velocity ratio during heat transfer will be greater than for the corresponding adiabatic condition due to the presence of momentum forces. At the end of evaporation there will, therefore, be a period in which the velocity ratio in the unheated tube adjusts itself to the velocity ratio normally associated with adiabatic flow. In effect, during this period the steam will be giving up kinetic energy to the water.

The velocity ratios at the top of the heated length, and in the length where the steam-water mixture flows adiabatically, do not show a marked difference. The error introduced by neglecting this effect will, therefore, be small consequently in determining the pressure change from the furnace top of the riser top tapping point the method detailed in the previous section is used.

Pressure Change During Heat Transfer. Where heat transfer occurs the pressure change is obtained from Equation 53

$$-\left(\frac{db}{dl}\right)_2 \cdot \delta \ell = 1.25 \cdot \frac{\lambda \cdot \delta \ell \cdot U_L^2 \cdot \rho_L}{2g \cdot d} + \left\{ \frac{q + K(1-q)}{q/\rho_G + K(1-q)/\rho_L} \right\} \delta \ell \sin \theta$$

$$+ \left\{ \frac{q}{g} \cdot \frac{M}{X} \cdot \delta U_G + \frac{1-q}{g} \cdot \frac{M}{X} \cdot \delta U_L + \frac{\delta q}{g} \cdot \frac{M}{X} (U_G - U_L) \right\}$$

The velocity ratio is obtained from Equation 54.

$$K = 1 + Z \sqrt{\frac{\rho_L \cdot \left(\frac{db}{dl}\right)_2 + \rho_G \sin \theta + \frac{\rho_G \cdot U_2 \cdot \delta U_2}{\delta \ell \cdot g}}{\rho_G \cdot -1.25 \cdot \frac{\lambda \cdot U_L^2 \cdot \rho_L}{2g \cdot d}}}$$

(The friction term is multiplied by 1.25 to allow for the effects of evaporation).

The theoretical values of the velocity ratio and of the pressure change are again those which make the above equations compatible. It will be appreciated that the above equations cannot be integrated, and consequently the method of obtaining the overall pressure change is by determining the pressure gradient at five points along the heated length, plotting the results to a base of heated length and measuring the area of the figure. The area represents to a particular scale the pressure change over the heated section. The procedure is detailed in Appendix H.

In all such evaluations the dryness fraction of the steam is assumed to vary linearly over the evaporation length.

The experimental and theoretical pressure changes over/

over the riser top and riser bottom tapping points are plotted to a base of boiler gauge pressure in Figures 43 to 47. In certain tests the theoretical pressure change assuming homogeneous flow is also plotted. The procedure is detailed in Appendix H.

Discussion.

The agreement of the experimental and theoretical results is extremely good, all but two tests agreeing within 0.2 lb/in.^2 (i.e. within 6%). This would appear a considerable improvement on the figures obtained in the adiabatic case, but it should be remembered that, in certain tests, as much as 2 lb/in.^2 of the pressure change is due to the water flow before the commencement of evaporation. Over the evaporation length the maximum error is of the order of 15%. In general, however, the accuracy is better than this.

The agreement obtained with the homogeneous theory is slightly better than for the adiabatic case. This is presumably due to two reasons:

- (a) The large contribution to the pressure change due to the flow before evaporation commences, as mentioned above.
- (b) The pressure change due to momentum forces calculated on the assumption of homogeneous flow will be greater than obtained by introducing the respective phase velocities.

Nevertheless/

PRESSURE DIFFERENCE, RISER TOP TO RISER BOTTOM - BOILER PRESSURE

TUBE: $2\frac{1}{4}$ " O.D. x 2 S.W.G.

HEATING: UNIFORM.

RESTRICTING ORIFICE: - NONE

TUBE POSITION: VERTICAL

HEATED LENGTH: 10'-6"

○— EXPERIMENTAL —·—·— ANNULAR FLOW THEORY - - - - - HOMOGENEOUS FLOW THEORY

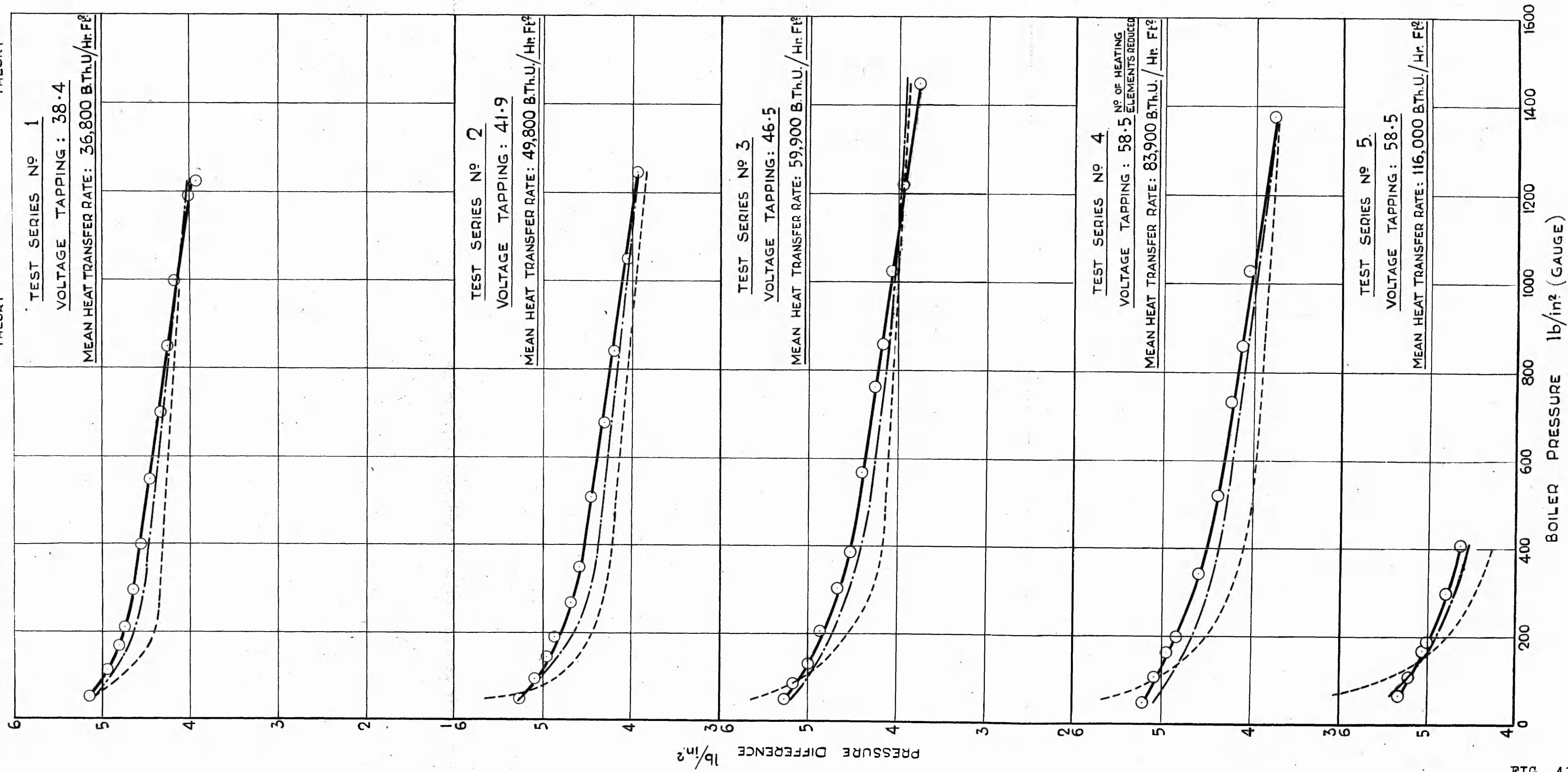
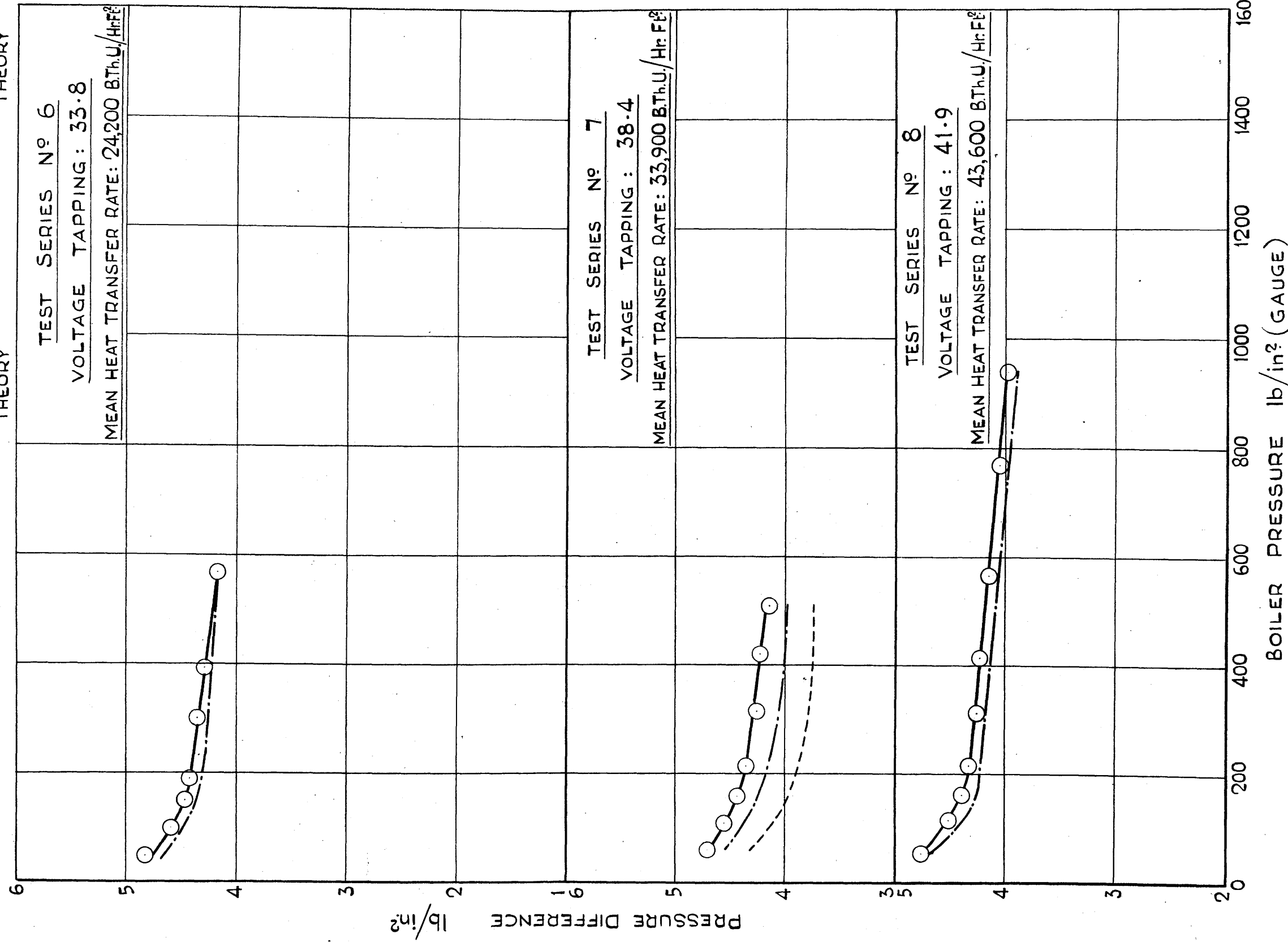


FIG. 43.

PRESSURE DIFFERENCE, RISER TOP TO RISER BOTTOM - BOILER PRESSURE
 TUBE: $2\frac{1}{4}$ " O.D. x 2 S.W.G. HEATING: UNIFORM RESTRICTING ORIFICE: $\frac{1}{8}$ " DIA.
 TUBE POSITION: VERTICAL HEATED LENGTH: 10'-6"

○—○ EXPERIMENTAL ——— ANNULAR FLOW THEORY - - - - - HOMOGENEOUS FLOW THEORY



PRESSURE DIFFERENCE, RISER TOP TO RISER BOTTOM — BOILER PRESSURE.

TUBE: $2\frac{1}{2}$ " O.D. x 2 S.W.G.

HEATING: UNIFORM.

RESTRICTING ORIFICE: $\frac{3}{4}$ " DIA.

TUBE POSITION: VERTICAL.

HEATED LENGTH: 10' - 6"

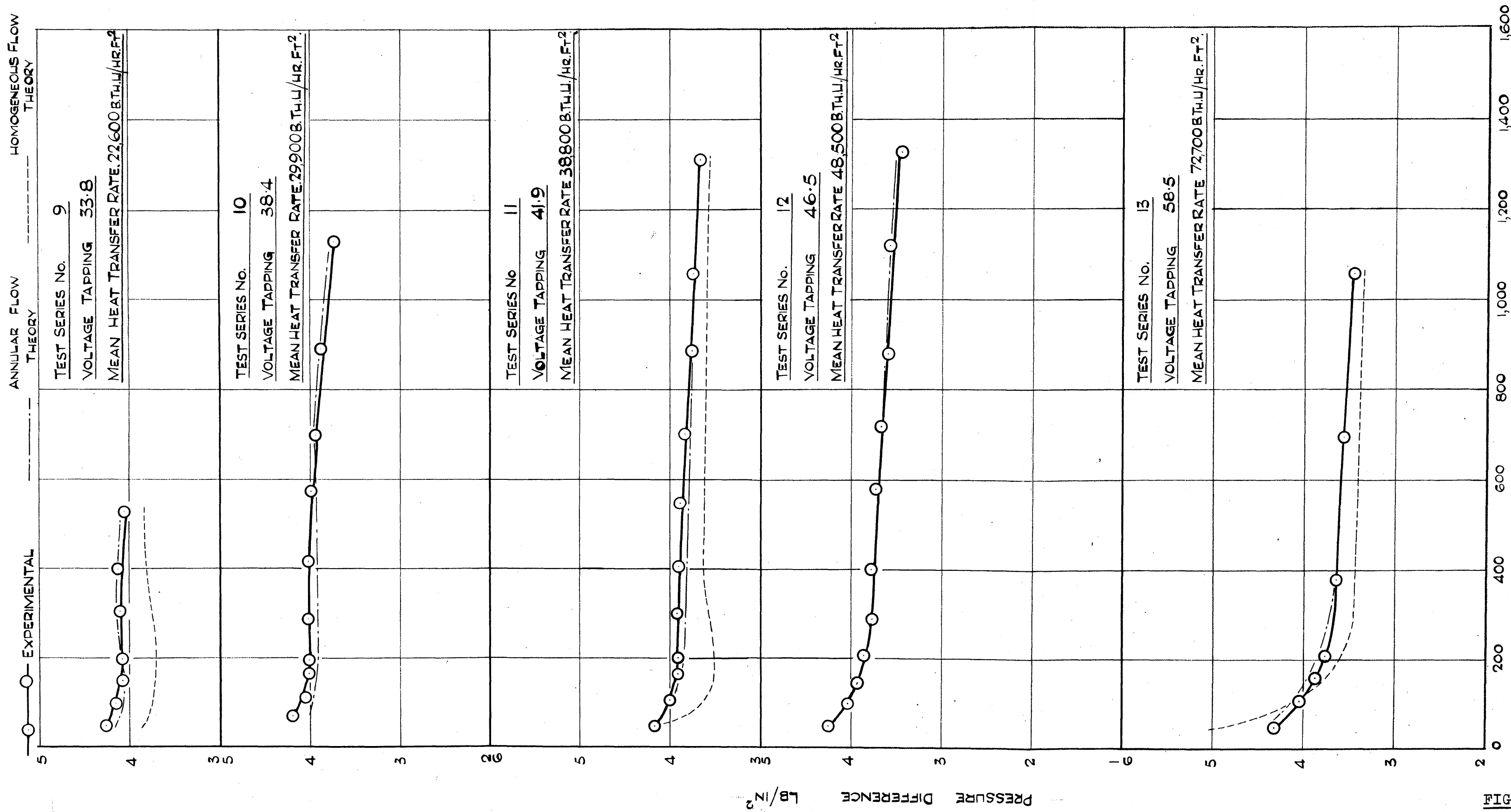


FIG. 45.

PRESSURE DIFFERENCE, RISER TOP TO RISER BOTTOM - BOILER PRESSURE

TUBE: $\frac{1}{4}$ " DIA. x 2 S.W.G. HEATING: UNIFORM RESTRICTING ORIFICE $\frac{5}{8}$ " DIA.
TUBE POSITION: VERTICAL HEATED LENGTH: 10'-6"

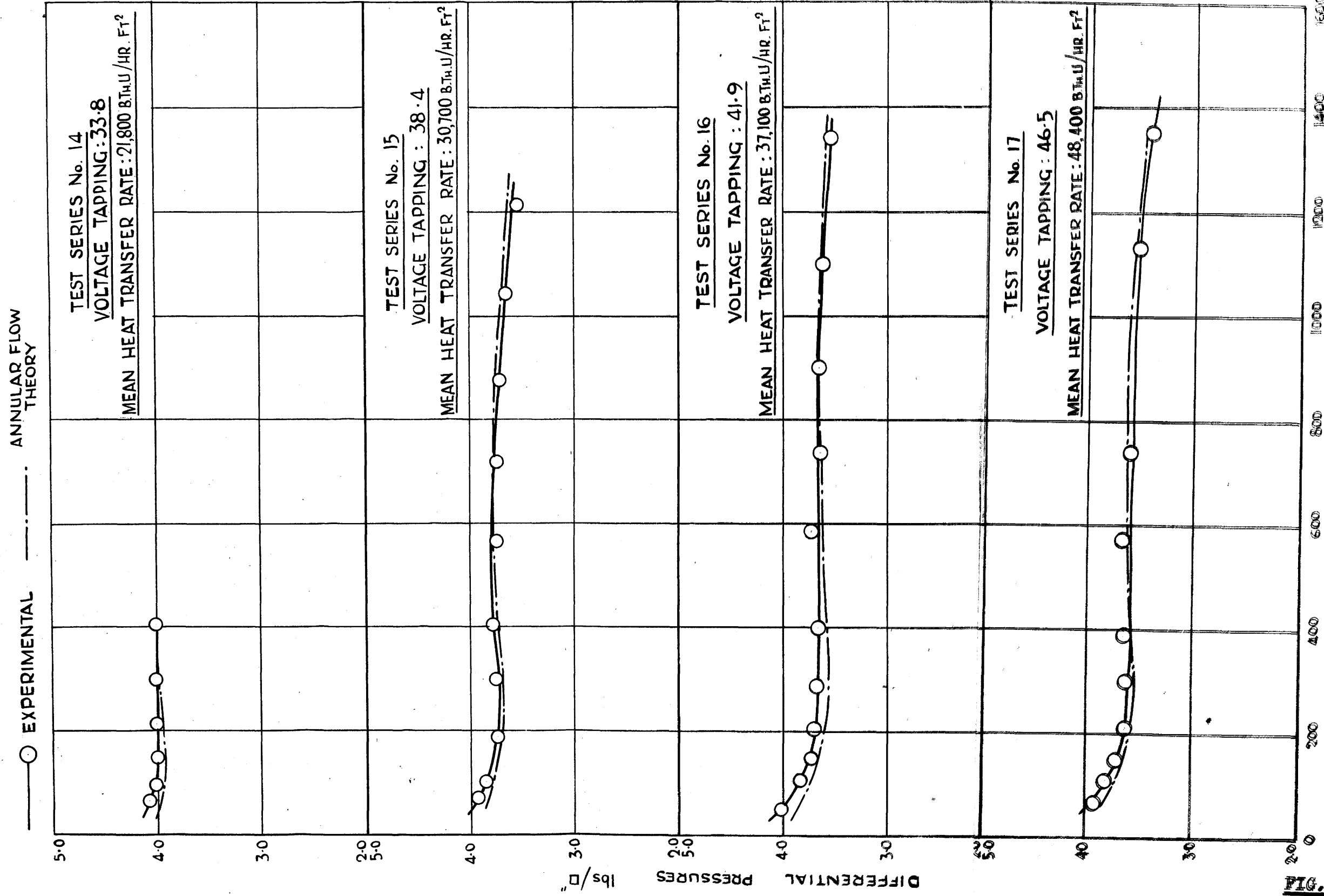


FIG. 46.

PRESSURE DIFFERENCE, RISER TOP TO RISER BOTTOM - BOILER PRESSURE

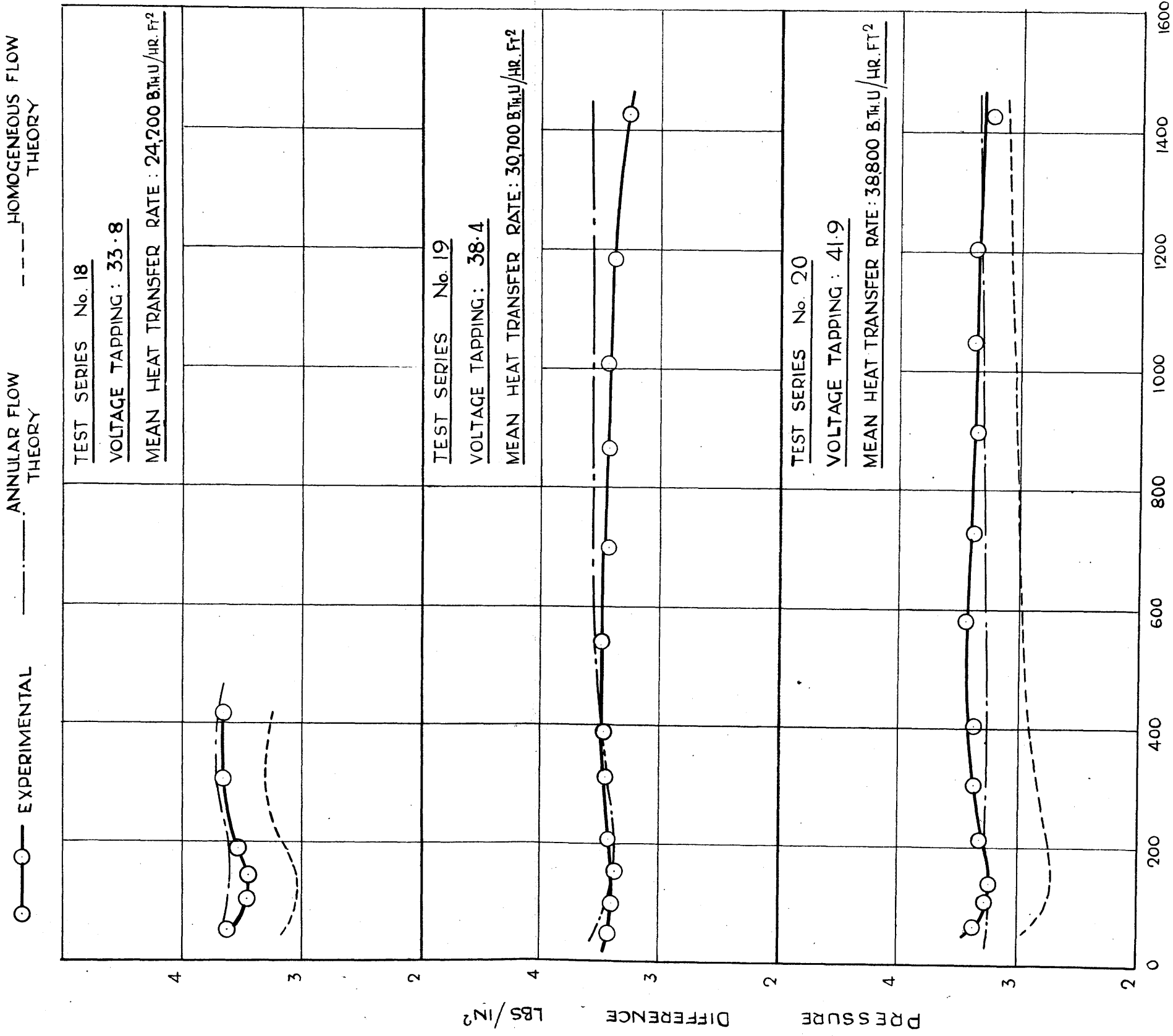
TUBE: $2\frac{1}{4}$ OD x 2 SWG.

HEATING: UNIFORM

RESTRICTING ORIFICE: $\frac{1}{2}$ DIA

TUBE POSITION: VERTICAL

HEATED LENGTH: 10'-6"



BOILER PRESSURE LBS/IN² (GAUGE)

FIG. 47.

Nevertheless the errors assuming homogeneous flow are still large when based on the pressure change over the tapping points, being as much as 27% at low pressures. Over the evaporation length the errors will be of the order of 40%.

33. THE STEAM-WATER VELOCITY RATIO.

The previous sections have shown the application of the theoretical equations to the prediction of pressure changes during two-phase flow. Contained in that analysis was the estimate of the ratio of the velocities of the steam and water phases. It is of interest to estimate from the accuracy of the predicted pressure changes, the accuracy of the estimated velocity ratio, and to investigate the relative importance of the various terms contained in the equation for velocity ratio. (Equation 13).

$$K = 1 + Z \sqrt{\frac{\rho_L}{\rho_G} \cdot \frac{T_2}{T_1}}$$

This was the form used in analysing the results in the previous sections. Figure 48 shows for adiabatic flow the velocity ratio to a base of boiler pressure for three representative test series. Velocity ratios as high as four were obtained.

The values of Z , the density ratio ρ_L/ρ_G , and the shear stress ratio T_2/T_1 used in calculating the velocity ratio K , are shown in Figures 49, 50 and 51 respectively.

These figures indicate that each of the three terms varies considerably during the test series. The values of Z range from 0.01 to 0.123. The ratio T_2/T_1 varies from just greater than unity to 57.5 and the ratio ρ_L/ρ_G varies from 360 to 10. This indicates that the variation of each of/

FIG. 4-8. VELOCITY RATIO K TO A BASE OF BOILER GAUGE PRESSURE
FOR THREE REPRESENTATIVE TESTS

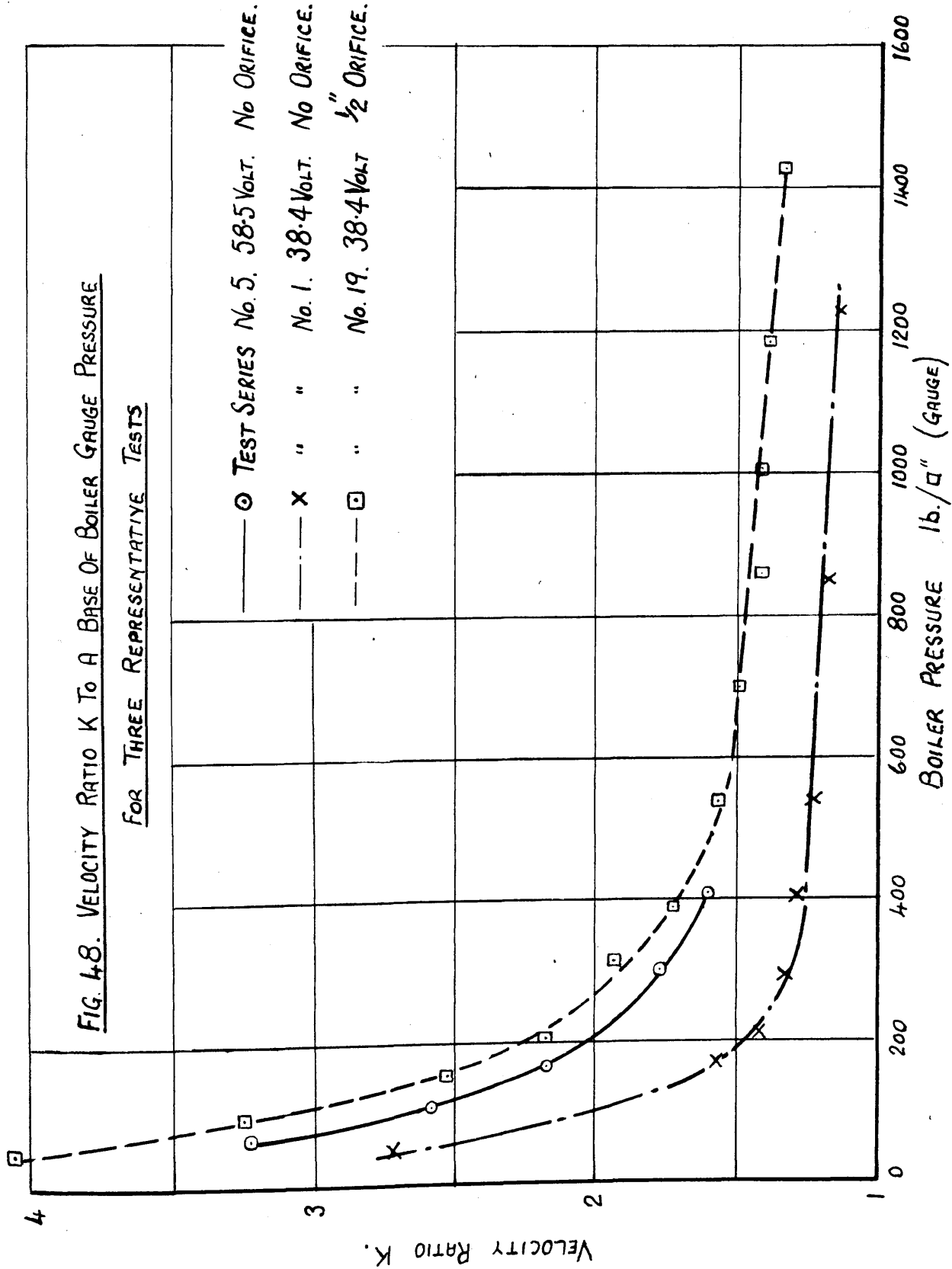
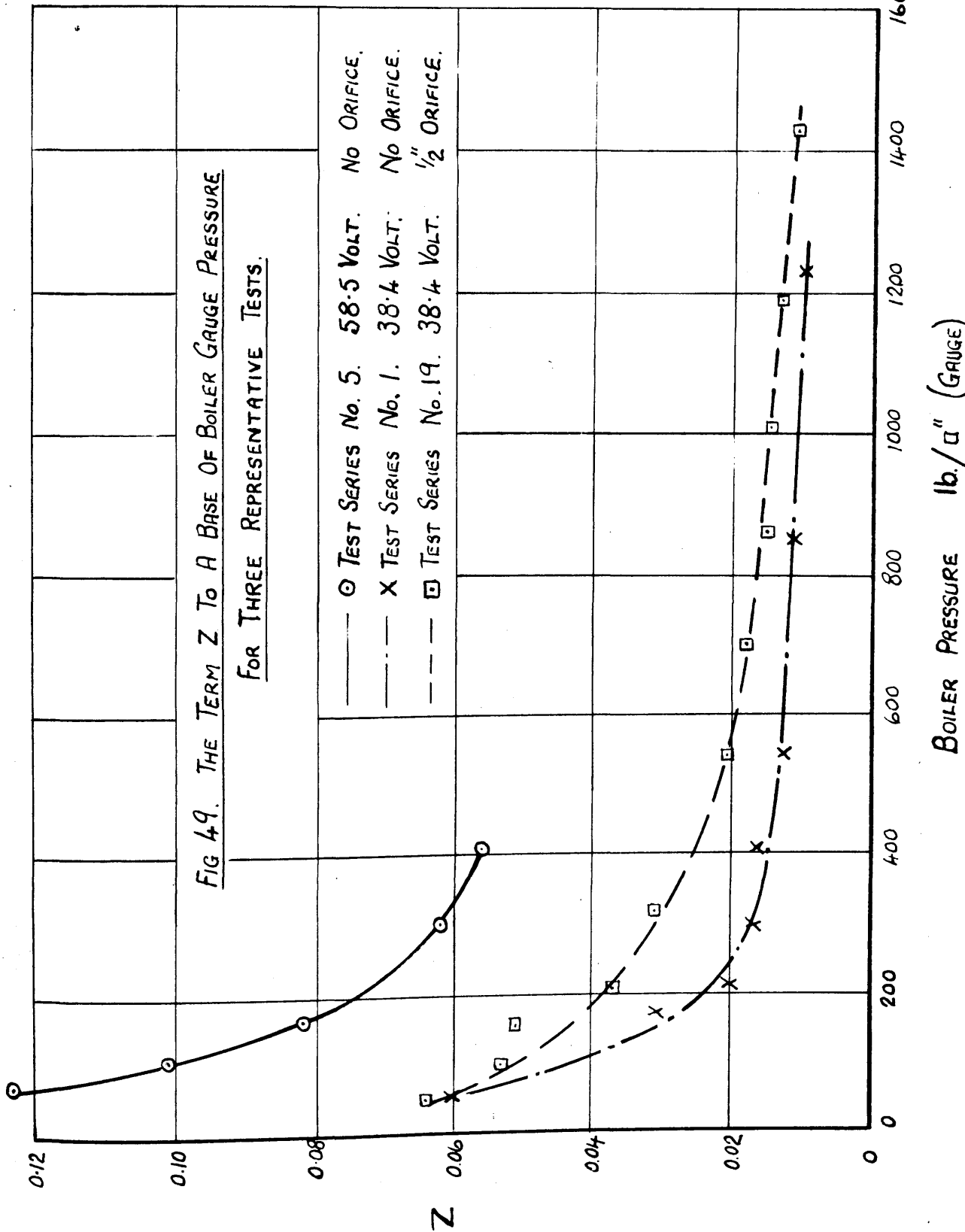


FIG 49. THE TERM Z TO A BASE OF BOILER GAUGE PRESSURE
FOR THREE REPRESENTATIVE TESTS.

— O TEST SERIES No. 5. 58.5 VOLT. No ORIFICE.
- - X TEST SERIES No. 1. 38.4 VOLT. No ORIFICE.
- - - □ TEST SERIES No. 19. 38.4 VOLT. 1/2" ORIFICE.



BOILER PRESSURE lb./sq. (GAUGE)

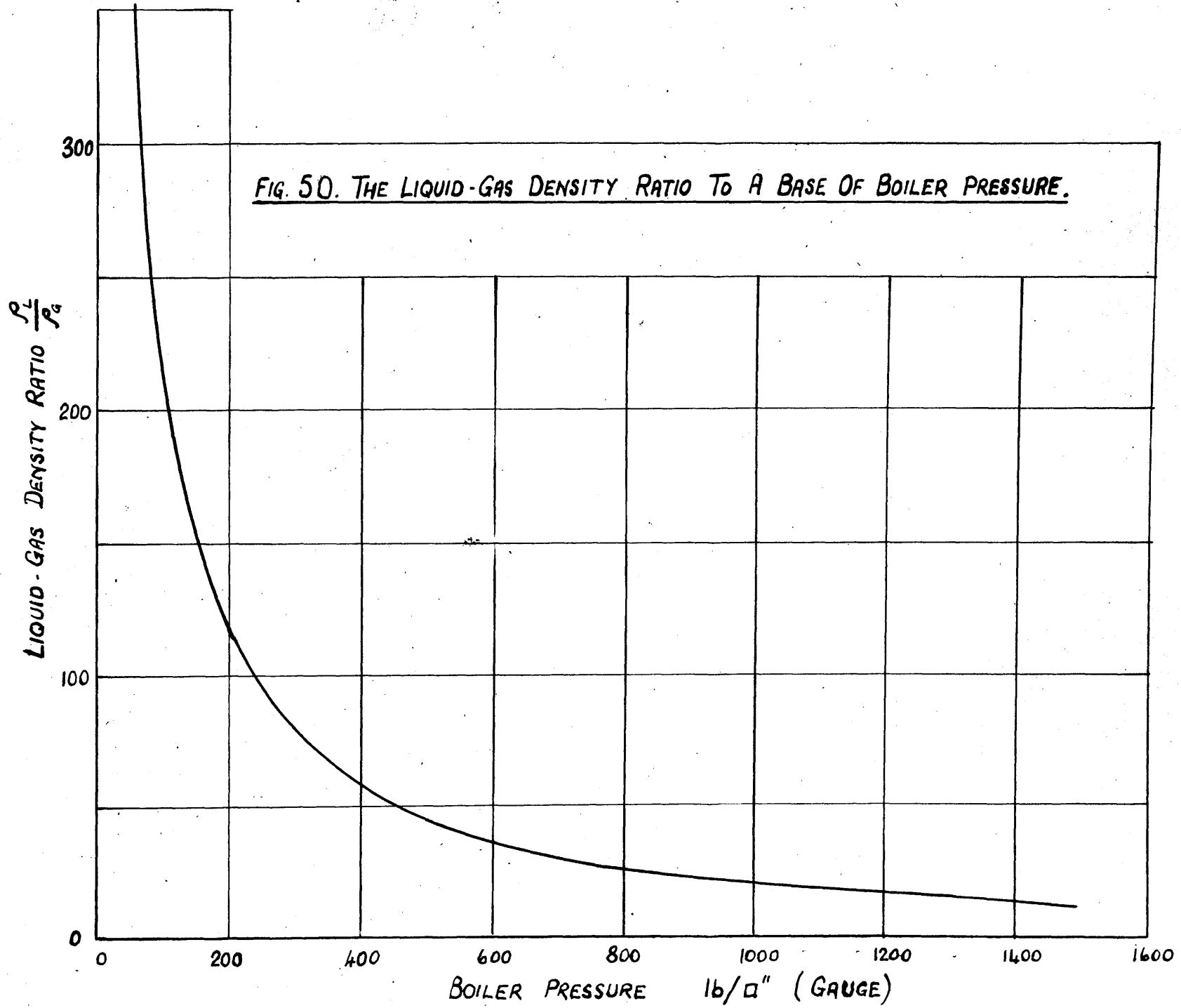
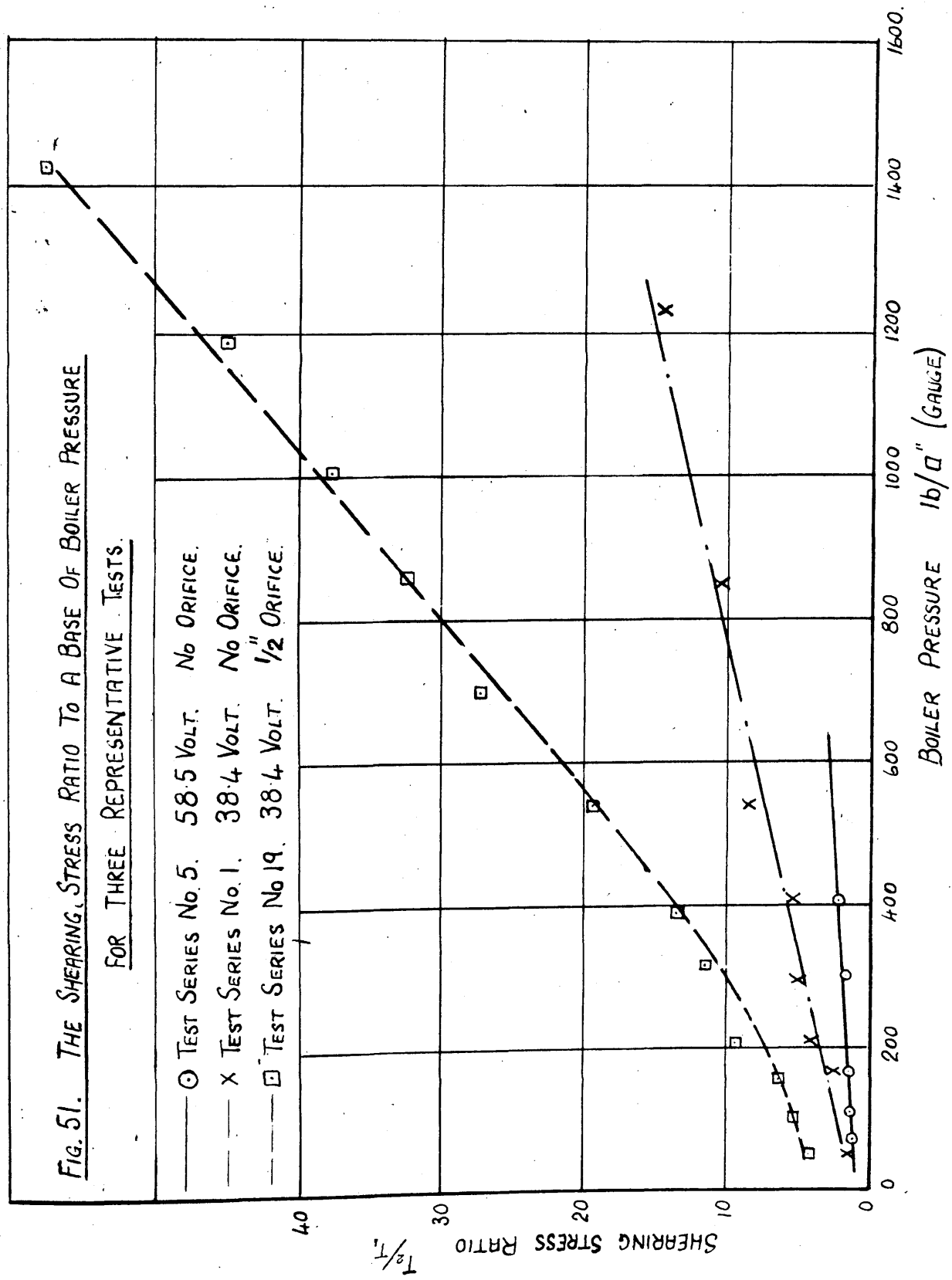


Fig. 51. THE SHEARING STRESS RATIO TO A BASE OF BOILER PRESSURE
FOR THREE REPRESENTATIVE TESTS.

—○— TEST SERIES No. 5. 58.5 Volt. No ORIFICE.
 —X— TEST SERIES No. 1. 38.4 Volt. No ORIFICE.
 —□— TEST SERIES No. 19. 38.4 Volt. 1/2" ORIFICE.



of the three terms is of importance.

The apparent accuracy of the estimated velocity ratio may be studied with reference to Figure 52. This figure shows the estimated pressure change over a foot length of tube plotted to a base of assumed values of the velocity ratio. Figures (a) to (d) illustrate the change in relationship between the pressure change and the velocity ratio when the contribution of the friction pressure change to the total pressure change decreases.

On the assumption that the discrepancy between the theoretical and experimental values of the pressure change is due to errors in the predicted velocity ratio, the slope of the various lines suggests that a 15% error in the predicted pressure change may be due to errors in the velocity ratio of 10%, 30%, 65% and 24% for cases (a), (b), (c) and (d) respectively. As 87% of the test results agree within 15%, this would suggest that the majority of the values of velocity ratio are determined within 65%.

The above errors are, however, based on the slope of the curves in the vicinity of the theoretical velocity. Over a greater range of velocity ratio the relationship between the pressure changes and the velocity ratio no longer approaches a straight line. This is illustrated in Figure 53 which consists of the pressure change to a base of velocity ratio for the test represented in Figure 52(c).

From this diagram it will be seen that if the theoretical value of the velocity ratio is 4.05 (as was the case in this test) the error in the velocity ratio associated with/

FIG. 52. PRESSURE CHANGE TO A BASE OF ASSUMED VELOCITY RATIO.

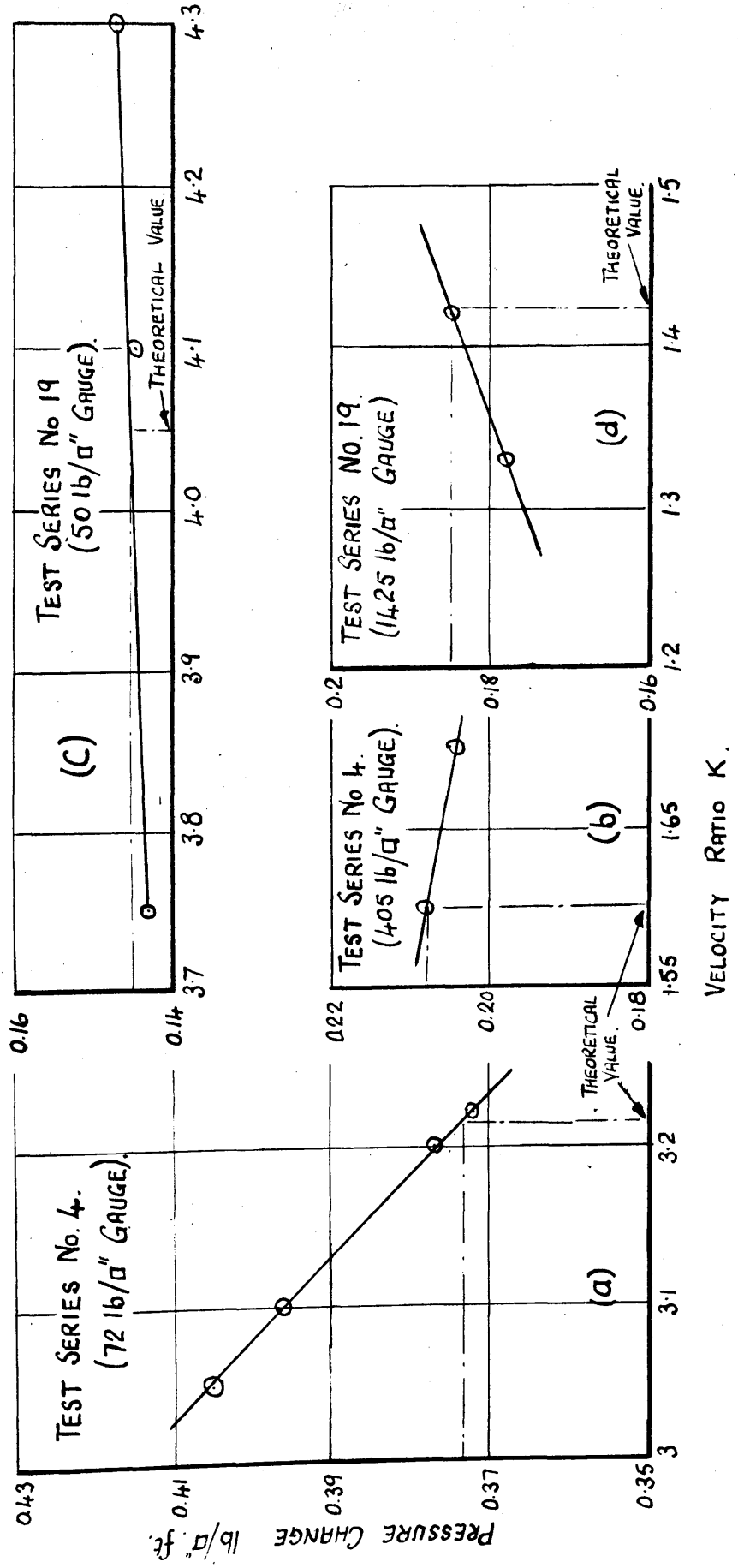
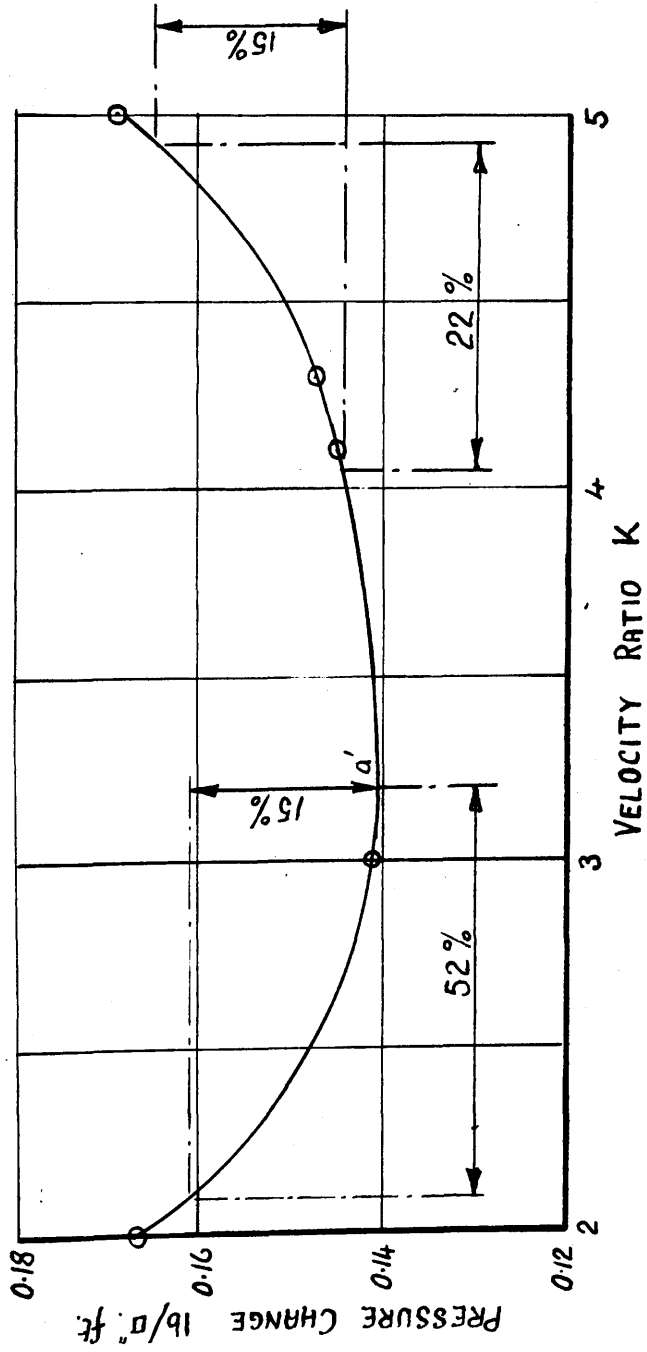


FIG. 53. PRESSURE CHANGE TO A BASE OF VELOCITY. RATIO.

TEST SERIES No 19 (50 lb/ft² GAUGE)



with a 15% error in the pressure change is 22% which is considerably less than that estimated on the basis of the mean slope of the curve.

Greater errors would occur if the theoretical velocity were at the turning point α' in Figure 53. At this point a 15% error in the pressure change is associated with a 52% in the velocity ratio. In the majority of the tests, however, the theoretical velocity does not coincide with the turning point. It may be concluded that in the majority of the tests the velocity ratio is determined within approximately 20%.

Flow with Heat Transfer. The equations are the same as those used with adiabatic flow with the addition of the momentum forces which are now no longer negligible. The effect of heat transfer on the theoretical equation for the velocity ratio has already been discussed in Section 13.

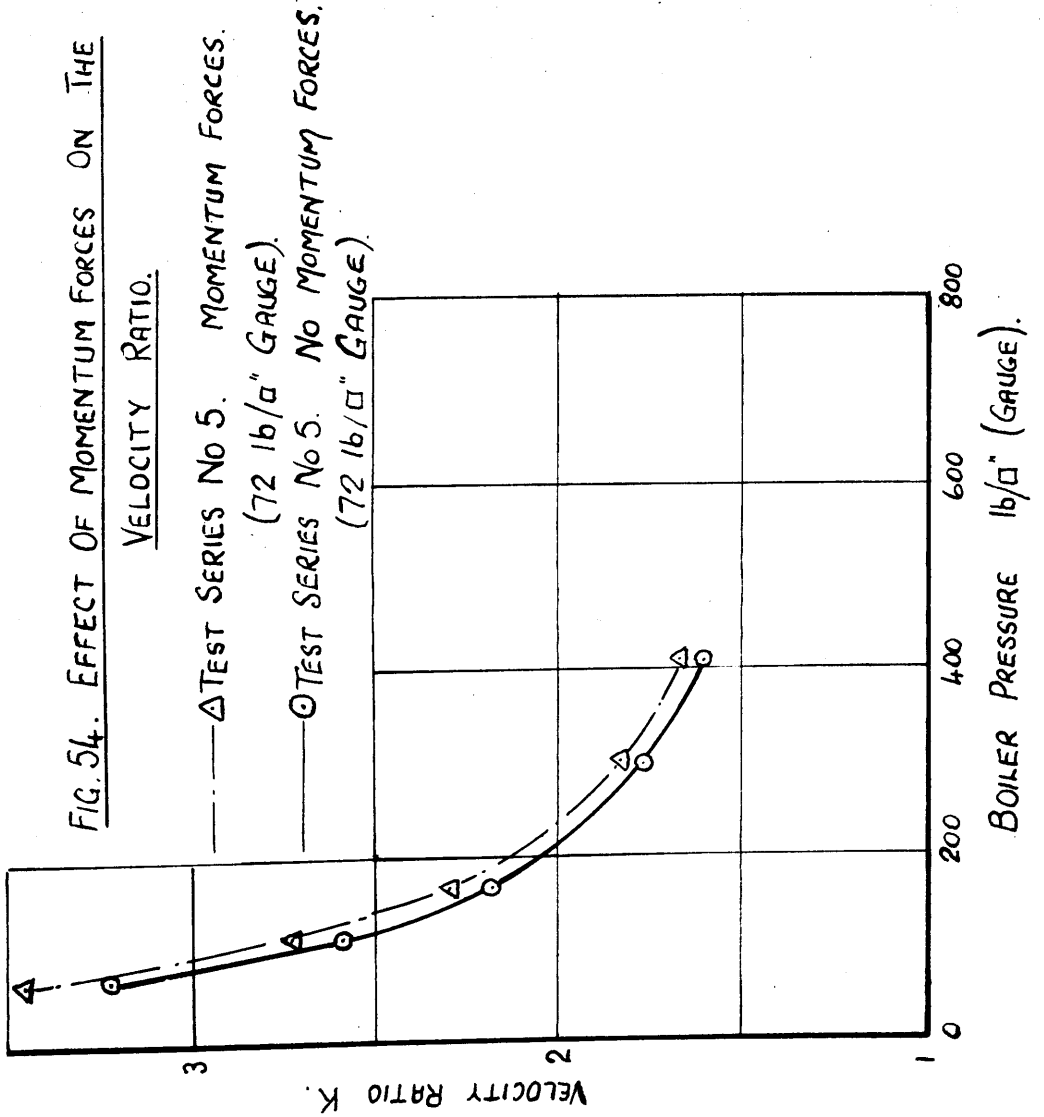
The two predominant effects were considered to be:-

- (a) the breaking down of the laminar wall film due to bubble formation near the wall,
- and (b) the decrease of the effective density in the annular ring due to steam bubbles.

The effects tend to counter balance each other. It was not possible to allow for either.

The influence of heat transfer is shown in Figure 54. Here are shown two curves of velocity ratio for Test Series Numbers 5, plotted to a base of boiler pressure. One shows the velocity ratio during adiabatic flow and the other/

FIG. 54. EFFECT OF MOMENTUM FORCES ON THE VELOCITY RATIO.



other the velocity ratio at the end of the heated section where the quality will be the same as in the adiabatic length. Test Series Number 5 was chosen on account of its high heat transfer rate.

It can be seen that the effect of heat transfer is to increase the velocity ratio. The maximum increase is approximately 7%. This indicates that the effect of heat transfer on the velocity ratio is not negligible.

The variation in the velocity ratio along the heated length is shown in Figure 55.

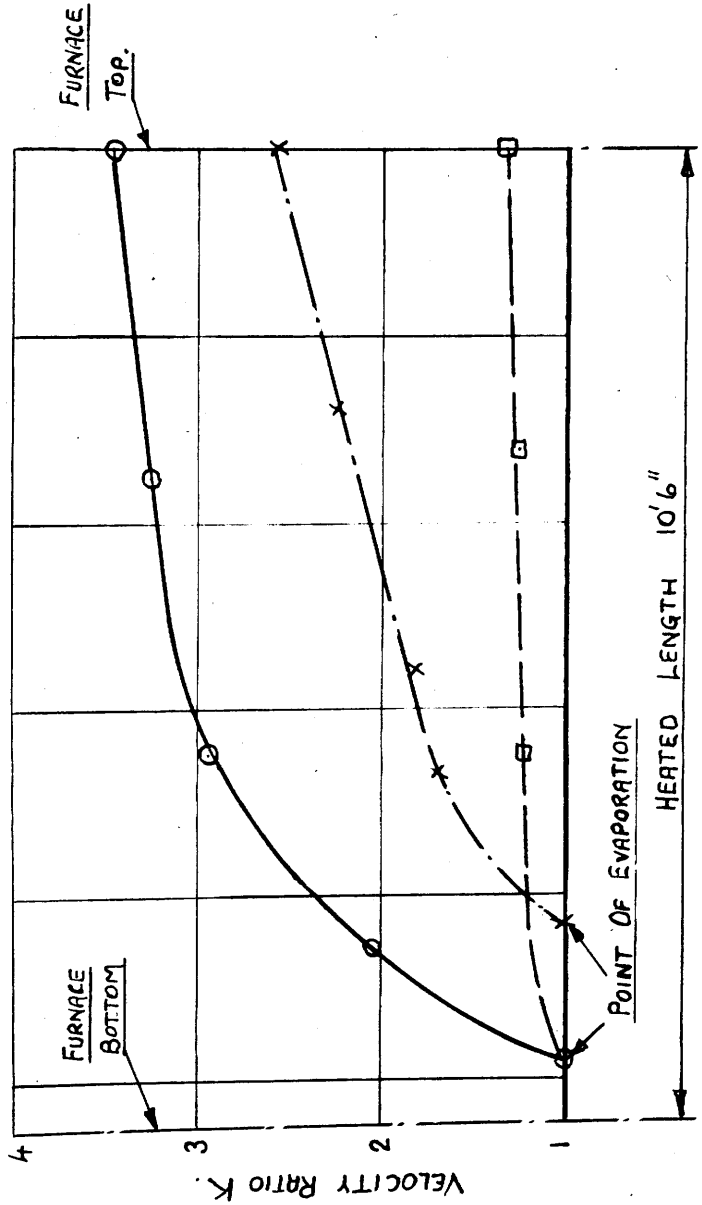
Since only overall pressure readings were taken, it is not possible to estimate the error in the velocity ratio calculations for intermediate points along the heated length. The agreement between the theoretical and experimental pressure changes suggests that the accuracy is of the same order as obtained with adiabatic flow.

FIG. 55. VELOCITY RATIO TO A BASE OF HEATED LENGTH.

--- X TEST SERIES No 1. (55 lb/ft² GAUGE).

— O TEST SERIES No 5. (72 lb/ft² GAUGE).

--- □ TEST SERIES No 19. (14.25 lb/ft² GAUGE).



34. PRESSURE CHANGES OVER THE DOWNCOMER TUBE
AND AT RISER ENTRY.

179.

The calculation of the pressure change over the downcomer tube was complicated by the change in roughness of the downcomer tube during the testing period. This change in roughness was not apparent with the riser tube.

The values adopted for λ were as follows:-

Test Series Numbers 1-3, 5-8.	$\lambda = 0.022$
14-20.	$\lambda = 0.024$
9-13.	$\lambda = 0.026$
4.	$\lambda = 0.0288$

The test series numbers above are given in the order in which they were carried out. The friction characteristics of the tube were checked in the horizontal position both when new and after the last test. When new, the tube behaved as a smooth tube, but at the end of the test programme it conformed to the behaviour of a rough tube, having a value of $\lambda = 0.0288$. The choice of the values of λ indicated above therefore seemed reasonable.

The change in pressure between the steam drum and water drum tapping points is due to the following causes:-

(a) Static head difference due to the water in the downcomer - 17.833 ft

(The water level in the steam drum is 1" below mid-drum level).

(b) Static head due to the steam between the water level and the steam drum volume chamber - 1.205 ft

(c)/

(c) Loss at entry to downcomer - $\frac{1}{2} \cdot \frac{U^2}{2g} \cdot \rho_L$

(d) Loss due to restriction of Pitot and thermocouple pockets - $\frac{1}{2} \cdot \frac{U^2}{2g} \cdot \rho_L$

(Approximately. Evaluated from tests in horizontal plane.)

(e) Loss of kinetic energy $\frac{U^2}{2g} \cdot \rho_L$. This is assumed lost as heat in the water drum.

(f) Friction loss $\frac{\lambda \cdot \ell \cdot U^2 \cdot \rho_L}{2g \cdot d} = \frac{\lambda \times 16.7 \times 12 \times U^2 \times \rho_L}{2g \times 1.7} = 1.83 \cdot \lambda \cdot U^2 \cdot \rho_L$

Ft. Lb. Sec. Units are used throughout.

The total pressure change which is the sum of the above terms is, therefore

$$\rho_L \left(17.833 - \frac{U^2}{g} - 1.83 \lambda U^2 \right) + 1.205 \rho_G \dots \dots \dots 78$$

For the various friction factors during the tests this reduces to:

Test Series Numbers

1-3, 5-8	$\rho_L \left(17.833 - 0.0713 \cdot U^2 \right) + 1.205 \rho_G \dots \dots \dots 79$
14-20	$\rho_L \left(17.833 - 0.075 \cdot U^2 \right) + 1.205 \rho_G$
9-13	$\rho_L \left(17.833 - 0.0786 \cdot U^2 \right) + 1.205 \rho_G$
4	$\rho_L \left(17.833 - 0.0840 \cdot U^2 \right) + 1.205 \rho_G$

The theoretical values are compared with the experimental values in Tables 10 and 11.

The experimental pressure changes between the riser bottom and the water drum tapping points are shown in Tables 12 and 13.

For the case of no restricting orifice the theoretical values/

TABLE 10

PRESSURE CHANGE - STEAM DRUM TO WATER DRUM.

ORIFICE: NONE		VOLTAGE TAPPING: 46.5										TEST SERIES No. 3.		
BOILER PRESS ^E (GAUGE)	lb/d"	48	87	133	202	300	390	570	760	1025	1220	1450		
PRESSURE CHANGE	EXPERIMENTAL	"	6.74	6.49	6.29	6.09	5.90	5.76	5.60	5.42	5.24	5.09	4.91	
	THEORETICAL	"	6.75	6.56	6.28	6.11	5.92	5.79	5.60	5.43	5.22	5.06	4.87	
ORIFICE: NONE		VOLTAGE TAPPING: 58.5 (ELEMENTS REDUCED)										TEST SERIES No. 4.		
BOILER PRESS ^E (GAUGE)	lb/d"	51	105	160	200	339	525	735	860	1030	1380			
PRESSURE CHANGE	EXPERIMENTAL	"	6.75	6.55	6.26	6.14	5.87	5.65	5.47	5.36	5.22	4.88		
	THEORETICAL	"	6.74	6.41	6.21	6.08	5.80	5.57	5.34	5.25	5.12	4.86		
ORIFICE: NONE		VOLTAGE TAPPING: 58.5										TEST SERIES No. 5.		
BOILER PRESS ^E (GAUGE)	lb/d"	72	110	169	200	300	405							
PRESSURE CHANGE	EXPERIMENTAL	"	6.81	6.61	6.36	6.29	6.00	5.80						
	THEORETICAL	"	6.73	6.55	6.31	6.22	5.98	5.80						
ORIFICE: 7/8"		VOLTAGE TAPPING: 33.8										TEST SERIES No. 6		
BOILER PRESS ^E (GAUGE)	lb/d"	50	100	149	185	300	395	570						
PRESSURE CHANGE	EXPERIMENTAL	"	6.75	6.54	6.41	6.32	6.16	6.05	5.89					
	THEORETICAL	"	6.76	6.56	6.44	6.36	6.22	6.10	5.91					
ORIFICE: 7/8"		VOLTAGE TAPPING: 38.4										TEST SERIES No. 7.		
BOILER PRESS ^E (GAUGE)	lb/d"	62	111	159	215	315	420	510						
PRESSURE CHANGE	EXPERIMENTAL	"	6.69	6.54	6.43	6.34	6.2	6.05	5.96					
	THEORETICAL	"	6.69	6.54	6.42	6.33	6.16	6.05	5.95					
ORIFICE: 7/8"		VOLTAGE TAPPING: 41.9.										TEST SERIES No. 8.		
BOILER PRESS ^E (GAUGE)	lb/d"	58	115	160	215	315	415	565	770	940				
PRESSURE CHANGE	EXPERIMENTAL	"	6.74	6.52	6.41	6.32	6.18	6.03	5.95	5.75	5.62			
	THEORETICAL	"	6.73	6.5	6.39	6.30	6.15	6.03	5.90	5.70	5.58			
ORIFICE: 3/4"		VOLTAGE TAPPING: 33.8										TEST SERIES No. 9.		
BOILER PRESS ^E (GAUGE)	lb/d"	50	100	151	200	305	400	530						
PRESSURE CHANGE	EXPERIMENTAL	"	6.80	6.60	6.47	6.40	6.29	6.16	6.00					
	THEORETICAL	"	5.86	6.66	6.56	6.46	6.3	6.18	6.05					
ORIFICE: 3/4"		VOLTAGE TAPPING: 38.4.										TEST SERIES No. 10		
BOILER PRESS ^E (GAUGE)	lb/d"	68	110	164	197	290	415	570	700	890	1130			
PRESSURE CHANGE	EXPERIMENTAL	"	6.81	6.65	6.52	6.45	6.30	6.18	6.01	5.87	5.71	5.50		
	THEORETICAL	"	6.79	6.62	6.50	6.43	6.29	6.12	5.95	5.85	5.67	5.46		
ORIFICE: 3/4"		VOLTAGE TAPPING: 41.9.										TEST SERIES No. 11.		
BOILER PRESS ^E (GAUGE)	lb/d"	50	105	165	200	300	402	550	700	890	1060	1310		
PRESSURE CHANGE	EXPERIMENTAL	"	6.81	6.65	6.46	6.43	6.27	6.16	6.00	5.87	5.71	5.58	5.37	
	THEORETICAL	"	6.82	6.64	6.45	6.38	6.23	6.10	5.95	5.80	5.65	5.47	5.27	
ORIFICE: 3/4"		VOLTAGE TAPPING: 46.5.										TEST SERIES No. 12.		
BOILER PRESS ^E (GAUGE)	lb/d"	51	100	145	207	295	400	580	720	880	1120	1330		
PRESSURE CHANGE	EXPERIMENTAL	"	6.85	6.65	6.52	6.40	6.25	6.15	5.96	5.81	5.67	5.48	5.27	
	THEORETICAL	"	6.85	6.61	6.50	6.37	6.23	6.10	5.91	5.80	5.66	5.40	5.26	
ORIFICE: 3/4"		VOLTAGE TAPPING: 58.5.										TEST SERIES No. 13.		
BOILER PRESS ^E (GAUGE)	lb/d"	49	105	160	208	380	700	1060						
PRESSURE CHANGE	EXPERIMENTAL	"	6.85	6.63	6.45	6.29	6.10	5.80	5.505					
	THEORETICAL	"	6.8	6.60	6.45	6.35	6.07	5.74	5.41					

TABLE II.

PRESSURE CHANGE - STEAM DRUM TO WATER DRUM.

ORIFICE: 5/8"

VOLTAGE TAPPING: 33.8

TEST SERIES No. 14.

BOILER PRESS ^E (GAUGE)		1b/d"	63	95	150	207	298	405					
PRESSURE CHANGE	EXPERIMENTAL	"	6.81	6.7	6.6	6.47	6.32	6.20					
	THEORETICAL	"	6.87	6.75	6.62	6.52	6.38	6.22					

ORIFICE: 5/8"

VOLTAGE TAPPING: 38.4

TEST SERIES No. 15.

BOILER PRESS ^E (GAUGE)		1b/d"	68	100	190	300	410	570	720	880	1040	1215	
PRESSURE CHANGE	EXPERIMENTAL	"	6.79	6.7	6.46	6.3	6.17	6.01	5.81	5.71	5.56	5.40	
	THEORETICAL	"	6.84	6.74	6.51	6.32	6.21	6.04	5.90	5.79	5.60	5.44	

ORIFICE: 5/8"

VOLTAGE TAPPING: 41.9

TEST SERIES No. 16.

BOILER PRESS ^E (GAUGE)		1b/d"	50	104	148	202	290	400	585	740	900	1100	1335
PRESSURE CHANGE	EXPERIMENTAL	"	6.85	6.72	6.60	6.49	6.32	6.20	6.01	5.85	5.71	5.53	5.31
	THEORETICAL	"	6.90	6.69	6.60	6.48	6.35	6.21	6.01	5.87	5.66	5.52	5.28

ORIFICE: 5/8"

VOLTAGE TAPPING: 46.5

TEST SERIES No. 17.

BOILER PRESS ^E (GAUGE)		1b/d"	68	103	151	210	304	390	575	740	940	1130	1350
PRESSURE CHANGE	EXPERIMENTAL	"	6.83	6.72	6.61	6.49	6.34	6.26	6.05	5.89	5.75	5.57	5.33
	THEORETICAL	"	6.83	6.70	6.55	6.46	6.32	6.22	6.00	5.81	5.62	5.48	5.26

ORIFICE: 1/2"

VOLTAGE TAPPING: 33.8

TEST SERIES No. 18.

BOILER PRESS ^E (GAUGE)		1b/d"	56	104	145	191	308	420					
PRESSURE CHANGE	EXPERIMENTAL	"	7.1	6.85	6.74	6.65	6.49	6.34					
	THEORETICAL	"	6.96	6.80	6.69	6.60	6.42	6.27					

ORIFICE: 1/2"

VOLTAGE TAPPING: 38.4

TEST SERIES No. 19.

BOILER PRESS ^E (GAUGE)		1b/d"	50	100	157	205	315	390	540	700	865	1010	1425
PRESSURE CHANGE	EXPERIMENTAL	"	7.03	6.85	6.69	6.60	6.40	6.31	6.11	5.93	5.84	5.67	5.33
	THEORETICAL	"	7.00	6.85	6.70	6.61	6.43	6.31	6.14	5.97	5.77	5.65	5.28

ORIFICE: 1/2"

VOLTAGE TAPPING: 41.9

TEST SERIES No. 20.

BOILER PRESS ^E (GAUGE)		1b/d"	64	108	137	213	304	405	580	730	1060	1205	1425
PRESSURE CHANGE	EXPERIMENTAL	"	6.95	6.8	6.74	6.58	6.49	6.34	6.18	6.00	5.71	5.51	5.31
	THEORETICAL	"	6.95	6.81	6.75	6.58	6.42	6.29	6.10	5.93	5.63	5.49	5.28

TABLE 12.

PRESSURE CHANGE - RISER BOTTOM TO WATER DRUM.

ORIFICE: NONE.		VOLTAGE TAPPING: 38.4.								TEST SERIES No. 1.				
BOILER PRESSURE (GAUGE)		16/8"	55	116	167	210	298	400	550	700	1000	1225		
PRESSURE CHANGE	EXPERIMENTAL.	"	0.8	0.85	0.85	0.8	0.8	0.78	0.74	0.69	0.69	0.71		
	THEORETICAL.	"	0.78	0.80	0.79	0.78	0.76	0.74	0.72	0.68	0.63	0.61		
ORIFICE: NONE.		VOLTAGE TAPPING: 41.9.								TEST SERIES No. 2.				
BOILER PRESSURE (GAUGE)		16/8"	49	99	146	192	270	350	510	680	1050	1250		
PRESSURE CHANGE	EXPERIMENTAL	"	0.74	0.79	0.78	0.8	0.81	0.8	0.76	0.72	0.71	0.69		
	THEORETICAL.	"	0.79	0.76	0.8	0.8	0.78	0.77	0.74	0.72	0.65	0.63		
ORIFICE: NONE.		VOLTAGE TAPPING: 46.5								TEST SERIES No. 3.				
BOILER PRESSURE (GAUGE)		16/8"	49	87	133	202	300	390	570	760	1025	1450		
PRESSURE CHANGE	EXPERIMENTAL	"	0.74	0.74	0.78	0.78	0.78	0.76	0.72	0.71	0.71	0.65		
	THEORETICAL	"	0.74	0.77	0.78	0.8	0.78	0.77	0.74	0.71	0.67	0.62		
ORIFICE: NONE.		VOLTAGE TAPPING: 58.5 (ELEMENTS REDUCED)								TEST SERIES No. 4.				
BOILER PRESSURE (GAUGE)		16/8"	54	105	160	200	339	525	735	860	1030	1380		
PRESSURE CHANGE	EXPERIMENTAL	"	0.76	0.80	0.80	0.80	0.80	0.80	0.76	0.76	0.72	0.69		
	THEORETICAL	"	0.72	0.74	0.76	0.76	0.76	0.74	0.71	0.69	0.67	0.64		
ORIFICE: NONE.		VOLTAGE TAPPING: 58.5.								TEST SERIES No. 5.				
BOILER PRESSURE (GAUGE)		16/8"	72	110	169	200	300	405						
PRESSURE CHANGE	EXPERIMENTAL	"	0.65	0.71	0.71	0.71	0.71	0.71						
	THEORETICAL	"	0.71	0.72	0.74	0.74	0.76	0.76						
ORIFICE: 7/8"		VOLTAGE TAPPING: 33.8.								TEST SERIES No. 6.				
BOILER PRESSURE (GAUGE)		16/8"	50	100	149	185	300	395	570					
PRESSURE CHANGE - EXPER +		"	1.41	1.46	1.46	1.44	1.28	1.23	1.10					
ORIFICE: 7/8"		VOLTAGE TAPPING: 38.4.								TEST SERIES No. 7.				
BOILER PRESSURE (GAUGE)		16/8"	62	111	159	215	315	420	510					
PRESSURE CHANGE - EXPER +		"	1.48	1.50	1.46	1.44	1.43	1.32	1.28					
ORIFICE: 7/8"		VOLTAGE TAPPING: 41.9.								TEST SERIES No. 8.				
BOILER PRESSURE (GAUGE)		16/8"	58	115	160	215	315	415	565	770	940			
PRESSURE CHANGE - EXPER +		"	1.44	1.52	1.52	1.48	1.43	1.37	1.26	1.16	1.07			
ORIFICE: 3/4"		VOLTAGE TAPPING: 33.8.								TEST SERIES No. 9.				
BOILER PRESSURE (GAUGE)		16/8"	50	100	151	200	305	400	530					
PRESSURE CHANGE - EXPER +		"	2.10	2.06	1.93	1.86	1.66	1.57	1.45					
ORIFICE: 3/4"		VOLTAGE TAPPING: 38.4.								TEST SERIES No. 10.				
BOILER PRESSURE (GAUGE)		16/8"	68	110	164	197	290	415	570	700	890	1130		
PRESSURE CHANGE - EXPER +		"	2.17	2.12	2.02	1.97	1.83	1.68	1.57	1.46	1.32	1.21		
ORIFICE: 3/4"		VOLTAGE TAPPING: 41.9.								TEST SERIES No. 11.				
BOILER PRESSURE (GAUGE)		16/8"	50	105	165	200	300	402	550	700	1060	1310		
PRESSURE CHANGE - EXPER +		"	2.15	2.24	2.15	2.08	1.93	1.82	1.72	1.61	1.34	1.23		
ORIFICE: 3/4"		VOLTAGE TAPPING: 46.5.								TEST SERIES No. 12.				
BOILER PRESSURE (GAUGE)		16/8"	51	100	145	207	295	400	580	720	1120	1330		
PRESSURE CHANGE - EXPER +		"	2.04	2.17	2.19	2.13	2.04	1.95	1.81	1.68	1.48	1.35		

TABLE 13.

PRESSURE CHANGE - RISER BOTTOM TO WATER DRUM.

ORIFICE: 3/4" VOLTAGE TAPPING: 58.5 TEST SERIES No. 13.

BOILER PRESSURE (GAUGE)	1b/d"	49	105	160	208	380	700	1060			
PRESSURE CHANGE - EXPER:	"	1.94	2.10	2.13	2.12	2.06	1.84	1.64			

ORIFICE: 5/8" VOLTAGE TAPPING: 33.8 TEST SERIES No. 14.

BOILER PRESSURE (GAUGE)	1b/d"	63	95	150	207	298	405				
PRESSURE CHANGE - EXPER:	"	2.30	2.30	2.15	2.02	1.86	1.72				

ORIFICE: 5/8" VOLTAGE TAPPING: 38.4 TEST SERIES No. 15.

BOILER PRESSURE (GAUGE)	1b/d"	68	100	190	300	410	570	720	880	1060	1215
PRESSURE CHANGE - EXPER:	"	2.49	2.48	2.35	2.15	1.97	1.79	1.65	1.52	1.45	1.34

ORIFICE: 5/8" VOLTAGE TAPPING: 41.9 TEST SERIES No. 16.

BOILER PRESSURE (GAUGE)	1b/d"	50	104	148	202	290	400	585	740	1100	1335
PRESSURE CHANGE - EXPER:	"	2.37	2.55	2.46	2.37	2.24	2.04	1.84	1.75	1.46	1.43

ORIFICE: 5/8" VOLTAGE TAPPING: 46.5 TEST SERIES No. 17.

BOILER PRESSURE (GAUGE)	1b/d"	68	103	151	210	304	390	575	740	1130	1350
PRESSURE CHANGE - EXPER:	"	2.44	2.48	2.49	2.44	2.31	2.19	1.99	1.90	1.61	1.50

ORIFICE: 1/2" VOLTAGE TAPPING: 33.8 TEST SERIES No. 18.

BOILER PRESSURE (GAUGE)	1b/d"	56	104	145	191	308	420				
PRESSURE CHANGE - EXPER:	"	3.13	3.08	2.95	2.75	2.39	2.24				

ORIFICE: 1/2" VOLTAGE TAPPING: 38.4 TEST SERIES No. 19.

BOILER PRESSURE (GAUGE)	1b/d"	50	100	157	205	315	390	540	700	1010	1425
PRESSURE CHANGE - EXPER:	"	3.26	3.11	2.95	2.73	2.53	2.39	2.21	2.04	1.75	1.57

ORIFICE: 1/2" VOLTAGE TAPPING: 41.9 TEST SERIES No. 20.

BOILER PRESSURE (GAUGE)	1b/d"	64	108	137	213	304	405	580	730	1050	1425
PRESSURE CHANGE - EXPER:	"	3.27	3.25	3.18	2.89	2.77	2.55	2.33	2.17	1.86	1.72

values are also tabulated.

The pressure change is due to:-

(a) Static head of the water between the tapping points - $1.5 \rho_L$

(b) Loss at riser entry - $\frac{1}{2} \cdot \frac{U^2}{2g} \cdot \rho_L$

(c) Kinetic energy at riser entry - $\frac{U^2}{2g} \cdot \rho_L$

(d) Friction loss from riser entry to the riser bottom tapping point

$$\frac{\lambda \cdot \rho_L \cdot U^2 \cdot R_L}{2g \cdot d} = \frac{\lambda \times 13.375 \times U^2 \times R_L}{2g \times 1.7} = 0.00269 U^2$$

(The friction factor λ is assumed to have the value in the downcomer i.e. $\lambda = 0.022$)

Therefore, the pressure change between the water drum and riser bottom tapping points is the sum of the above terms, i.e.

$$\rho_L \left(1.5 + 1.5 \frac{U^2}{2g} + 0.00269 U^2 \right) = \rho_L (1.5 + 0.026 U^2) \quad 80$$

The above formula was used where there was no restricting orifice. With a restricting orifice the experimental pressure change (δp) between water drum and riser bottom tapping points was used in any pressure summation corresponding to the experimental velocity (U). The pressure change (δp_c) corresponding to a velocity (U_c) other than the experimental velocity was determined by assuming the losses due to the orifice and friction vary directly as the square of the velocity. This gives the pressure change in terms of/

of the measured value as

$$\delta p_t = \left[1.5 + \left\{ \frac{\delta p}{\rho_L} - 1.5 \right\} \left\{ \frac{u_t}{u} \right\}^2 \right] \rho_L$$

(The riser bottom tapping point is 1.5 feet above the water drum tapping point).

Very close agreement is obtained between calculated and measured values of pressure change between (1) the steam drum and water drum via the downcomer, and (2) the water drum and riser bottom tapping points.

PART VII.PREDICTION OF NATURAL CIRCULATION
IN TWO-TUBE BOILER.

	<u>Page.</u>
35. Pressure change over riser and downcomer tubes	188.
36. Circulation velocity	195.

INTRODUCTION.

The preceding sections have been devoted to the development and confirmation of a theory enabling the prediction of the pressure change over lengths of tube where steam-water mixtures flow. It is now possible to proceed to the application of this theory to the prediction of the theoretical circulation velocity.

35. PRESSURE CHANGES OVER RISER AND DOWNCOMER TUBES.

In a tube bank of a water-tube boiler each tube is subject to a common pressure change. In addition, the net flow into a particular drum is zero.

For the simple case of a two-tube circuit, where the diameters of both tubes are the same, the velocity in the downcomer will be the same as in the riser tube up to the point where evaporation commences.

As the pressure change over each tube is the same the theoretical pressure change obtained using the measured velocity should be identical for both riser and downcomer if the theoretical equations are correct.

The theoretical pressure changes over the riser calculated from the measured velocity are compared with the measured values in Figures 56 to 60. The pressure change over the riser was obtained by adding the theoretical values obtained from Sections 30 and 32 respectively, to the measured value over the restricting orifice, except in the case of no restricting orifice, when the theoretical values were used.

The experimental values over the orifice were used as this was considered more accurate than theoretical values. It was undesirable to introduce errors, however small, due to inaccuracies in the prediction of a theoretical pressure change/

PRESSURE DIFFERENCE - STEAM DRUM TO WATER DRUM — BOILER PRESSURE
 TUBE: 2 1/4" O.D. x 2 SWG HEATING: UNIFORM RESTRICTING ORIFICE: NONE
 TUBE POSITION: VERTICAL HEATED LENGTH: 10'-6"

○— EXPERIMENTAL ——— ANNULAR FLOW THEORY - - - - - HOMOGENEOUS FLOW THEORY

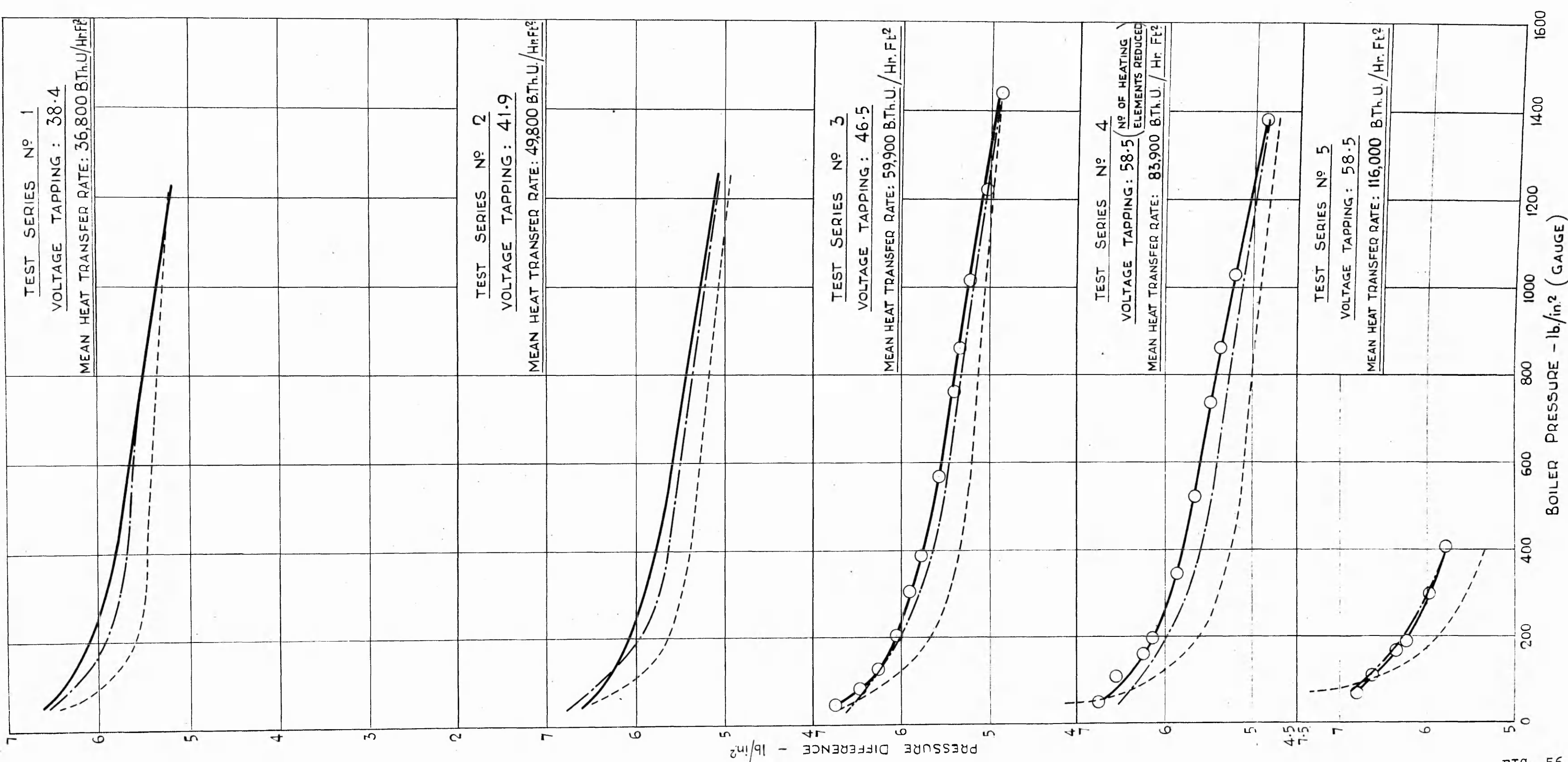


FIG. 56.

PRESSURE DIFFERENCE, STEAM DRUM TO WATER DRUM - BOILER PRESSURE

TUBE: 2 1/4" O.D. x 2 SW.G.

HEATING: UNIFORM

RESTRICTING ORIFICE: 8 DIA. 7"

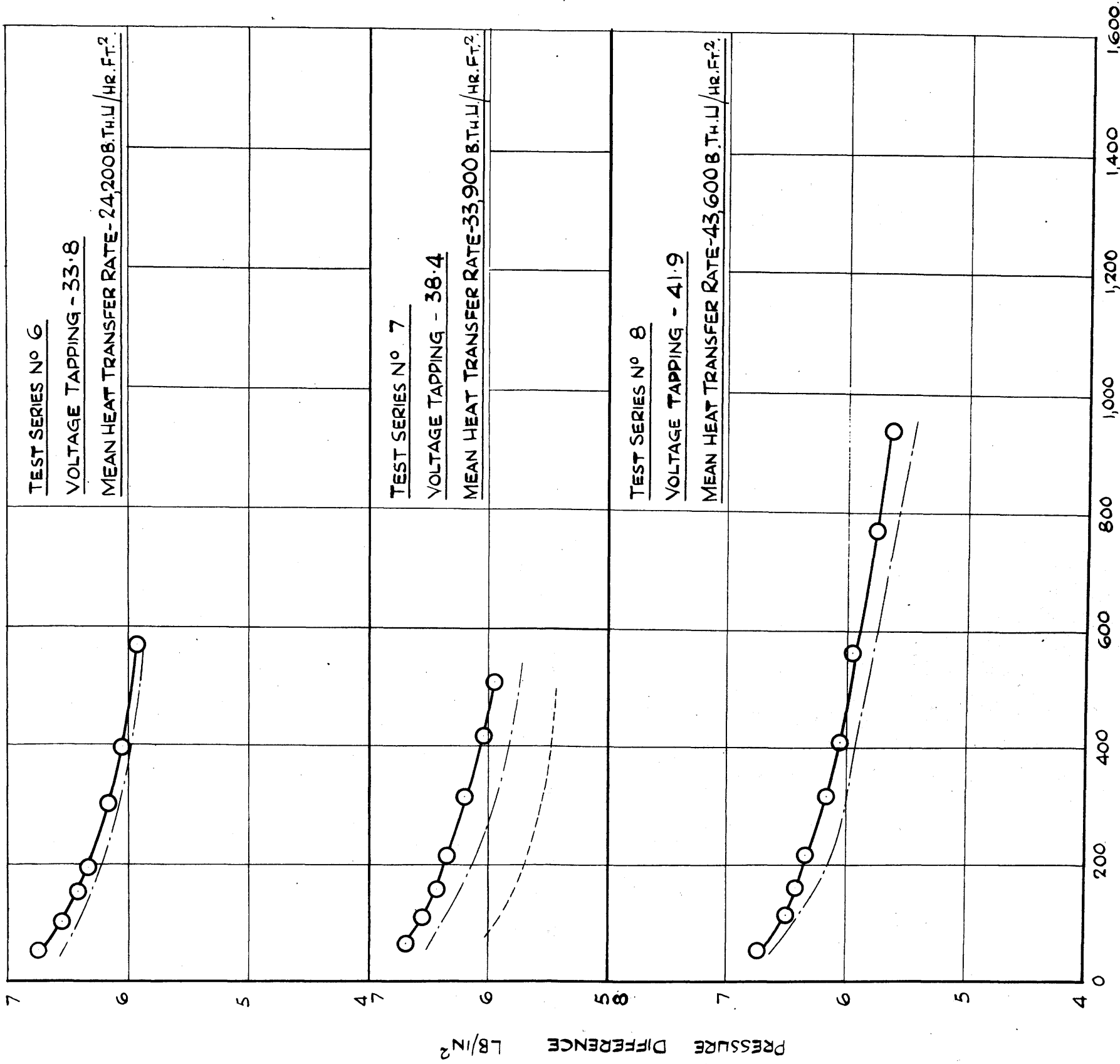
TUBE POSITION: VERTICAL

HEATED LENGTH: 10'-6"

----- HOMOGENEOUS FLOW THEORY

----- ANNULAR FLOW THEORY

○— EXPERIMENTAL



BOILER PRESSURE LB/IN² (GAUGE)

FIG. 57.

PRESSURE DIFFERENCE, STEAM DRUM TO WATER DRUM - BOILER PRESSURE
 TUBE: 2 1/4" O.D. x 2 S.W.G. HEATING: UNIFORM RESTRICTING ORIFICE: 3/4" DIA.
 TUBE POSITION: VERTICAL HEATED LENGTH: 10'-6"

○ EXPERIMENTAL — ANNULAR FLOW THEORY - - - - - HOMOGENEOUS FLOW THEORY

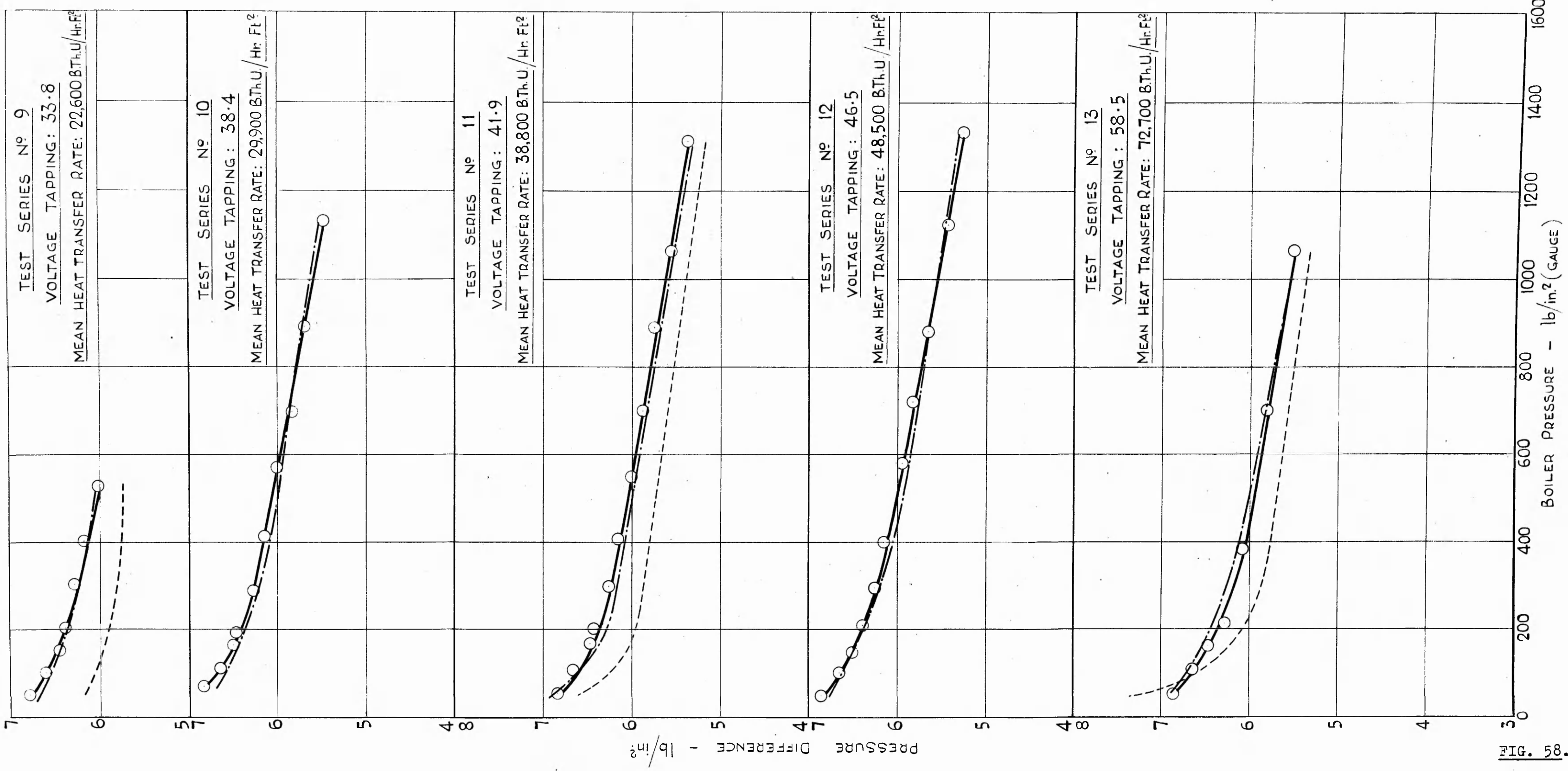


FIG. 58.

PRESSURE DIFFERENCE, STEAM DRUM TO WATER DRUM - BOILER PRESSURE

TUBE: $2\frac{1}{4}$ O.D. x 2 S.W.G. HEATING: UNIFORM RESTRICTING ORIFICE: $\frac{5}{8}$ " DIA.

TUBE POSITION: VERTICAL HEATED LENGTH: 10'-6"

○—○ EXPERIMENTAL -·-·-·- ANNULAR FLOW THEORY - - - - - HOMOGENEOUS FLOW THEORY

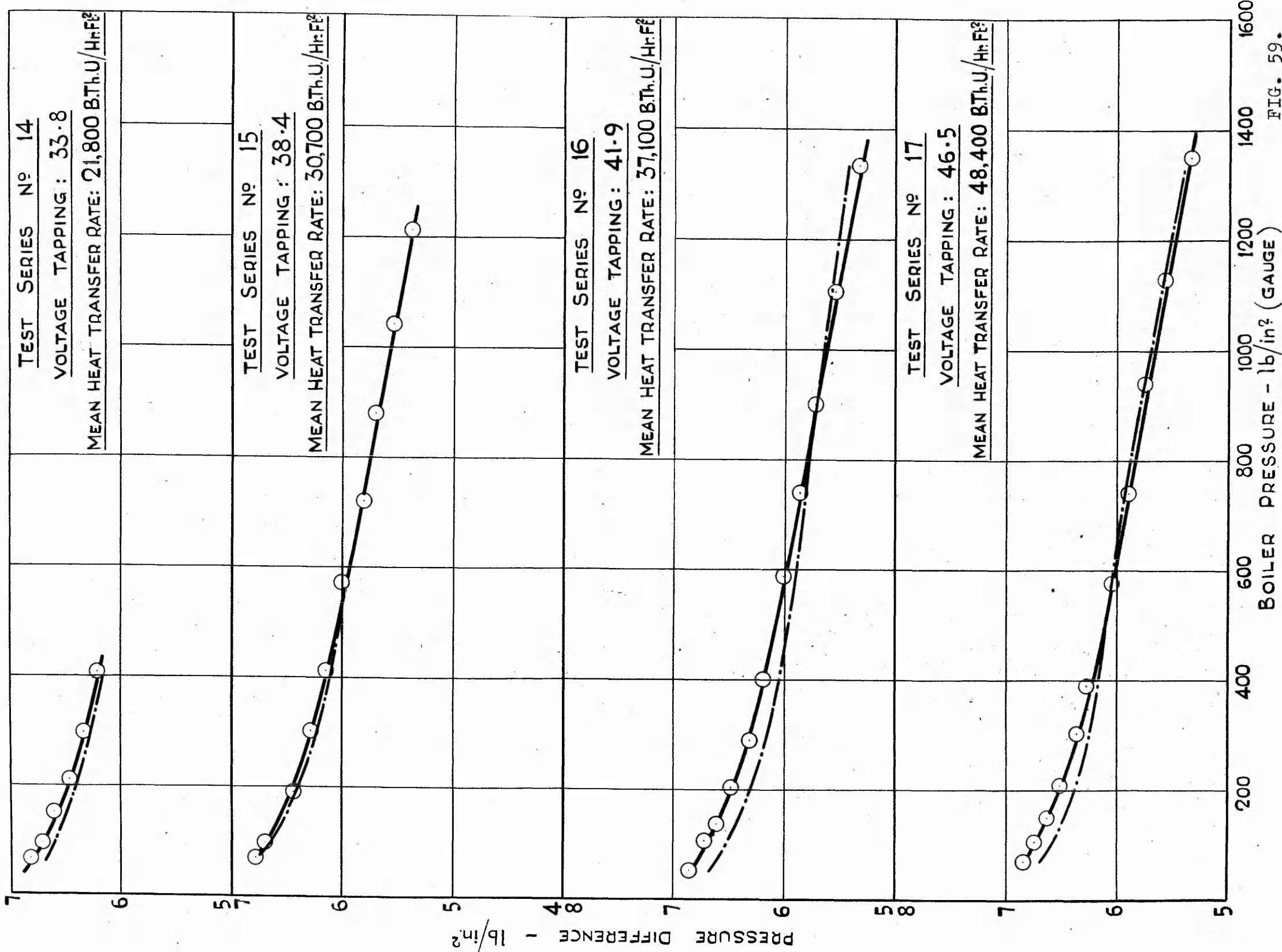


FIG. 59.

PRESSURE DIFFERENCE, STEAM DRUM TO WATER DRUM - BOILER PRESSURE

TUBE: $\frac{1}{2}$ " O.D. x 2 SWG.
TUBE POSITION: VERTICAL

HEATING: UNIFORM
HEATED LENGTH 10'-6"

RESTRICTING ORIFICE $\frac{1}{2}$ " DIA.

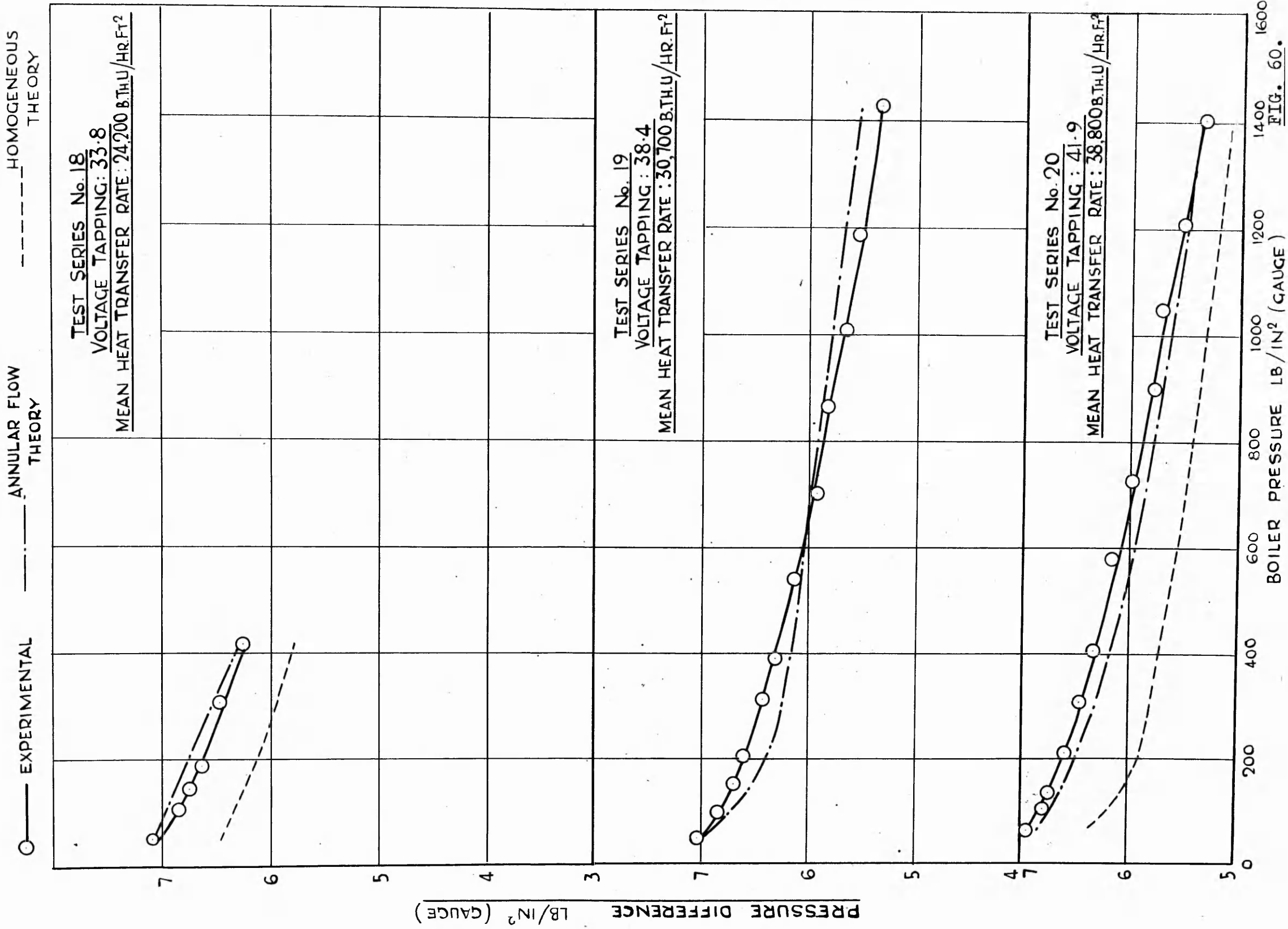


FIG. 60.

change over an orifice.

Discussion.

The agreement between the theoretical and measured pressure changes over the riser is extremely satisfactory the maximum error being approximately 0.3 lb/in.^2 in 6 lb/in.^2 (i.e. $\pm 5\%$).

The theoretical values obtained using the homogeneous theory are also shown in Figures 56 to 60 for the purposes of comparison. The maximum error here is approximately 0.7 lb/in.^2 in 6 lb/in.^2 (i.e. $\pm 11.5\%$).

Due to the close agreement shown in the preceding section between the theoretical and measured pressure changes over the downcomer, the agreement quoted above will also be approximately that between the theoretical pressure changes over the riser and downcomer corresponding to the measured circulation velocity. It is, therefore, to be expected that the proposed theory will give extremely close predictions of the circulation velocity and this is shown to be the case in the following section.

The theoretical circulation velocity will be that velocity giving the same pressure change over the riser and downcomer tubes.

A trial and error procedure is used to obtain this velocity. The pressure changes over the downcomer and riser are determined as described in the preceding sections for a number of assumed velocities. By graphical means the velocity which gives the same pressure change over downcomer and riser is obtained.

The procedure is detailed in Appendix H. The theoretical velocity values are compared with the experimental values in Figures 61 to 64 for eight representative test series. It will be seen that very close agreement is obtained. This was only to be expected in view of the close agreement obtained between the theoretical pressure changes over the riser and downcomer tubes as shown in the preceding section. Since this agreement was common to all tests, it was considered unnecessary to evaluate the theoretical velocities for more than the eight tests.

Also shown in Figures 61 to 64 is the circulation velocity calculated on the assumption of homogeneous flow.

Discussion.

The velocity curves shown in Figures 61 to 64 indicate that the proposed theory gives values within 0.25 ft./sec. ($\pm 6\%$) of the experimental values, which is considered satisfactory./

CIRCULATION VELOCITY - BOILER PRESSURE

TUBE: 2 1/4" O.D. x 2 S.W.G.

HEATING: UNIFORM

RESTRICTING ORIFICE: NONE

TUBE POSITION: VERTICAL.

HEATED LENGTH: 10'-6"

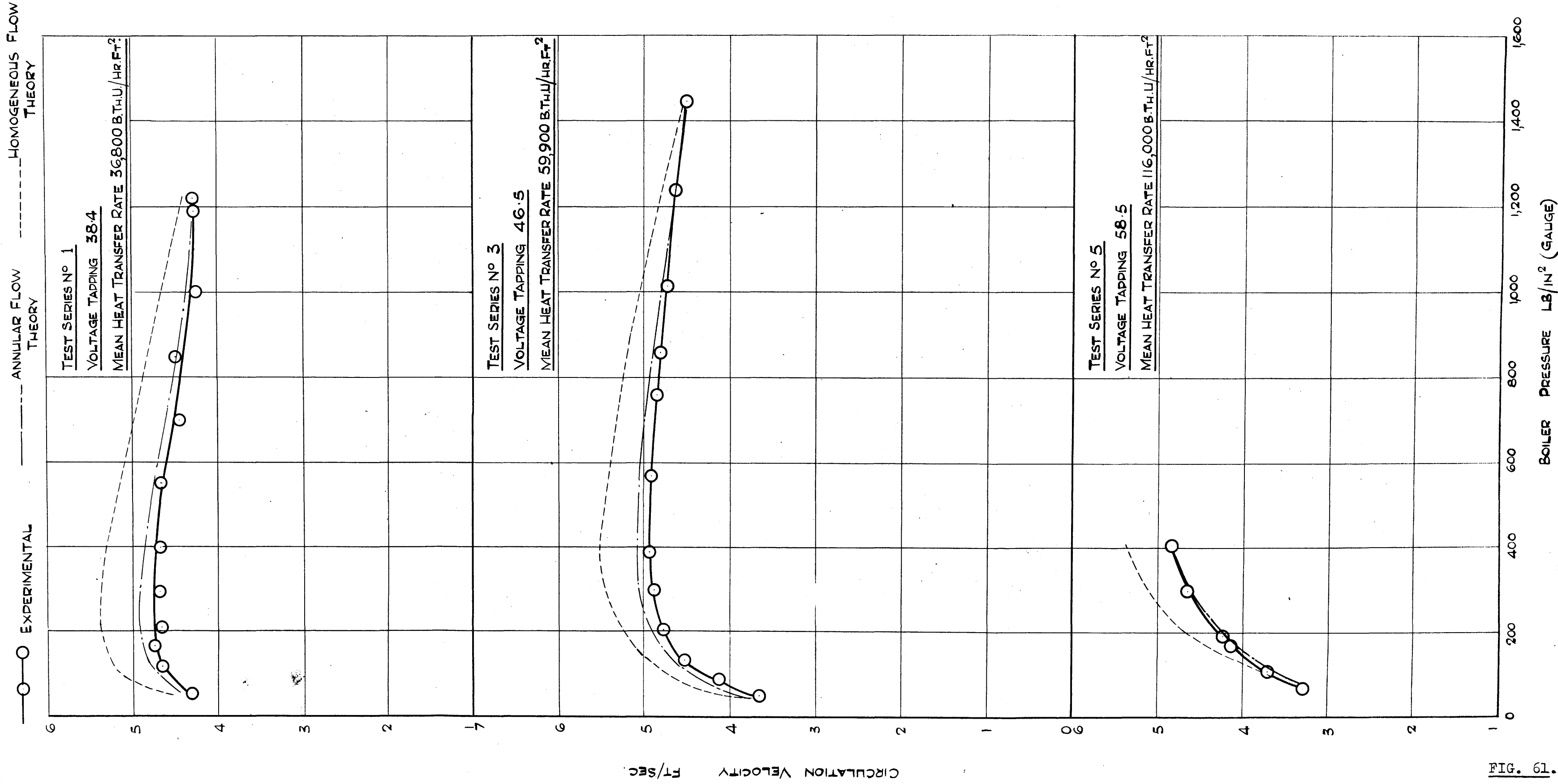


FIG. 61.

CIRCULATION VELOCITY - BOILER PRESSURE

TUBE: $2\frac{1}{4}$ " O.D. x 2 S.W.G. HEATING: UNIFORM RESTRICTING ORIFICE: $\frac{1}{8}$ " DIA.
 TUBE POSITION: VERTICAL HEATED LENGTH: 10'-6"

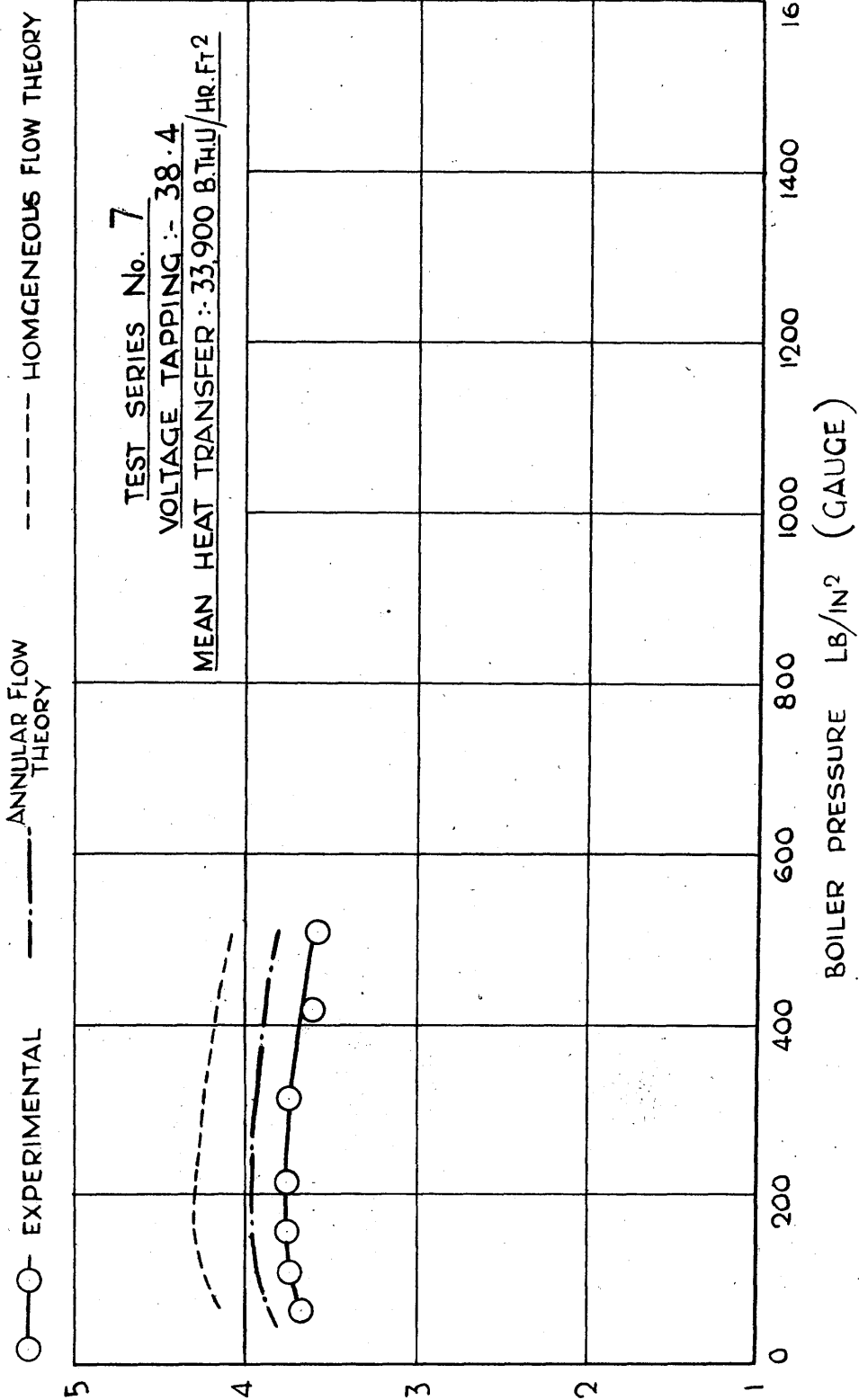


FIG. 29

CIRCULATION VELOCITY - BOILER PRESSURE

TUBE: $2\frac{1}{4}$ " O.D. x 2 S.W.G. HEATING: UNIFORM RESTRICTING ORIFICE: $\frac{5}{32}$ " DIA.

TUBE POSITION: VERTICAL HEATED LENGTH: 10'-6"

EXPERIMENTAL
 ANNULAR FLOW THEORY
 HOMOGENEOUS FLOW THEORY

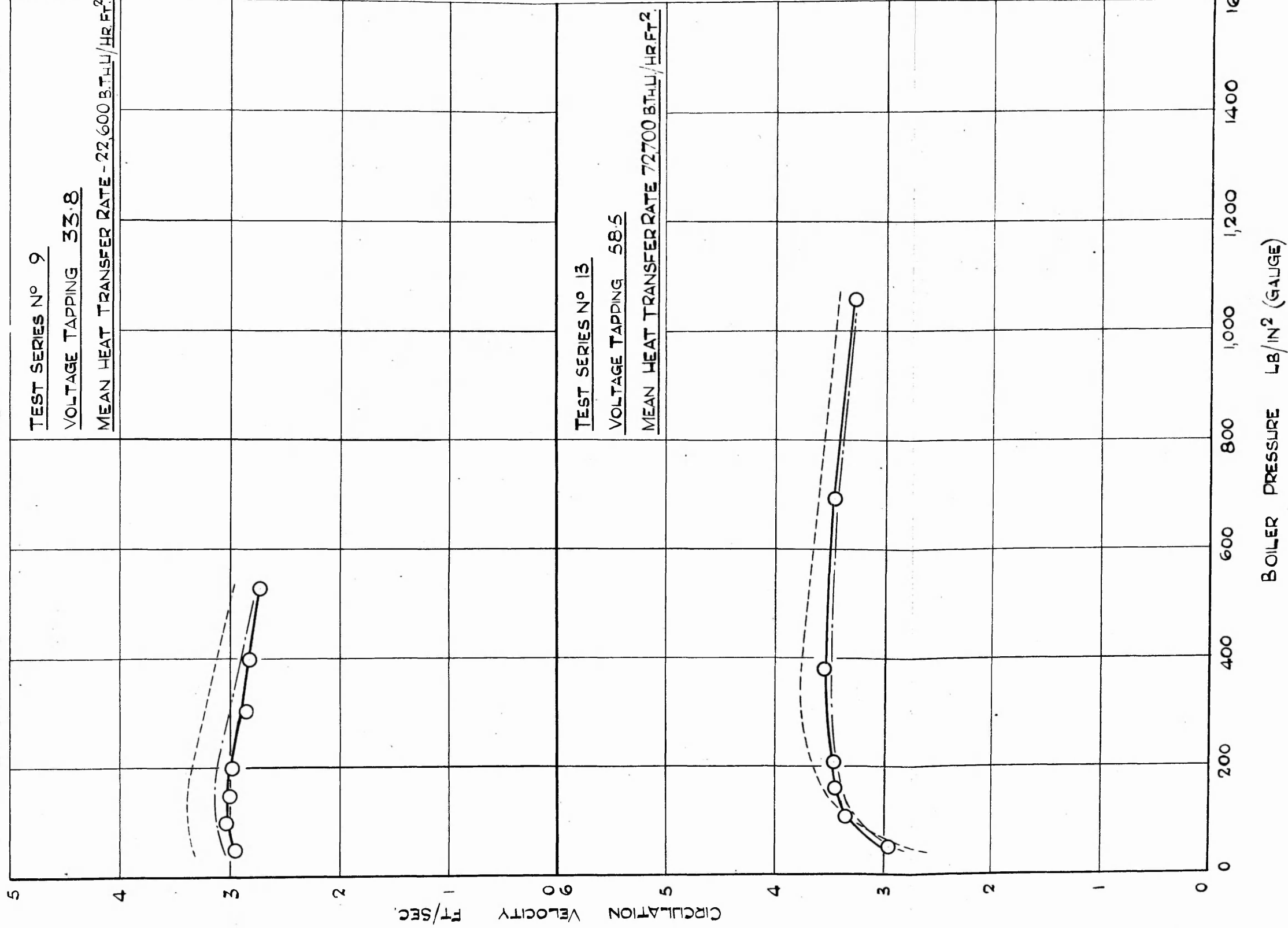
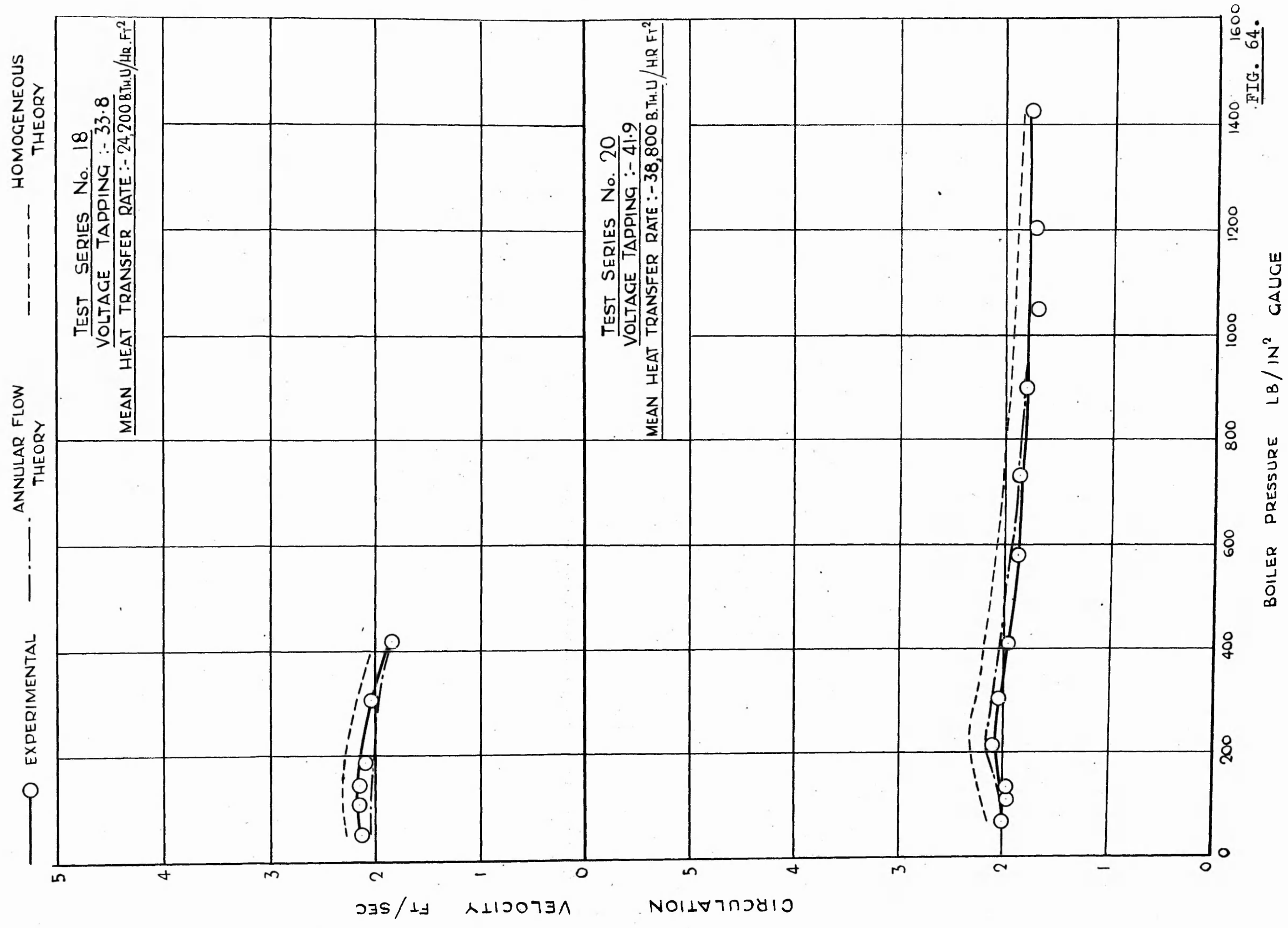


FIG. 63.

CIRCULATION VELOCITY - BOILER PRESSURE

TUBE :- 2 1/4" O.D. x 2 S.W.G. HEATING :- UNIFORM RESTRICTING ORIFICE :- 1/2" DIA
TUBE POSITION :- VERTICAL HEATED LENGTH :- 10'-6"



TEST SERIES No. 18
 VOLTAGE TAPPING :- 33.8
 MEAN HEAT TRANSFER RATE :- 24,200 B.Th.U./HR. FT.²

TEST SERIES No. 20
 VOLTAGE TAPPING :- 41.9
 MEAN HEAT TRANSFER RATE :- 38,800 B.Th.U./HR. FT.²

FIG. 64.

satisfactory.

The homogeneous theory gives values within 0.65 ft./sec. ($\pm 15\%$). While this may be accurate enough for certain purposes, there is no doubt that the proposed theory reduces possible errors considerably.

However, in assessing the relative merits of the two theories it is necessary to consider the diverse conditions met with in actual boiler practice and to examine the possible influence these conditions might have on the accuracy of the results.

The following are some of the more important considerations:-

- (a) Change in Adiabatic Length. In practice the unheated length will be small. On the other hand, however, over appreciable lengths of tubes the heat input may be very small, and indeed approximate to the adiabatic condition. It should be remembered that the homogeneous flow theory gave comparatively large discrepancies in pressure change over the adiabatic lengths. It might be expected, therefore, that the proposed theory would give greater satisfaction in actual boiler calculations.
- (b) Change in Heated Length. In practice the heated tube length is often considerably greater than in the two-tube boiler. An increased heating length for/

for the same heat input causes a reduction in the momentum forces relative to the other force actions. Thus the error incurred by using the homogeneous theory is again increased since the present agreement found with that theory is due in part to the excessive momentum force obtained by assuming both phases to have the same velocity.

- (c) Tube Inclination. The velocity ratio will decrease with decreasing tube inclination. It is to be presumed, therefore, that the error due to the assumption of homogeneous flow will tend to decrease.
- (d) Heated Downcomers. In practice, particularly where no unheated downcomer is provided, it is possible that some downcomer tubes will contain steam-water mixtures. When determining the circulation for such circuits additional errors will be introduced in the prediction of the pressure change over the downcomer. It is expected that the proposed theory will enable more accurate calculation of pressure changes during downcomer flow than the homogeneous theory, particularly in view of the satisfactory application to the prediction of stagnation conditions and to the prediction of the pressure change during the downward flow of air-water mixtures in Sections 22 and 23 respectively.

The question arises as to whether the incidence of steam in the downcomer will render the homogeneous flow theory even more inaccurate. This is seen to be the case by/

by referring to Figure 65. The curves NO and LM are taken to represent the pressure changes in the riser as predicted by the homogeneous and proposed theories respectively. Where no steaming occurs in the downcomer, curve GH is taken to represent the predicted pressure change in the downcomer. The discrepancy in predicted circulation velocity between the theories is represented by the horizontal distance CA. If, where steaming occurs, curve GH is now taken to represent the pressure change in the downcomer as predicted by the homogeneous theory, and curve JK as predicted by the proposed theory, then the discrepancy between the theories is increased and is represented by the horizontal distance EA.

In Figure 66 the same factors are plotted, but for the case in which the gradient of the curve GH has been assumed negative. Here also it is seen that the formation of steam in the downcomer increases the discrepancy between the two theories.

While in Figures 65 and 66 the curve JK has been shown below the curve GH, there are circumstances under which the position would be reversed. Where the steam flowed downward with a velocity greater than that of the water JK would lie above GH. In this case the discrepancy involved by use of the homogeneous theory would be reduced. It can be shown that the conditions necessary for this type of flow exist only where there is a considerable quantity of steam generated in the downcomer.

It/

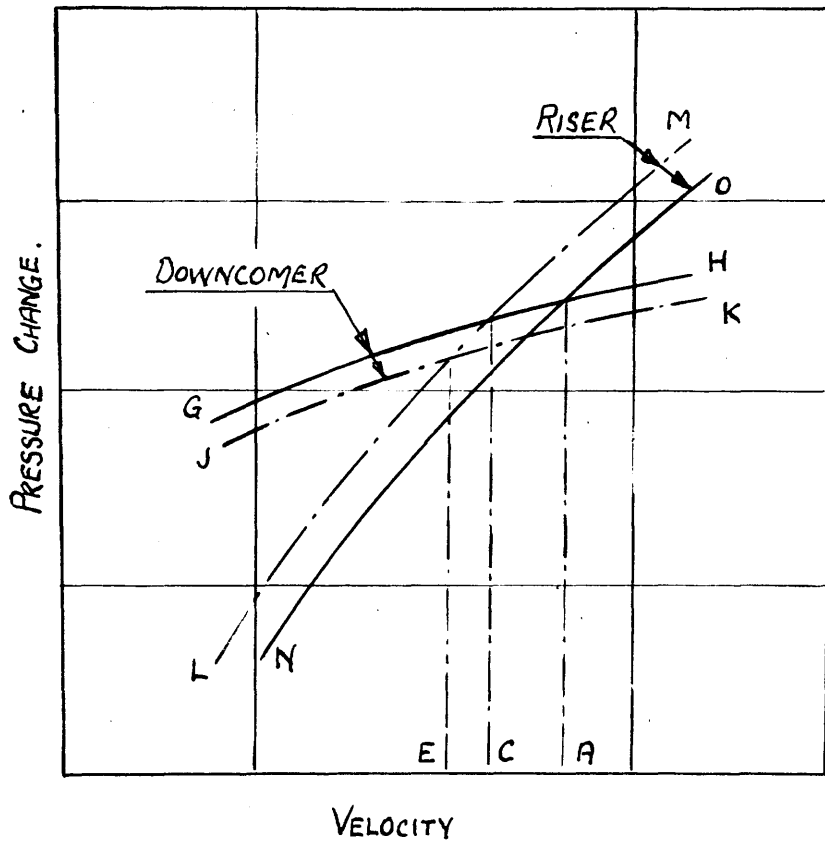


FIG. 65. DIAGRAMMATIC SKETCH OF GRAPHICAL PROCEDURE
TO DETERMINE CIRCULATION VELOCITY WITH HEATED DOWNCOMERS.

————— THEORETICAL - HOMOGENEOUS THEORY.
 - - - - - " - PROPOSED THEORY.

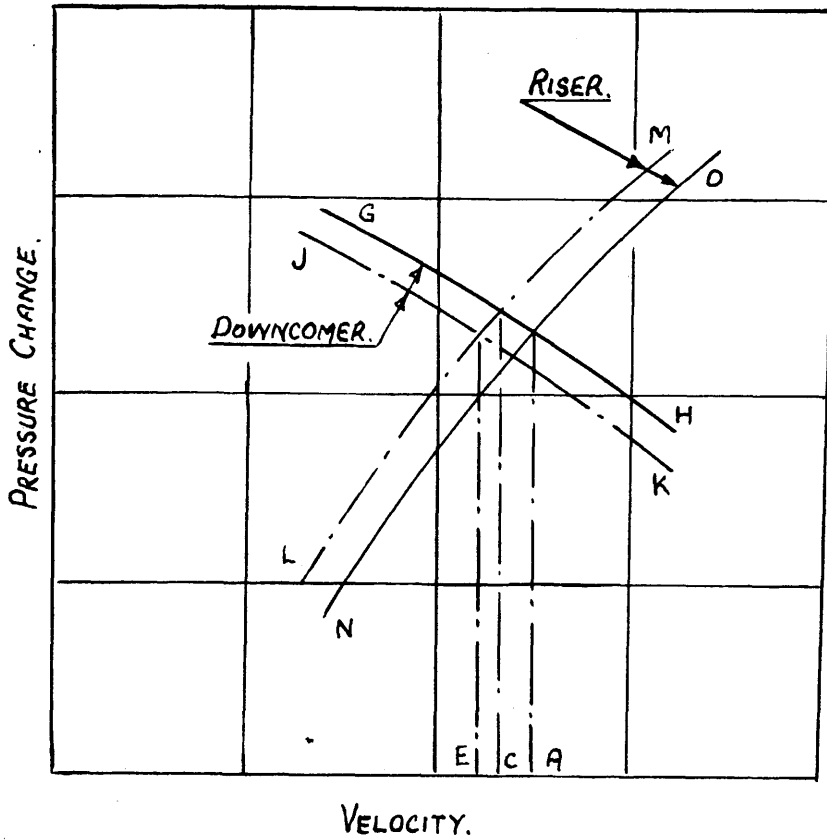


FIG 66. DIAGRAMMATIC SKETCH OF GRAPHICAL PROCEDURE TO DETERMINE CIRCULATION VELOCITY WITH HEATED DOWNCOMERS.

————— THEORETICAL - HOMOGENEOUS THEORY.
 - - - - - " - PROPOSED THEORY.

It can be reasonably concluded that if the downcomer in the experimental plant were heated, the agreement between the measured and theoretical values deduced from the proposed theory would be confirmed, whereas the discrepancy between the measured and theoretical values based on the homogeneous flow theory would be increased.

It may be said that comparisons between theoretical and experimental velocities in a two-tube circuit, interesting as they are, give only overall impressions. The true merits of any theory are more readily obtained by a comparison in detail of the pressure changes over the various parts of the circuit.

RESUMÉ.

This research was initiated to investigate the principles of natural circulation in water-tube boilers. Previous investigators such as Schmidt, Waeselynk and Schwab had appreciated that the standard theory which assumed that the steam-water mixture flowing in the heated tubes behaved as a homogeneous fluid, was inadequate, due primarily to the steam velocity relative to the water. There was ample evidence to indicate that even during the horizontal flow of steam-water mixtures the steam velocity was considerably greater than the water velocity. Several theories had been developed to include this relative movement, but they either contained assumptions unacceptable in the light of present knowledge of the mechanism of turbulent flow, or were in such a form as to render them inapplicable to the wide range of conditions met with in boiler practice. These remarks apply not only to theories and experimental work directly connected with boilers, but to all work connected with the flow of two-phase mixtures.

It was, therefore, necessary to develop the theoretical equations governing the flow of two-phase mixtures. It became clear that the problem was essentially twofold; firstly the determination of the phase distribution, and secondly the determination of the velocities of the respective phases. It has been possible, by consideration of the fundamental mechanism of turbulent flow, to develop

the relationships governing the respective phase velocities for a particular phase distribution. On the other hand, present knowledge does not extend to the point of specifying the distribution of the phases.

The experimental work of previous investigators indicated the persistence, during two-phase flow, of an annular flow pattern in which a ring of liquid wets the entire wall and the inner core comprises gas, or vapour, with associated liquid. The theory was developed for this case. It was assumed that, (a) the liquid in the core was uniformly distributed, (b) the core mixture behaved as a homogeneous fluid, and (c) the core was symmetrically dispersed about the tube axis. The experimental work of Martinelli suggested that both phases flow turbulently for the mass flow rates met with in boiler practice.

During two-phase flow, as during homogeneous flow, the internal shearing stresses must be transferred by viscous or momentum shear. It was assumed that Prandtl's Equation relating shearing stresses and velocity profile gradient would hold throughout the two phases, and that the Prandtl mixing length distribution is the same as for single-phase flow. From these assumptions the velocity profile may be determined for any given shear distribution and in turn the respective phase velocities could be obtained.

The practical application of the theoretical equation embodying the above ideas is not normally possible, as the liquid content in the core is unknown. Where conditions are such that there is no liquid content in the core, a

ready solution is possible, as is illustrated by the analysis of Bergelin's tests. In the majority of cases, and certainly in the case of natural circulation, the liquid content of the core is important, but so far no information directly applicable to the natural circulation problem is available. In fact, the only information on the subject was derived from the results of Armand for air-water mixtures. This information made possible the application of the theoretical equation in a simplified form, to the case of steam-water mixtures.

The procedure is best understood with reference to the equations. The theoretical equations for the gas-liquid velocity ratio is obtained in the form

$$K = \frac{U_b}{U_1} \cdot \frac{1-q-\omega+\omega/k_2}{1-q} + \frac{U_3}{U_1} \cdot \frac{1-q-\omega+\omega/k_2}{1-q} \sqrt{\frac{q}{q+\omega} \cdot \frac{\rho_L}{\rho_G} \cdot \frac{T_2}{T_1}}$$

As the water content in the core is not known, the equation is reduced to the form

$$K = 1 + Z \sqrt{\frac{\rho_L}{\rho_G} \cdot \frac{T_2}{T_1}}$$

The term Z, containing the liquid of the core, is assumed independent of the phase densities and viscosities and it is shown that this is approximately the case. Its values were determined by applying the above equation to Armand's experiments for air-water flow, and were assumed to hold for the flow of steam-water mixtures for corresponding liquid/

liquid flow rates and ratios of gas to tube cross-sectional areas.

The water content in the core is also involved in the shear stress ratio as

$$\frac{T_2}{T_1} = \frac{\left(\frac{dp}{dl}\right)_2 + \rho_2 \sin \theta + \frac{\rho_2 \cdot U_2 \delta U_2}{\delta l \cdot g}}{\left(\frac{dp}{dl}\right)_{F2}}$$

The core density is ρ_2 . In evaluating the shear stress ratio, the core density was, of necessity, assumed that of the steam.

Using the gas to liquid velocity ratio K , the equation for the pressure change is obtained in the form

$$-\left(\frac{dp}{dl}\right)_2 \cdot \delta l = G \cdot \frac{\lambda \cdot \delta l \cdot U_L^2 \cdot \rho}{2g \cdot d} + \left\{ \frac{q + K(1-q)}{q/\rho_g + K(1-q)/\rho} \right\} \delta l$$

$$+ \left\{ \frac{q}{g} \cdot \frac{M}{X} \cdot \delta U_g + \frac{1-q}{g} \cdot \frac{M}{X} \cdot \delta U_L + \frac{\delta q}{g} \cdot \frac{M}{X} (U_g - U_L) \right\}$$

The terms are, in turn, due to mixture weight, friction, and inertia force. The corresponding equation assuming homogeneous flow is

$$-\left(\frac{dp}{dl}\right)_2 \cdot \delta l = \frac{\lambda \cdot \delta l \cdot U^2 \cdot \rho}{2g \cdot d} + \rho \cdot l \cdot \sin \theta + \frac{M}{X} \cdot \frac{\delta U}{g}$$

where

$$\rho = \frac{1}{q/\rho_g + (1-q)/\rho_L}$$

and

$$U = \frac{M}{X} \cdot \frac{1}{\rho}$$

In the friction equation the term G allows for the fact that (a) the liquid is mainly contained in a ring at the wall/

wall, and (b) the core contains a certain amount of liquid.

It was shown that G would have a magnitude close to unity and this assumption has, therefore, been made throughout the application of the theoretical equations. Where evaporation occurs at the wall due to heat transfer the bubble formation at the wall would presumably break up the laminar layer at the wall with an increase in friction. This would tend to increase the friction pressure change. Inspection of the data over the heated length from the two-tube boiler suggested an increase of 25% on the adiabatic friction equation to allow for this effect.

The fundamental relationships governing the velocity ratio K were approximately confirmed by using them to evaluate the water content of the core during Armand's experiments with air-water mixtures. The small magnitudes of the water so found to be concentrated in the core were consistent with the flow pattern assumed.

Further confirmation of the proposed theory in its fundamental form was obtained for Bergelin's tests with air-water mixtures flowing down vertical tubes. In these tests the mass flow rates and the ratio of the gas to tube cross-sectional areas had such values that the water content of the core could be regarded as negligible.

The form of the proposed friction equation was confirmed by applying it to analyse the pressure changes during the air-water flow experiments reported by Martinelli, and also the/

the pressure changes during the adiabatic flow of steam-water mixtures in the two-tube boiler experiments.

The theoretical pressure changes, using both the proposed theory and the standard homogeneous theory, were compared with the experimental values for the upward flow of steam-water mixtures in smooth vertical tubes for the following conditions.

- (a) The adiabatic flow of steam-water mixtures in 1" bore tubes, for pressures in the region of 170 lb./in.² and 1600 lb/in.² (Schwab's results).
- (b) The adiabatic flow of steam-water mixtures in 1.7" bore tubes for pressures between 50 to 1500 lb./in.² (Two-tube boiler results).
- (c) Steam-water mixtures flowing through 1.7" bore tube with heat transfer (Two-tube boiler results).

The proposed theory was also used to determine the circulation velocity producing "stagnation" conditions in downcomer tubes, and the results compared with the experimental observations of Lowenstein.

Finally, both the proposed theory and the homogeneous theory were used to determine the circulation velocity in the two-tube boiler.

DISCUSSION.

The application of the theory to a wide range of experimental results gave extremely good agreement. When applied to the analysis of the adiabatic flow of steam-water mixtures in the two-tube boiler, the proposed theory gave 45% of the predicted pressure changes within 5% of the measured values, 87% within 15%, and all within 22%. The homogeneous theory, on the other hand, gave only 40% of the results within 22%, and all within 55%. It is, therefore, seen that the proposed theory gives considerable improvement over the homogeneous theory. In the analysis of Schwab's results for the flow of steam-water mixtures through 1" tubes the improvement was even more marked, the proposed theory agreeing within 14% and the homogeneous theory within 60%.

In general, the large errors quoted for the homogeneous theory decrease with increasing pressure, as is to be expected, since the steam-water velocity ratio decreases with increasing steam density.

The only data available relating to the flow of steam-water mixtures with heat transfer is that obtained from the two-tube boiler. The proposed theory enables the calculation of the pressure change over the evaporation length within 15%. The great majority of the results gave agreement much closer than this maximum error. Here again the homogeneous theory gave considerable errors, the maximum error being as much as 40%. While this is an improvement on/

on the figure obtained for the adiabatic case, it is undoubtedly due to the excessive momentum force obtained by assuming both phases to flow with the same velocity thus compensating for the error involved in this assumption where momentum forces do not exist.

Part of the error in the proposed theory must be attributed to the term G in the friction equation. This was assumed unity. The analysis of Martinelli's tests for air-water flow through horizontal tubes confirmed that friction varies as the square of the liquid velocity, but gave a value of $G = 0.75$. The analysis of the steam-water mixtures flowing adiabatically in vertical tubes, obtained from the two-tube boiler, also confirmed that the friction varied as the square of the liquid velocity, providing in this instance that G varied with the boiler pressure. On this basis G was found to have a value of 1.25 at 50 lb./in.² gauge decreasing to 0.95 at 130 lb/in.², and remaining constant thereafter. It seems reasonable that G should be dependent on the pressure, as G is dependent on the water content in the core which will be affected in turn by the change in the phase densities with pressure variation. The introduction of the changing value of G , to the theoretical calculation for the pressure change during adiabatic flow, would have produced considerable improvement particularly at low pressures, and 55% of the tests would then have agreed within 5% as against 45% when assuming $G = 1$. The explanation of the lower values of G (0.75) obtained with the horizontal/

horizontal flow of air-water mixtures may be that, with horizontal flow, the pattern is no longer strictly symmetrical.

There was no appreciable error due to the neglect of distortion effects in the friction equation. Distortion is large, where the friction pressure change is small relative to the total pressure change, as for this condition the shearing stress ratio T_2/T_1 is large. Hence where the error in the friction equation introduced by neglecting distortion is likely to be largest, the contribution of friction to the total pressure change is smallest.

Data was not available to confirm the accuracy of the equations when applied to rough tubes (Appendix K). The theoretical equation indicates that with horizontal tubes the velocity ratio will be increased with increasing surface roughness. However, with vertical tubes the influence of the increased friction on the internal shearing stresses tends to make the velocity ratio independent of the surface roughness. Tests with rough tubes afford an excellent opportunity of checking the form of the equation for the gas-liquid velocity ratio.

The prediction of the point of stagnation by the proposed equations gave good agreement with Lowenstein's observations. This suggests that the equations may be satisfactorily applied to the prediction of flow in down-comers. This was also supported by the analysis of Bergelin's results for air-water mixtures flowing vertically downwards./

downwards. These tests, while they gave errors in the predicted pressure change as large as 62%, gave agreement between the theoretical velocity ratio and that velocity ratio which would give the actual pressure change within 20%. This was the estimated accuracy of the velocity ratio for the steam-water experiments with upward flow in vertical tubes. The explanation of the greater errors in the predicted pressure change with downward flow is that, unlike the case where the flow is upwards, the resultant pressure change is due to the difference between the friction and mixture weight pressure changes. Any errors naturally tend to be magnified, particularly where the pressure changes due to friction and mixture weight tend to be of the same magnitude. In addition it should be noted that any error in the predicted velocity ratio has opposite effects on the pressure change due to mixture weight and friction. If the pressure change due to mixture weight increases the friction decreases, and vice versa. Where the two components of the pressure change are being added, the errors due to inaccuracies, therefore, tend to balance. Where they subtract, as in the analysis of Bergelin's experiments, the errors are cumulative.

The analysis of Bergelin's experiments, where as already mentioned the theoretical velocity and that velocity ratio which would give the measured pressure change were found to agree within 20%, also indicates that the controversial assumption that the Prandtl mixing length distribution is/

is the same during single and two-phase flow is approximately true.

When applying the proposed theory to determine the circulation velocity, agreement within 6% was obtained. The homogeneous theory, on the other hand, gave agreement within 15%. Thus, despite the large errors in the pressure change over various tube lengths, the homogeneous theory gives an agreement which, from practical purposes would not seem unsatisfactory. If, in addition, the relative simplicity of the homogeneous theory is considered, it may appear unnecessary to use the more complicated proposed theory. However, it has already been shown that the inclusion of greater tube lengths with adiabatic flow and of heated downcomers could appreciably increase the errors quoted above. Also, in multi-tube banks the large errors in the pressure change may produce inaccurate conclusions as to the flow rates occurring in different tubes. The errors may give quite erroneous ideas as to the number of tubes acting as risers and downcomers. Care should, therefore, be taken in applying the homogeneous theory, as in certain circumstances the errors in the predicted circulation may be considerably greater than those obtained with the two-tube boiler. On the other hand, the close agreement obtained with the proposed theory in the step-by-step analysis of the circuit in the two-tube boiler, and in the analysis of widely differing experimental work of previous investigators, inspires confidence in its general application.

CONCLUSIONS.

Over the range of pressures and heat input rates investigated, natural circulation provides adequate flow in a two-tube circuit. With increasing pressure the circulation velocity rises to a maximum value above which it decreases slowly. With no restriction to flow the maximum circulation velocity occurs at pressures in the region of 400 lb/in². The maximum velocity was independent of the heat input, and the pressure corresponding to the maximum velocity increased with the heat input to the tube.

With restricting orifices the trends are similar, except that the maximum velocity now occurs at pressures lower than 400lb/in².

The proposed theory, based on an annular flow pattern where the water forms a ring at the wall with a core of steam and entrained liquid, gives much closer and more consistent agreement between experimental and calculated values than the homogeneous theory. This is illustrated in the following tables:

Annular Theory.

Pressure Gradients.

	Tests per 100 lying within the following % errors.		
	5%	15%	22%
Adiabatic flow. 1.7" bore tube. (Two-tube boiler)	45	87	100

Flow with heat transfer. 1.7" bore tube. (Two-tube boiler)	70	100	-
Adiabatic flow. 1.0" bore tube. (Schwab's experiments)	76	100	-

Homogeneous Theory.

Pressure Gradients.

	Tests per 100 lying within the following % errors.		
	22%	40%	55%
Adiabatic flow . 1.7" bore tube. (Two-tube boiler)	40	92	100
Flow with heat transfer. 1.7" bore tube. (Two-tube boiler)	75	100	-
Adiabatic flow. 1.0" bore tube. (Schwab's experiments)	64	77	<100

The annular theory gives the ratio of the steam to water velocities as high as 5.7, for which condition the steam velocity is 57.5 ft/sec. and the water velocity 10.1 ft/sec. In the majority of tests the velocity ratio would appear to be estimated within 20%.

At pressures above 1000 lb/in² the velocity ratio is normally near unity, and for such circumstances the homogeneous theory gives closer agreement than indicated in the above tables. At 1615 lb/in² with a 1" bore tube

the maximum error was 18%.

The proposed theory enabled the prediction of the circulation velocity within 6% as against 15% using the homogeneous theory. With circuits other than the two-tube boiler the errors assuming homogeneous flow could be considerably greater than those quoted. The more detailed agreement obtained with the proposed theory would suggest it could be applied with confidence to other circuits.

The above results indicate that while the flow pattern assumed may not occur at all flow conditions, the theory based on such a pattern may be applied with considerable accuracy over a wide range of flow conditions. This is further confirmed by the good agreement obtained in analysing experiments for air-water flow in horizontal and vertical tubes.

Nevertheless there is still scope for further improvement. Due to the limited information available certain assumptions and approximations were necessary in developing the proposed theory. The problems implicit in these assumptions can only be answered by further detailed investigation into the flow of two-phase mixtures. The study of steam-water flow is fraught with difficulties due to the effects of condensation or evaporation. In the first instance the most satisfactory field of investigation would appear to be that of air-water flow. The work of Armand suggests the natural starting point.

In conclusion it can be said that a theory has been developed allowing for the different velocities of the

phases during two-phase flow. The relationships are in a form permitting their application to the problem of circulation in tube banks. The proposed theory is more laborious in application than the homogeneous theory but the preparation of suitable charts would substantially reduce the labour at present required. Considerable improvement is obtained over the homogeneous theory in predicting pressure changes and circulation rates.

- Thornycroft, J.I. Watertube Steam Boilers for Marine Engineers. Proc. I.C.E. Vol. 99, 1889.
- Thornycroft, J.I. Circulation in the Thornycroft Watertube Boiler. Trans. I.N.A. Vol. 35, 1894.
- Thornycroft, J.I. The Influence of Circulation on Evaporative Efficiency. Trans. I.N.A. Vol. 36, 1895.
- Watkinson, Prof.W.H. On Watertube Boilers. Trans. I.E. and S. Vol.39, 1895.
- Yarrow, A.F. Description of Some Experiments with a Watertube Boiler. Trans. I.N.A. Vol.40, 1898.
- Schmidt, E. Experiments Regarding Circulation in Vertical Tube Boilers. Combustion, August, 1933.
- Dight, J.R. Eng. Capt. R.N. Naval Watertube Boilers. Trans. I.N.A.Vol. 75, 1933.
- Davis and Timmins. Some Technical Aspects of High Pressure Boiler Design. Proc. I. Mech.E. Vol. 125, 1933.
- Robinson, S.M. Rear Adm. Water Circulation and Gas Path in Naval Boilers. Trans. S.N.A. and Mar. E. Vol.41, 1933.
- Schmidt, E. Circulation in Steam Boilers. V.O.L. Verlag G.M.B.H. Berlin 1934
- Jones and Solberg Marine and Naval Boilers. Trans. S.N.A. and Mar.E. Vol.42, 1934.
- Dight, J.R. Eng. Capt. Naval Watertube Boilers. Trans. I.N.A. Vol. 78, 1936.
- Worthen, E.F. Water Circulation in A. Type Marine Boilers. Journal A.S.N.E. Vol. 52, 1940.
- Lewis and Robertson Circulation of Water and Steam in Watertube Boilers and Rational Simplification of Boiler Design. Proc.I.Mech.E. Vol.143,1940.

- Brunt, J.V. A Study of Circulation in High Pressure Boilers and Water Cooled Surfaces.
Trans. A.S.M.E. Vol.63, 1941.
- Midtlying, C. Development of a Graphical General Solution for Thermal Circulation in U-Tube Hydraulic Circuits.
Journal A.S.N.E. Vol. 54, 1942.
- Markson, Ravese and Humphreys. A Method of Estimating the Circulation in Steam Boiler Furnace Circuits.
Trans. A.S.M.E. Vol. 64, 1942.
- Nothman, G.A. and Binder, R.C. Slip Velocity in Boilertube Circuits.
Combustion, June, 1943.
- McAdams, W.H. and others. Vaporisation inside Horizontal Tubes II Benzene - Oil Mixtures.
Trans. A.S.M.E. Vol. 65, no.6.
- Martinelli, R.C. and others Isothermal Pressure Drop for Two-Phase, Two-Component Flow in a Horizontal Pipe.
Trans.A.S.M.E. Vol. 66, 1944.
- Ledineg, Dr. Water Circulation in Bent-Tube and Radiant Boilers.
Engineer's Digest, 1944.
- Rowand and Allardice. Natural Circulation Test Results on a 2500 lb/in² Twin Branch Boiler.
Trans.A.S.M.E. Vol. 66, 1944.
- Silver, R.S. A Thermodynamic Theory of Circulation in Water tube Boilers.
Proc.I.Mech.E. 1945.
- Lowenstein. Reports on Tests of the Wagner Boiler Co. with a Model Boiler.
British Intelligence Object Sub-Committee. Final Report No. 580.
Item 29.
- Armand, A.A. Resistance to Two-Phase Flow in Horizontal Tubes.
Izvestia W.T.I. No.1, 1946.
- Burnell, J.G. Flow of Boiling Water through Orifices and Pipes.
Engineering. Vol.164, 1947.

Davis, R.

Expansion Theory of Circulation in ^{223.}
Water-Tube Boilers.
Engineering, Vol.163, n 431, Feb.1947.

Armand, A.A. and
Treshchew, G.G.

Investigation of Resistance during
The Motion of Steam-Water Mixtures
in a Heated Boiler Tube at High
Pressure.
Izvestia W.T.I. No.4, 1947.

S

Schwab, V.A.

Hydraulics of Two-Phase Flow in a
Vertical Branch of a Free Circulation
Boiler.
Kotloturbostroenie No.4, 1947.

Waeselynk, R.

Investigation on the Natural
Circulation in Boiler Tubes.
Bull. Assoc. Techn. Mar. et Aero. 1948.

Baldina, D.M. and
Petersen, D.F.

The Application of Dimensionless
Co-ordinates for the Generalisation
of Experimental Results of
Circulation in Steam Boilers.
Kotloturbostroenie No.2, 1949.

Bergelin, O.P. and
Gazley, C.

Co-Current Gas-Liquid Flow -
1. Flow in Horizontal Tubes.
A.S.M.E. Heat Transfer and Fluids
Mechanics Institute, 1949.

Bergelin, O.P. and
others.

Co-Current Gas-Liquid Flow -
2. Flow in Vertical Tubes.
A.S.M.E. Heat Transfer and Fluid
Mechanics Institute, 1949.

Baker, L.

Design of Marine Water-Tube Boilers.
Charles Griffen and Co. Ltd. London.
1950.

Allen, W.F. Jr.

Flow of a Flashing Mixture of Water
and Steam through Pipes and Valves.
A.S.M.E. Vol.73, 1951.

Heywood, R.W.

Research into the Fundamentals of
Boiler Circulation Theory.
I. Mech. E. } 1951
A.S.M.E. }

Linning, D.L.

The Adiabatic Flow of Evaporating
Fluids in Pipes of Uniform Bore.
Proc. I. Mech. E. Vol. 1B, No.2, 1952.

APPENDICES.

	<u>Page.</u>
A. Continuity equations during two-phase flow ...	225.
B. Velocities and velocity changes	227.
C. Relationship between core velocities	228.
D. Determination of the velocity ratio K , the term Z , and the water concentration ω	229.
E. Determination of the pressure change during the downward flow of air-water mixtures in vertical tubes..	234.
F. Determination of stagnation point during flow in downcomer tubes.	238.
G. Conversion of experimental readings - two-tube boiler	242.
H. Specimen calculations - two-tube boiler... ..	244.
J. Equipment to enable the study of the flow of steam-water mixtures through horizontal tubes...	256.
K. Velocity ratio equation for rough tubes... ..	259.

The continuity equation for the core is

$$\frac{(q+\omega)M}{X_2} = U_2 \cdot \rho_2 \dots \dots \dots A1$$

The continuity equation for the annular ring is

$$\frac{(1-q-\omega)M}{X_1} = U_1 \cdot \rho_1 \dots \dots \dots A2$$

Combining Equations A1 and A2

$$\begin{aligned} X &= X_1 + X_2 = \frac{(q+\omega)M}{U_2 \cdot \rho_2} + \frac{(1-q-\omega)M}{U_1 \cdot \rho_1} \\ &= \frac{(q+\omega)M}{U_2 \cdot \rho_2} + \frac{K_2(1-q-\omega)M}{U_1 \cdot \rho_1} \dots \dots \dots \text{as } U_1 = \frac{U_2}{K_2} \\ &= \frac{M}{U_2} \left[\frac{q+\omega}{\rho_2} + \frac{K_2(1-q-\omega)}{\rho_1} \right] \dots \dots \dots A3 \end{aligned}$$

Treating now the continuity equations for the gas and liquid

$$\frac{qM}{X_g} = U_g \cdot \rho_g \dots \dots \dots A4$$

and

$$\frac{(1-q)M}{X_L} = U_L \cdot \rho_L \dots \dots \dots A5$$

Combining Equations A4 and A5

$$\begin{aligned} X &= \frac{q \cdot M}{U_g \cdot \rho_g} + \frac{(1-q)M}{U_L \cdot \rho_L} \\ &= \frac{M}{U_g} \left[\frac{q}{\rho_g} + \frac{K(1-q)}{\rho_L} \right] \dots \dots \dots A6 \end{aligned}$$

The core mixture is treated as homogeneous, hence

$$U_g = U_2 \dots \dots \dots A7$$

and the annulus is assumed to contain liquid only, hence

$$\rho_L = \rho_1 \dots \dots \dots 9$$

Combining Equations A3, A6, A7 and 9

$$\frac{q+w}{P_2} + \frac{K_2(1-q-w)}{P_L} = \frac{q}{P_G} + \frac{K(1-q)}{P_L} \dots \dots \dots A8$$

and from Equation 7

$$P_2 = (q+w) / (q/P_G + w/P_L)$$

Substituting Equation 7 in Equation A8

$$\frac{q}{P_G} + \frac{w}{P_L} + \frac{K_2(1-q-w)}{P_L} = \frac{q}{P_G} + \frac{K(1-q)}{P_L}$$

Hence

$$K = K_2 \cdot \frac{1-q-w+w/K_2}{1-q} \dots \dots \dots A9$$

That is

$$\frac{U_G}{U_L} = \frac{U_2}{U_1} \cdot \frac{1-q-w+w/K_2}{1-q} \dots \dots \dots A10$$

Therefore

$$U_1 = U_L \cdot \frac{1-q-w+w/K_2}{1-q} \dots \dots \dots A11$$

as

$$U_G = U_2$$

Combining Equations A4 and A6,

$$\frac{X_G}{X} = \frac{q/P_G}{q/P_G + K(1-q)/P_L} \dots \dots \dots A12$$

and

$$\begin{aligned} \frac{X_L}{X} &= 1 - \frac{X_G}{X} \\ &= \frac{K(1-q)/P_L}{q/P_G + K(1-q)/P_L} \dots \dots \dots A13 \end{aligned}$$

Velocities and Velocity Change.

APPENDIX B.

From Equations A6 and A7,

$$U_2 = U_G = \frac{M}{X} \left[\frac{q}{\rho_G} + \frac{K(1-q)}{\rho_L} \right] \dots \dots \dots A14$$

As $K = \frac{U_G}{U_L}$ it follows from the above equation that

$$U_L = \frac{U_G}{K} = \frac{1}{K} \cdot \frac{M}{X} \left[\frac{q}{\rho_G} + \frac{K(1-q)}{\rho_L} \right] \dots \dots \dots A15$$

In determining the change in velocity due to the changing conditions along the tube, changes in the densities and in the velocity ratio are ignored, as the influence of both effects is small for the experimental conditions.

The velocity of the gas or vapour after a change in dryness fraction δq is

$$U_G + \delta U_G = \frac{M}{X} \left[\frac{q + \delta q}{\rho_G} + \frac{K(1-q - \delta q)}{\rho_L} \right] \dots \dots \dots A16$$

Therefore subtracting Equation A15 from A16

$$\delta U_G = \frac{M}{X} \left[\frac{\delta q}{\rho_G} - \frac{K \cdot \delta q}{\rho_L} \right] \dots \dots \dots A17$$

$$\doteq \frac{M}{X} \cdot \frac{\delta q}{\rho_G} \dots \dots \dots A18$$

as ρ_L is large compared with ρ_G in the experiments analysed.

Similarly

$$\delta U_L \doteq \frac{1}{K} \cdot \frac{M}{X} \cdot \frac{\delta q}{\rho_G} \dots \dots \dots A19.$$

RELATIONSHIP BETWEEN CORE VELOCITIES. APPENDIX C.

From Equation 4

$$\left(\frac{du}{dy}\right)_2 = \left(\frac{du}{dy}\right)_1 \sqrt{\frac{\rho_1}{\rho_2} \cdot \frac{T_2}{T_1}} \dots \dots \dots 4$$

As the term within the square root sign is a constant for a particular flow condition, this may be integrated with respect to y , giving, after the constant of integration has been obtained,

$$U' = U \sqrt{\frac{\rho_1}{\rho_2} \cdot \frac{T_2}{T_1}} \dots \dots \dots A21$$

where the velocity symbols are as indicated in Figure 14.

The mean velocity of the core relative to the boundary of the phases during single-phase flow (i.e. curve dc in Figure 14) is

$$U_3 = \frac{\int_{r_b}^{r_o} 2 \pi r U dy}{\pi r_b^2} \dots \dots \dots A22$$

where r_b is the radius of the cylindrical core.

The mean velocity of the core mixture during two-phase flow relative to the boundary is

$$U_3' = \frac{\int_{r_b}^{r_o} 2 \pi r U' dy}{\pi r_b^2} \dots \dots \dots A23$$

which, on substituting Equation A21, becomes

$$\begin{aligned} U_3' &= \frac{\int_{r_b}^{r_o} 2 \pi r U \sqrt{\frac{\rho_1}{\rho_2} \cdot \frac{T_2}{T_1}} dy}{\pi r_b^2} \\ &= U_3 \sqrt{\frac{\rho_1}{\rho_2} \cdot \frac{T_2}{T_1}} \dots \dots \dots 5 \end{aligned}$$

Armand, as previously discussed in Section 6, weighed the tube through which a mixture of air and water flowed, from which it was possible to determine the respective cross-sectional areas occupied by the phases. The ratio of the gas to tube cross-sectional areas ($\frac{X_g}{X}$) to a base of the ratio of the gas flow volume to the total flow volume (β) obtained in this manner are shown in Figure 12.

From this information the velocity ratio K may be obtained.

Determine the velocity ratio K when

$$\frac{X_g}{X} = \frac{q/\rho_g}{q/\rho_g + K(1-q)/\rho_L} = 0.6 \dots \dots \dots A24$$

From Figure 12 corresponding to this value of $\frac{X_g}{X}$

$$\beta = \frac{q/\rho_g}{q/\rho_g + (1-q)/\rho_L} = 0.715 \dots \dots \dots A25$$

Hence

$$\frac{1-q}{q} \cdot \frac{\rho_g}{\rho_L} = \frac{1}{0.715} - 1 = 0.4 \dots \dots \dots A26$$

Now Equation A24 may be written

$$\frac{1}{1 + K \frac{1-q}{q} \frac{\rho_g}{\rho_L}} = \frac{1}{1 + K \times 0.4} = 0.6$$

$$\therefore K = 1.675$$

In Section 11 the approximate form of the velocity ratio K during horizontal flow has been obtained in the form (Equation 20)

$$\begin{aligned}
 K &= 1 + Z \sqrt{\frac{\rho_L}{\rho_G}} \\
 &= 1 + Z \sqrt{62.5 \times 13.35} \\
 &= 1 + Z \times 28.9 \dots \dots \dots A27
 \end{aligned}$$

as $\rho_L = 62.5 \text{ lb/ft}^3$ and $\rho_G = 1/13.35 \text{ lb/ft}^3$. The density of air used is that at atmospheric pressure and a temperature of 70°F .

Now, for the particular case of $\frac{X_G}{X} = 0.6$ already considered

$$\begin{aligned}
 Z &= \frac{1}{28.9} (K - 1) = \frac{1}{28.9} (1.675 - 1) \\
 &= 0.0234
 \end{aligned}$$

By this procedure Figure 15 was constructed.

Above the critical $\frac{X_G}{X}$ ratio the value of Z is dependent on the mass flow of the liquid phase. Considerable interpolation was necessary in this region. The continuous lines are mean lines obtained from the experimental data. Where the line is obtained by interpolation or extrapolation it is shown as a broken line.

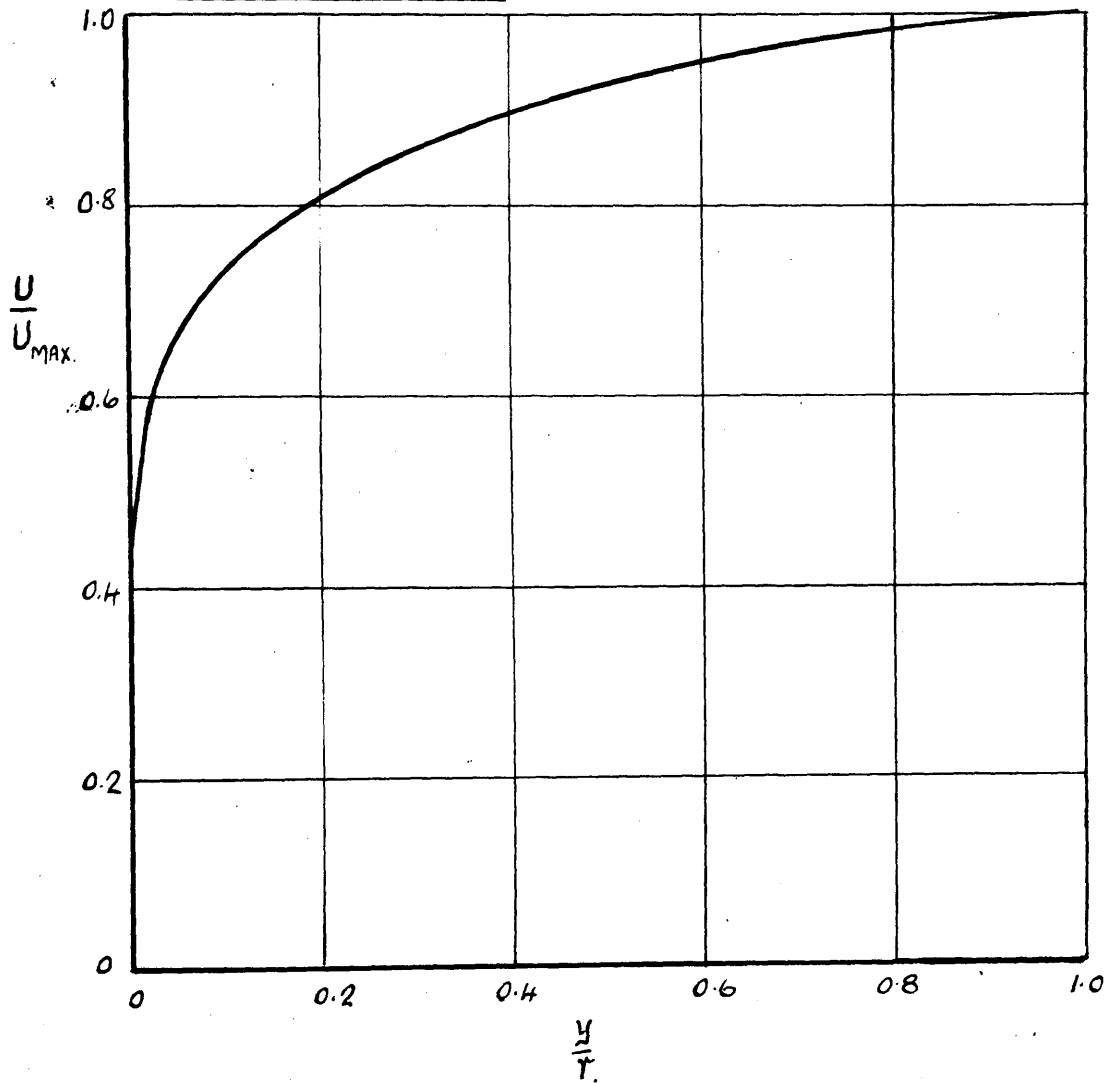
.

An approximate estimate of the water concentration in the core may be made by using Equation 59.

$$K = 1 + \frac{U_3}{U_1} \sqrt{\frac{q}{q+w} \cdot \frac{\rho_L}{\rho_G}} \dots \dots \dots 59$$

The ratio $\frac{U_3}{U_1}$ was determined from the single-phase velocity profile shown in Figure 67. This is the velocity profile corresponding to a Reynold's Number of 105,000.

FIG. 67. VELOCITY DISTRIBUTION IN SMOOTH TUBES
AT A REYNOLD'S NUMBER OF 105,000.
(SOURCE: NIKURADSE FROM BAKHMETEFF'S "MECHANICS
OF TURBULENT FLOW.")



The Reynold's Number used should, in fact, be the Reynold's Number corresponding to the flow in the annulus. The value quoted is an approximate mean value throughout Armand's tests. As the ratio $\frac{U_3}{U_1}$ varies only slightly with Reynold's Number the error involved in this assumption is small. The calculated values of $\frac{U_3}{U_1}$ are shown in Figure 68 to a base of X_2/X .

Continuing the numerical example where $\frac{X_G}{X} = 0.6$, from Equation A31

$$\frac{1-q}{q} \cdot \frac{\rho_G}{\rho_L} = \frac{1-q}{q} \cdot \frac{1}{62.5 \times 13.35} = 0.4$$

Therefore

$$\frac{1}{q} = 334$$

From Figure 68 $\frac{U_3}{U_1} = 0.112$ when $\frac{X_G}{X} = 0.6$ (N.B. $\frac{X_G}{X} = \frac{X_2}{X}$)

Regrouping Equation 59 in the form

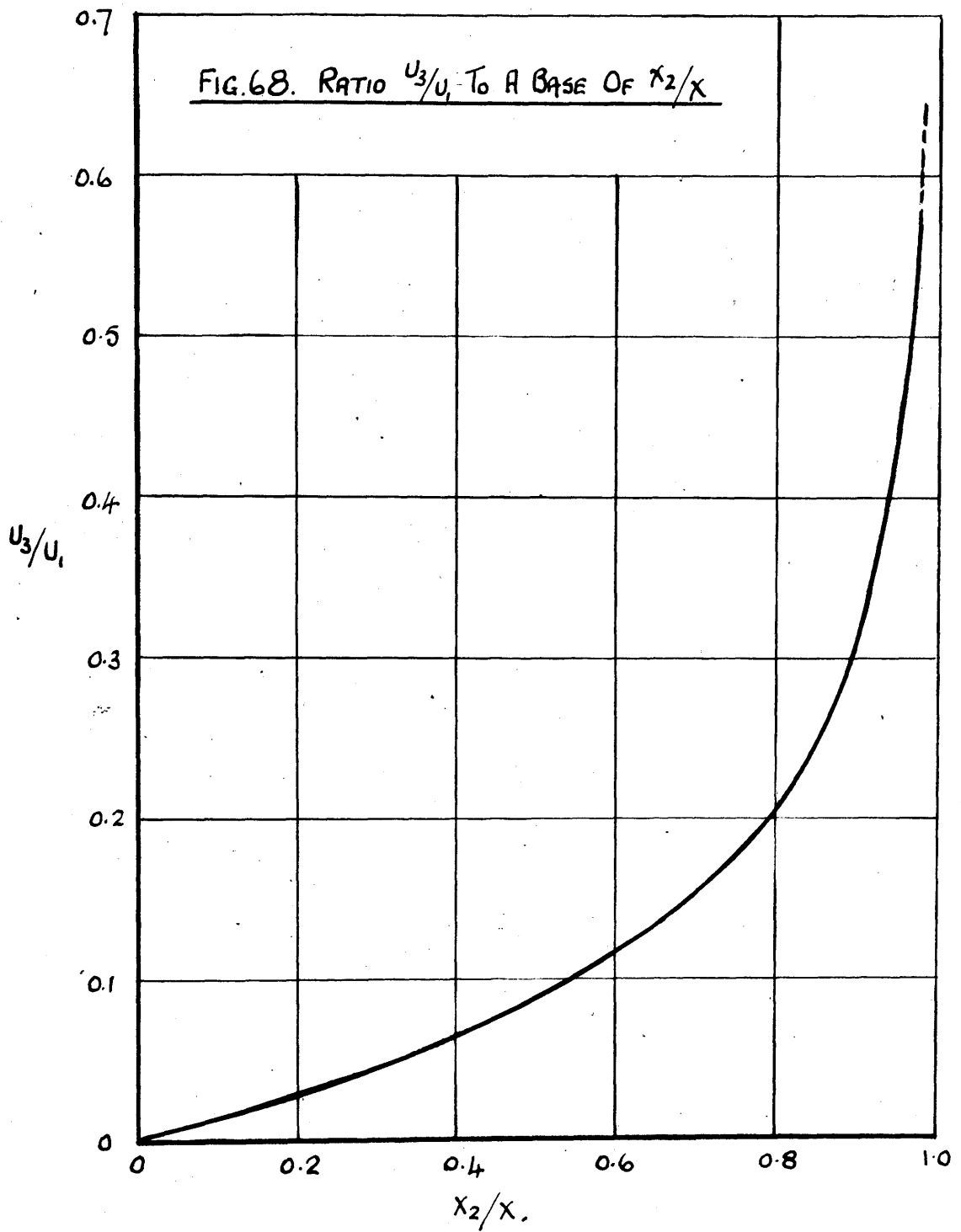
$$K = 1 + \frac{U_3}{U_1} \sqrt{\frac{1}{1 + \frac{\omega}{q}} \cdot \frac{\rho_L}{\rho_G}}$$

Substituting numerical values

$$1.675 = 1 + 0.112 \sqrt{\frac{62.5 \times 13.35}{1 + 334 \omega}}$$

Hence $\omega = 0.073$

Figure 20 was constructed in this manner.



DETERMINATION OF THE PRESSURE CHANGE DURING
THE DOWNWARD FLOW OF AIR-WATER MIXTURES IN
VERTICAL TUBES.

APPENDIX E.

Consider the case where the air and water flow rates are respectively 80 and 1400 lb/hr.

The other properties are:

$$\rho_L = 62.5 \text{ lb/ft}^3. \quad \rho_g = 0.0749 \text{ lb/ft}^3. \quad \mu_L = 2.42 \text{ lb/hr.ft.}$$

$$q = \frac{80}{80 + 1400} = 0.054 \quad \text{Tube diameter } 1". \quad X = \frac{\bar{n}}{4} \times \frac{1}{144}$$

$$\frac{M}{X} = \frac{1480 \times 183.5}{3600} = 75.5 \text{ lb/sec.ft}^2 \quad = \frac{1}{183.5} \text{ ft}^2$$

Assume $K=7$.

The pressure change is obtained from Equation 65.

$$-\left(\frac{dp}{dl}\right)_2 \cdot 8l = \frac{\lambda \cdot 8l \cdot u_L^2 \cdot \rho_L}{2g \cdot d} - \left[\frac{q + K(1-q)}{q/\rho_g + K(1-q)/\rho_L} \right] 8l$$

From Equation A15

$$u_L = \frac{1}{K} \cdot \frac{M}{X} \left[\frac{q}{\rho_g} + \frac{K(1-q)}{\rho_L} \right]$$

$$= \frac{75.5}{7} \left[\frac{0.054}{0.0749} + \frac{7 \times 0.946}{62.5} \right]$$

$$= 8.92 \text{ ft/sec.}$$

Reynold's Number (Equation 46)

$$Re = \frac{u_L \cdot d \cdot \rho_L}{\mu_L}$$

$$= \frac{8.92 \times 1 \times 62.5 \times 3600}{12 \times 2.42} = 69,100$$

From the friction curves shown in Figure 69 $\lambda = 0.0195$.

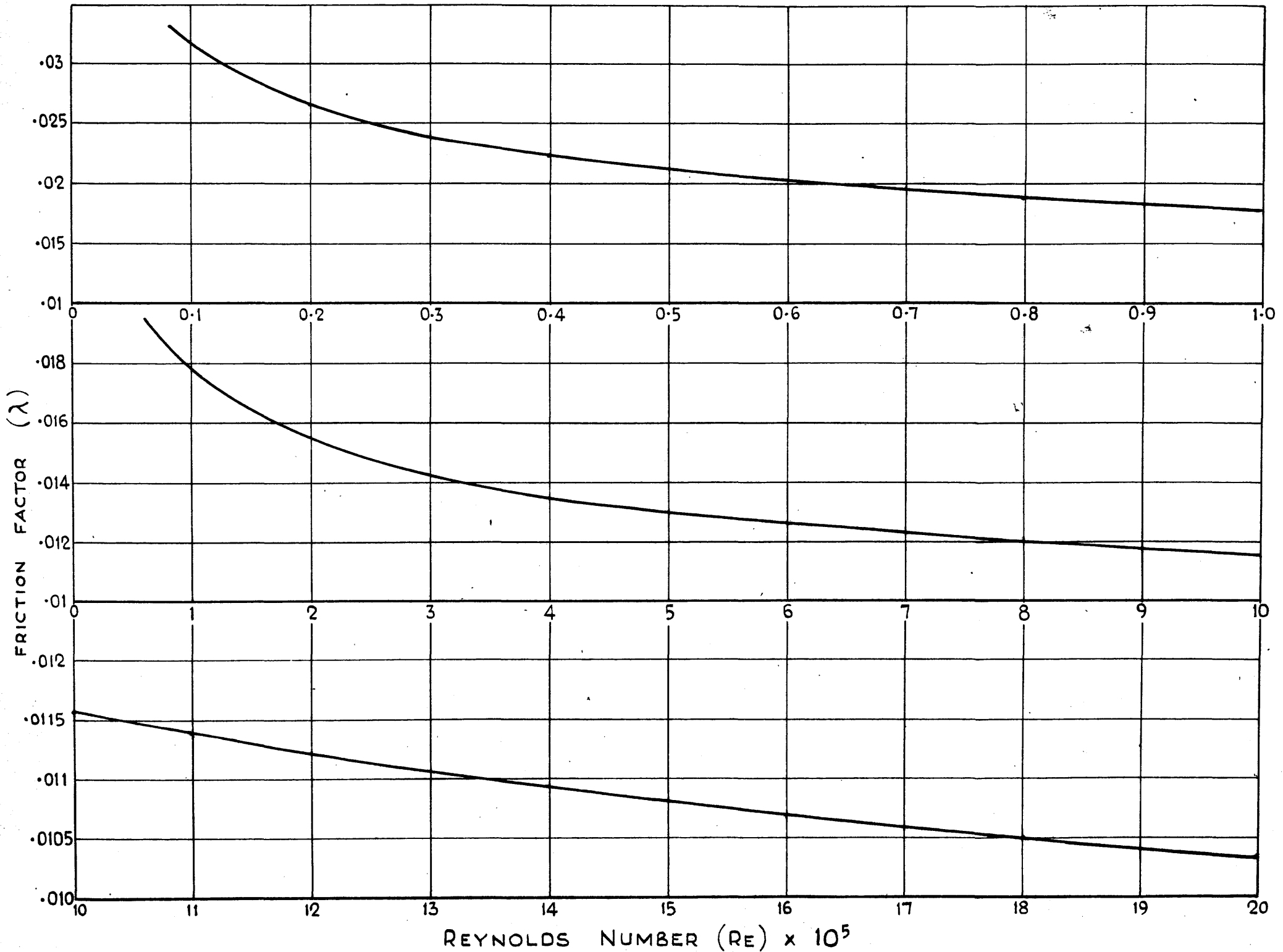
The pressure change per unit length is therefore

$$-\left(\frac{dp}{dl}\right)_2 = \frac{0.0195 \times 12 \times 8.92^2 \times 62.5}{2g \times 1} - \frac{0.054 + 7 \times 0.946}{\frac{0.054}{0.0749} + \frac{7 \times 0.946}{62.5}}$$

CURVES OF FRICTION FACTOR - REYNOLDS NUMBER

LAWS : $\lambda = \frac{0.316}{Re^{.25}}$ FOR $Re < 10^5$ (BLASIUS)

$\lambda = 0.0032 + \frac{0.221}{Re^{.237}}$ FOR $Re \geq 10^5$ (NIKURADSE)



$$= 18.6 - 8.05$$

$$= 10.55 \text{ lb/ft}^2 \cdot \text{ft.}$$

The theoretical velocity ratio is obtained using Equation 65.

$$K = 1 \pm \frac{U_3}{U_1} \sqrt{\frac{\rho_L + \left[\left(\frac{dp}{dl} \right)_2 - \rho_G \right]}{\rho_G - \frac{\lambda \cdot U_1^2 \cdot \rho_L}{2g \cdot d}}}$$

The value of U_3/U_1 is obtained from Figure 68. The values correspond to a Reynold's Number of 105,000. A certain error is therefore introduced here as the ratio U_3/U_1 should theoretically be that corresponding to Reynold's Number for the annulus flow.

From Equation A12

$$\begin{aligned} \frac{X_G}{X} &= \frac{q/\rho_G}{q/\rho_G + K(1-q)/\rho_L} = \frac{0.054/0.0749}{0.054/0.0749 + 7 \times 0.946/62.5} \\ &= 0.873 \end{aligned}$$

From Figure 68

$$\frac{U_3}{U_1} = 0.27$$

Therefore

$$K = 1 \pm 0.27 \sqrt{\frac{62.5}{0.0749} \frac{\pm(-10.55 - 0.0749)}{-18.6}}$$

The appropriate signs give

$$\begin{aligned} K &= 1 + 0.27 \sqrt{\frac{62.5}{0.0749} \frac{10.625}{18.6}} \\ &= 6.95 \end{aligned}$$

It will be seen that this disagrees slightly with the assumed value. The theoretical pressure change is that obtained when the assumed and theoretical values of the

velocity ratio are identical. This is obtained by a trial and error procedure, which is detailed in Appendix H. In this case the pressure change was found to be 10.62 lb/ft²ft. and the velocity ratio 6.97.

"Stagnation Point" as previously discussed in Section 23, occurs when $K=0$. The equations are however not in a form enabling their application to the limiting condition. For example, the dryness fraction q ceases to have meaning when the steam phase is no longer moving. Consequently the equations were applied to find the mass flow corresponding to $K=0.1$.

Lowenstein obtained stagnation with pressure drops from 60 to 40 atmospheres. The calculations were carried out for a mean pressure of 50 atmospheres (720 lb/in² gauge) and the mass flow rates corresponding to $K=0.1$ and a range of qualities determined for this condition.

The procedure was to assume a value of the dryness fraction (e.g. $q=0.015$) and $K=0.1$. Then for a series of mass flows the velocity ratio calculated. The mass flow approximating to the stagnation condition will be that for which the calculated K agrees with the assumed value of 0.1. This procedure is now detailed.

From Equation 57

$$-\left(\frac{dp}{dl}\right)_2 \cdot \delta l = \frac{\lambda \cdot \delta l \cdot u_L^2 \cdot \rho}{2g \cdot d} - \left[\frac{q + K(1-q)}{q/\rho_g + K(1-q)/\rho_l} \right] \delta l$$

The various properties are:

$$\begin{array}{lll} \rho_l = 48.7 \text{ lb/ft}^3. & \rho_g = 1.6 \text{ lb/ft}^3. & \mu_L = 0.26 \text{ lb/hr.ft.} \\ q = 0.015 & K = 0.1 & \frac{M}{X} = 48.8 \text{ lb/sec.ft}^2. \end{array}$$

From Equation A15

$$u_L = \frac{1}{K} \cdot \frac{M}{X} \left[\frac{q}{\rho_g} + \frac{K(1-q)}{\rho_l} \right]$$

$$= 0.1 \times 48.8 \left(\frac{0.015}{1.6} + \frac{0.1 \times 0.985}{48.7} \right)$$

$$= 5.55 \text{ ft/sec.}$$

From Equation 46 Reynold's Number

$$Re = \frac{U_L \cdot d \cdot \rho_L}{\mu_L} = \frac{5.55 \times 1.18 \times 48.7 \times 3600}{12 \times 0.26} = 368,000$$

From Figure 69 $\lambda = 0.0137$.

The pressure change per unit length is therefore

$$-\left(\frac{dp}{dl}\right)_2 = \frac{0.0137 \times 12 \times 5.55^2 \times 48.7}{29 \times 1.18} - \frac{0.015 + 0.1 \times 0.985}{\frac{0.015}{1.6} + \frac{0.1 \times 0.985}{48.7}}$$

$$= 3.26 - 9.98 = -6.72 \text{ lb/ft}^2 \cdot \text{ft.}$$

The velocity ratio is now obtained from Equation 32,

$$K = 1 \pm Z \sqrt{\frac{\rho_L}{\rho_G} \cdot \frac{\pm \left[\left(\frac{dp}{dl}\right)_2 - \rho_G \right]}{\left(\frac{dp}{dl}\right)_{F2}}}$$

The term Z is that corresponding to (Equation A12)

$$\frac{x_G}{x} = \frac{q/\rho_G}{q/\rho_G + K(1-q)/\rho_L}$$

$$= \frac{0.015/1.6}{0.015/1.6 + 0.1 \times 0.985/48.7} = 0.823$$

and $(1-q)\frac{M}{x} = 0.985 \times 48.8 = 48 \text{ lb/ft}^2 \cdot \text{sec}$. In obtaining Z from Figure 15 the value of Z was taken as that corresponding to $(1-q)\frac{M}{x} = 54$. The curves could not be extrapolated with any accuracy beyond this point. From Figure 15 $Z = 0.306$.

Hence

$$K = 1 \pm 0.306 \sqrt{\frac{48.7}{1.6} \cdot \frac{\pm (6.72 - 1.6)}{-3.26}}$$

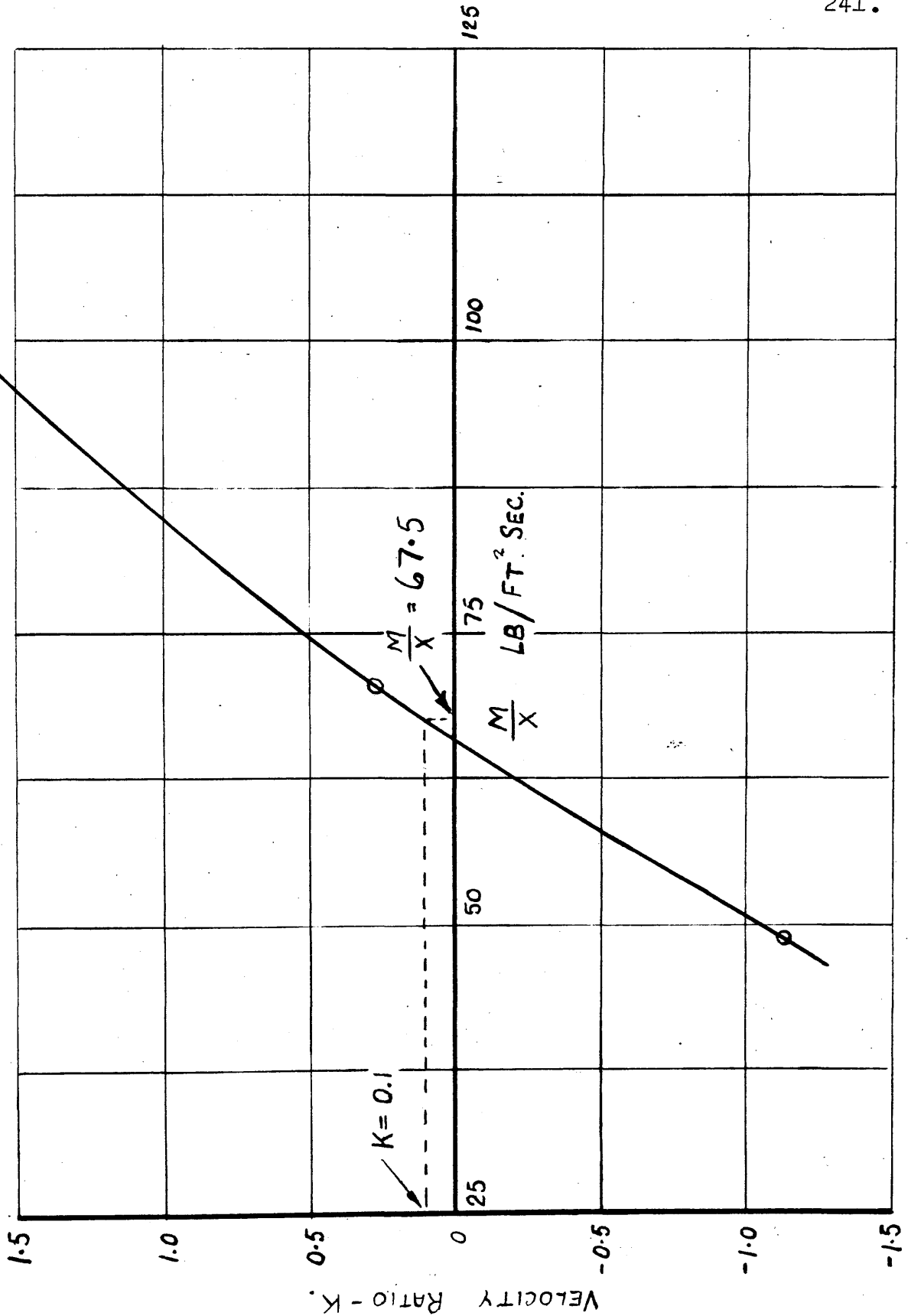
Using the appropriate signs

$$K = 1 - 0.306 \sqrt{\frac{48.7}{1.6} \cdot \frac{5.12}{3.26}}$$
$$= -1.13$$

This procedure was repeated for $\frac{M}{X} = 73.1$ and 97.5 lb/sec.ft^2 and K plotted to $\frac{M}{X}$ as shown in Figure 70. From this figure it is seen that $K = 0.1$ for $\frac{M}{X} = 67.5 \text{ lb/sec.ft}^2$. This entire procedure was repeated for various assumed qualities and Figure 24 constructed.

FIGURE 70. GRAPH OF K TO M/X .

($q = 0.015$. ASSUMED $K = 0.1$.)



Pressure Changes.

As already discussed in Section 28 the ratios of P_c/P_a adopted over the various lengths of pressure limbs were:

$$\text{Water drum to riser bottom} - P_c/P_a = 0.99.$$

$$\text{Riser bottom to riser top} - P_c/P_a = 0.98.$$

$$\text{Riser top to steam drum} - P_c/P_a = 0.99.$$

Over the other combinations of tapping points the ratios were calculated as follows:

$$\text{Water drum to riser top} - \frac{P_c}{P_a} = \frac{18 \times 0.99 + 172 \times 0.98}{18 + 172} = 0.981$$

$$\text{Water drum to steam drum} - \frac{P_c}{P_a} = \frac{18 \times 0.99 + 172 \times 0.98 + 38.5 \times 0.99}{18 + 172 + 38.5} = 0.982$$

$$\text{Riser bottom to steam drum} - \frac{P_c}{P_a} = \frac{172 \times 0.98 + 38.5 \times 0.99}{172 + 38.5} = 0.982$$

(The various dimensions are obtained from Figure 26)

The pressure changes are therefore for Test Series No. 11 at 51 lb/in² using Equations 72 to 76:

$$\text{Steam drum to water drum} - \frac{228.5 \times 0.982 - 36}{144} \times \frac{62.5}{12} = 6.81 \text{ lb/in}^2.$$

$$\text{Steam drum to riser bottom} - \frac{210.5 \times 0.982 - 78}{144} \times \frac{62.5}{12} = 4.66 \text{ lb/in}^2.$$

$$\text{Steam drum to riser top} - \frac{38.5 \times 0.99 - 25}{144} \times \frac{62.5}{12} = 0.47 \text{ lb/in}^2.$$

$$\text{Riser top to riser bottom} - \frac{172 \times 0.98 - 53}{144} \times \frac{62.5}{12} = 4.18 \text{ lb/in}^2.$$

$$\text{Riser top to water drum} - \frac{190 \times 0.981 - 11}{144} \times \frac{62.5}{12} = 6.35 \text{ lb/in}^2.$$

$$\text{Riser bottom to water drum} - \frac{18 \times 0.99 + 41.5}{144} \times \frac{62.5}{12} = 2.15 \text{ lb/in}^2.$$

Velocities.

For Test Series No. 11 at 50 lb/in² the Pitot head reading was 3.125 inches. The density of saturated water at 50 lb/in² is 57.5 lb/ft³.

Hence from Equation 70, the circulation, or downcomer

velocity

$$U = \sqrt{\frac{2g}{1.938} \cdot \frac{h_R}{12} \cdot \frac{\rho_a}{\rho_b}} = \sqrt{\frac{29}{1.938} \times \frac{3.125}{12} \times \frac{62.5}{57.5}}$$
$$= 3.06 \text{ ft/sec.}$$

DATA.

Test Series No. 5. Heating: Uniform.
 Restricting Orifice: None. Heated Length: 10'6".
 Tube: 1.698" = 1.7" I.D. Tube Position: Vertical.
 Gauge Pressure: 72 lb/in². Saturation Temperature: 318°F.
 Pressure Difference (Steam Drum To Water Drum): 6.81 lb/in².
 Water Velocity In Downcomer: 3.31 ft/sec.
 Condenser Heat Transfer: 7.04 × 10⁵ B.Th.U./hr.
 Boiler Heat Loss (Equation 67): Q_B = 50(t_s - 200) = 5900 B.Th.U./hr.
 Latent Heat: 897.6 B.Th.U./lb. $\frac{dH}{dp} = 0.85 \text{ B.Th.U. in}^2/\text{lb}^2$.
 $\frac{1}{\rho_L} = 0.0176 \text{ ft}^3/\text{lb.}$ $\frac{1}{\rho_G} = 5.07 \text{ ft}^3/\text{lb.}$
 $\frac{M}{X} = U \cdot \rho_L = 3.31/0.0176 = 188 \text{ lb/sec.ft}^2$.
 $M = 188 \times \frac{\pi}{4} \times \frac{1.7^2}{144} = 2.955 \text{ lb/sec.}$ $\mathcal{N}_L = 0.42 \text{ lb/hr.ft.}$

(a) Dryness Fraction at furnace top. It has been shown in Section 28 that approximately $\frac{1}{5}$ of the boiler heat loss is from the steam.

$$\begin{aligned} \therefore \text{Heat transfer from steam} &= 704,000 + 1180 \\ &= 705,180 \text{ B.Th.U./hr.} \end{aligned}$$

$$q = \frac{705,180}{2.955 \times 3600 \times 897.6} = 0.0739$$

(b) Point at which Evaporation begins. From Equation 77 the heat transfer between furnace bottom and point of evaporation is

$$\frac{dH}{dp} \cdot \delta p + \frac{4}{5} \cdot \frac{Q_B}{M \times 3600}$$

Commence by assuming that the point of evaporation is 2 ft. from the furnace bottom, . i.e. 3.915 ft. from the riser bottom tapping point. At the tapping

point the pressure relative to the steam drum is 6.13 lb/in².

Then

$$\begin{aligned} \Delta p &= 6.13 - \frac{3.915}{144 \times 0.0176} - \frac{0.02 \times 3.915 \times 12 \times 3.31^2}{2g \times 1.7 \times 144 \times 0.0176} \\ &= 4.55 \text{ lb/in}^2 \end{aligned}$$

(The friction factor λ is assumed 0.02. The small magnitude of the pressure change does not warrant a detailed determination.)

∴ Heat supply to point of evaporation/hr.

$$\begin{aligned} &= 0.85 \times 4.55 \times 2.955 \times 3600 + 5900 \times 0.8 \\ &= 45,800 \text{ B.Th.U.} \end{aligned}$$

∴ Distance from furnace bottom to point of evaporation

$$\begin{aligned} &= 10.5 \times 45,800 / 709,900 \\ &= 0.677 \text{ ft.} \end{aligned}$$

This compares with 2 ft. assumed. By further trial and error the point of evaporation is found to be 0.74 ft. from the furnace bottom, i.e. evaporation length $l_e = 10.5 - 0.74 = 9.76$ ft.

(c) Pressure Gradient and Velocity Ratio at Furnace Top. A velocity ratio of 3.5 is assumed and the pressure gradients due to friction, mixture weight, and momentum forces are evaluated in turn.

(I) Friction.

Now from Equation A6

$$\begin{aligned} U_L &= \frac{M}{K \cdot X} \left[\frac{q}{\rho_g} + \frac{K(1-q)}{\rho_L} \right] = \frac{188}{3.5} \left[0.0739 \times 5.07 + 3.5 \times 0.926 \times 0.0176 \right] \\ &= \frac{188}{3.5} \times 0.431 = 23.2 \text{ ft/sec.} \end{aligned}$$

$$\therefore Re = \frac{23.2 \times 1.7 \times 3600}{12 \times 0.0176 \times 0.42} = 1,600,000.$$

From Figure 69, the friction factor $\lambda = 0.0107$.

Hence from Equation 39

$$\begin{aligned} -\left(\frac{dp}{dl}\right)_{F2} &= 1.25 \frac{\lambda \cdot U_L^2 \cdot \rho_L}{2g \cdot d} = 1.25 \frac{0.0107 \times 23.2^2 \times 12}{2 \times 32.2 \times 1.7 \times 0.0176} \\ &= 45 \text{ lb/ft}^3 \end{aligned}$$

(II) Tube Mixture Weight. From Equation 52

$$-\left(\frac{dp}{dl}\right)_{\rho_2} = \frac{q + K(1-q)}{q/\rho_g + K(1-q)/\rho_L} = \frac{0.0739 + 3.5 \times 0.926}{0.431} = 7.7 \text{ lb/ft}^3$$

(III) Momentum Forces. From Equation 52

$$-\left(\frac{dp}{dl}\right)_{M2} = \frac{q}{g} \cdot \frac{M}{X} \cdot \frac{\delta U_g}{\delta l} + \frac{1-q}{g} \cdot \frac{M}{X} \cdot \frac{\delta U_L}{\delta l} + \frac{\delta q}{g} \cdot \frac{M}{X} \cdot \frac{U_g - U_L}{\delta l}$$

As uniform heat transfer is assumed $\frac{\delta q}{\delta l} = \frac{q}{\ell_e}$ where

ℓ_e is the evaporation length. If, in addition, Equations A14, A15, A18 and A19 are substituted in Equation 52,

$$\begin{aligned} -\left(\frac{dp}{dl}\right)_{M2} &= \frac{1}{g} \cdot \frac{q}{\ell_e} \left(\frac{M}{X}\right)^2 \left\{ \frac{q}{\rho_g} + \frac{1-q}{K \cdot \rho_g} + \left(\frac{q}{\rho_g} + \frac{K(1-q)}{\rho_L} \right) \left(1 - \frac{1}{K} \right) \right\} \\ &= \frac{0.0739 \times 188^2}{g \times 9.76} \left\{ 0.0739 \times 5.07 + \frac{0.926 \times 5.07}{3.5} + 0.431 \left(1 - \frac{1}{3.5} \right) \right\} \\ &= 16.81 \text{ lb/ft}^3 \end{aligned}$$

(IV) Total Pressure Gradient.

$$-\left(\frac{dp}{dl}\right)_2 = 45 + 7.7 + 16.81 = 69.51 \text{ lb/ft}^3 = 0.484 \text{ lb/in}^2 \text{ per ft.}$$

(V) Velocity Ratio (K). From the total pressure gradient the velocity ratio can be calculated and compared with the assumed value. The correct solution is obtained when assumed and calculated values agree.

The value of Z is that corresponding to:-

$$\frac{X_G}{X} = \frac{q/\rho_G}{q/\rho_G + K(1-q)/\rho_L} = \frac{0.0739 \times 5.07}{0.431} = 0.867$$

and to $(1-q)\frac{M}{X} = 0.926 \times 188 = 174 \text{ lb/sec.ft}^2$.

From Figure 15 the value of Z is 0.118.

From Equation 17

$$\frac{T_2}{T_1} = \frac{\left(\frac{dp}{dl}\right)_2 + \rho_G \sin \theta + \frac{\rho_G \cdot U_2 \cdot \delta U_2}{\delta l \cdot g}}{\left(\frac{dp}{dl}\right)_{F2}}$$

$\sin \theta$ is unity, as the tube is vertical. Therefore substituting for U_2 and δU_2

$$\begin{aligned} \frac{T_2}{T_1} &= \frac{\left(\frac{dp}{dl}\right)_2 + \rho_G + \left(\frac{M}{X}\right)^2 \frac{q/\rho_G + K(1-q)/\rho_L}{g} \cdot \frac{q}{le}}{\left(\frac{dp}{dl}\right)_{F2}} \\ &= \frac{-69.51 + 1/5.07 + 188^2 \frac{0.431}{32.2} \times \frac{0.0739}{9.76}}{-45} \\ &= 1.46. \end{aligned}$$

From Equation 13

$$K = 1 + 0.118 \sqrt{\frac{5.07}{0.0176} \times 1.46} = 3.42$$

This compares with the value of 3.5 assumed. The correct value is best obtained graphically from three assumed values. These two further values of K , in this case 3.42 and 3.46, are taken and the calculations repeated. Figure 71 is then plotted and the correct values of K and the pressure gradient deduced, viz. 3.44 and 0.492 lb/in² per ft. respectively.

(d) Pressure Change. The pressure change between steam drum and water drum can be evaluated either via the riser or via the downcomer. In the case of the riser there are three distinct lengths decided by the flow conditions, from steam drum to furnace top, the evaporation length, and the evaporation point to the water drum. To allow comparison with the measured values these are further divided and grouped as follows.

(I) Steam drum to riser top.

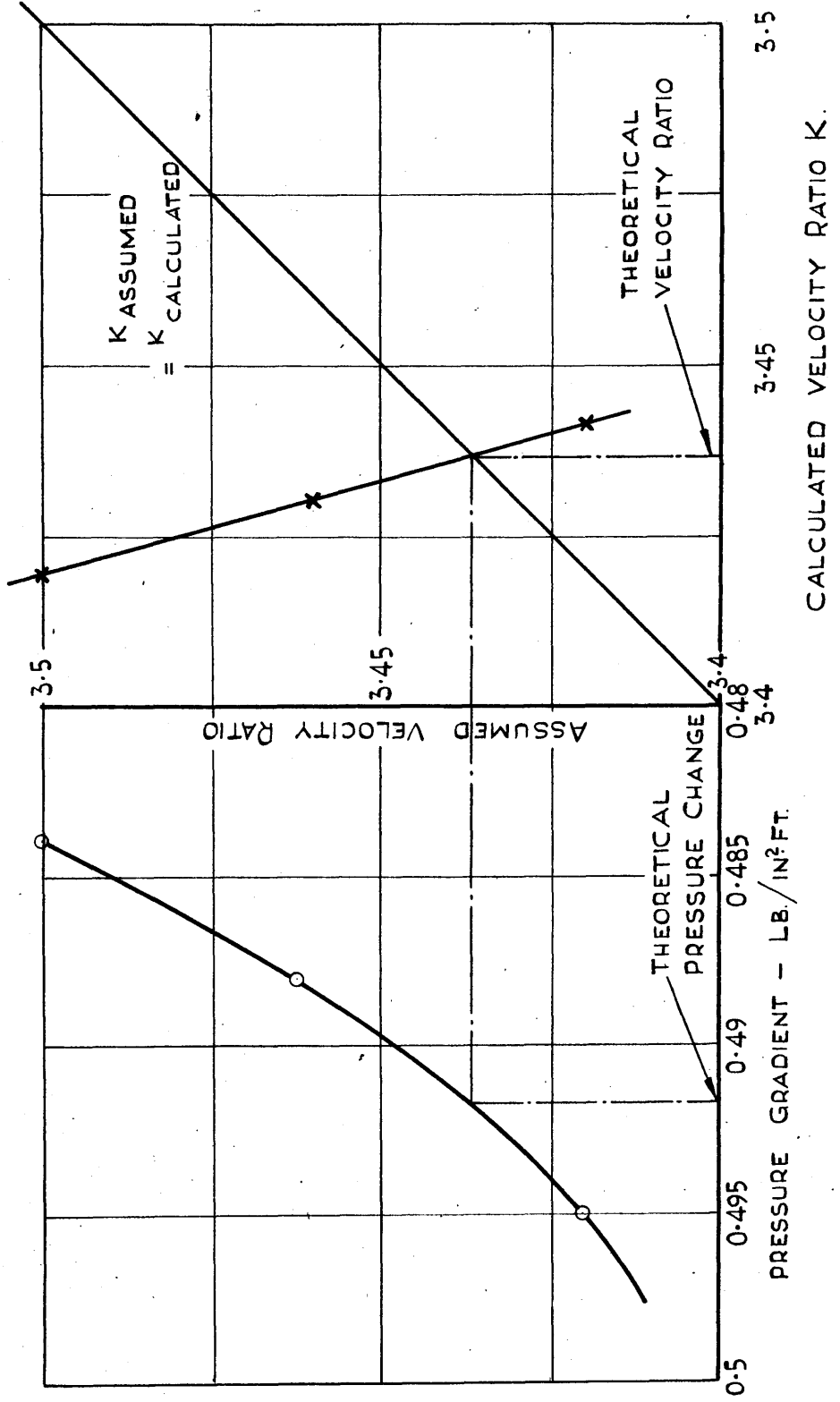
(II) Riser top to furnace top; furnace top to evaporation point; and evaporation point to riser bottom.

(III) Riser bottom to water drum.

These sections are now considered:

(I) Steam drum to riser top. By assuming a velocity

FIG: 71. DETERMINATION OF THE THEORETICAL VELOCITY RATIO AND PRESSURE GRADIENT
TEST N^o 5 (72 LB./IN² GAUGE)



ratio of 3.5 as in the previous calculation for the furnace top position, the only modifications required in the pressure gradient calculations are that the factor 1.25 allowed for the effect of evaporation is omitted, and the momentum terms are now negligible.

Friction. $-\left(\frac{dp}{dl}\right)_{F2} = 45/1.25 = 35.9 \text{ lb/ft}^3$.

Tube Mixture Weight. As before 7.7 lb/ft^3 .

Total Pressure Gradient. $-\left(\frac{dp}{dl}\right)_2 = 35.9 + 7.7 = 43.6 \text{ lb/ft}^3$.

Velocity Ratio K . As before $Z = 0.118$.

The shearing stress ratio is now (Momentum forces negligible)

$$\frac{T_2}{T_1} = \frac{\left(\frac{dp}{dl}\right)_2 + \rho_g}{\left(\frac{dp}{dl}\right)_{F2}} = \frac{-43.6 + 1/5.07}{-35.9} = 1.21$$

$$K = 1 + 0.118 \sqrt{\frac{5.07}{0.0176} \times 1.21} = 3.2$$

By repeating calculations for two more assumed values of K and plotting, the correct values of K and pressure gradient are found to be 3.23 and 0.336 lb/in^2 per ft.

∴ Pressure change steam drum to riser top tapping point

$$= 0.336 \times 2.33 + \frac{10.5}{12 \times 5.07 \times 144} = 0.784 \text{ lb/in}^2$$

The second term is the allowance for the weight of steam between the exit of tube and the steam drum tapping point.

(II) Riser top to riser bottom.

(a) Riser top to furnace top - conditions as above.

$$\therefore \text{Pressure difference riser top to furnace top} \\ = 0.336 \times 23/12 = 0.643 \text{ lb/in}^2.$$

(b) Furnace top to evaporation point. The pressure gradient at the top of this length i.e. at furnace top, has already been calculated and found to be 0.492 lb/in² per foot. The same calculations are made for four other points along the evaporation length and the pressure gradients plotted as in Figure 72. The pressure change over the evaporation length is given by the area under the pressure gradient curve multiplied by the scale. Hence

$$\text{Pressure change furnace top to evaporation point} \\ = 9.25 \times 0.4 = 3.7 \text{ lb/in}^2.$$

(c) Evaporation point to riser bottom. In this length water only is flowing hence, the pressure gradient

$$-\left(\frac{db}{dl}\right)_f = R_L + \frac{\lambda \cdot U^2 \cdot R}{2g \cdot d} \\ = \frac{1}{0.0176} + \frac{0.015 \times 3.31^2 \times 12}{2g \times 1.7 \times 0.0176} \\ = 56.8 + 1.02 = 57.82 \text{ lb/ft}^3$$

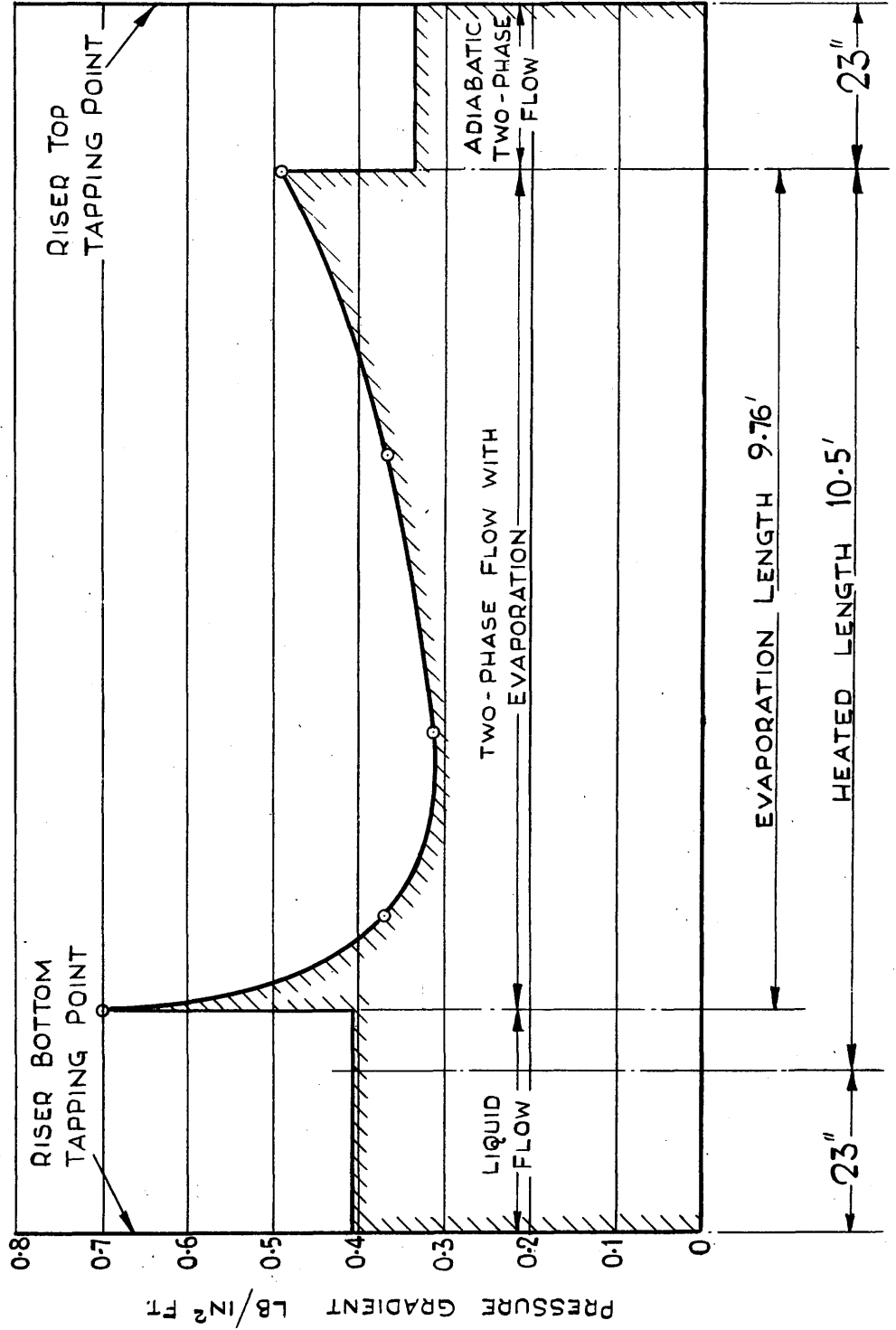
$$\text{(N.B. } Re = \frac{3.31 \times 1.7 \times 3600}{12 \times 0.0176 \times 0.42} = 228,000 \quad \text{From Figure 69, } \lambda = 0.015)$$

$$\therefore \text{Pressure change evaporation point to riser bottom} \\ = 57.82 \times 2.655/144 = 1.065 \text{ lb/in}^2.$$

$$\therefore \text{Pressure change riser top to riser bottom} \\ = 0.643 + 3.7 + 1.065 = 5.408 \text{ lb/in}^2.$$

(III) Riser bottom to water drum. This is summation due to 1.5ft. head of water, friction loss in 1.115ft. of riser tube, water kinetic energy, and entry loss. From Equation 80

FIG. 72. PRESSURE GRADIENTS BETWEEN RISER BOTTOM AND TOP TAPPING POINTS.



$$\begin{aligned} \text{Pressure change} &= (1.5 + 0.026 \times 3.31^2) / 0.0176 \\ &= 101.4 \text{ lb/ft}^2 = 0.705 \text{ lb/in}^2. \end{aligned}$$

$$\begin{aligned} \therefore \text{Pressure change steam drum to water drum} \\ &= 0.784 + 5.408 + 0.705 = 6.897 \text{ lb/in}^2. \end{aligned}$$

The pressure change over the downcomer is obtained using Equation 79

$$\begin{aligned} &\rho_L (17.833 - 0.0713 U^2) + 1.205 \rho_G \\ &= \frac{17.833 - 0.0713 \times 3.31^2}{0.0176 \times 144} + \frac{1.205}{5.07 \times 144} = 6.74 \text{ lb/in}^2 \end{aligned}$$

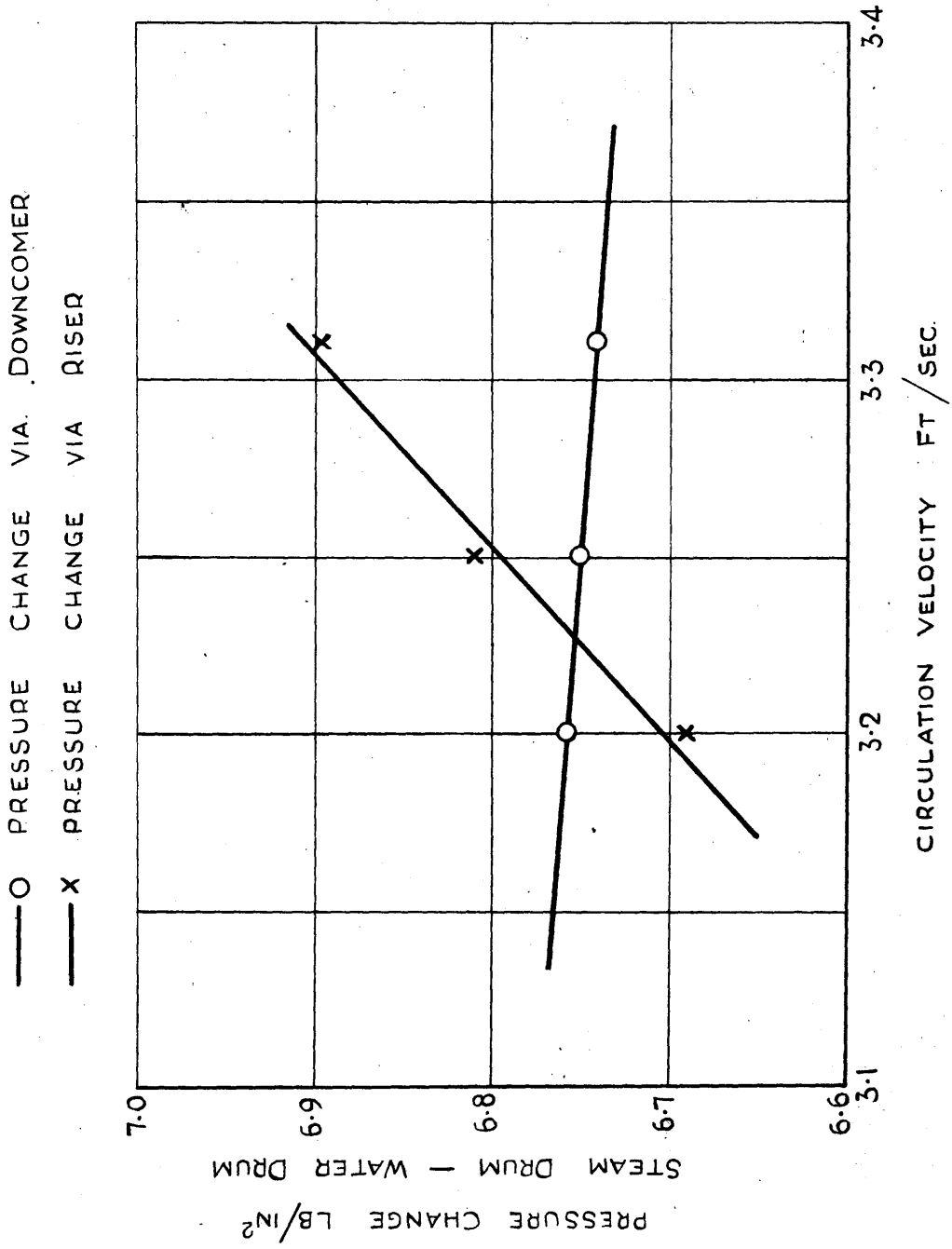
This compares with 6.897 lb/in² above, or an error of 2½%.

(e) Determination of Circulation Velocity. The theoretical circulation velocity is found to be 3.225 ft/sec by the graphical construction shown in Figure 73. This figure was constructed by making two further assumptions as to the circulation velocity, and evaluating the pressure changes over the riser and downcomer as indicated above.

(f) Pressure Change (Homogeneous Theory) Over the heated length the assumption of homogeneous flow, and of a uniform change of quality over the evaporation length gives (see Section 2)

$$\begin{aligned} -\sum \left(\frac{dp}{dl} \right)_2 \cdot dl &= \frac{\rho_L}{q \left(\frac{1}{\rho_G} - \frac{1}{\rho_L} \right)} \text{Log}_e \left\{ 1 + q \frac{\rho_L - \rho_G}{\rho_G} \right\} + \frac{\lambda \cdot \rho_L \cdot U^2 \cdot \rho_L}{2g \cdot d} \left\{ 1 + \frac{q}{2} \frac{\rho_L - \rho_G}{\rho_G} \right\} \\ &\quad + \frac{q}{g} \cdot U^2 \cdot \rho_L \left\{ \frac{\rho_L - \rho_G}{\rho_G} \right\} \\ &= \frac{9.76}{0.0739(5.07 - 0.0176)} \text{Log}_e \left\{ 1 + 0.0739 \frac{1/0.0176 - 1/5.07}{1/5.07} \right\} + \end{aligned}$$

FIG. 73. DETERMINATION OF THEORETICAL CIRCULATION VELOCITY



$$\begin{aligned}
& + \frac{0.02 \times 9.76 \times 12 \times 3.31^2}{2g \times 1.7 \times 0.0176} \left\{ 1 + \frac{0.0739}{2} \cdot \frac{1/0.0176 - 1/5.07}{1/5.07} \right\} \\
& + \frac{0.0739 \times 3.31^2}{g \times 0.0176} \left\{ \frac{1/0.0176 - 1/5.07}{1/5.07} \right\} \\
& = 79.5 + 154 + 406 = 717.5 \text{ lb/ft}^2 = 4.99 \text{ lb/in}^2.
\end{aligned}$$

The friction factor λ is assumed 0.02 as recommended by Lewis and Robertson.

Over the length where the steam-water mixture flows adiabatically the pressure gradient is given by

$$-\left(\frac{dp}{dl}\right)_2 = \frac{1}{q/\rho_a + (1-q)/\rho_L} + \frac{\lambda \cdot U^2}{2g \cdot d} \cdot \frac{1}{q/\rho_a + (1-q)/\rho_L}$$

where

$$\begin{aligned}
U &= \frac{M}{X} \left\{ \frac{q}{\rho_a} + \frac{1-q}{\rho_L} \right\} \\
&= 188 (0.0739 \times 5.07 + 0.926 \times 0.0176) \\
&= 188 \times 0.392 = 73.6 \text{ ft/sec.}
\end{aligned}$$

Hence

$$\begin{aligned}
-\left(\frac{dp}{dl}\right)_2 &= \frac{1}{0.392} + \frac{0.02 \times 73.6^2 \times 12}{2g \times 1.7 \times 0.392} \\
&= 33 \text{ lb/ft}^3 = 0.23 \text{ lb/in}^2 \text{ per ft.}
\end{aligned}$$

The pressure change over the riser was once more obtained by summing the pressure changes over the various lengths as already indicated.

EQUIPMENT TO ENABLE THE STUDY OF THE FLOW OF STEAM-WATER MIXTURES THROUGH HORIZONTAL TUBES. APPENDIX J.

Attempts were made to investigate the flow of steam-water mixtures in horizontal tubes at pressures close to atmospheric, but had eventually to be abandoned due to water-hammer effects, and difficulty in maintaining steady conditions.

Two methods were tried. First by the arrangement shown in Figure 74, the water was delivered from a pump at pressures up to 40 lb/in² and temperatures in the region of 170° F. At the preheater, steam was added to the water to bring it up to saturation temperature. The steam was passed from an annular chamber through holes in the pipe. At the steam mixer further steam was added to make up the mixture steam content. The steam pipe was placed inside, and axial with the main pipe, in order that the steam maintained its momentum when mixing with the water. The mixture then passed along the test length, through a throttling valve to a condenser then to the measuring tanks.

This apparatus is practically identical to the used by Armand in 1946. The writer was unaware of this when the apparatus was constructed. Armand also experienced difficulty in maintaining steady conditions, however Armand's experiments differed from the writer's in two important aspects. Armand used superheated steam, and the lowest pressure at which the plant was operated was 150 lb/in². As the difficulty of maintaining steady conditions is

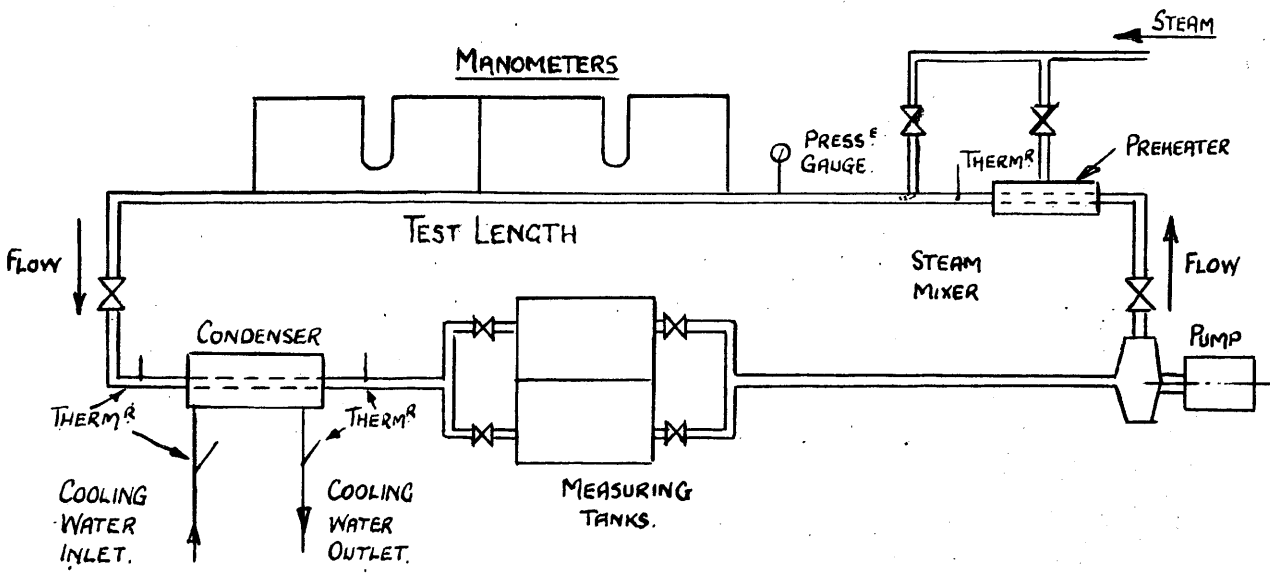


FIG 74. CIRCUIT FOR STEAM-WATER TESTS.

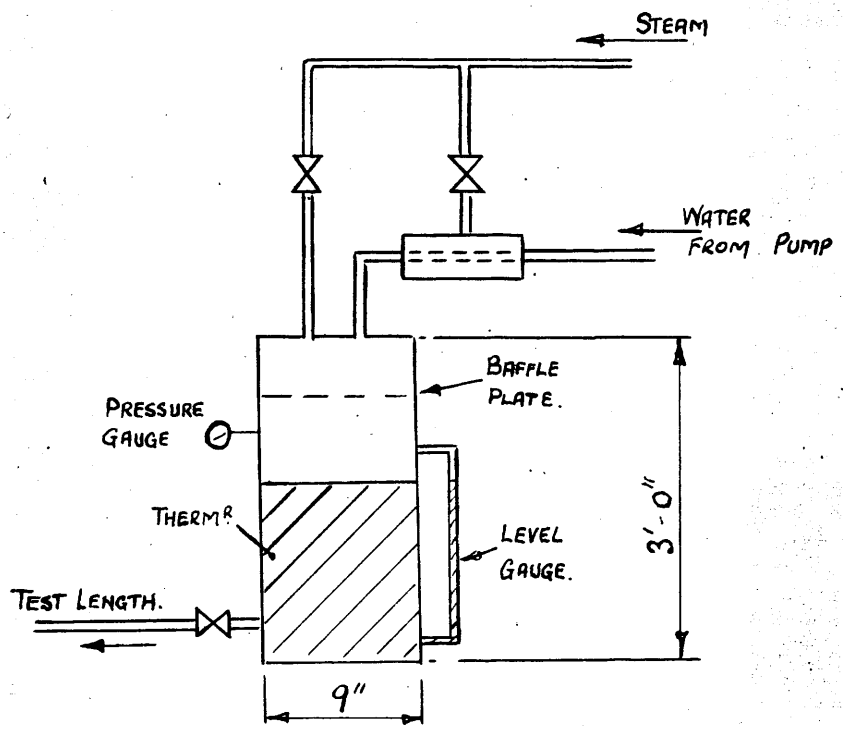


FIG. 75. ALTERNATIVE MIXING ARRANGEMENT.

undoubtedly associated with the collapse of the steam when mixing with water below saturation temperature, both the points quoted would enable Armand to obtain more readily steady conditions. He was unable, however, to obtain sufficiently steady conditions to adopt the technique of weighing the tube, which he used with air-water flow.

The second arrangement was similar to the first except that the steam mixer was now replaced by a large chamber as shown in Figure 75. Water close to saturation temperature was taken from the foot of the chamber and throttled to give the necessary mixture steam content.

THE VELOCITY RATIO EQUATION FOR ROUGH TUBES. APPENDIX K.

The term Z in the applied form of the velocity ratio equation was determined from experiments with smooth tubes. The equations are further developed here to allow for the effect of rough tubes.

The effect of rough tube walls on the velocity profile during single phase flow is the starting point. The most comprehensive experimental work to date is that of Nikuradse. The roughness of the artificially roughened tube was correlated using the ratio of the roughness indentation to the tube radius. This ratio is referred to as the relative roughness. The reciprocal is referred to as the relative smoothness. Nikuradse found this ratio a satisfactory method of correlating his results. The geometric forms of the roughness during the tests were similar. The behaviour with rough surfaces of other geometric forms has yet to be investigated.

Nikuradse's analysis utilises Prandtl's idea of a "friction velocity"

$$U_* = \sqrt{\frac{T \cdot g}{\rho}}$$

where T is the shearing stress at the walls.

Figure 76 illustrates the outline of the observed velocity curves, in terms of the friction velocity U_* for different relative roughness.

It will be seen that the profiles are parallel over the central region, from which it follows that U_3 in Equation 11 (for example) will be independent of the surface roughness. However U_1 , the velocity in the annulus is very

much dependent on the roughness.

For a particular value of U_3 , consider the variation of the ratio U_3/U_1 with surface roughness. Let C be the decrease in the ratio of the maximum velocity to the friction velocity due to the influence of tube roughness as indicated in Figure 76. Here it will be seen that the ratio of the velocity at any radius to the friction velocity decreases by approximately the same amount, hence the ratio of the mean velocity in the annulus to the friction velocity will also decrease by C .

Let $(U_1)_s$ represent the annulus velocity with smooth

tubes, and $(U_1)_R$ the annulus velocity with rough tubes.

Then
or

$$\frac{(U_1)_s}{(U_1)_R} = \frac{(U_1)_R}{(U_1)_R} + C U_* \dots \dots \dots A29$$

Consider now the behaviour of the term Z with tube roughness.

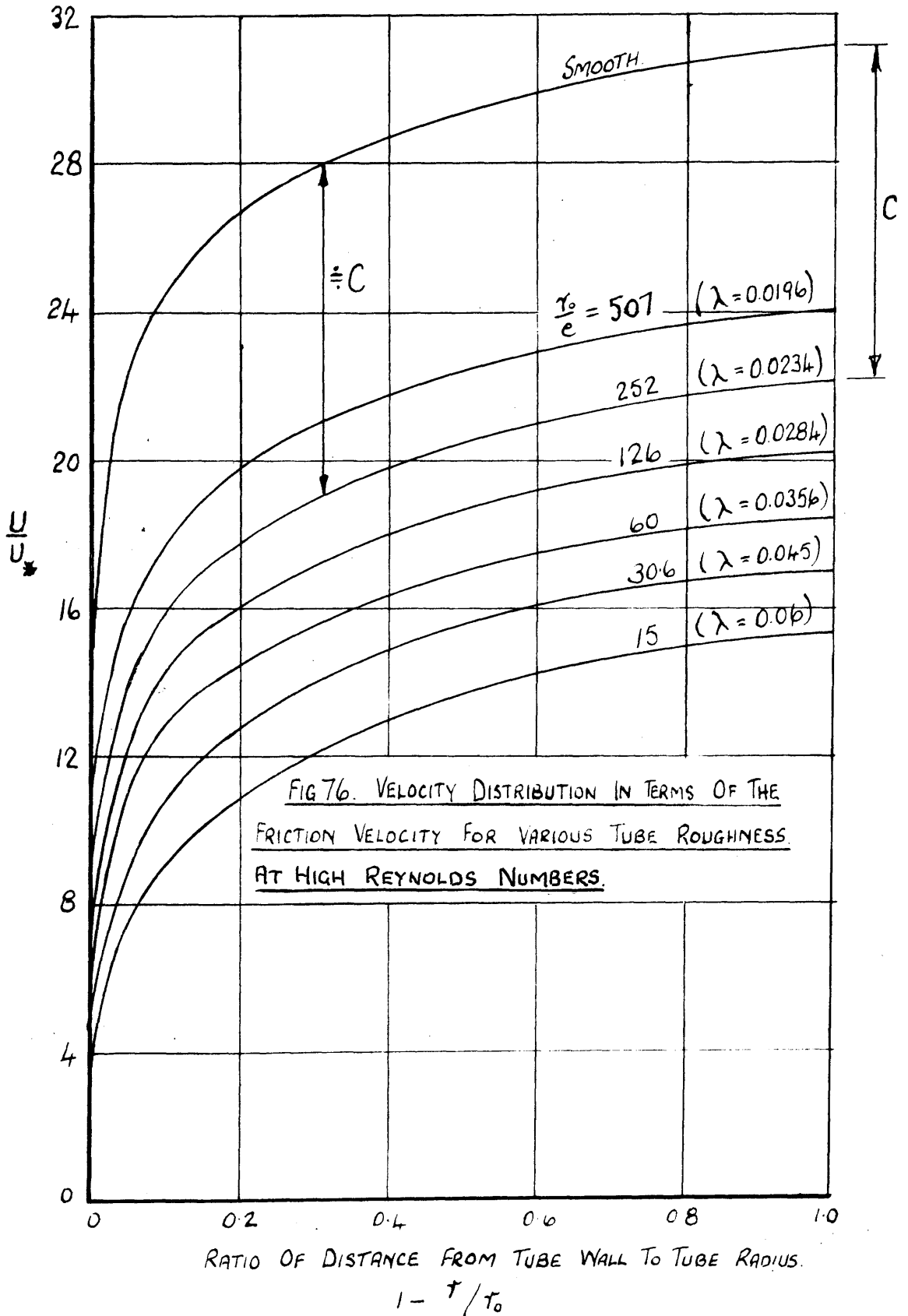
$$Z = \frac{U_3}{U_1} \cdot \frac{1-q-\omega+\omega/k_2}{1-q} \sqrt{\frac{q}{q+\omega}} \dots \dots \dots 63$$

As Z is calculated from the experiments with a smooth tube this should now be written

$$Z = \frac{U_3}{(U_1)_s} \cdot \frac{1-q-\omega+\omega/k_2}{1-q} \sqrt{\frac{q}{q+\omega}} \dots \dots \dots A30$$

Let Z_R be the term with rough tubes where

$$Z_R = \frac{U_3}{(U_1)_R} \cdot \frac{1-q-\omega+\omega/k_2}{1-q} \sqrt{\frac{q}{q+\omega}}$$



$$= \frac{U_3}{(U_1)_s} \cdot \frac{1-q-\omega+\omega/k_2}{1-q} \sqrt{\frac{q}{q+\omega}} \cdot \frac{(U_1)_s}{(U_1)_R} \dots \dots \dots A31$$

Substituting Equations A29 and A30 in A31

$$Z_R = Z \cdot \frac{(U_1)_s}{(U_1)_s - C U_*}$$

$$= \frac{Z}{1 - C U_* / (U_1)_s} \dots \dots \dots A32$$

The approximate general form of the Gas-Liquid Velocity Ratio Equation may therefore be written

$$K = 1 + \frac{Z}{1 - C U_* / (U_1)_s} \sqrt{\frac{P_2 T_2}{P_1 T_1}} \dots \dots \dots A33$$

It should be noted that the ratio U_b/U_1 in Equation 11 is also slightly affected by the roughness. The expression $\frac{U_b}{U_1} \cdot \frac{1-q-\omega+\omega/k_2}{1-q}$ will however still be approximately unity.

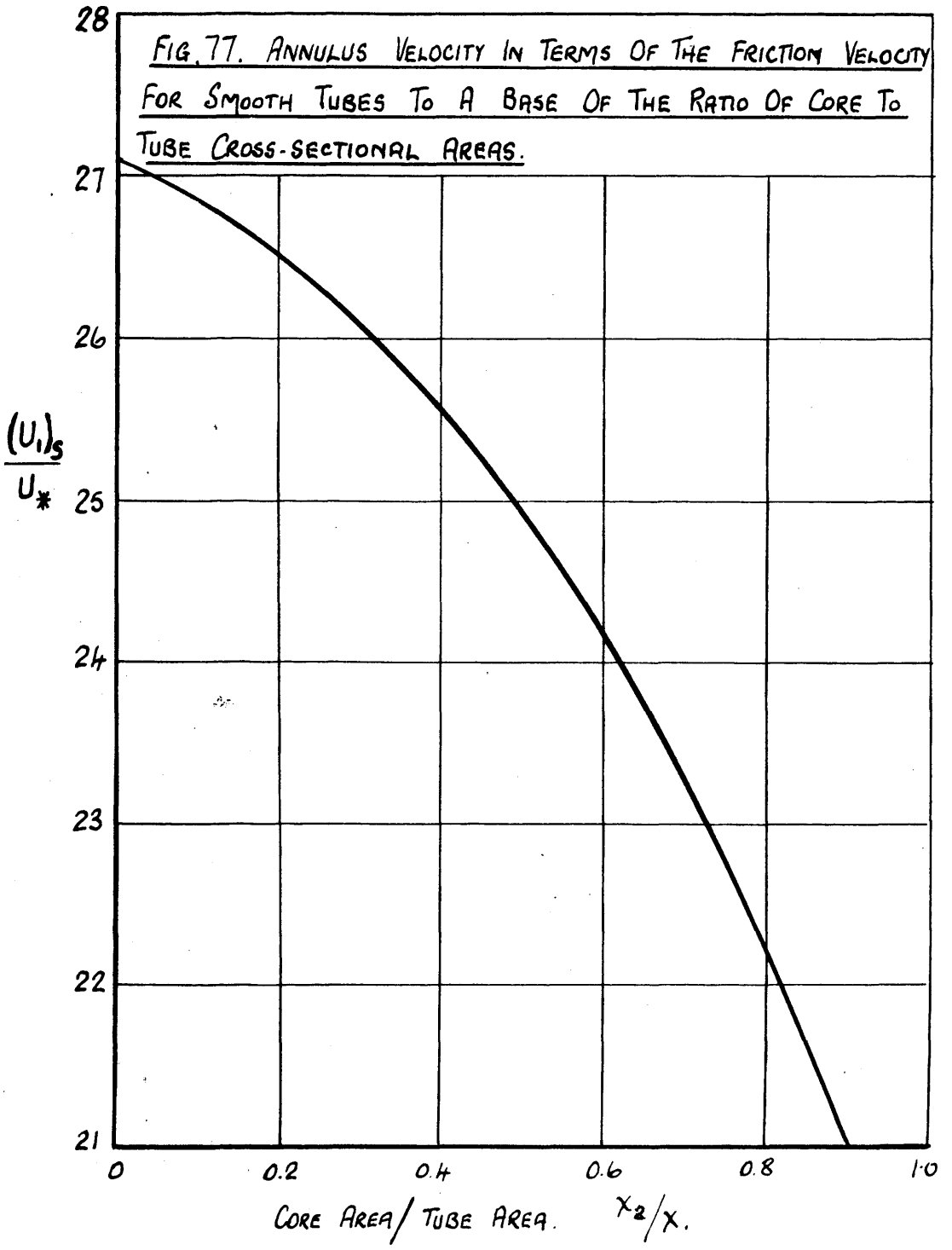
During the experiments of Nikuradse, the friction factor λ was related to the surface roughness in the expression

$$\frac{1}{\sqrt{\lambda}} = 1.74 + 2 \text{Log} \frac{r_0}{e} \dots \dots \dots A34$$

where $\frac{r_0}{e}$ is the relative smoothness.

In applying Equation A33 to the analysis of rough tube data, the above expression should be utilised. It must be remembered, however, that Equation A34 will presumably hold accurately only where the geometric form of the roughness is the same as in Nikuradse's experiments.

Appropriate values of $(U_1)_s/U_*$ and C can be obtained from Figures 77 and 78 respectively.



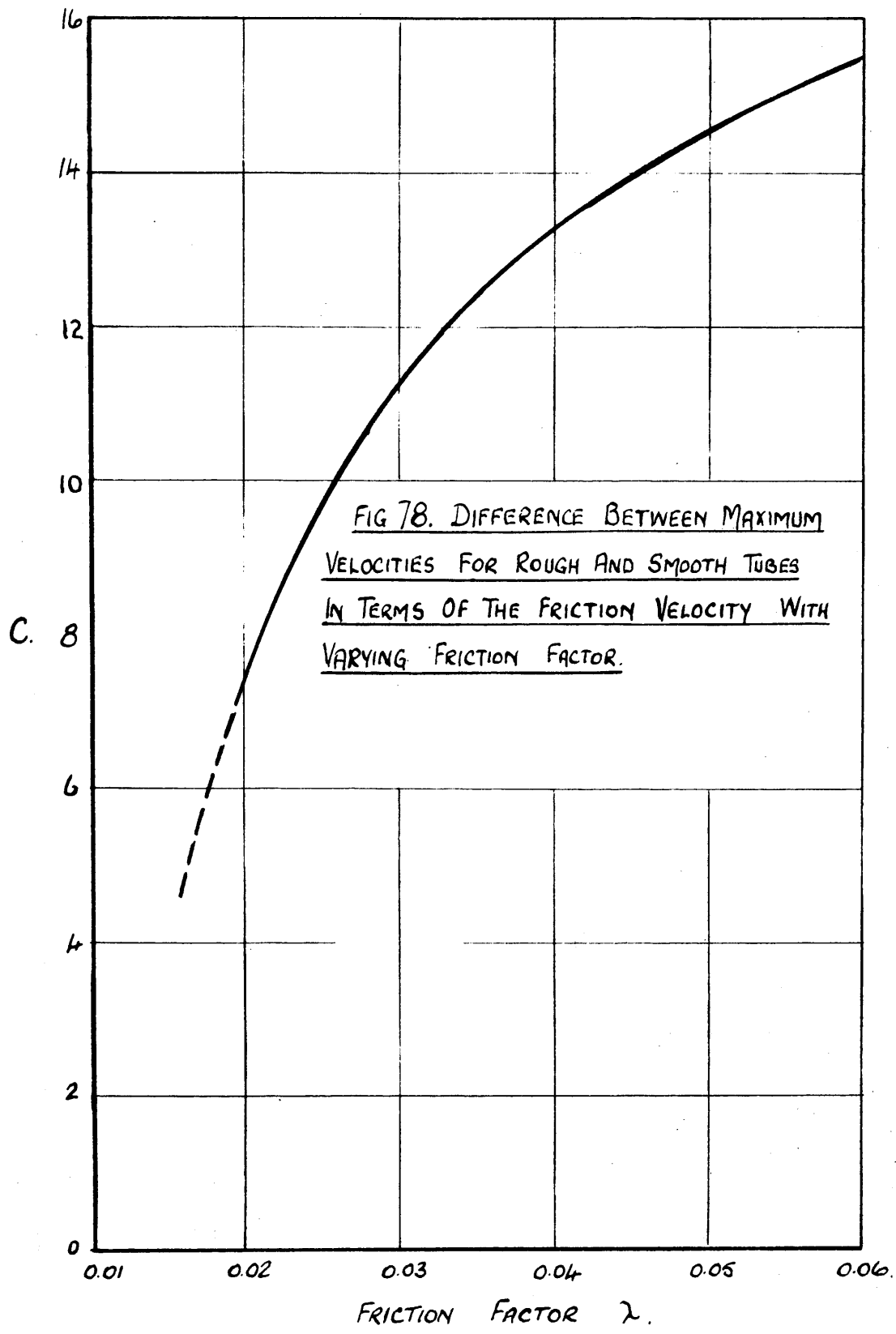


FIG 78. DIFFERENCE BETWEEN MAXIMUM VELOCITIES FOR ROUGH AND SMOOTH TUBES IN TERMS OF THE FRICTION VELOCITY WITH VARYING FRICTION FACTOR.